

MODERN DEVELOPMENT OF MAGNETIC RESONANCE

abstracts

2020

KAZAN * RUSSIA





MODERN DEVELOPMENT OF MAGNETIC RESONANCE

ABSTRACTS OF THE
INTERNATIONAL CONFERENCE
AND WORKSHOP "DIAMOND-BASED
QUANTUM SYSTEMS FOR SENSING
AND QUANTUM INFORMATION"

Editors:
ALEXEY A. KALACHEV
KEV M. SALIKHOV

KAZAN, SEPTEMBER 28–OCTOBER 2, 2020

This work is subject to copyright.

All rights are reserved, whether the whole or part of the material is concerned, specifically those of translation, reprinting, re-use of illustrations, broadcasting, reproduction by photocopying machines or similar means, and storage in data banks.

© 2020 Zavoisky Physical-Technical Institute, FRC Kazan Scientific Center of RAS, Kazan

© 2020 Igor A. Aksenov, graphic design

Printed in Russian Federation

Published by Zavoisky Physical-Technical Institute, FRC Kazan Scientific Center of RAS, Kazan

www.kfti.knc.ru

CHAIRMEN

Alexey A. Kalachev
Kev M. Salikhov

PROGRAM COMMITTEE

Kev Salikhov, chairman (Russia)
Vadim Atsarkin (Russia)
Elena Bagryanskaya (Russia)
Pavel Baranov (Russia)
Marina Bennati (Germany)
Robert Bittl (Germany)
Bernhard Blümich (Germany)
Michael Bowman (USA)
Gerd Buntkowsky (Germany)
Sergei Demishev (Russia)
Sabine Van Doorslaer (Belgium)
Rushana Eremina (Russia)
Jack Freed (USA)
Philip Hemmer (USA)
Konstantin Ivanov (Russia)
Alexey Kalachev (Russia)
Vladislav Kataev (Germany)
Walter Kockenberger (Great Britain)
Wolfgang Lubitz (Germany)
Anders Lund (Sweden)
Sergei Nikitin (Russia)
Klaus Möbius (Germany)
Hitoshi Ohta (Japan)
Igor Ovchinnikov (Russia)
Vladimir Skirda (Russia)
Alexander Smirnov (Russia)
Graham Smith (Great Britain)
Mark Smith (Great Britain)
Murat Tagirov (Russia)
Takeji Takui (Japan)
Valery Tarasov (Russia)
Violeta Voronkova (Russia)

LOCAL ORGANIZING COMMITTEE

Kalachev A.A., chairman	Kupriyanova O.O.
Mamin R.F., vice-chairman	Kurkina N.G.
Khantimerov S.M., vice-chairman	Latypov V.A.
Voronkova V.K., scientific secretary	Mosina L.V.
Akhmin S.M.	Oladoshkin Yu.V.
Fazlizhanov I.I.	Sukhanov A.A.
Galeev R.T.	Zaripov R.B.
Gavrilova T.P.	Yanduganova O.B.
Guseva R.R.	Yurtaeva S.V.
Konovalov D.A.	

SCIENTIFIC SECRETARIAT

Violeta K. Voronkova
Laila V. Mosina
Vladislav A. Latypov

The conference is organized under the auspices of the AMPERE Society

ORGANIZERS

Zavoisky Physical-Technical Institute, FRC Kazan Scientific Center of RAS
Kazan Federal University

SUPPORTED BY

The Government of the Russian Federation (Mega-grant no. 14.W03.31.0028)
Russian Foundation for Basic Research (project no. 20-02-22031)

CONTENTS

PLENARY LECTURES

From High Power to Low Power – Recipes for a Successful Scientific Life! <i>K.-P. Dinse</i>	1
DNP Enhanced Solid-State NMR Spectroscopy of Functional Materials <i>G. Buntkowsky</i>	2
New Paradigm of Spin Exchange <i>K. M. Salikhov</i>	3
Interplay of Magnetism and Topological Electronic Structure of Magnetic Van Der Waals Compounds <i>V. Kataev</i>	4

SECTION 1

CHEMICAL AND BIOLOGICAL SYSTEMS

Invited Talks

Molecular Mobility in a Set of Imidazolium-Based Ionic Liquids [bmim] ⁺ A ⁻ and Their Mixtures with Water <i>V. I. Chizhik, S. S. Bystrov, V. V. Matveev, A. V. Egorov, V. Balevičius</i>	6
On the Nature of Radicals in Titania Photocatalysts: New Approach Based on EPR Spectroscopy <i>E. A. Konstantinova, E. V. Kytina, G. V. Trusov, A. I. Kokorin</i>	7
Application of EPR to Porphyrin-Protein Agents for Photodynamic Therapy <i>O. A. Krumkacheva, N. E. Sannikova, I. O. Timofeev, A. S. Chubarov, N. Sh. Lebedeva, A. S. Semeikin, I. A. Kirilyuk, Y. P. Tsentalovich, M. V. Fedin, E. G. Bagryanskaya</i>	9
Application of Time-Resolved EPR in Study of Charge-Recombination Induced Intersystem Crossing in Compact Electron Donor/Acceptor Dyads <i>X. Zhang, Y. Dong, Y. Yan, J. Zhao</i>	10

Oral Talks

- Investigation of Pathological Calcification and Synthetic Calcium Phosphates by Magnetic Resonance Techniques
M. Gafurov, G. Mamin, S. Orlinskii, P. Grishin, I. Ignatyev, M. Goldberg, N. Petrakova, A. Fedotov, V. S. Komlev 11
- A Test of the Poisson-Boltzmann Double Layer Theory on Mesoporous Silicas by EPR of pH-Sensitive Nitroxides
E. G. Kovaleva, A. Marek, A. I. Smirnov, D. O. Antonov, D. P. Tambasova 12
- Stable Novel Biradicals for Dynamic Nuclear Polarization
N. Asanbaeva, D. Morozov, S. Dobrynin, V. Tormyshev, I. Kirilyuk, E. Bagryanskaya 14
- Isotope Substitution in EPR Studies of Nitroxide Biradicals
R. B. Zaripov, I. T. Khairutdinov, T. Kálai, K. Kish, A. I. Kokorin, K. M. Salikhov 16

SECTION 2

STRONGLY CORRELATED ELECTRON SYSTEMS

Plenary Lectures

- New Concept of Magnetism of Topological Kondo Insulator SmB_6 on the Basis of Electron Spin Resonance Experiments
S. V. Demishev 18
- Thermodynamic, Dynamic and Transport Properties of Quantum Spin Liquid
V. R. Shaginyan 20

Invited Talk

- Dynamic Diamagnetism of the Anisotropic Chain Antiferromagnet
A. I. Smirnov, T. A. Soldatov, K. Yu. Povarov, A. Paduan-Filho, A. Zheludev 21

Oral Talks

- Antiferromagnetic Resonance Modes of the Quasi-Two-Dimensional Antiferromagnet $\text{Cu(en)(H}_2\text{O)}_2\text{SO}_4$
V. N. Glazkov, Yu. V. Krasnikova, I. K. Rodygina, J. Chovan, R. Tarasenko, A. Orendáčová 23
- Glassy Features in the NMR and μSR Response of Na_2IrO_3 with 3d Transition Metal Ion Impurities
E. Vavilova, G. Prando, V. Kataev 25

SECTION 3
LOW-DIMENSIONAL SYSTEMS AND NANO-SYSTEMS

Plenary Lecture

ESR Investigation of Functional Molecular Magnetic Materials <i>T. Nakamura</i>	27
------------------------------------------------------------------------------------	----

Oral Talks

Synthesis of Carbon Quantum Dots and Their Characterization by 2D DOSY NMR Method <i>I. I. Geru, A. N. Barba, E. C. Gorincioi, I. E. Midoni</i>	29
-------------------------------------------------------------------------------------------------------------------------------------------------------	----

Ferromagnetic Resonance in CoFeB-LiNbO Nanogranular Films Near Metal-Insulator Transition <i>A. B. Drovosekov, N. M. Kreines, A. S. Barkalova, S. N. Nikolaev, A. V. Sitnikov, V. V. Rylkov</i>	30
-----------------------------------------------------------------------------------------------------------------------------------------------------------------------------------------------------------	----

Formation of Ferromagnetic Clusters in $\text{La}_{1-x}\text{Sr}_x\text{Mn}_{0.9}\text{Fe}_{0.1-y}\text{M}_y\text{O}_3$ ($\text{M} = \text{Mg}^{2+}; \text{Zn}^{2+}$) <i>R. M. Eremina, I. V. Yatsyk, A. G. Badelin, V. K. Karpasyuk, Z. Y. Seidov</i>	32
--------------------------------------------------------------------------------------------------------------------------------------------------------------------------------------------------------------------------------------------------------------------	----

Local Structure of Pillared Mordenite and ZSM-5 Zeolites and Water Behavior in Their Interlayer Space Studied by NMR <i>M. G. Shelyapina, D. Nefedov, A. Tyurtyaeva, A. Arteaga, R. Yocupicio-Gaxiola, A. V. Petranovskii, S. Fuentes</i>	33
-----------------------------------------------------------------------------------------------------------------------------------------------------------------------------------------------------------------------------------------------------	----

Synthesis and Studies of Structural, Magnetic and Ferromagnetic Resonance Properties of Epitaxial $\text{Pd}_{0.96}\text{Fe}_{0.04}/\text{VN}/\text{Pd}_{0.92}\text{Fe}_{0.08}$ Superconducting Spin-Valve Heterostructure <i>W. M. Mohammed, I. V. Yanilkin, A. I. Gumarov, A. G. Kiiamov, A. A. Rodionov, R. V. Yusupov, L. R. Tagirov</i>	35
-----------------------------------------------------------------------------------------------------------------------------------------------------------------------------------------------------------------------------------------------------------------------------------------------------------------------------------------------------------	----

Ferromagnetic Resonance Versus Spin-Hall Effect in Heteroepitaxial $\text{W}/\text{Pd}_{0.92}\text{Fe}_{0.08}$ Thin Film Structure <i>R. V. Yusupov, A. I. Gumarov, A. A. Rodionov, I. V. Yanilkin, G. A. Zhivov, L. R. Tagirov</i>	38
-----------------------------------------------------------------------------------------------------------------------------------------------------------------------------------------------------------------------------------------------	----

VSM and FMR Studies of Fe-Ion Implanted Epitaxial Films of Palladium <i>R. I. Khaibullin, A. I. Gumarov, V. I. Nuzhdin, I. R. Vakhitov, V. F. Valeev, I. V. Yanilkin, R. V. Yusupov, L. R. Tagirov</i>	39
------------------------------------------------------------------------------------------------------------------------------------------------------------------------------------------------------------------	----

Electron Spin Resonance in Multiferroic Spin-Chain Cuprate LiCuVO_4 <i>S. Gotovko, L. Svistov</i>	42
---------------------------------------------------------------------------------------------------------------	----

Spin Resonance on Electrons of Zero Modes Stabilized at Atomically Smooth Graphene Edges <i>A. M. Ziatdinov</i>	44
-----------------------------------------------------------------------------------------------------------------------	----

SECTION 4 MAGNETIC RESONANCE INSTRUMENTATION

Plenary Lectures

- Multi-Extreme THz ESR: Present and Future
*H. Ohta, S. Okubo, E. Ohmichi, T. Sakurai, H. Takahashi,
S. Hara, Y. Saito* 47

- EPR/ODMR Instrument Complex and its Application for the Study
of Wide Band Gap Materials
*R. A. Babunts, A. N. Anisimov, A. S. Gurin, N. G. Romanov,
A. G. Badalyan, P. G. Baranov* 48

Oral Talk

- Accounting Material Imperfections in the Design of Halbach Magnets
A. Bogaychuk, V. Kuzmin 50

SECTION 5 ELECTRON SPIN-BASED METHODS FOR ELECTRONIC AND SPATIAL STRUCTURE DETERMINATION IN PHYSICS, CHEMISTRY AND BIOLOGY

Plenary Lecture

- Experimental Features of Enhanced Nuclear Magnetic Resonance
in Van Vleck Paramagnets
M. Tagirov 53

Invited Talk

- Enhancing Coordination-Based Copper(II) Spin Labelling for Accurate
Distances at Sub-Micromolar Concentrations
*J. L. Wort, K. Ackermann, A. Giannoulis, A. J. Stewart,
D. G. Norman, B. E. Bode* 55

Oral Talks

- NMR of ^3He in Contact with Nanoparticles
*E. M. Alakshin, G. A. Dolgorukov, A. V. Klochkov, E. I. Kondratyeva,
V. V. Kuzmin, K. R. Safiullin, A. A. Stanislavovas, M. S. Tagirov* 56

- Investigations of Substituted Calcium Phosphates for Biomedical
Applications Using Double Resonance EPR Techniques
*F. F. Murzakhanov, M. R. Gafurov, G. V. Mamin, S. B. Orlinskii,
M. A. Goldberg, S. M. Barinov, V. S. Komlev* 57

- On the Manifestation of the Le Chatelier-Braun Principle
in Photosystem I Complexes Embedded in Dry Trehalose Matrices
A. Sukhanov, M. Mamedov, A. Semenov, K. Salikhov 59

SECTION 6
MOLECULAR MAGNETS AND LIQUID CRYSTALS

Plenary Lecture

- EPR Study of Intrinsically Disordered Proteins in Cell
*E. G. Bagryanskaya, S. Ovchenko, O. A. Chinak,
O. A. Krumkacheva, S. A. Dobrynin, V. Tormyshev, I. A. Kirilyuk* 61

Invited Talks

- Tuning the Magnetic Properties of Co(II)-Based Single-Ion Magnets
by Magnetic Dilution
*S. L. Veber, J. Nehr Korn, I. V. Valuev, A. S. Bogomyakov,
A. M. Sheveleva, V. I. Ovcharenko, M. A. Kiskin, E. A. Suturina,
K. Holldack, A. Schnegg, M. V. Fedin* 62
- Cation Dynamics in Ionic Liquid Crystals
D. Majhi, J. Dai, B. B. Kharkov, A. V. Komolkin, S. V. Dvinskikh 64

SECTION 7
OTHER APPLICATIONS OF MAGNETIC RESONANCE

Invited Talks

- New Insights from the Study of Triplet States
A. Barbon 66
- Hydration, Self-Diffusion and Ionic Conductivity
of One Charge Cations in Nafion Membranes Studied by NMR
V. I. Volkov, A. V. Chernyak, O. I. Gnezdilov, V. D. Skirda 67

Oral Talks

- Spin Kinetics of Gaseous ^3He in Nematically Oriented Aerogels
at Low Temperatures
V. Kuzmin, K. Safullin, A. Stanislavovas, M. Tagirov 68
- Magnetoelastic Effect in CoNi Particles Caused by Thermal Resizing
of Crystal Substrate
*D. A. Bizyaev, A. A. Bukharaev, N. I. Nurgazizov, A. P. Chuklanov,
S. A. Migachev* 70
- Modern Fundamentals of the Development of Agricultural *Solanum
Tuberosum L.* Using Targeted Delivery of Manganese with Novel
Bionanocomposites Based on Polysaccharides
*S. S. Khutsishvili, A. I. Perfil'eva, O. A. Nozhkina, T. V. Ganenko,
N. I. Tikhonov, I. A. Graskova, T. I. Vakul'skaya* 72

SECTION 8
 PERSPECTIVES OF MAGNETIC RESONANCE IN SCIENCE AND
 SPIN TECHNOLOGY. SPIN-BASED INFORMATION PROCESSING.
 THEORY OF MAGNETIC RESONANCE

Oral Talks

- Magnon Bose Condensed State for Quantum Computing
Yu. Bunkov 75
- On Certain Algebraic Properties of the Sub-Block of Zero Field
 Hyperfine Hamiltonian with Penultimate Total Spin Projection
 for a Radical with an Arbitrary Set of Spin-1/2 Nuclei and Visualizing
 its Eigenvalues
D. V. Stass 76
- Energy Transfer in Spin-Polarized Photo-Excited Triplet States:
 Two-Site Model
Y. E. Kandrashkin 78
- Conduction Electron Spin Resonance Study of $\text{Bi}_{1.08}\text{Sn}_{0.02}\text{Sb}_{0.9}\text{Te}_2\text{S}$
 Topological Insulator
V. O. Sakhin, I. I. Gimazov, E. F. Kukovitskii, Yu. I. Talanov,
G. B. Teitel'baum 79
- EPR Study of Light-Induced Charges in Ternary Organic Photovoltaic
 Blend PCDTBT/PC60BM/ICBA
M. N. Uvarov, L. V. Kulik 80
- Theoretical Basis for Switching a Kramers Single Molecular Magnet
 by Circularly-Polarized Radiation
A. G. Maryasov, M. K. Bowman, M. V. Fedin, S. L. Veber 81

SECTION 9
 MEDICAL PHYSICS.
 MAGNETIC RESONANCE IMAGING

Oral Talks

- Application of EPR Spectroscopy to Determine the Content
 of Nitric Oxide in the Brain and Heart of Rats after Some Pathology
Kh. L. Gainutdinov, V. V. Andrianov, G. G. Yafarova,
T. K. Bogodvid, M. N. Paveliev, N. G. Shayakhmetov,
S. G. Pashkevich, V. A. Kulchitchky 83
- Using of Special MRI-0.4 T for the Selection of Sugar Beets
Ya. Fattakhov, A. Bayazitov, A. Fakhruddinov, R. Khabipov,
K. Salikhov, V. Shagalov, A. Kornienko, O. Stognienko 86
- Investigation of Functional Voice Diseases Using MRI and Spectral Voice
 Analysis Method
M. Fattakhova, V. Krasnozhon, R. Khabipov, Ya. Fattakhov 87

SECTION 10
DIAMOND-BASED QUANTUM SYSTEMS
FOR SENSING AND QUANTUM INFORMATION

Invited Talks

Color Centers in Diamond for Biological Sensing and Quantum Information <i>P. Hemmer</i>	89
Diamond Quantum Sensing of Cell Mechanics and Cell Dynamics <i>Q. Li</i>	90
Single Nuclear Spin Detection Using Electrical Spin State NV Readout <i>M. Nesladek</i>	91
Picoliter NMR Spectroscopy with Diamond NV Centers <i>V. Acosta</i>	92
Optically Hyperpolarized Nanodiamonds: Applications in Accelerated NMR and Sensing <i>A. Ajoy</i>	93
Coherent Control of the Single Photon Interaction with Atomic and Nuclear Ensembles of Quantum Emitters in Solids <i>Y. Shi, A. Akimov, P. Hemmer, A. A. Kalachev, F. G. Vagizov, Y. V. Radeonychev, O. Kocharovskaya</i>	94
Prospects of Tin Vacancy Centers in Diamond for Quantum Sensing and Information <i>C. Becher</i>	96
Quantum Photonics with hBN – from Fundamental Studies to Emerging Applications <i>I. Aharonovich</i>	97
Photonic Crystal Cavities for GeV SnV Diamond <i>A. Akimov</i>	98
Fiber-Optic Diamond-Based Biothermometry <i>A. Zheltikov</i>	100
Sensitive Magnetometry in Challenging Environments <i>Kai-Mei C. Fu, G. Z. Iwata, A. Wickenbrock, D. Budker</i>	101
Oral Talks	
Development of Upconversion YVO_4 $\text{Yb}^{3+}\text{Er}^{3+}$ Nanoparticles for Biological Applications <i>V. G. Nikiiforov, D. K. Zharkov, A. G. Shmelev, A. V. Leontyev, V. S. Lobkov, M. H. Alkahtani, P. R. Hemmer</i>	102

Biocompatibility Testing of Vanadate Oxide Based Upconversion Nanoparticles with Helix Lucorum Grape Snails <i>A. G. Shmelev, V. G. Nikiforov, D. K. Zharkov, V. V. Andrianov, L. N. Muranova, A. V. Leontyev, Kh. L. Gainutdinov, V. S. Lobkov, P. R. Hemmer</i>	104
Fluorescent Properties of Diamonds Doped with Germanium and Erbium <i>D. K. Zharkov, A. G. Shmelev, A. V. Leontyev, V. G. Nikiforov, R. I. Khaibullin, M. H. Alkahtani, P. R. Hemmer</i>	106
 POSTERS	
Section	
Chemical and Biological Systems	
Kinetics of Paramagnetic Centers Formation in the Calcium Gluconate Subjected to Mechanochemical Treatment <i>M. M. Akhmetov, G. G. Gumarov, V. Yu. Petukhov, G. N. Konygin, D. S. Rybin</i>	108
Quantification of Protein Aggregation using NMR Relaxation of Nuclei of Water and Ions: a Study of the RRM2 Domain of TDP-43 Protein <i>S. O. Rabdano, S. S. Bystrov, C. Cabal, V. I. Chizhik</i>	111
Identification of the Radiation-Induced Radicals in Calcium Gluconate <i>A. R. Gafarova, G. G. Gumarov, M. M. Bakirov, R. B. Zaripov, V. Yu. Petukhov</i>	112
The Content of Nitric Oxide and Copper in the Olfactory Bulbs of Rat's Brain after Modeling of Brain Stroke and Administration of Mesenchymal Stem Cells <i>Kh. L. Gainutdinov, V. V. Andrianov, G. G. Yafarova, S. G. Pashkevich, M. O. Dosina, A. S. Zamaro, Y. P. Tokalchik, T. Kh. Bogodvid, L. V. Bazan, A. A. Denisov, V. A. Kulchitchky</i>	114
Structural and Functional Properties of the Nanosized Al/V ₂ O ₅ Termites Obtained by Mechanochemical Activation <i>A. I. Kokorin, E. A. Konstantinova, A. N. Streletskii</i>	116
NMR and DLS Study of Intermolecular Interactions of the Blood Plasma Fibrinogen. The pH and Ionic Strength Effects on the Prelude of Fibrin Clotting <i>A. M. Kusova, A. E. Sitnitsky, Yu. F. Zuev</i>	118
Mechanism of Intrinsically Disordered Protein Penetration into Cells: Monitoring by EPR and Confocal Microscopy <i>S. Ovcherenko, O. Chinak, O. Krumkacheva, S. Dobrynin, I. Kirilyuk, E. Bagryanskaya</i>	119

DFT Calculations of EPR Parameters for Substituted Calcium Phosphates <i>D. Shurtakova, G. Mamin, M. Gafurov, S. Orlinskii, F. Murzakhanov, A. Fedotov, V. Komlev</i>	121
¹ H NMR Study of Blood Plasma of Rats with the Experimental Model of SCI <i>S. V. Yurtaeva, M. Yu. Volkov, G. G. Yafarova</i>	123
Photoinduced States of Some Compact Electron Donor/Acceptor Dyads <i>A. A. Sukhanov, V. K. Voronkova, J. Zhao</i>	124
Nitric Oxide in Restriction of Motor Activity, Including Spin Cord Injury <i>G. G. Yafarova, V. V. Andrianov, V. S. Iyudin, T. V. Baltina, A. A. Ereemeev, I. A. Lavrov, R. I. Zaripova, T. L. Zefirov, Kh. L. Gainutdinov</i>	125
Study of the Radiation-Induced at Room Temperature Stable Radicals in Octacalcium Phosphate Synthesized by Wet Method with XRD and EPR <i>B. Yavkin, D. Shurtakova, F. Murzakhanov, M. Gafurov, G. Mamin, S. Orlinskii, V. Smirnov, V. Sirotinkin, A. Fedotov, V. S. Komlev, A. Shinkarev</i>	127
Section	
Strongly Correlated Electron Systems	
NMR Study of the Ion Mobility in Frustrated Li _{1-x} CuSbO ₄ Compound <i>D. Gafurov, M.-I. Sturza, E. Vavilova</i>	128
ESR Investigation of Magnetic Properties and Vanadium Oxidation State in α-Li ₃ V ₂ (PO ₄) ₃ /C Composite <i>T. P. Gavrilova, S. M. Khantimerov, R. R. Fatykhov, I. V. Yatsyk, P. Balaya, N. M. Suleimanov</i>	129
Zn-Doped Frustrated S = 1/2 Spin Chains LiCu _(1-x) Zn _(x) SbO ₄ Studied by NMR <i>A. Kamalov, M.-I. Sturza, H.-J. Grafe, E. Vavilova</i>	131
Modification of the Properties of Barium Strontium Titanate Films on Silicon Substrate <i>D. P. Pavlov, R. I. Batalov, A. V. Leontyev, D. K. Zharkov, S. A. Migachev, I. V. Lunev, T. S. Shaposhnikova, R. F. Mamin</i>	132
The Delay Time of Phase Transition to the Polar Phase in Relaxors <i>T. S. Shaposhnikova, S. A. Migachev, R. F. Mamin</i>	134
Cluster Spin Glass State as a Result of Lithium Deficiency in the Honeycomb System Li ₃ Ni ₂ SbO ₆ <i>E. Vavilova, T. Salikhov, E. Zvereva, V. Nalbandyan</i>	135

Superparamagnetic Properties in $\text{La}_{0.83}\text{Sr}_{0.17}\text{Mn}_{0.9}\text{Zn}_{0.1-x}\text{Fe}_x\text{O}_3$ ($x = 0, 0.025, 0.075, 0.1$) <i>R. M. Eremina, I. V. Yatsyk, Z. Y. Seidov, A. Badelin</i>	136
Photostimulated Properties of Ferroics and Photoconductivity at the Interface of the $\text{Ba}_{0.8}\text{Sr}_{0.2}\text{TiO}_3/\text{LaMnO}_3$ <i>D. P. Pavlov, T. S. Shaposhnikova, A. V. Leontyev, D. K. Zharkov,</i> <i>T. M. Salikhov, R. F. Mamin</i>	137
Electron Spin Resonance Study of $\text{Sm}_{1-x}\text{Yb}_x\text{B}_6$ Solid Solutions <i>S. V. Demishev, M. I. Gilmanov, A. N. Samarin, A. V. Semeno,</i> <i>N. E. Sluchanko, N. Yu. Shitsevalova, V. B. Filipov, V. V. Glushkov</i>	139
Section	
Electron Spin-Based Methods for Electronic and Spatial Structure Determination in Physics, Chemistry and Biology	
Comparative Analysis of Electrosurface Properties of Mesoporous Alumina Grafted with Silanes Using EPR of pH-Sensitive Nitroxide Radicals <i>D. Tamasova, P. Lyubyakina, E. Kovaleva</i>	141
EPR Study of Yb^{3+} Impurity Ions in Mg_2SiO_4 Single Crystals <i>V. Tarasov, A. Sukhanov, R. Zaripov, K. Subbotin, E. Zharikov,</i> <i>V. Dudnikova</i>	143
Development of Fullerene-Based Spin Label for Nanometer Distance Measurements <i>I. Timofeey, E. Tretyakov, G. Fazleeva, P. Troshin,</i> <i>E. Bagryanskaya, M. Fedin, O. Krumkacheva</i>	144
Synthesis and ESR Study of Copper Doped CdSe and “Core-Shell” CdSe/CdS Quantum Dots <i>D. O. Sagdeev, R. R. Shamilov, V. K. Voronkova, A. A. Sukhanov,</i> <i>Yu. G. Galyametdinov</i>	145
Determination of the Energy Level Position of Radicals in the Band Gap of TiO_2 Based Microspheres Using EPR Spectroscopy <i>E. V. Kytina, E. R. Parkhomenko, E. A. Konstantinova</i>	147
Specific Features and Application Examples of a High-Frequency Electron Spin Resonance Spectrometer with Frequency Modulation <i>Yu. A. Uspenskaya, R. A. Babunts, E. V. Edinach, A. S. Gurin,</i> <i>H. R. Asatryan, D. O. Tolmachev, N. G. Romanov, A. G. Badalyan,</i> <i>P. G. Baranov</i>	149

Section

Medical Physics

- Connective Tissue Dysplasia: Computer Analysis
of Serum Fe³⁺-Transferrin ERR Spectra
*G. Gumarov, M. Ibragimova, A. Chushnikov, D. Khaibullina,
V. Petukhov, I. Yatsyk* 151
- Inter-Protein Molecular Interactions in Solutions of Human Serum
Albumin, Studied by NMR-Diffusometry and Dynamic Light Scattering
A. K. Iskhakova, A. M. Kusova, A. E. Sitnitsky, Yu. F. Zuev 154

Section

Theory of Magnetic Resonance

- Collective Modes in Solutions of Nitroxyl Radicals Detected
by CW EPR
M. M. Bakirov, K. M. Salikhov, I. T. Khairutdinov, B. Bales 155
- Spin-Echo Diffusion Attenuation and Spin Relaxation of a Particle
Moving in a Random Magnetic Field
R. Shagvaleev, N. Fatkullin 157

Section

Low-Dimensional Systems and Nano-Systems

- Abnormal Magnetism of Nano- and Microscaled Tetrafluorites
LiTbF₄ and LiDyF₄
*G. Yu. Andreev, A. G. Kiyamov, S. L. Korableva, A. A. Rodionov,
I. V. Romanova, A. S. Semakin, M. S. Tagirov* 158
- Spin-Polarized Current in Non-Collinear Magnetic Tunnel Junction
Ch. A. Fam, N. Kh. Useinov, A. P. Chuklanov, A. A. Bukharaev 159
- Epitaxial Growth and Ferromagnetic Resonance Study of Magnetic
Anisotropies in Thin Pd_{1-x}Fe_x Films on the Single-Crystal
MgO(110) Substrate
*B. F. Gabbasov, A. I. Gumarov, A. A. Rodionov, I. V. Yanilkin,
R. R. Khabibullin, R. V. Yusupov, L. R. Tagirov* 161
- Ultrafast Magnetization Dynamics in Thin Films of L10-Ordered
FePt and FePd Compounds
*A. V. Petrov, M. V. Pasyukov, R. V. Yusupov, S. I. Nikitin,
A. I. Gumarov, I. V. Yanilkin, A. G. Kiiamov, L. R. Tagirov* 162
- Femtosecond Optical and Magneto-Optical Studies of Magnetic and
Electronic Inhomogeneities in Pd_{1-x}Fe_x Thin Films
*A. V. Petrov, R. V. Yusupov, I. V. Yanilkin, A. I. Gumarov,
A. G. Kiiamov, S. I. Nikitin, L. R. Tagirov* 163
- Hidden Magnetic Order in Triangular-Lattice Magnet Li₂MnTeO₆
*G. V. Raganyan, T. M. Vasilchikova, V. B. Nalbandyan,
D. A. Gafurov, E. L. Vavilova, A. E. Susloparova, A. I. Kurbakov,
M.-H. Whangbo, E. A. Zvereva* 165

Magnetic Properties of $\text{La}_{1-x}\text{Sr}_x\text{Mn}_{0.9}\text{Fe}_{0.1-y}\text{Mg}_y\text{O}_3$ <i>R. M. Eremina, A. V. Shestakov, I. V. Yatsyk, D. V. Mamedov, A. G. Badelin, V. K. Karpasyuk</i>	166
EPR Study of Highly Branched Mesomorphic Iron(III) Complexes <i>V. Vorobyeva, U. Chervonova, M. Gruzdev, A. Kolker</i>	168
Epitaxial Growth, Structural and Magnetic Properties of $\text{Pd}_{0.95}\text{Fe}_{0.05}/\text{Pd}_{0.92}\text{Fe}_{0.08}$ Bilayers <i>A. I. Gumarov, I. V. Yanilkin, R. V. Yusupov, R. I. Khaibullin, M. N. Aliyev, L. R. Tagirov</i>	170
2D Triangular Lattice Magnet GdFeTeO_6 with Large Magnetocaloric Characteristics <i>T. Vasilchikova, V. Nalbandyan, M. Evstigneeva, E. Zvereva</i>	172
EPR in Conductive Polymer Composites with Carbon Nanotubes <i>A. M. Zyuzin, N. V. Yantsen, A. A. Karpeev, V. V. Naumkin</i>	173
High Temperature Ferromagnetism in Thin Films of $\text{Mn}_x\text{Si}_{1-x}$ ($x \approx 0.5$) Nonstoichiometric Alloys: Ferromagnetic Resonance Studies <i>A. B. Drovoskov, A. S. Barkalova, L. S. Parshina, O. A. Novodvorsky, O. D. Khramova, D. S. Gusev, E. A. Cherebilo, K. Yu. Chernoglazov, A. S. Vedenev, V. V. Rylkov</i>	174
Section	
Other Applications of Magnetic Resonance	
The Effect of Halloysite Nanotubes Surface Modification on its Acid-Base Properties <i>D. O. Antonov, D. P. Tambasova, D. D. Davydov, E. G. Kovaleva</i>	176
TR EPR Study of Spin-Orbit Charge Transfer Intersystem Crossing in Bodipy-Anthracene Compact Dyads <i>A. A. Sukhanov, Z. Mahmood, J. Zhao, V. K. Voronkova</i>	178
Capabilities of Nuclear-Magnetic Resonance Tools for Detailed Scanning of Fluid Properties in Core Samples and in Wells Under Drilling. <i>V. Murzakaev, N. Belousova, A. Bragin, D. Kistler, V. Skirda, A. Alexandrov</i>	179
Spin Properties of the Fe(III) Complexes with Tetradentate Schiff Bases and Photosensitive 4-Alkoxystryrylpyridine Axial Ligands <i>E. N. Frolova, L. V. Bazan, O. A. Turanova, M. Yu. Volkov, L. G. Gafiyatullin, I. V. Ovchinnikov, A. N. Turanov</i>	181
EPR Measurements of Guest Diffusion in Magneto-Concentrated Porous Metal Organic Frameworks (MOFs) <i>D. Polyukhov, A. Poryvaev, M. Fedin</i>	182

Section

Magnetic Resonance Imaging

Development of a Conform Sensor “Hand” for Receiving an NMR Signal in a Small-Size Traumatological MRI System with a Field of 0.4 T

A. A. Bayazitov, Ya. V. Fattakhov, A. R. Fakhrutdinov, V. A. Shagalov 183

The First Results of Using a Specialized MRI System with Magnetic Field of 0.4 T

Ya. Fattakhov, A. Anikin, A. Bayazitov, A. Fakhrutdinov, R. Khabipov, V. Odivanov, K. Salikhov, V. Shagalov, N. Reshetnikov, D. Abdulganieva, M. Mikhailov, S. Ryzhkin, V. Anisimov 184

Section

Related Phenomena

Photon Echo Oscillations in $\text{LuLiF}_4:\text{Er}^{3+}$ (0.025%) Depending on the Magnetic Field Perpendicular to the C Axis of the Sample

V. Lisin, A. Shegeda, V. Samartsev 185

Propagation Single-Photon Wave-Packet with Orbital Angular Momentum in a Turbulent Atmosphere

D. O. Akatiev, D. A. Turaikhanov, A. V. Shkalikov, I. Z. Latypov, A. A. Kalachev 187

Electric Polarization in Small Particles of Multiferroics

T. S. Shaposhnikova, R. F. Mamin 189

Effect of UV Laser Modification on Intramolecular Energy Transfer Processes in a Vitrified Film Based on a Europium(III) β -Diketonate Complex

D. V. Lapaev, V. G. Nikiforov, V. S. Lobkov, A. A. Knyazev, Yu. G. Galyametdinov 190

Section

Perspectives of Magnetic Resonance in Science and Spin Technology

Effect of Random Flips of Spins and Conformational Transitions in PELDOR Signal of Spin Labels with Overlapping EPR Spectra

I. T. Khairutdinov, K. M. Salikhov 191

NMR Study ^{169}Tm in Diluted Van Vleck Paramagnet $\text{LiTm}_{0.02}\text{Y}_{0.98}\text{F}_4$

A. S. Parfishina, A. V. Egorov, S. L. Korableva, I. V. Romanova, K. R. Safiullin, M. S. Tagirov 193

Jahn-Teller Centers of Cr^{2+} in a CdSe Crystal

G. S. Shakurov, V. V. Gudkov, I. V. Zhevstovskikh, M. N. Sarychev, Yu. V. Korostelin 194

Features of the ESR on the Mn^{2+} Impurities in the 3D Dirac Semimetal Cd_3As_2 <i>Yu. Goryunov, A. Nateprov</i>	195
Electron Spin Relaxation of Photoexcited Porphyrin in Water-Glycerol Glass <i>N. Sannikova, I. Timofeev, E. Bagryanskaya, M. Bowman, M. Fedin, O. Krumkacheva</i>	196
ESR of Dy^{3+} Ions at Cubic Sites in Cs_2NaYF_6 and $CsCaF_3$ Single Crystals <i>M. L. Falin, V. A. Latypov, S. L. Korableva, N. M. Khaidukov</i>	197
Section	
Diamond-Based Quantum Systems for Sensing and Quantum Information	
Specific Features of High-Frequency EPR/ESE/ODMR Spectroscopy of NV Defects in Diamond <i>R. A. Babunts, D. D. Kramushchenko, A. S. Gurin, A. P. Bundakova, M. V. Muzafarova, A. G. Badalyan, N. G. Romanov, P. G. Baranov</i>	199
Investigation of Vacancy Diffusion and NV Center Formation in the Annealed Electron Beam Irradiated Diamond <i>A. M. Gorbachev, S. A. Bogdanov, M. A. Lobaev, A. L. Vikharev, D. B. Radishev, V. A. Isaev, M. N. Drozdov, V. A. Gusev, D. A. Tatarsky</i>	201
The Study of SiV Centers Formation in Diamond During the Process of CVD Growth by Optical Emission Spectroscopy <i>S. A. Bogdanov, A. M. Gorbachev, A. L. Vikharev, D. B. Radishev, M. A. Lobaev</i>	202
Electroluminescence of Silicon Vacancy Centers in Diamond p-i-n Diode <i>M. A. Lobaev, D. B. Radishev, S. A. Bogdanov, A. L. Vikharev, A. M. Gorbachev, V. A. Isaev, S. A. Kraev, A. I. Okhapkin, E. A. Arhipova, M. N. Drozdov</i>	203
Bose Condensation and Spin Superfluidity of Magnons in YIG Film <i>P. M. Vetoshko, G. A. Knyazev, A. N. Kuzmichev, A. A. Kholin, V. I. Belotelov, Yu. M. Bunkov</i>	204
AUTHOR INDEX	205

PLENARY LECTURES

From High Power to Low Power – Recipes for a Successful Scientific Life!

K.-P. Dinse

Fachbereich Physik, FU Berlin, Germany

Magnetic Resonance is a multi-dimensional space in science, allowing people to explore it with a non-trivial individual trace. Most probably such a trace is correlated with technological developments, but this alone is not sufficient for success, because scientific guidance as well as access to financial funds is required. If personal interests and capabilities match by chance with an expanding field like EPR in the 60ties, one might be rewarded with the possibility contributing significantly to its development. I will give some examples in which by lucky circumstances I was led to interesting places in the field of EPR.

DNP Enhanced Solid-State NMR Spectroscopy of Functional Materials

G. Buntkowsky

Institute of Physical Chemistry, Technical University Darmstadt, Alarich-Weiss-Str. 8, D-64287,
Darmstadt, Germany, gerd.buntkowsky@chemie.tu-darmstadt.de

Recent results about standard and dynamic nuclear polarization (DNP) enhanced solid-state nuclear magnetic resonance (NMR) spectroscopy on nanostructured and functional materials are reported. The first example reports studies on materials based on crystalline nanocellulose (CNC) or microcrystalline cellulose (MCC), which are used as support material for functionalization or in combination with heterocyclic molecules as ion conducting membranes. The second example reports studies on mixed metal oxides such as V-Mo-W oxides, which are employed as heterogeneous catalyst in bulk-scale production of basic chemicals. The third example reports confined systems with functionalized surfaces and different guest molecules. These materials are discussed in terms of their application and physico-chemical characterization by solid-state NMR techniques, combined with gas-phase NMR and quantum-chemical modelling on the density functional theory (DFT) level. Moreover, the analytic power of the combination of these techniques with DNP for the identification of low-concentrated carbon and nitrogen containing surface species in natural abundance is discussed.

New Paradigm of Spin Exchange

K. M. Salikhov

Zavoisky Physical-Technical Institute, FRC Kazan Scientific Center of RAS, Kazan 420029,
Russian Federation

The lecture is devoted to a new paradigm of the bimolecular spin exchange process and its manifestations in electron paramagnetic resonance (ESR) spectroscopy. This is a bimolecular process of changing the state of electron spins of paramagnetic particles caused by their exchange interaction during collisions.

The study of spin exchange in solutions using EPR spectroscopy has become an important method for determining the frequency of bimolecular collisions of particles, including in complex media such as polymer solutions, porous structures, and biological objects.

Several issues can be identified in this issue:

- Theoretical analysis of the elementary act of changing the spin state of a colliding pair of particles.
- Measurement of the contribution of electron-electron interaction to the dynamics of electron spins of paramagnetic particles.
- Separation of the exchange and dipole-dipole interaction contributions, since the desired frequency of bimolecular particle collisions is directly characterized only by the contribution of the exchange interaction to the molecular-kinetic parameters of electron spins.

In all these aspects, the new paradigm of spin exchange formulates fundamental changes in comparison with the widespread and applied paradigm.

The “return” of quantum spin coherence plays a fundamental role. Thanks to this “return”, collective modes of motion of the coherence of the spins of the entire system are formed. Each collective mode gives an asymmetric resonant line in the EPR spectrum: the sum of a symmetric (even) absorption line and a non-symmetric (odd) dispersion line.

The lines of collective resonances widen with the growth of spin exchange frequencies. Their frequency also depends on the spin exchange. This effect of exchange narrowing of the spectrum is due to the fact that in conditions of sufficiently rapid spin exchange, the external microwave field effectively excites only one of the collective modes of spin motion. The remaining collective modes, with other resonant frequencies, become “forbidden” lines in the spectrum.

The new paradigm of spin exchange also offers a new algorithm for determining the speed of spin exchange from the analysis of the shape of EPR spectra, which ultimately improves the accuracy of determining the frequency of bimolecular collisions.

1. Salikhov K.M.: *Physics-Uspekhi* **189**, no. 10, 1017–1043 (2019)
2. Salikhov K.M.: *Fundamentals of spin exchange. Story of paradigm shift.* Springer Verlag (2019)
3. Salikhov K.M.: *J. Phys. Chem. B* **124**, no. 30, 6628–6641 (2020)

Interplay of Magnetism and Topological Electronic Structure of Magnetic Van Der Waals Compounds

V. Kataev

Leibniz Institute for Solid State and Materials Research IFW Dresden,
01069 Dresden, Germany

Layered van der Waals magnetic compounds attract currently large attention as they may display an intrinsically low-dimensional magnetic behavior and as such offer an extensive materials base for exploring fundamental magnetic properties of strongly correlated two-dimensional (2D) electron systems. Here, the results of a detailed electron spin resonance (ESR) spectroscopic study of two representatives of this family will be discussed:

1) $\text{Cr}_2\text{Ge}_2\text{Te}_6$ is a quasi-2D magnet showing intriguing intrinsic ferromagnetism down to atomically thin films [1]. We could obtain new detailed insights into the magnetocrystalline anisotropy of this compound which should be responsible for the stabilization of magnetic order in the 2D limit and find evidence for an intrinsically 2D character of the dynamics of Cr spins even in bulk single crystals [2]. These results are supported by calculations of the electronic structure revealing that the low-lying conduction band carries almost completely spin-polarized, quasi-homogeneous, two-dimensional states [2].

2) MnBi_2Te_4 [3, 4] is the first antiferromagnetic topological insulator featuring Dirac cones in the electronic structure due to the topological surface states [5,6]. In this material we observe a surprisingly anisotropic spin dynamics of bulk conduction electrons and Mn localized states which, as we argue, could be responsible for the persistence of the band gap in the topological surface state even above the magnetic ordering temperature [5].

1. Gong C. *et al.*: Nature **546**, 265 (2017)
2. Zeisner J. *et al.*: Phys. Rev. B **99**, 165109 (2019)
3. Zeugner A. *et al.*: Chem. Mater. **31**, 2795 (2019)
4. Vidal R.C. *et al.*: arXiv: 1903.11826 (2019)
5. Otrokov M. *et al.*: Nature **576**, 416 (2019)
6. Lee S.H. *et al.*: Phys. Rev. Research **1**, 012011(R) (2019)

SECTION 1

CHEMICAL AND BIOLOGICAL SYSTEMS

INVITED TALKS

Molecular Mobility in a Set of Imidazolium-Based Ionic Liquids [bmim]⁺A⁻ and Their Mixtures with Water**V. I. Chizhik¹, S. S. Bystrov¹, V. V. Matveev¹, A. V. Egorov¹,
V. Balevičius²**¹ Saint-Petersburg State University, Saint-Petersburg, Russian Federation, v.chizhik@spbu.ru² Vilnius University, Vilnius, Lithuania

Room temperature ionic liquids (ILs) are ionic compounds that are composed of asymmetric organic cations and nearly any type of anions. In contrast to typical salts these substances remain in liquid phase at the room temperature or at temperatures close to it. Unique physical and chemical properties of ionic liquids (neat and in solutions) such as high thermal stability, low vapor pressure, high boiling point, and the ability to dissolve a wide range of chemical species, determine numerous applications in “green” chemistry and material science.

The detailed investigation of the local mobility in a set of dried imidazolium-based ionic liquids (1-butyl-3-methylimidazolium) in a wide temperature range and varying anions (BF₄⁻, I⁻, Cl⁻, Br⁻, NO₃⁻, TfO⁻) is presented. The measurements of temperature dependencies of the spin-lattice relaxation times of ¹H and ¹³C nuclei are motivated by the need to obtain a fundamental characterization of molecular mobility of the substances under study, namely, to estimate the correlation times for the motion of individual molecular groups. The effect of the influence of an anion type on the cation mobility is also analyzed.

In the past few years, the hypothesis about the existence of so-called “water pockets” in mixtures of water with a number of ionic liquids has been discussed in the literature. The concept of “water pockets” was introduced by Japanese researchers [1]. They believed that in the region of water concentrations of 75÷90 mol%, water molecules were grouped (formed “water pockets”), and in these structures water existed in a special state, which was characterized by a slow hydrogen exchange. In the report we give a critical review of existing models of the microstructure of mixtures “IL–water” and the justification of a new hypothesis about the structure of systems such as “[bmim]A–H₂O”. In addition, we carried out measurements of the self-diffusion coefficients of various components of mixtures at different temperatures and computer simulations of molecular dynamics.

The work was funded by RFBR, project 17-03-00057a.

On the Nature of Radicals in Titania Photocatalysts: New Approach Based on EPR Spectroscopy

E. A. Konstantinova^{1,2}, E. V. Kytina¹, G. V. Trusov³, A. I. Kokorin⁴

¹ Department of Physics, M. V. Lomonosov Moscow State University, Russian Federation

² National Research Center Kurchatov Institute, Moscow, Russian Federation, liza35@mail.ru

³ National University of Science and Technology "MISIS", Moscow 119049, Russian Federation

⁴ N. Semenov Institute of Chemical Physics RAS, Moscow, Russian Federation

Titania and titania based nanomaterials have attracted the attention of researchers for many decades [1, 2]. Their structural, electrophysical and photoelectronic properties are being actively studied [2, 3]. Such interest is due to their unique properties, first of all, availability of a huge specific surface area – several hundred of square meters per gram. The presence of such specific surface opens up new prospects for investigation of features of adsorption processes, properties of defects (radicals) on the surface of nanocrystals and mechanisms of their interaction with environmental molecules [1–3]. In this work we offer new insight into investigation of photocatalytic processes using EPR spectroscopy. Our original approach is to implement the photocatalytic process directly in the cavity of EPR spectrometer. Thus, we carry out “in situ” monitoring of radicals participating in redox reactions on the surface of the samples under investigation.

We have studied nitrogen doped TiO₂ nanocrystals, TiO₂ based nanoheterostructures (TiO₂/MoO₃, TiO₂/WO₃, TiO₂/V₂O₅, TiO₂/MoO₃/V₂O₅) and microspheres (TiO₂/MoO₃, TiO₂/WO₃, TiO₂/V₂O₅, TiO₂/MoO₃/V₂O₅, TiO₂/WO₃/V₂O₅, TiO₂/MoO₃/WO₃, TiO₂/MoO₃/V₂O₅/WO₃) using our new approach. We have studied initial samples and ones with test dye. Dye Rhodamine 6G in an amount of $4 \cdot 10^{-8}$ mol/cm² was applied to the surface of the TiO₂ based photocatalyst from an aqueous solution. All EPR experiments were made both in dark and under illumination. The dynamics of radicals was studied under visible illumination both in the initial samples and in the photocatalysts with Rhodamine 6G. N[•], Ti³⁺, Mo⁵⁺, V⁴⁺, O⁻, O₂⁻ paramagnetic centers were found in the initial samples in dark. The concentration of N[•], Ti³⁺, Mo⁵⁺, V⁴⁺ centers increases under illumination which can be explained by the capture of photoexcited charge carriers by initially non-paramagnetic centers. It was revealed that the concentration of O⁻, O₂⁻ radicals decreases under illumination in the samples with Rhodamine 6G. This result indicates their consumption in the process of redox reactions on the surface of the samples. After the illumination is switched off, the concentration of revealed paramagnetic centers returned to its original state for a very long time (approximately within 50 hours). Therefore we have detected the effect of separation and accumulation of photoexcited electrons and holes in TiO₂ based nanoheterostructures.

The obtained results can be useful for understanding the mechanism of photocatalytic reactions and contribute to the development of energy-efficient heterostructure photocatalysts.

The reported study was funded by RFBR according to the research project № 18-29-23051.

1. Fujishima A., Hashimoto K., Watanabe T.: *TiO₂ Photocatalysis. Fundamentals and Applications*. Tokyo: BKC Inc. 1999.
2. Sviridova T.V., Sadovskaya L.Yu., Konstantinova E.A., Belyasova N.A., Kokorin A.I., Sviridov D.V.: *Cat. Lett.* **149**, 1147 (2019)
3. Polliotto V., Livraghi S., Giamello E.: *Res. Chem. Intermed.* **44**, 3905 (2018)

Application of EPR to Porphyrin-Protein Agents for Photodynamic Therapy

**O. A. Krumkacheva¹, N. E. Sannikova¹, I. O. Timofeev¹, A. S. Chubarov²,
N. Sh. Lebedeva³, A. S. Semeikin⁴, I. A. Kirilyuk⁵, Y. P. Tsentalovich¹,
M. V. Fedin¹, E. G. Bagryanskaya⁵**

¹International Tomography Center SB RAS, Russian Federation, olesya@tomo.nsc.ru

²Institute of Chemical Biology and Fundamental Medicine SB RAS, Russian Federation

³G. A. Krestov Institute of Solution Chemistry RAS, Russian Federation

⁴Ivanovo State University of Chemistry and Technology, Russian Federation

⁵N. N. Vorozhtsov Institute of Organic Chemistry SB RAS, Russian Federation

Recently, a new type of spin labels based on photoexcited triplet molecules was proposed for nanometer scale distance measurements by pulsed dipolar electron paramagnetic resonance (PD EPR). However, such molecules are also actively used within biological complexes as photosensitizers for photodynamic therapy (PDT) of cancer. Up to date, the idea of using the photoexcited triplets simultaneously as PDT agents and as spin labels for PD EPR has never been employed. In this work [1], we demonstrate that PD EPR in conjunction with other methods provides valuable information on the structure and function of PDT candidate complexes, exemplified here with porphyrins bound to human serum albumin (HSA). Two distinct porphyrins with different properties were used: amphiphilic mesotetrakis(4-hydroxyphenyl)porphyrin (mTHPP) and water soluble cationic meso-tetra(N-methyl-4-pyridyl)porphyrin (TMPyP4); HSA was singly nitroxide-labeled to provide a second tag for PD EPR measurements. We found that TMPyP4 locates in a cavity at the center of the four-helix bundle of HSA subdomain IB, close to the interface with solvent, thus being readily accessible to oxygen. As a result, the photolysis of the complex leads to photo-oxidation of HSA by generated singlet oxygen and causes structural perturbation of the protein. Contrary, in case of mTHPP porphyrin, the binding occurs at the proton-rich pocket of HSA subdomain IIIA, where the access of oxygen to a photosensitizer is hindered. Structural data of PD EPR were supported by other EPR techniques, laser flash photolysis and protein photocleavage studies. Therefore, pulsed EPR on complexes of proteins with photoexcited triplets is a promising approach for gaining structural and functional insights into such PDT agents.

This work was supported by Russian Science Foundation (no. 20-73-10239).

1. Sannikova N.E., Timofeev I.O., Chubarov A.S., Lebedeva N.Sh., Semeikin A.S., Kirilyuk I.A., Tsentalovich Yu.P., Fedin M.V., Bagryanskaya E.G., Krumkacheva O.A.: Application of EPR to Porphyrin-Protein Agents for Photodynamic Therapy, *Journal of Photochemistry & Photobiology, B: Biology* 2020.

Application of Time-Resolved EPR in Study of Charge-Recombination Induced Intersystem Crossing in Compact Electron Donor/Acceptor Dyads

X. Zhang, Y. Dong, Y. Yan, J. Zhao

State Key Laboratory of Fine Chemicals, School of Chemical Engineering,
Dalian University of Technology, Dalian 116024, P.R. China, zhaojzh@dlut.edu.cn (J. Z.)

Compact electron donor/acceptor dyads with orthogonal geometry of the electron donor and acceptor have been used as novel heavy atom-free triplet photosensitizers [1]. The intersystem crossing (ISC) of these orthogonal dyads is due to the spin orbit charge transfer ISC (SOCT-ISC). The photophysical processes involved in these dyads include photo-induced charge separation, and charge recombination to either the ground state or the localized triplet state. The ISC mechanisms involved in these dyads may include spin-orbit ISC (SO-ISC), SOCT-ISC, or radical pair ISC (RP-ISC). However, the detail study of these processes is rare. Recently we used time-resolved EPR (TREPR) spectroscopy to study series such dyads [2–4]. We observed upper 3LE (localized excited) state as well as 3CT states, which are rare for electron donor/acceptor dyads. Normally spin-correlated radical pair (SC RP) was observed, not the 3CT state. We also found that the electron spin polarization (ESP) patten of the triplet state formed via SOCT-ISC may be similar to that of SO-ISC, which is different from what concluded in literatures.

1. Hou Y., Zhang X., Zhao J., Barbon A. *et al.*: J. Mater. Chem. C 7, 12048 (2019)
2. Wang Z., Sukhanov A.A., Toffoletti A., Zhao J., Barbon A., Voronkova V.K., Dick B.: J. Phys. Chem. C 123, 265 (2019)
3. Imran M., Sukhanov A.A., Wang Z., Zhao J., Voronkova V.K., Hayvali M., Weber S. *et al.*: J. Phys. Chem. C. 123, 7010 (2019)
4. Dong Y., Sukhanov A.A., Zhao J., Dick B., Karatay A., Voronkova V.K.: J. Phys. Chem. C 123, 22793 (2019)

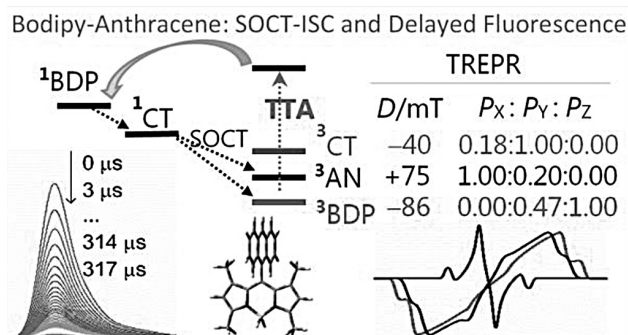


Fig. 1. TRERP spectra of the orthogonal anthryl-Bodipy electron donor/acceptor dyads.

ORAL TALKS

Investigation of Pathological Calcification and Synthetic Calcium Phosphates by Magnetic Resonance Techniques

**M. Gafurov¹, G. Mamin¹, S. Orlinskii¹, P. Grishin², I. Ignatyev^{2,3},
M. Goldberg⁴, N. Petrakova⁴, A. Fedotov⁴, V. S. Komlev⁴**

¹ Kazan Federal University, Kazan 420008, Russian Federation, marat.gafurov@kpfu.ru

² Kazan State Medical University, Kazan 420012, Russian Federation

³ Interregional Clinic and Diagnostic Centre, Kazan 420111, Russian Federation

⁴ A. A. Baikov Institute of Metallurgy and Materials Science Russian Academy of Sciences, Moscow 119334, Russian Federation

The majority of strokes in patients with moderate and severe carotid artery stenoses are due to thromboembolism caused by unstable atherosclerotic plaques (ASP) characterized by the cap rupture, large lipid core, intraplaque hemorrhage, cap/plaque inflammation and neovascularization. ASP formation, calcification and reliable factors/markers of their stability are a matter of controversy demanding various tools for their investigation.

92 patients (56 y.o.) and their tissues obtained after carotid endarterectomy operations were investigated histologically, with ultrasound duplex scanning and ultrasound elastography (LOGIQ E9, Aplio XG), scanning electron microscopy (SEM, Merlin), electron dispersive spectrometer (EDS, AZtec), X-ray diffraction (XRD, D8 Advance), thermogravimetry/scanning calorimetry (TG/DSC/MS STA-449Jupiter), pulsed electron paramagnetic resonance at X- and W-bands (EPR, Bruker E680). The results are compared with the data obtained on synthesized calcium phosphates (CaP) - hydroxyapatite (HA), dicalcium phosphate dihydrate (DCPD), tricalcium phosphate (TCP) and octacalcium phosphate (OCP) doped by various divalent cations in amount 0–20 mol.%.

Presence of only HA in the calcified ($\text{Ca/P} > 1.0$) was found. No traces of Cu^{2+} or Fe^{3+} ions but Mn^{2+} and carbonate radicals were detected by EPR. Their EPR spectral and relaxation characteristics depend on the calcification degree, location (cap, shoulders or core) and ASP stability. Correlations ($p < 0.05$) between the CO_2^- concentration and calcification, relaxation characteristics of Mn^{2+} and ASP stability was proved [1, 2].

The work is supported by Russian Foundation for Basic Research (grant # 18-29-11086).

1. Gabbasov B. *et al.*: J. Magn. Magn. Mater **470**, 109 (2019)

2. Chelyshev Yu. *et al.*: Biomed. Res. Int. **2016**, 3706280 (2016)

A Test of the Poisson-Boltzmann Double Layer Theory on Mesoporous Silicas by EPR of pH-Sensitive Nitroxides

**E. G. Kovaleva¹, A. Marek², A. I. Smirnov², D. O. Antonov¹,
D. P. Tamasova¹**

¹ Ural Federal University, Mira str., 19, Yekaterinburg 620002, Russian Federation
e.g.kovaleva@urfu.ru

² Department of Chemistry, North Carolina State University, 2620 Yarbrough Drive, Raleigh,
North Carolina, 27695-8204, USA

Chemical and physical processes occurring within the nanochannels of mesoporous materials are known to be determined by both chemical nature of the solution inside the pores/channels as well as the channel surface properties, including surface electrostatic potential. Such properties are important for numerous practical applications such as heterogeneous catalysis and chemical adsorption including chromatography. However, for solute molecules diffusing inside the pores the surface potential is expected to be effectively screened by counter ions for the distances exceeding the Debye length. Here we employed EPR spectroscopy of ionizable nitroxide spin probes to experimentally examine

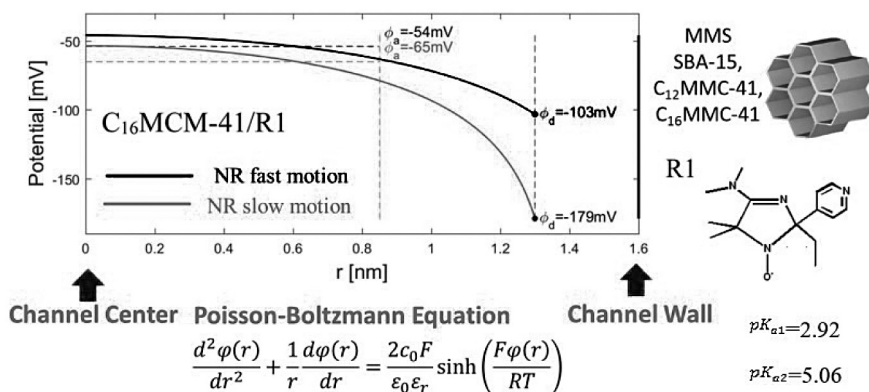


Fig. 1. Radial profiles of electrostatic potential $\varphi(r)$ obtained from numerical solutions of the Poisson-Boltzmann equation using different boundary conditions. Vertical lines denote integration limits inside the channel: solid black corresponds to the channel wall, dashed black – to the distance of the immobilized probe to the wall, $d = 0.3$ nm, and dashed grey delimits the mobile probe region (up to the radius of nitroxide probes, $l = 0.45$ nm, away from the immobilized distance). For example, for channel/probe combination for C16MCM-41/R1, two sets of profiles were calculated. The first (black curves) is calculated using the experimental boundary condition given by $\varphi_a = \langle \varphi(r) \rangle$ an average potential over the mobile probe region (i.e., from the channel center to the distance indicated by vertical grey dashed lines). The second set (grey curves) is calculated using the experimental boundary condition, φ_d , the electrostatic potential measured by an immobilized NR at a distance d from the channel wall. The corresponding numerical values are indicated in the graph. Averaging of the electrostatic potential over the pore region accessible to the mobile NR probe has been carried out assuming a homogeneous distribution inside the pore and the corresponding values are indicated by horizontal black and grey dashed lines.

the conditions for the efficient electrostatic surface potential screening inside the nanochannels of chemically similar silica-based mesoporous molecular sieves (MMS) filled with water at ambient conditions and a moderate ionic strength of 0.1 M. Three silica MMS having average channel diameters of $D = 2.3, 3.2$ and 8.1 nm (C12MCM-41, C16MCM-14, and SBA-15, respectively) were chosen to investigate effects of the pore diameter at the nanoscale. EPR titration of the aqueous phase confined in MMS channels with water-soluble ionizable nitroxides (NR) which pH-sensitive in the range of 2 and 7.5 pH provide the means to determine an average effective local pH_{loc} experienced by such molecules confined but diffusing in aqueous volume inside the nanopores of the mesoporous molecular sieves.

The results are compared with the classical Poisson–Boltzmann (PB) double layer theory developed for diluted electrolytes and applied to a cylindrical capillary of infinite extent. While the surface electrostatic potential was effectively screened by the counter ions inside the largest channels of 8.1 nm in diameter (SBA-15) the effect of the surface electrostatic potential on local effective pH was significant for the 3.2 nm channels (C16MCM-14). The smaller pores of C12MCM-41 (2.3 nm in diameter) provided the most critical test for the PB equation that is based on a continuum electrostatic model and demonstrated its inapplicability likely due to discrete nature of molecular systems at the nanoscale and nanoconfinement effects leading to larger spatial heterogeneity (Fig. 1) [1].

We acknowledge the financial support of the Foundation for Basic Research grants 18-29-12129 mk.

1. Kovaleva E.G., Molochnikov L.S., Antonov D.O., Tambasova D.P. (Stepanova), Hartmann M., Tsmokalyuk A.N., Marek A., Smirnov A.I.: *J. Phys. Chem. C* **122**(35), 20527–20538 (2018)

Stable Novel Biradicals for Dynamic Nuclear Polarization

**N. Asanbaeva^{1,2}, D. Morozov¹, S. Dobrynin¹, V. Tormyshev¹, I. Kirilyuk¹,
E. Bagryanskaya¹**

¹ Novosibirsk Institute of Organic Chemistry SB RAS, Novosibirsk 630090, Russian Federation, m_falcon@nioch.nsc.ru; s.a.dobrynin@gmail.com; torm@nioch.nsc.ru; kirilyuk@nioch.nsc.ru; egbagryanskaya@nioch.nsc.ru

² Physics Department, Novosibirsk State University, Novosibirsk 630090, Russian Federation, nasanbaeva@nioch.nsc.ru

Nitroxide biradicals are common polarizing agents used to increase the sensitivity of solid state NMR experiments using dynamic nuclear polarization. But their low resistance to reduction by low-molecular-weight antioxidants limits their use in the study of biological systems. It is supposed that the combination of trityl and nitroxyl will overcome this problem. According to previous studies, the optimum CE DNP enhancement was observed due to the relatively strong exchange interaction between the trityl and nitroxide moieties in such biradicals

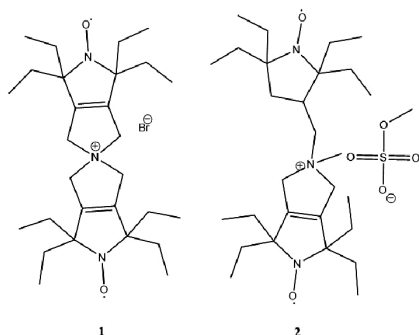


Fig. 1. Chemical structures of the nitroxide biradicals.

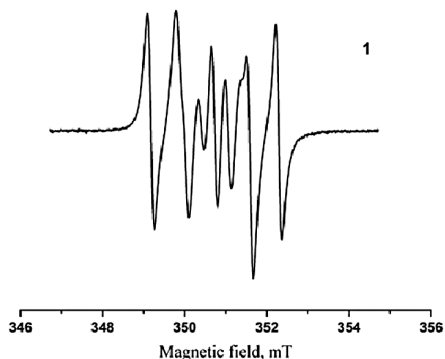


Fig. 2. EPR spectrum of 0.1 mM solution of biradical 1.

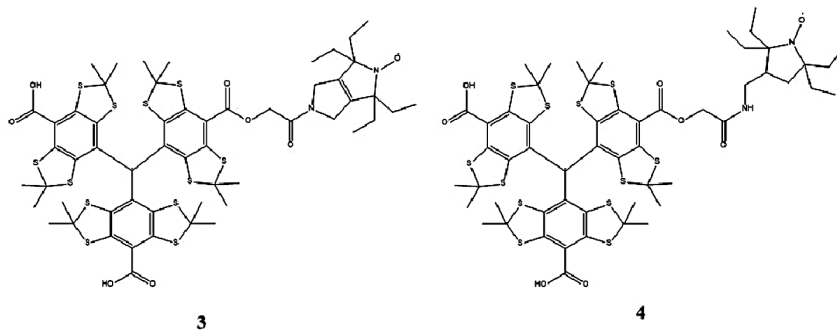


Fig. 3. Chemical structures of the trityl-nitroxyl biradicals.

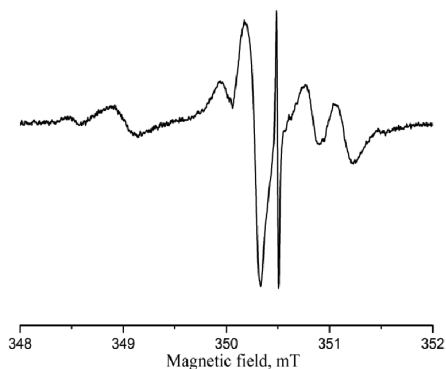


Fig. 4. EPR spectrum of 0.1 mM solution of biradical 3.

[1]. For further promote the promising effort of developing effective polarization sources the novel stable biradicals (Fig. 1 and Fig. 3) were synthesized in NIOCH SB RAS.

The EPR spectra (Fig. 2 and Fig. 4) in aqueous and water–methanol solutions at 295 K at concentrations of 0.1 mM were recorded by means of a commercial Bruker X Band (9 GHz) spectrometer, Elexsys E 540 (Bruker Corporation, Billerica, MA, USA). Simulations of the solution ESR lines were carried out in the EasySpin software [2]. The g -values, hfc and J were determined.

Kinetics of new nitroxyl-nitroxyl and trityl-nitroxyl biradicals at concentrations 0.3 mM were measured in presence of 0.01–0.1 M ascorbate and 2 mM glutathione. The rate constants of the biradicals were obtained by fitting to a monoexponential function. The influence of the structural composition of biradicals on their stability and the magnitude of the spin-spin exchange interaction was analyzed.

The work was supported by the Ministry of Science and Higher Education of Russia (project number 14.W03.31.0034).

1. Mathies G. *et al.*: *Angew. Chem., Int. Ed.* **54**, 11770–11774 (2015)
2. Stoll S., Schweiger A.: *J. Magn. Reson.* **178**, 42–55 (2006)

Isotope Substitution in EPR Studies of Nitroxide Biradicals

**R. B. Zaripov¹, I. T. Khairutdinov¹, T. Kálai^{2,3}, K. Kish²,
A. I. Kokorin^{4,5}, K. M. Salikhov¹**

¹ Zavoisky Physical-Technical Institute, FRC Kazan Scientific Center of RAS, Kazan 420029, Russian Federation

² Institute of Organic and Medicinal Chemistry, University of Pécs, H-7624 Pécs, Hungary

³ Szentágotthai Research Center, H-7624 Pécs, Hungary

⁴ N. N. Semenov Federal Research Center for Chemical Physics, Russian Academy of Sciences, Moscow, Russian Federation

⁵ Plekhanov Russian University of Economics, Moscow, Russian Federation

New nitroxide biradicals $^{15}\text{NR}_6\text{-C}\equiv\text{C-(p-C}_6\text{H}_4)_2\text{-C}\equiv\text{C-}^{14}\text{NR}_6$ (**B3**) and $^{15}\text{NR}_6\text{-C}\equiv\text{C-(p-C}_6\text{H}_4)_2\text{-C}\equiv\text{C-}^{15}\text{NR}_6$ (**B2**), where R_6 denotes 1-oxy-2,2,6,6-tetramethyl-1,2,3,6-tetrahydropyridine ring, are synthesized and studied in liquid solutions by continuous-wave electron paramagnetic resonance (EPR) spectroscopy. Hyperfine splitting constants and exchange integrals are determined from the simulation and fitting of experimental spectra and calculated ones.

The best fitting of the EPR spectra detected in experiments and their temperature dependence was achieved under the assumption that the biradicals perform transitions between conformations with different exchange integrals. The conformation of about 75% of biradicals has the exchange integral $|J| = 4.4$ G. About 20% of biradicals have the conformation with the zero exchange integral. It is shown that the isotope substitution provides a valuable resource in the EPR studies of the exchange interaction in biradicals.

At the Fig. 1 simulation of the experimental spectra for three biradicals **B1** (contain only ^{14}N isotopes) [1], **B2** and **B3** are shown. The best fitting was achieved with a simulation model according to which a biradical can be in two conformations ($|J| = 4.4$ G and $J = 0$).

Authors T. Kálai and K. Kish (Pécs University) gratefully acknowledge the support of the grant GINOP-2.3.2-15-2016-00049.

1. Kokorin A.I., Gromov O.I., Kálai T., Hideg K.: Appl. Magn. Reson. **47**, 1283 (2016)

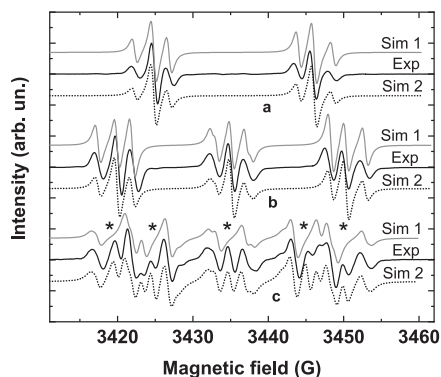


Fig. 1. Experimental (Exp) and simulated (Sim) EPR spectra of biradicals B1 (b), B2 (c) and B3 (a). Grey curves show spectra calculated at the assumption that all biradicals exist in only one conformation (Sim1). Dotted curves present the case of two conformations (Sim2).

SECTION 2

STRONGLY CORRELATED ELECTRON SYSTEMS

PLENARY LECTURES

New Concept of Magnetism of Topological Kondo Insulator SmB_6 on the Basis of Electron Spin Resonance Experiments

S. V. Demishev

Prokhorov General Physics Institute of RAS, Moscow 119991, Russian Federation,
demis@lt.gpi.ru

We suggest a new spin-polaron concept for describing the low-temperature magnetic properties of the surface of the topological Kondo insulator SmB_6 based on the study of dynamic (electron spin resonance, ESR) and static magnetic properties. It is experimentally established that (1) the paramagnetic centers responsible for the static and ESR magnetic response arise in a threshold manner at temperatures below $T^* \sim 5$ K [1, 2]. (2) These centers have an anomalously large value of the localized magnetic moment (LMM) $\mu^* \sim (7-14)\mu_B$, determined from the field dependences of the magnetization [2]. (3) The ESR data suggest that paramagnetic centers are characterized by a spin relaxation time $\tau \sim 10^{-8}$ s, which is no less than 5 orders of magnitude bigger than the time of charge and spin fluctuations of the Sm ion in a uniform mixed valence state [3].

To explain the experimental facts, a model has been proposed that relates the indicated features of magnetic properties to the formation of a spin polaron with antiferromagnetic interaction between elementary magnetic moments [3, 4]. Such spin polarons can be considered as ferrimagnetic clusters containing n_1 electrons with magnetic moment μ_1 and n_2 localized magnetic moments (LMM) with magnetic moment μ_2 . The number of LMMs and electrons in a cluster is determined by the condition of thermodynamic stability $\mu_1^2 n_1 = \mu_2^2 n_2$ [4]. The field dependence of the magnetization of such spin structure behaves similarly to a paramagnetic center with an enhanced (with respect to μ_1 and μ_2) the effective magnetic moment μ^* . The dynamic properties of a spin cluster (spin polaron) correspond to the rotation of the magnetization at the same frequency with the g factor $g \sim 2$ [4]. The paramagnetic response of the spin cluster ($\mu^* > 0$) is possible only when the moment of the sublattice with the biggest elementary magnetic moment is directed opposite to the direction of the external magnetic field. Additionally, this sublattice contains fewer particles, due to the mentioned conditions of thermodynamic stability. Within the framework of this model, we calculated the μ^* for different numbers of electrons and LMM and various alignments of the sublattices magnetization in the spin cluster under the assumption that $\mu_1 = \mu_B$. The requirement for the formation of a paramagnetic response of

the cluster ($\mu^* > 0$) leads to the conditions $n_1 = n_e$ and $n_1 = n\text{Sm}^{3+}$, whereas maximization of the effective moment gives $n_e = n\text{Sm}^{3+} + 1$. Here n_e and $n\text{Sm}^{3+}$, mean the number of electrons and the number of Sm^{3+} ions in the spin-polaron state respectively. Realistic μ^* values corresponding to experimental data [2] may be obtained for the number of Sm^{3+} ions in an isolated unit cell, i.e. for the spin clusters of nano size. Estimates considered make it possible to qualitatively explain the low-temperature magnetic transition in SmB_6 , which is characterized by the appearance of a large effective moment μ^* and anomalous spin relaxation time. In this ansatz, the spin cluster (spin polaron) can be composed of Kondo singlets that bind one additional electron. These spin states can persist on the surface of the sample in the form of a rare exception, while most of the Kondo singlets decay [3]. In the regime of homogeneous mixed valence, this situation can arise as a result of “frozen” fluctuation, leading to formation of considered spin states at sufficiently low temperatures. Thus, the transition temperature T^* will correspond to the binding energy of spin polarons. After the formation, in a magnetic field, the spin polaron behaves like a paramagnetic center with a significantly increased effective magnetic moment μ^* , and the mode of magnetic oscillations will correspond to a g factor of ~ 2 , in accordance with experiment [1]. The many-particle nature of spin-polaron states suggests that electronic transitions that provide spin relaxation with a characteristic time of $\tau \sim 10^{-8}$ s will occur on a time scale different from the time of charge fluctuations. The formation of spin polarons should be advantageous in energy below T^* , which may be a consequence of the localization of an additional electron inside spin cluster constructed of several “frozen” Kondo singlets.

This work was supported by the program of the Presidium of the Russian Academy of Sciences “Photonic technologies in probing inhomogeneous media and biological objects”.

1. Demishev S.V. *et al.*: Scientific Reports **8**, 7125 (2018)
2. Demishev S.V. *et al.*: JETP Lett. **109**, 150 (2019)
3. Demishev S.V. *et al.*: Applied Mag. Res. **51**, 71 (2020)
4. Demishev S.V. *et al.*: J. Low Temp. Phys. **41**, 971 (2015)

Thermodynamic, Dynamic and Transport Properties of Quantum Spin Liquid

V. R. Shaginyan

Petersburg Nuclear Physics Institute of NRC “Kurchatov Institute”, vrshag@thd.pnpi.spb.ru

The exotic substances have exotic properties. One class of such substances is geometrically frustrated magnets, where correlated spins reside in the sites of triangular or kagome lattice. In some cases such magnet would not have long-range magnetic order. Rather, its spins tend to form kind of pairs, called valence bonds. At low temperatures these highly entangled quantum objects condense in the form of a liquid, called quantum spin liquid (QSL). The observation of a gapless QSL in actual materials is of fundamental significance both theoretically and technologically, as it could open a path to creation of topologically protected states for quantum information processing and computation. In the present review we consider QSL formed by spinons that are chargeless fermionic quasiparticles with spin $1/2$, filling up the

Fermi sphere. The excitations of QSL are spinons, which are chargeless fermionic quasiparticles with spin $1/2$. We expose a state of the art in the investigations of physical properties of geometrically frustrated magnets with QSL. As the QSL excitations are fermions, the most appropriate description of observed phenomena should be based on some fermionic formalism rather than on different forms of standard spin-wave approaches. So, one more purpose of our review centers on a theory employed, demonstrating its range of applicability to a novel expression of magnetic behavior. Unique feature of our review is to elucidate the nature of the used QSL in terms of both experimental facts and the theory of fermion condensation (FC). Our analysis, based on FC concept, permits to describe the multitude of experimental results regarding the thermodynamic and transport properties of QSL in geometrically frustrated. Based on the experimental facts and the theory, we show that the considered magnets exhibit the universal scaling behavior resembling that of heavy-fermion metals, including T/B scaling with T being temperature and B magnetic field [1]. We also show that QSL as a member of strongly correlated Fermi systems represents a new state of matter. We make predictions, which can help to stabilize gapless QSL in frustrated magnets.

1. Shaginyan V.R. *et al.*: J. Mater. Sci. **55**, 2257 (2020)

INVITED TALK

Dynamic Diamagnetism of the Anisotropic Chain Antiferromagnet

**A. I. Smirnov¹, T. A. Soldatov¹, K. Yu. Povarov², A. Paduan-Filho³,
A. Zheludev²**

¹ P. L. Kapitza Institute for Physical Problems, RAS, Moscow 119334, Russian Federation

² Laboratory for Solid State Physics, ETH Zürich, 8093 Zürich, Switzerland

³ High Magnetic Field Laboratory, University of São Paulo, BR-05315-970 São Paulo, Brazil

We studied magnetic resonance and microwave susceptibilities of $S = 1$ chain antiferromagnet with a strong single-ion anisotropy $\text{NiCl}_2\cdot 4\text{SC}(\text{NH}_2)_2$ (abbreviated as DTN). In this compound the exchange energy is lower than the energy of easy-plane anisotropy. DTN is a rare example of a quantum magnet with a disordered ground state stabilized by anisotropy. This is different from a classical magnet, where anisotropy helps ordering. The low-temperature electron spin resonance of DTN near a zero field is mainly analogous to that of spins $S=1$ in a crystal field [1]. However, in a specific field-induced antiferromagnetic phase found between the fields of 2 and 12 T, the ESR spectrum consists of two branches of unusual antiferromagnetic resonance. One of these branches has minimum frequency 80 GHz in the field of 7 T, while the other is zero-frequency Goldstone mode. Nevertheless, the Goldstone mode acquires a gap

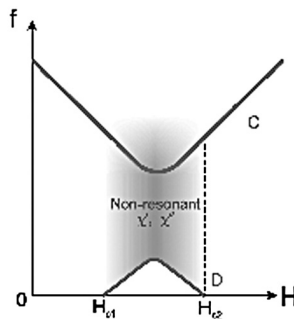


Fig. 1. Outline of the frequency-field domain of the nonresonant dynamic diamagnetic susceptibility, caused by two-magnon absorption. Line C denotes the upper antiferromagnetic resonance mode and line D is a quasi-Goldstone node in a slightly tilted field. H_{c1} and H_{c2} are field limits of the antiferromagnetic phase.

at a tiny tilting of the field against the fourfold axis. In the field range of the ordered phase we observe an unusual effect of a nonresonant strong dynamic diamagnetism in a wide frequency range, schematically shown in the Figure. Diamagnetic susceptibility reaches a value of dynamic susceptibility of the paramagnetic resonance in this compound. This very strong diamagnetic response differs from that of a conventional paramagnetic resonance via its very wide frequency band of 100 GHz. This frequency band has a sharp lower limit at a quasi-Goldstone mode indicating, that the effect is a two magnon like absorption in a dispersion range of magnons of the lower branch.

The work at the Kapitza Institute (ESR experiments, microwave measurements, and data processing) was supported by the Russian Science Foundation, Grant No. 17-12-01505. Construction and installation of the 4.5-GHz spectrometric unit was supported by the Russian Foundation for Fundamental Research (Grant No. 19-02-00194). Analysis of two-magnon absorption was supported by the Program of Presidium of RAS. The sample preparation work performed at the University of São Paulo was supported by the Brazilian Agency FAPESP (Grant No. 2015-16191-5).

1. Soldatov T.A., Smirnov A.I., Povarov K.Yu., Paduan-Filho A., Zheludev A.: Phys. Rev. B **101**, 104410 (2020)

ORAL TALKS

Antiferromagnetic Resonance Modes of the Quasi-Two-Dimensional Antiferromagnet $\text{Cu}(\text{en})(\text{H}_2\text{O})_2\text{SO}_4$

**V. N. Glazkov^{1,2}, Yu. V. Krasnikova^{1,2}, I. K. Rodygina^{1,2}, J. Chovan^{3,4},
R. Tarasenko⁵, A. Orendáčová⁵**

¹ P. Kapitza Institute for Physical Problems, Moscow 119344, Russian Federation,
glazkov@kapitza.ras.ru

² National Research University “Higher School of Economics”, Moscow 101000, Russian Federation

³ IT4Innovations National Supercomputing Center, VSB-Technical University of Ostrava, 708 33
Ostrava, Czech Republic

⁴ International Clinical Research Center, St. Anne’s University Hospital, 656 91 Brno, Czech Republic

⁵ Institute of Physics, P. J. Šafárik University, 040 00 Košice, Slovakia

We report on the low-temperature electron spin resonance (ESR) study of the quasi-two dimensional antiferromagnet $\text{Cu}(\text{en})(\text{H}_2\text{O})_2\text{SO}_4$ (here $(\text{en})=\text{C}_2\text{H}_8\text{N}_2$). Magnetic subsystem of this compound consists of weakly coupled plains with

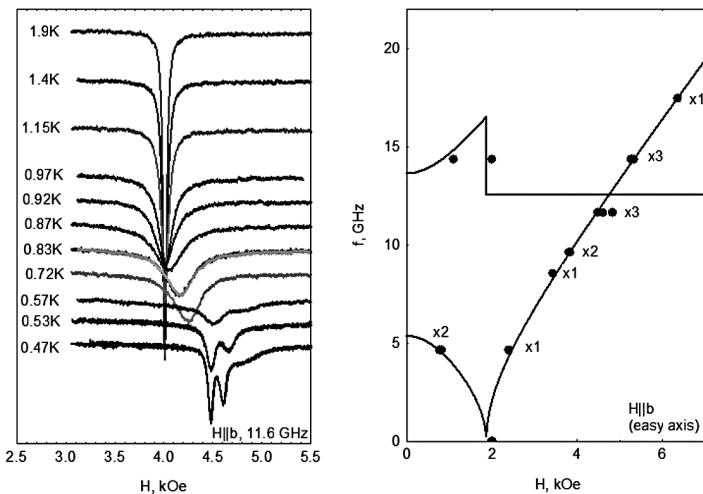


Fig. 1. Left panel: Temperature evolution of the ESR absorption spectra in $\text{Cu}(\text{en})(\text{H}_2\text{O})_2\text{SO}_4$. Right panel: Frequency-field diagram for $\text{Cu}(\text{en})(\text{H}_2\text{O})_2\text{SO}_4$ at $T = 0.45$ K. Symbols – experimental data, curve – model of biaxial collinear antiferromagnet. Notations “x1”, “x2”, “x3” mark number of split components of low-temperature antiferromagnetic resonance absorption spectra.

the strongest in-plane coupling strength about 3.5 K. $\text{Cu(en)(H}_2\text{O)}_2\text{SO}_4$ orders antiferromagnetically at $T_N = 0.91$ K [1–3].

We have studied evolution of the electron spin resonance absorption spectra down to 0.4 K using a custom-made multifrequency ESR spectrometer (4–120 GHz, 0–12 T) equipped with He-3 cryostat. We have observed that below the Neel point paramagnetic resonance signal continuously transforms to antiferromagnetic resonance absorption signal with nonlinear frequency-field dependency typical for a collinear antiferromagnet with biaxial anisotropy (Fig. 1). Anisotropy axes are identified and strength of the anisotropy parameters is evaluated, it turns out that the anisotropy of the antiferromagnetically ordered phase of $\text{Cu(en)(H}_2\text{O)}_2\text{SO}_4$ is dominated by dipolar interaction.

Besides of the conventional antiferromagnetic resonance behavior we observed weak splitting of the antiferromagnetic resonance absorption. We conclude that the most plausible explanation of this splitting is a coexistence of decoupled slightly inequivalent magnetic subsystems in $\text{Cu(en)(H}_2\text{O)}_2\text{SO}_4$. [4]

The study was partially supported by RFBR Grant 19-02-00194 and Russian Science Foundation Grant 17-02-01505. Work at P. J. Šafárik University was supported by VEGA grant No. 1/0269/17. One of the authors (J.Ch.) acknowledge support of his work by the Path to Exascale project No. CZ.02.1.01/0.0/0.0/16-013/0001791, and by project LQ1605 from the National Program of Sustainability II.

1. Lederová L., Orendáčová A.: J. Chovan *et al.*: Phys. Rev. B **95**, 054436 (2017)
2. Kajňáková M., Orendáč M., Orendáčová A. *et al.*: Phys. Rev. B **71**, 014435 (2005)
3. Sýkora R., Legut D.: Journal of Applied Physics **115**, 17B305 (2014)
4. Glazkov V.N., Krasnikova Yu.V., Rodygina I.K. *et al.*: Phys. Rev. B **101**, 014414 (2020)

Glassy Features in the NMR and μ SR Response of Na_2IrO_3 with 3d Transition Metal Ion Impurities

E. Vavilova¹, G. Prando², V. Kataev³

¹ Zavoisky Physical-Technical Institute, FRC Kazan Scientific Center of RAS, Kazan 420029, Russian Federation, jenia.vavilova@gmail.com

² Department of Physics of the University of Pavia, Pavia I-27100 Italy

³ Leibniz Institute for Solid State and Materials Research IFW Dresden, Dresden 01069, Germany

Recently, systems like A_2IrO_3 ($\text{A} = \text{Na}, \text{Li}$) have attracted great attention as model systems for Kitaev honeycomb physics. The impact of inhomogeneities in the crystalline and magnetic structures as well as of non-Kitaev interactions in such highly frustrated systems are one of the subjects of the most active study. Here we present the results of ^7Li NMR, μSR and magnetization measurements in the compounds $\text{Na}_{0.92}\text{Ni}_{1/3}\text{Ir}_{2/3}\text{O}_2$, $\text{Na}_{0.86}\text{Cu}_{1/3}\text{Ir}_{2/3}\text{O}_2$, and $\text{Na}_{0.89}\text{Zn}_{1/3}\text{Ir}_{2/3}\text{O}_2$ where 3d ions replace the sodium in the centers of iridium hexagons in Ir-planes. We demonstrate that the peculiar properties of the spin-glass behavior and critical characteristics of the systems strongly depend on the interaction of the 3d ion with the Ir magnetic lattice of the compound.

The work was supported by RFBR through grant No. 18-02-00664.

SECTION 3

LOW-DIMENSIONAL SYSTEMS AND NANO-SYSTEMS

PLENARY LECTURE

ESR Investigation of Functional Molecular Magnetic Materials

T. Nakamura

Institute for Molecular Science, Okazaki 444-8585, Japan, t-nk@ims.ac.jp

At the Institute of Molecular Science (IMS), we are conducting joint researches using multi-frequency (X-, Q-, and W-bands) and pulsed ESR measurements. For example, a) functional molecular materials, b) organic conductors, c) photoconductive materials, and d) bio-related substances and so on. In this paper, we briefly introduce several topics of our recent researches.

a) Organic conductors based on TTF (tetrathiafulvalene) derivatives have attracted much attention because they have various electronic phases and exhibit strange physical properties. Recently, Nishikawa *et al.* of Ibaraki University have developed organic conductors based on chiral and racemic reduced π electron donors. $[\pm\text{-DM-MeDH-TTP}]_2\text{AsF}_6$, which are composed of racemic molecules, have an average structure. The magnetic behavior is similar to conventional one-dimensional TTF salts. Figure 1 (a) shows the temperature dependence of ESR Linewidth ΔH of the racemic $[\pm\text{-DM-MeDH-TTP}]_2\text{AsF}_6$. The ΔH decreases as lowering temperatures, and turns to increase below 30K. It shows a maximum at around 22 K, and the ESR signal suddenly disappeared below 22 K. Theses behavior indicates that $[\pm\text{-DM-MeDH-TTP}]_2\text{AsF}_6$ undergoes an antiferromagnetic transition. On the other hand, the spin susceptibility of the chiral system $[(S, S)\text{-DM-MeDH-TTP}]_2\text{AsF}_6$ shows a low-dimensional antiferromagnetic behavior with a gentle peak near 250 K. This insulating phase is not understood. The ESR linewidth shows curious temperature dependence, following T^{-1} . At around 40 K, ESR signal suddenly disappeared. In the chiral system $[(S, S)\text{-DM-MeDH-TTP}]_2\text{AsF}_6$, the chiral molecule uniformly stacks to one-dimensional column. As a result, this system has no inversion symmetry. The chiral system shows a low-dimensional antiferromagnetic behavior with a gentle peak near 250 K. This insulating phase is not understood. The ESR linewidth ΔH is proportional to the reciprocal of temperature T^{-1} . At around 40 K, ESR signal suddenly disappeared. There is no such kind of enhancement of ΔH in one-dimensional TTF salts. The behavior of T^{-1} rules out the possibility of motional narrowing effect. It cannot be explained by the Oshikawa-Affleck mechanism since there is no alternating magnetic field in this system. The low-temperature electronic state and possible spin relaxation mechanism are discussed.

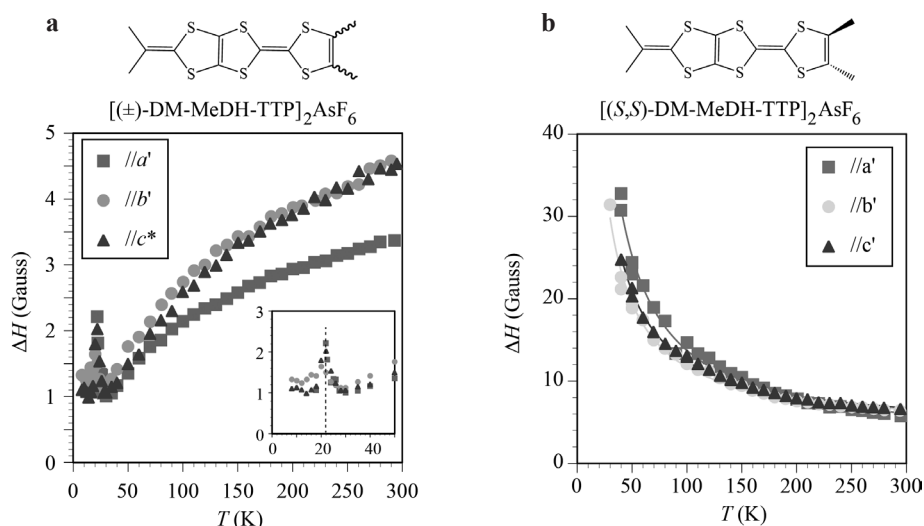


Fig. 1. Temperature dependence of the ESR linewidth ΔH of (a) racemic $[(\pm)\text{-DM-MeDH-TTP}]_2\text{AsF}_6$ and (b) chiral $[(S,S)\text{-DM-MeDH-TTP}]_2\text{AsF}_6$.

b) Noble metal clusters are attracting attention in the field of basic science because of their curious physicochemical properties arising from distinct electronic structures. Thiolate-protected alloy cluster $[\text{PtAu}_{24}(\text{SC}_2\text{H}_4\text{Ph})_{18}]^0$ ($[\text{PtAu}_{24}]^0$) is one of the model systems to study the novel electronic structures.[1] $[\text{PtAu}_{24}]^0$ has a distorted icosahedral Pt@Au_{12} core protected by six units of $\text{Au}_2(\text{SC}_2\text{H}_4\text{Ph})_3$. Because of Jahn-Teller distortion of the core, one of the 1P orbitals aligned along the compressed axis is destabilized and constitutes the LUMO. As a result, $[\text{PtAu}_{24}]^0$ takes a subshell closed electron configuration of $(1S)^2(1P)^4$, where 1S and 1P represent superatomic orbitals with angular momenta of 0 and 1, respectively. $[\text{PtAu}_{24}]^0$ was fully and selectively converted to $[\text{PtAu}_{24}]^-$ upon the reaction with an equiamount of NaBH_4 . In order to understand the electronic states of these systems, ESR measurements were carried out for solid and frozen solution of $[\text{PtAu}_{24}]^0$ and $[\text{PtAu}_{24}]^-$. $[\text{PtAu}_{24}]^0$ is ESR silent, indicating that the system is closed shell. On the other hand, $[\text{PtAu}_{24}]^-$ give us a clear ESR signal. We discuss the electronic state of a noble metal cluster from a microscopic viewpoint.

This research was supported by the “Nanotechnology Platform” of the Ministry of Education, Culture, Sports, Science, and Technology of Japan, and by Joint Research by Institute for Molecular Science.

1. Suyama M., Takano S., Nakamura T., Tsukuda T.: J. Am. Chem. Soc. **141**, 14048–14051 (2019)

ORAL TALKS

Synthesis of Carbon Quantum Dots and Their Characterization by 2D DOSY NMR Method

I. I. Geru, A. N. Barba, E. C. Gorincioi, I. E. Midoni

Department of Quantum Chemistry, Catalysis and Physical Methods, Institute of Chemistry,
Str. Academiei 3, Chisinau, MD-2028, Republic of Moldova, iongeru11@gmail.com

The carbon quantum dots (CQDs) were synthesized by the method described in [1] with modified chemical reactions durations and temperature treatment. The amine terminated compound 4, 7, 10-trioxa-1, 13-tridecanediamine was used as a surfactant. The Fig. 2 shows the values of the antilogarithms of the diffusion coefficients of water molecules, CQDs coated with a surfactant, and acetone. The acetone was added to an aqueous solution of the CQDs to determine their hydrodynamic diameter, d_{CQD} , by 2D DOSY NMR method using both known diameters of water molecule ($d_{\text{H}_2\text{O}} = 0.265 \text{ nm}$ [2]) and acetone molecule ($d_{\text{A}} = 0.469 \text{ nm}$ [3]) as standards. It was obtained $d_{\text{CQD}} = (1.16 \pm 0.06) \text{ nm}$, which is consistent with the value of $\sim 1 \text{ nm}$ estimated from the optical spectrum of the CQDs in the UV range (Fig. 1).

1. Shen L., Zhang L., Chen M. *et al.*: Carbon **55**, 345–349 (2013)
2. Tsuru T., Igi R., Kanezashi M. *et al.*: AIChE J. **57**, 618–629 (2011)
3. Murayama N.: J. Ceram. Soc. Jpn. **166**, 1167–1174 (2008)

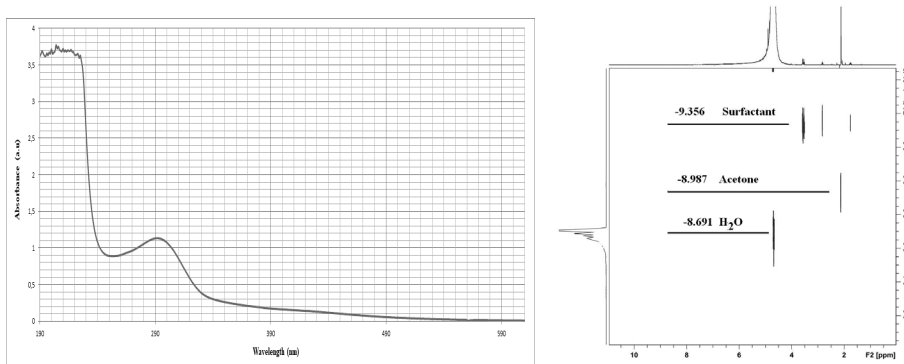


Fig. 1. UV absorption spectrum of CQDs in the aqueous solution of a concentration 0.17 mg/mL and 2D DOSY NMR spectrum of CQD at concentration 0.03 mg/mL.

Ferromagnetic Resonance in CoFeB-LiNbO Nanogranular Films Near Metal-Insulator Transition

**A. B. Drovosekov¹, N. M. Kreines¹, A. S. Barkalova^{1,2}, S. N. Nikolaev³,
A. V. Sitnikov⁴, V. V. Rylkov³**

¹ P. L. Kapitza Institute for Physical Problems RAS, Moscow 119334, Russian Federation, drovosekov@kapitza.ras.ru

² National Research University "Higher School of Economics", Moscow 101000, Russian Federation

³ National Research Center "Kurchatov Institute", Moscow 123182, Russian Federation

⁴ Voronezh State Technical University, Voronezh 394026, Russian Federation

The granular $(\text{CoFeB})_x(\text{LiNbO}_3)_{100-x}$ metal-insulator nanocomposite is a synthetic multiferroic system that can be of great interest due to possibilities of non-trivial magneto-electric effects [1]. Recently, this nanocomposite was proposed as promising material for realizing resistive switching memory elements for potential applications in neuromorphic networks [2].

In this work, $(\text{CoFeB})_x(\text{LiNbO}_3)_{100-x}$ nanocomposite films with different content of the ferromagnetic (FM) phase x are investigated by ferromagnetic resonance (FMR) technique. The room temperature measurements show a strong change of the FMR line shape in the vicinity of metal-insulator transition (MIT) of the film, $x_c \sim 43$ at.% (Fig. 1a, b), where the hopping-type conductivity σ modifies to the regime of a strong intergranular tunneling with logarithmic dependence $\sigma(T)$ [2]. It is shown that below MIT ($x < x_c$), the FMR linewidth is mainly determined by the inhomogeneous distribution of the local anisotropy axes in the film plane. Above MIT ($x > x_c$), the contribution of this inhomogeneity to the line broadening decreases. At the same time, two-magnon magnetic relaxation processes begin to play a significant role in the formation of the linewidth. The observed behavior indicates the critical role of interparticle exchange in the tunnelling regime above MIT of the nanocomposite [3].

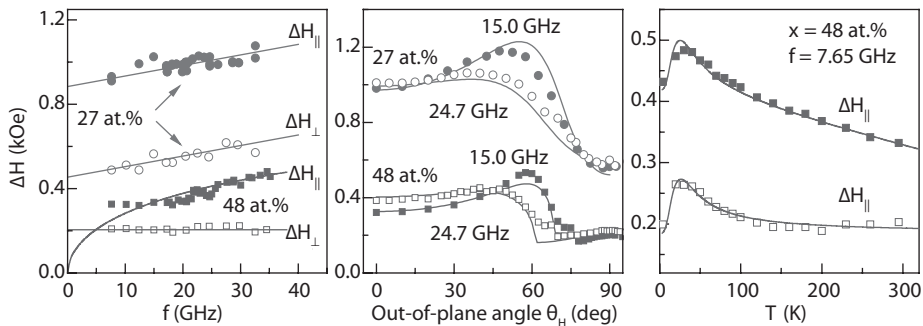


Fig. 1. a, b Room temperature FMR linewidth, ΔH , as a function of frequency, f , and out-of-plane angle, θ_H , for $(\text{CoFeB})_x(\text{LiNbO}_3)_{100-x}$ nanocomposite films with $x = 27$ and 48 at.%. **c** Temperature dependencies of the FMR linewidth for the film with $x = 48$ at.% in parallel ($\Delta H_{||}$) and normal (ΔH_{\perp}) geometries. Points are experimental data, and solid lines are their theoretical approximation.

Temperature dependencies of the FMR linewidth demonstrate non-monotonic behavior with a maximum at low temperatures (Fig. 1c). The observed effect is explained in terms of magnetic damping by slow relaxing impurities. This mechanism was originally proposed to explain experiments on magnetic relaxation in rare earth-doped yttrium iron garnet [4]. More recently it has also been applied to layered FM metal-AFM oxide exchange bias systems (see references in review [5]). However, up to now there were no reports about possibility of this mechanism in granular metal-insulator nanocomposites.

In our case, the observed relaxation can be caused by Co and Fe paramagnetic ions dispersed in the dielectric matrix LiNbO and coupled to the FM CoFeB granules. Static magnetometry of the investigated films indicates the presence of such ions, demonstrating high magnetic susceptibility below $T \approx 40$ K [2]. This fact is in accordance with the FMR data, showing a peak in $\Delta H(T)$ dependence below $T \approx 40$ K.

The work is partially supported by the Russian Foundation for Basic Research (projects 18-07-00772, 18-07-00756, 19-07-00471), and by the Basic Research Program of the Presidium of Russian Academy of Sciences “Actual problems of low temperature physics”.

1. Udalov O.G., Beloborodov I.S.: *AIP Advances* **8**, 055810 (2018)
2. Rylkov V.V., Nikolaev S.N., Demin V.A. *et al.*: *J. Exp. Theor. Phys.* **126**, 353 (2018)
3. Drovosekov A.B., Kreines N.M., Barkalova A.S. *et al.*: *JMMM* **495**, 165875 (2020)
4. van Vleck J.H., Orbach R.: *Phys. Rev. Lett.* **11**, 65 (1963)
5. Mewes C.K.A., Mewes T. “Relaxation in Magnetic Materials for Spintronics”, in: “Handbook of Nanomagnetism: Applications and Tools” edited by R. A. Lukaszew (Pan Stanford Publishing, 2015).

Formation of Ferromagnetic Clusters in $\text{La}_{1-x}\text{Sr}_x\text{Mn}_{0.9}\text{Fe}_{0.1-y}\text{M}_y\text{O}_3$ ($\text{M} = \text{Mg}^{2+}; \text{Zn}^{2+}$)

**R. M. Eremina¹, I. V. Yatsyk¹, A. G. Badelin², V. K. Karpasyuk²,
Z. Y. Seidov³**

¹ Zavoiisky Physical-Technical Institute, FRC Kazan Scientific Center of RAS, Kazan 420029, Russian Federation, aleksey665@gmail.com

² Astrakhan State University, Astrakhan, 414056, Russian Federation, alexey_badelin@mail.ru

³ Institute of Physics, National Azerbaijan Academy of Sciences, AZ-1143, Baku, Azerbaijan

Hole doped manganites of the general composition $\text{Ln}_{1-x}\text{Me}_x\text{MnO}_3$, where Ln denotes a trivalent rare-earth ion and Me a divalent alkaline-earth metal like Ca, Sr or Ba, exhibit complex phase diagrams due to competing spin, orbital, charge, and lattice degrees of freedom. Interesting phenomena were observed such as complex magnetic structures, the colossal magnetoresistance effect and the existence of electronic phase separation in $\text{Ln}_{1-x}\text{Me}_x\text{MnO}_3$. The possible formation of ferromagnetically correlated regions in the paramagnetic phase of magnetic semiconductors much has been discussed in the literature, when an electron is captured by a ferromagnetic fluctuation of localized spins. The formation of ferromagnetically correlated regions in the paramagnetic regime is certainly not restricted to the cooperative Jahn-Teller phase, only, but is always expected to occur in the temperature regime of critical fluctuations above the onset of ferromagnetic order. While the distinct separation of additional FMR lines from the paramagnetic line demands a well-defined anisotropy which exists in the cooperative Jahn-Teller phase, in the general case of a random cluster distribution the anisotropy averages out and the averaged signal unites with the paramagnetic resonance line. Then the ESR linewidth, which reflects the spin-spin relaxation rate, usually exhibits a critical broadening on approaching magnetic order. We assume that ferromagnetically correlated regions in the paramagnetic phase should have a similar effect on the paramagnetic resonance spectrum like superparamagnetic particles. The substitution of manganese by divalent Zn^{2+} (Mg^{2+}) cations at a given Sr^{2+} concentration further suppresses the cooperative Jahn-Teller phase, as it decreases the concentration of Jahn-Teller active trivalent Mn^{3+} ions, while increasing in the content of tetravalent non Jahn-Teller ions Mn^{4+} . Moreover, the Zn^{2+} or Mg^{2+} ions do not participate in the exchange interaction, resulting in an increasing tendency to charge localization and reduced mobility of the carriers. To check our assumption, we systematically investigated the zinc (magnesium)-doped lanthanum-strontium manganite by means of ESR and magnetization measurements in temperature range 4.2–600 K. This work was supported by the Russian Foundation for Basic Research (grant no.18-52-06011).

Local Structure of Pillared Mordenite and ZSM-5 Zeolites and Water Behavior in Their Interlayer Space Studied by NMR

**M. G. Shelyapina¹, D. Nefedov¹, A. Tyurtyaeva¹, A. Arteaga²,
R. Yocupicio-Gaxiola², A. V. Petranovskii², S. Fuentes²**

¹ Saint Petersburg State University, Saint Petersburg 199034, Russian Federation, marina.shelyapina@spbu.ru

² Centro de Nanociencias y Nanotecnología, Universidad Nacional Autónoma de México, Ensenada, Baja California, C.P. 22860 México

Layered zeolites are used as precursor for mesoporous catalysts. For the successful development of these materials, knowledge on the structure and dynamics of both structural parts are highly required. In this contribution we report on the results of our studies of the local structure of the pillared mordenite and ZSM-5 zeolites, as well as the study of dynamics of water molecules inside the interlamellar space. The samples were synthesized according to the procedure described in our previous work [1]. The preparation method included four steps: (i) preparing of lamellar zeolites by self-assembling method using cetyltrimethylammonium bromide (CTAB) and polyethylene glycol (PEG) as mesopore creating agents in a one-pot synthesis; (ii) introduction of TEOS molecules into the interlamellar space; (iii) hydrolysis and formation amorphous SiO₂; (iv) calcination (evacuation of organic molecules).

Both X-ray diffraction patterns and transmission electron microscopy patterns confirm formation of first lamellar and then (after annealing) pillared structures. Magic angle spinning nuclear magnetic resonance (MAS NMR) at different nuclei ¹H, ¹³C, ¹⁵N, ²³Na, ²⁷Al, ²⁹Si was applied to control all the synthesis steps. The obtained results confirm formation of an ideal local structure of the as-synthesized samples. However, it was found that annealing results in appearing of non-framework Al atoms in a significant amount (without destruction of the zeolite framework). A simultaneous analysis of ²⁷Al and ²⁹Si MAS NMR spectra at all the preparation step allows us to suppose that when growing a layered zeolite in the presence of organic agents, aluminum atoms are located in the outer zeolite layer.

According to thermal gravimetric analysis, the water release in the both pillared zeolites occurs in one step. The mordenite sample exhibits both higher water content (14.0 and 9.8 mass% for the pillared mordenite and ZSM-5 samples, respectively) and higher temperature of water release (62 and 39 °C for the pillared mordenite and ZSM-5 samples, respectively). The ¹H MAS NMR spectra recorded within the temperature range from 160 to 293 K confirms that the majority of water molecules are situated inside the mesopores: at room temperature water molecules are bounded with the framework oxygen by hydrogen bonds. However, with temperature decreasing one observes disappearing of the water-framework hydrogen bonds due to formation of bulk water with further crystallization. For the both studied pillared zeolites the temperature dependences of ¹H spin-lattice relaxation times T_1 and $T_{1\rho}$ exhibit a rather complex behavior

that reflects the phase transitions that nanoconfined water undergoes. The activation energy, as determined from the $T_{1\rho}(1/T)$ dependence, was found equal to 25.9 and 30.7 kJ/mol for the mordenite and ZSM-5 samples, respectively.

The work was funded by SENER-CONACYT (project 117373), RFBR and CITMA in accordance with research Project No. 18-53-34004. The materials were synthesized and characterized at the Nanoscience and Nanotechnology Centre of the National Autonomous University of Mexico, and the Research Park of Saint Petersburg State University (Centre for Diagnostics of Functional Materials for Medicine, Pharmacology and Nanoelectronics, Magnetic Resonance Research Centre, Centre for X-ray Diffraction Studies, Thermogravimetric and Calorimetric Research Centre).

1. Yocupicio-Gaxiola R., Petranovskii V., Antúnez-García J., Moyado S.: Applied Nanoscience **9**, 557 (2019)

Synthesis and Studies of Structural, Magnetic and Ferromagnetic Resonance Properties of Epitaxial $\text{Pd}_{0.96}\text{Fe}_{0.04}/\text{VN}/\text{Pd}_{0.92}\text{Fe}_{0.08}$ Superconducting Spin-Valve Heterostructure

W. M. Mohammed¹, I. V. Yanilkin^{1,2}, A. I. Gumarov^{1,2}, A. G. Kiiamov¹,
A. A. Rodionov¹, R. V. Yusupov¹, L. R. Tagirov^{1,2}

¹ Institute of Physics, Kazan Federal University, Kazan, Russian Federation

² Zavoisky Physical-Technical Institute, FRC Kazan Scientific Center of RAS, Kazan 420029, Russian Federation, yanilkin-igor@yandex.ru

Thin ferromagnet/superconductor/ferromagnet (FSF) layered heterostructure is one of the possible logic elements in superconducting spintronics [1]. We synthesized a fully epitaxial FSF heterostructure, which consists of two layers of $\text{Pd}_{1-x}\text{Fe}_x$ as a ferromagnet and a VN layer as a superconductor. The $\text{MgO}/\text{Pd}_{0.96}\text{Fe}_{0.04}(20\text{ nm})/\text{VN}(30\text{ nm})/\text{Pd}_{0.92}\text{Fe}_{0.08}(12\text{ nm})$ heterostructure was deposited by molecular-beam epitaxy technique (MBE system by SPECS, Germany) and reactive magnetron sputtering (BESTEC, Germany) onto the (001)-oriented, epi-polished single-crystal MgO substrate [2–4]. The epitaxial growth mode of the layers was verified by low-energy electron diffraction (LEED) and X-ray diffraction (XRD) techniques (Fig. 1A). Magnetic properties were studied using VSM magnetometry (QD PPMS-9) and ferromagnetic resonance (FMR, X-band Bruker ESP300 spectrometer).

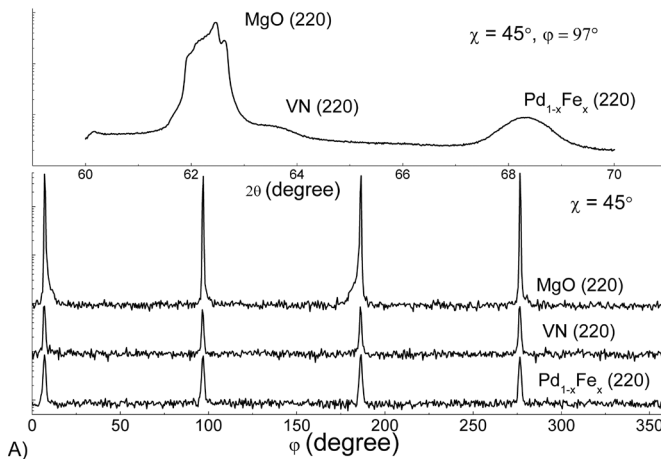
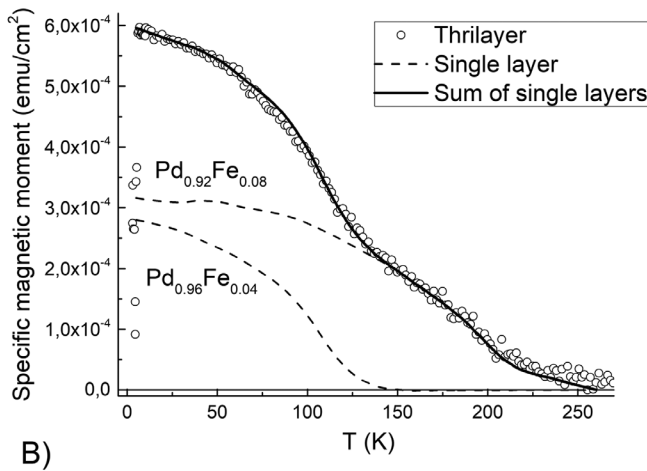
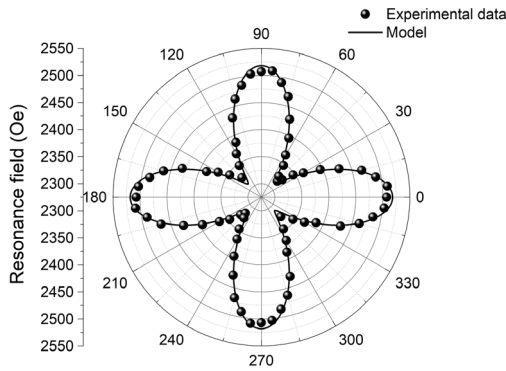


Fig. 1A Top: X-ray diffraction 2θ scan for the trilayer heterostructure; bottom: φ -scan for different 2θ corresponding to different materials.



B)



C)

Fig. 1B, C. Temperature dependences of the saturation specific magnetic moment for the trilayer film and the single films (B); Angular dependence of the FMR field of the epitaxial Pd_{0.96}Fe_{0.04}/VN film (C).

The specific magnetic moment versus temperature dependence $M(T)$ is presented in Fig. 1B. It exhibits a clear kink at a temperature of about 125 K, which can be well reproduced by decomposing the $M(T)$ dependence on the magnetic responses of the constituent Pd_{0.92}Fe_{0.08} and Pd_{0.96}Fe_{0.04} layers (shown by dash lines) using $M(T)$ data for single-layered films. At a temperature of 5.4 K, an additional diamagnetic contribution arises due to the superconducting transition in the VN layer. The FMR technique was used to study magnetic anisotropies in the Pd_{0.96}Fe_{0.04}/VN bilayer (Fig. 1C). The magnetic anisotropy of the bilayer is the same as for single Pd_{0.96}Fe_{0.04} layer – cubic with tetragonal distortion [2, 4].

Different concentration of iron in the ferromagnetic layers leads to different coercive fields [2], which makes it possible to utilize them like “free” and “fixed”

layers (soft-hard pseudo spin-valve). On the minor hysteresis loop we obtained parallel (P) and antiparallel (AP) mutual alignment of the ferromagnetic layers magnetizations. Resistive measurements showed the inverse superconductive spin-valve ($T_c(P) > T_c(AP)$) effect.

This work was supported by the RSF project No. 18-12-00459. Synthesis and analysis of the films were carried out at the PCR Federal Center of Shared Facilities of KFU.

1. Linder J., Robinson J.W.A.: *Nat. Phys.* **11**, 307 (2015)
2. Esmaili A., Yanilkin I.V., Gumarov A.I. *et al.*: *Thin Solid Films* **669**, 338 (2019)
3. Esmaili A., Mohammed W.M., Yanilkin I.V. *et al.*: *Magnetic Resonance in Solids. Electronic Journal* **21**, 4 (2019)
4. Mohammed W.M., Yanilkin I.V., Gumarov A.I. *et al.*: *Beilstein J. Nanotechnol* **11**, 807 (2020)
5. Esmaili A., Yanilkin I.V., Gumarov A.I. *et al.*, <https://arxiv.org/pdf/1912.04852>

Ferromagnetic Resonance Versus Spin-Hall Effect in Heteroepitaxial W/Pd_{0.92}Fe_{0.08} Thin Film Structure

**R. V. Yusupov¹, A. I. Gumarov¹, A. A. Rodionov¹, I. V. Yanilkin¹,
G. A. Zhivov¹, L. R. Tagirov^{1,2}**

¹ Institute of Physics, Kazan Federal University, Kazan, Russian Federation

² Zavoisky Physical-Technical Institute, FRC Kazan Scientific Center of RAS, Kazan 420029, Russian Federation, Roman.Yusupov@kpfu.ru

Spin-Hall effect (SHE) that has been predicted long ago by Dyakonov and Perel nowadays starts to play an important technological role in nano-patterned thin films structures. Phenomenologically, SHE reveals itself as a spin polarization/disbalance of the charge carriers in a thin film in the direction perpendicular to the flowing electric current. The magnitude of the effect is enhanced in heavy metals as the effect itself originates significantly from the spin-orbit interaction. Usual materials used for this kind of the actuators are platinum or iridium. Recently, high potential of the β -W was demonstrated.

In the recent years, we have elaborated an efficient way to grow high-quality epitaxial films of Pd_{1-x}Fe_x alloy with $x < 0.10$ that are the magnetically-soft low temperature easy-plane ferromagnets with a pronounced in-plane anisotropy [1]. Magnetic properties of these films have been studied extensively. Basing on our advanced understanding of Pd_{1-x}Fe_x film properties, we have initiated the study of the spin-Hall effect and related to it phenomena in heteroepitaxial W/Pd_{1-x}Fe_x bilayer structure.

The heterostructure has been grown by molecular beam epitaxy method, where Pd_{1-x}Fe_x layer was deposited by co-evaporation of Pd and Fe from high-temperature effusion cells, and W-layer – by electron-beam evaporation on the (001)-oriented MgO substrate. The structure of the produced samples were carefully characterized with X-ray diffractometry. It is shown that the type of epitaxy was W_[110]||Pd_{1-x}Fe_x_[001]||MgO_[001]. As a result, W-layer is represented by the α -phase and two or even four kinds of structural domains depending on its thickness. Occurrence of the spin-Hall effect will be demonstrated via the SHE-induced FMR, and its peculiarities in the given structure will be discussed.

This work was supported by the RSF project No. 18-12-00459. Synthesis and analysis of the films were carried out at the PCR Federal Center of Shared Facilities of KFU.

VSM and FMR Studies of Fe-Ion Implanted Epitaxial Films of Palladium

**R. I. Khaibullin¹, A. I. Gumarov^{1,2}, V. I. Nuzhdin¹, I. R. Vakhitov²,
V. F. Valeev¹, I. V. Yanilkin², R. V. Yusupov², L. R. Tagirov^{1,2}**

¹ Zavoisky Physical-Technical Institute, FRC Kazan Scientific Center of RAS, Kazan 420029, Russian Federation, rik@kfti.knc.ru

² Institute of Physics, Kazan Federal University, Kazan 420008, Russian Federation, amir@gumarov.ru

Thin films of palladium-rich Pd_{1-x}Fe_x alloys ($x = 0.01-0.1$), are of particular interest in superconducting spintronics (superspintronics) [1]. They reveal low-temperature ferromagnetism with a Curie temperature (T_C) depending on the concentration of iron dopant. Usually, such Pd_{1-x}Fe_x films are obtained by molecular-beam epitaxy (MBE) [2]. Since the electronic industry uses ion implantation (Ii) to dope semiconductors, we combined MBE with Ii to produce new nanostructured Pd_{1-x}Fe_x alloy films with unique magnetic properties.

At the first stage, epitaxial films of pure palladium (Pd) with a thickness of ~60 nm were grown on MgO (001) substrates by MBE. The crystal lattice perfection during film growth was controlled by low energy electron diffraction. Then, 40 keV Fe⁺ ions were implanted into epitaxial Pd films at three different fluences of (0.5, 1.0 and 3.0)×10¹⁶ ion/cm² in order to induce ferromagnetism in Pd films and to study the evolution of their magnetic properties as a function of the iron implant concentration. Depth profiles of the iron distribution were obtained by X-ray photoelectron spectroscopy in combination with argon ion etching technique. The magnetic properties of the implanted Pd films were measured utilizing vibrating sample magnetometry (VSM), and ferromagnetic resonance (FMR) at 9.5 GHz in a wide temperature range of 4–250 K and scanning the applied magnetic field either in-plane or out-of-plane of the Fe-implanted films of palladium.

VSM measurements have shown that after implantation with iron ions, the initially paramagnetic film of pure palladium reveals a ferromagnetic response with a narrow magnetic hysteresis loop (Fig. 1a). It is important to note that the width of the magnetic hysteresis loop (the value of the coercive field in the in-plane geometry) in the Fe-implanted films of palladium is significantly smaller than in similar films obtained by MBE [2] with the same average concentration of the iron impurity. A strong effect of the iron ion fluence on the Curie temperature was established: the implanted Pd films have $T_C \sim 40$ K, 100 K and 160 K for the samples implanted at the minimal, intermediate and maximal values of the iron fluence, respectively. Moreover, analysis of the FMR spectra recorded at different temperatures indicated the formation of a multiphase magnetic structure in the Fe-ion implanted Pd films. Namely, the FMR spectra of a sample with a maximum Fe fluence reveals up to three FMR lines in the out-of-plane geometry (Fig. 1b). Note that these FMR signals appeared one after

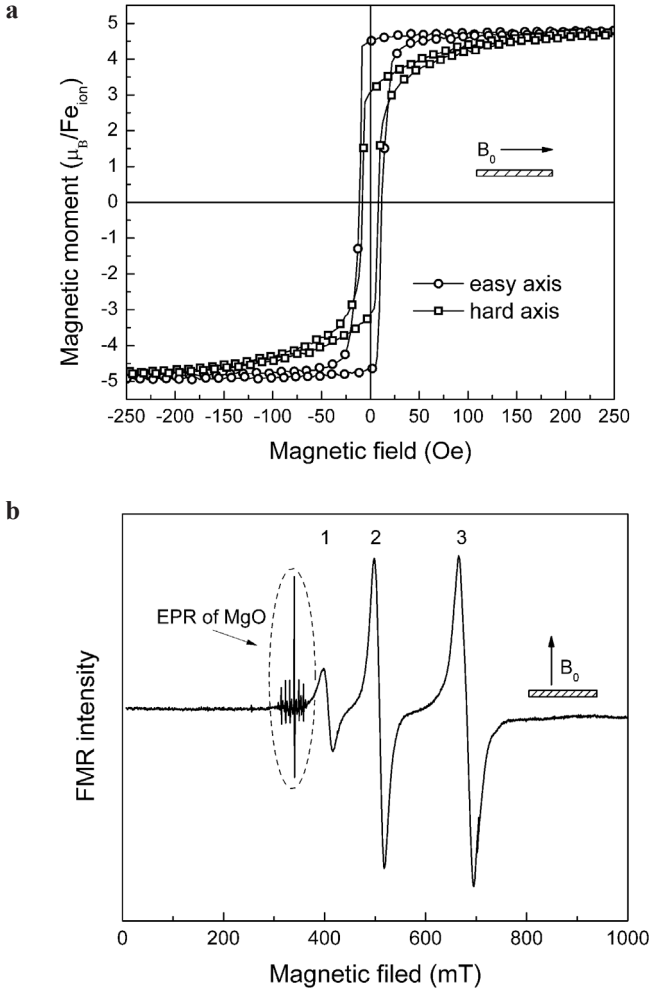


Fig. 1. In-plane magnetic hysteresis loops (a) and out-of-plane FMR spectrum (b) of the epitaxial Pd film implanted with Fe ions at the ion fluence of 3.0×10^{16} ions/cm², $T_{\text{meas.}} = 50$ K.

another when the temperature decreased from 160 K to 50 K. The film implanted with intermediate fluence shows only two FMR signals, and the sample with a minimum iron fluence reveals one FMR signal as is usually observed in FMR spectra of Pd_{1-x}Fe_x films prepared by the MBE method [3].

Argued by the appearance of three FMR signals at different temperatures in Fe-implanted films we propose a model of a spinodal decomposition of metastable Pd_{1-x}Fe_x solid solution with an initially inhomogeneous distribution of the iron dopant in regions with relatively well-defined x values. The current status of our understanding is that the implanted iron dopant forms something like well-defined sub-layers, the number and magnetic properties of which depend on

the implantation fluence. Subsequent annealing of the as-implanted samples in ultra-high vacuum led to a strong modification of the temperature dependences of the magnetization, as well the FMR spectra (not shown), which indicates a metastable state of our as-implanted samples: a quite intriguing conclusion for the Pd and Fe pair commonly considered as completely soluble in Pd-rich binary mixtures.

This work was supported by RFBR, grant No 20-02-00981. The epitaxial growth of pure palladium films and their microstructure analysis were carried out at the PCR Federal Center of Shared Facilities of KFU.

1. Ryazanov V.V., Bol'ginov V.V., Sobanin D.S. *et al.*: Phys. Procedia **36**, 35 (2012)
2. Esmaeili A., Yanilkin I.V., Gumarov A.I. *et al.*: Thin Solid Films **669**, 338 (2019)
3. Esmaeili A., Vakhitov I.R., Yanilkin I.V. *et al.*: Appl. Magn. Reson. **49**, 175 (2018)

Electron Spin Resonance in Multiferroic Spin-Chain Cuprate LiCuVO_4

S. Gotovko^{1,2}, L. Svistov¹

¹ P. L. Kapitza Institute for Physical Problems, RAS, Moscow 119334, Russian Federation

² National Research University Higher School of Economics, Moscow 101000, Russian Federation, sofyagotovko@gmail.com

We present an electron spin resonance (ESR) study of multiferroic quantum spin-chain compound LiCuVO_4 in presence of electric field. Magnetic ordering in this crystal is accompanied by the appearance of electric polarization which value and direction is connected with the magnetic structure. We expect that the ESR frequencies in LiCuVO_4 depend not only on anisotropy constants and applied magnetic field, but also on applied static electric field. The shifts of ESR absorption curves and, therefore, the shifts of resonance fields were observed with use of modulation technique: low-frequency alternating electric field was applied to the sample and oscillating part of absorption curve at the frequency of oscillations was measured.

LiCuVO_4 is a member of family of multiferroic frustrated spin-1/2 chain systems with competing nearest neighbor ferromagnetic and next-nearest neighbor antiferromagnetic exchange interactions. Elastic neutron scattering experiments

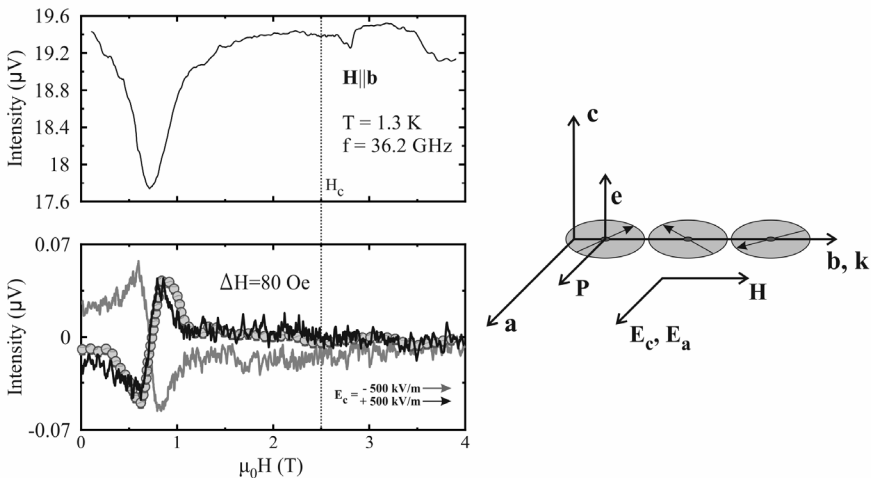


Fig. 1. Upper panel: field dependence of transmitted through the resonator HF power. Bottom panel: responses of transmitted power on alternating electric field (black line – $E_c = +500$ kV/m, grey line – $E_c = -500$ kV/m). Bubble line – scaled derivative of absorption line. Inset: mutual orientation of crystallographic axes, external \mathbf{H} and \mathbf{E} fields, electric polarization \mathbf{P} . Grey ellipses illustrate helical magnetic structure, \mathbf{e} is vector product of spins on neighbor copper ions.

[1] revealed that an incommensurate helical structure with wave vector $\mathbf{k} = (0, 0.532, 0)$ is established below $T_N = 2.3$ K at zero magnetic field as a result of such competition. Helical spin order in this crystal induces ferroelectricity. Spin current mechanism [2] predicts for LiCuVO_4 that with helical magnetic order the crystal acquires electric polarization \mathbf{P} directed within the helix spin plane and perpendicular to wave vector \mathbf{k} .

ESR study of LiCuVO_4 was conducted with use of multiple-mode rectangular resonator at $T = 1.3$ K and at frequencies $f = 17.2$ GHz, 36.2 GHz and 42.2 GHz. Alternating low-frequency electric field \mathbf{E}_a was applied along \mathbf{P} , and constant electric field \mathbf{E}_c was also applied to the sample to control the direction of electric polarization. Orientation of magnetic and electric fields and electric polarization in respect to crystallographic axes is shown in the inset to Fig. 1. The field dependence of transmitted through the resonator HF power at $f = 36.2$ GHz is shown on the upper panel of Fig. 1, the responses of transmitted power on the alternating electric field are shown on the bottom panel. The responses measured on the frequency of \mathbf{E}_c are proportional to derivative of absorption line. Change of electric polarization sign leads to change of the response sign (black and grey lines). Results of the experiments at different frequencies agree with the assumption that electric field influence magnetic properties of LiCuVO_4 .

The work was supported by Russian Foundation for Basic Research (grant №19-02-00194).

1. Gibson B.J., Kremer R.K., Prokofiev A.V., Assmus W., McIntyre G.J.: *Physica B* **350**, E253 (2004)
2. Katsura H., Nagaosa N., Balatsky A. V.: *Phys. Rev. Lett.* **95**, 057205 (2005)

Spin Resonance on Electrons of Zero Modes Stabilized at Atomically Smooth Graphene Edges

A. M. Ziatdinov

Institute of Chemistry, Far Eastern Branch of the RAS, Vladivostok 690022, Russian Federation, ziatdinov@ich.dvo.ru

On the zigzag edges of flat honeycomb carbon structures a specific π -electronic states (topological zero modes) with a sharp maximum of their density $D(E)$ near the Fermi level E_F are stabilized (Fig. 1) [1]. At given nanometer lateral sizes of such carbon structures (in nanographenes), the existence and the degree of manifestation of its specific quantum properties are completely controlled by these states [1-3]. In this report the results of ESR, conduction ESR (CESR) and magnetic susceptibility (MS) investigations of the electronic structure and magnetic properties of few-layer nanographenes (nanographites) – structural blocks of activated carbon fibers (ACFs), and the data on their changes under the influence of adsorbed acceptor molecules and covalent bonds of halogen with dangling σ -orbitals of edge carbon atoms are presented and discussed.

With the set of complementary physical methods we found that studied PAN-based ACFs consist of three dimensional disordered networks of nanographite domains, divided from each other by micropores and amorphous phase of carbon [4]. Each nanographite consists of ~ 3 nanographene layers. The mean in plane size of nanographite is ~ 2 nm [4].

The ESR, CESR and MS data show that there are two types of unpaired spins in studied ACFs: conduction electrons and localized centers, which are characterized with the near the same values of g -factors and ESR lineshape

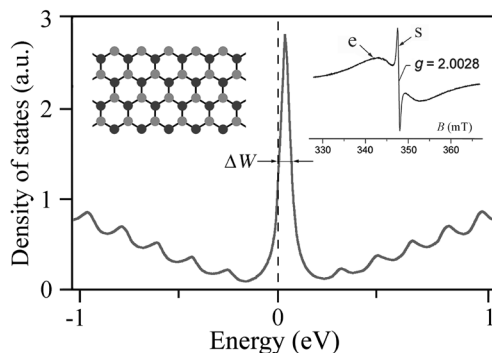


Fig. 1. The density of electronic states near the zigzag edges of graphene nanoribbon (shift of the $D(E)$ maximum relative to the E_F and full width at half maximum ΔW are equals to 30 and 80 meV, respectively [2, 3]; left inset: graphene nanoribbon with zigzag edges; right inset: the EPR spectrum of ACFs; arrows indicate the signals from mobile (e) and localized (s) electrons.

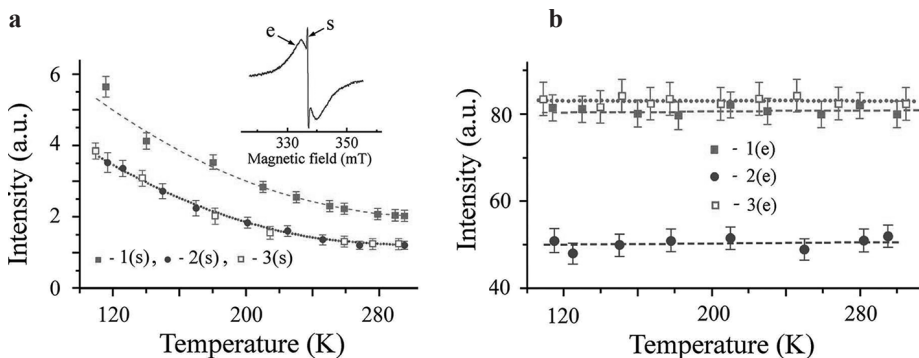


Fig. 2. **a** The temperature dependences of integrated intensities of the narrow (s) component of the EPR spectrum for initial – 1(s), chlorinated – 2(s) and dechlorinated – 3(s) ACFs. **b** The same dependences for the broad (e) component of EPR spectrum.

asymmetry (Fig. 1, right inset). The data of these methods (Fig. 2) show that the $D(E_F)$ in nanographites is several orders higher than that in the bulk graphite. This result suggests the existence of edge π -electronic states in them.

The energy of the $D(E)$ peak of honeycomb carbon network is slightly less than the E_F (Fig. 1) [2, 3]. Therefore, the expected result of their interactions with acceptor molecules is the increasing $D(E_F)$. However, we have observed the decreasing intensity of the CESR signal of nanographites, which is proportional to $D(E_F)$, both in cases of ACFs interaction with halogen and oxygen molecules. We assume that the reasons for this are the electron-electron interactions of edge π -electrons, which initiate spin-splitting of the edge states when $D(E_F)$ reaches a certain critical value. It has been shown that mentioned point of view on the nature considered phenomenon does not contradict the results of other physical methods of investigations of the edge π -electronic states, including scanning probe microscopy data [5, 6].

The experimental data obtained by us and theoretical models suggested for their explanation may be useful for understanding the reasons and mechanisms of changing the properties of nanocarbons resulting from the effect of different substances, for grading the factors determining their electronic structure and chemical reactivity and for opening prospects for their practical applications (for instance, in sensors, energy accumulators, electrochemical systems, catalysis etc.).

The work has been financially supported by the Ministry of Science and Higher Education of the Russian Federation (State assignment No. 265-2019-0001).

1. Nakada K., Fujita M., Dresselhaus G. *et al.*: Phys. Rev. B **54**, 17954 (1996)
2. Kobayashi Y., Fukui K., Enoki T. *et al.*: Phys. Rev. B **71**, 193406 (2005)
3. Takai K., Kumagai H., Sato H. *et al.*: Phys. Rev. B **73**, 035435 (2006)
4. Ziatdinov A.M., Skrylnik P.G., Saenko N.S.: Phys. Chem. Chem. Phys. **19**, 26957 (2017)
5. Ziatdinov M.A., Fujii S., Kusakabe K. *et al.*: Phys. Rev. B **87**, 115437 (2013)
6. Ohtsuka M., Fujii S., Kiguchi M. *et al.*: ACS Nano **7**, 6868 (2013)



SECTION 4

MAGNETIC RESONANCE INSTRUMENTATION

PLENARY LECTURES

Multi-Extreme THz ESR: Present and Future

**H. Ohta^{1,2}, S. Okubo^{1,2}, E. Ohmichi², T. Sakurai³, H. Takahashi^{1,2},
S. Hara³, Y. Saito³**

¹ Molecular Photoscience Research Center, Kobe University, Japan, hohta@kobe-u.ac.jp

² Graduate School of Science, Kobe University, Japan

³ Research Facility Center for Science and Technology, Kobe University, Japan

Multi-extreme THz ESR in Kobe can cover the frequency region between 0.03 and 7 THz [1], the temperature region between 1.8 and 300 K [1], the magnetic field region up to 55 T [1], and the pressure region up to 1.5 GPa [2] simultaneously.

Another aspect of multi-extreme THz ESR is the developments of the high-sensitive force-detected ESR. We succeeded in observing ESR up to 1.1 THz using micro-cantilever [3]. Then we extended our developments to the torque magnetometry [4] and ESR [5] measurements using a commercially available membrane-type surface stress sensor. Finally the membrane ESR is applied to the microliter solution sample (myoglobin) [6].

Recently we have developed the hybrid-type pressure cell, and achieved 2.5 GPa [7]. Using this pressure cell for our high-pressure THz ESR, we have discovered the first-order pressure-induced transition at 1.85 GPa in the Shastry-Sutherland Model Compound $\text{SrCu}_2(\text{BO}_3)_2$ [8]. Moreover, we have developed a new high pressure ESR system up to 25 T at the high field user facility in IMR, Tohoku University [9]. Recent applications of high-pressure THz ESR to Cs_2CuCl_4 [10] and CsCuCl_3 triangular antiferromagnets, which show new pressure induced phases such as the magnetization plateau, will be discussed.

1. Ohta H. *et al.*: *J. Low Temp. Phys.* **170**, 511 (2013)
2. Sakurai T. *et al.*: *Rev. Sci. Instr.* **78**, 065107 (2007); Sakurai T.: *J. Phys.: Conf. Series* **215**, 012184 (2010)
3. Ohta H. *et al.*: *AIP Conf. Proceedings* **850**, 1643 (2006); Ohmichi E. *et al.*: *Rev. Sci. Instrum.* **79**, 103903 (2008); Ohmichi E. *et al.*: *Rev. Sci. Instrum.* **80**, 013904 (2009); Ohta H., Ohmichi E.: *Appl. Mag. Res.*, **37**, 881 (2010); Ohmichi E. *et al.*: *J. Mag. Res.* **227**, 9 (2013); Ohmichi E. *et al.*: *Rev. Sci. Instrum.* **87**, 073904 (2016); Ohmichi E. *et al.*: *J. Inorganic Biochemistry* **162**, 160 (2016) (Invited paper); Takahashi H., Ohmichi E., Ohta H.: *Appl. Phys. Lett.* **107**, 182405 (2015)
4. Takahashi H. *et al.*: *J. Phys. Soc. Jpn.* **86**, 063002 (2017) (Editor's Choice).
5. Takahashi H. *et al.*: *Rev. Sci. Instrum.* **89**, 036108 (2018)
6. Okamoto T. *et al.*: *Appl. Phys. Lett.* **113**, 223702 (2018) (Editors Picks).
7. Fujimoto K. *et al.*: *Appl. Mag. Res.* **44**, 893 (2013); Sakurai T. *et al.*: *J. Mag. Res.* **259**, 108 (2015); *J. Mag. Res.* **280**, 3 (2017) (Invited review); Ohta H. *et al.*: *J. Phys. Chem. B* **119**, 13755 (2015) (Invited paper)
8. Sakurai T. *et al.*: *J. Phys. Soc. Jpn.* **87**, 033701 (2018)
9. Sakurai T. *et al.*: *J. Mag. Res.* **296**, 1–4 (2018)
10. Zvyagin S. A. *et al.*: *Nature Communications* **10**, 1064 (2019)

EPR/ODMR Instrument Complex and its Application for the Study of Wide Band Gap Materials

**R. A. Babunts, A. N. Anisimov, A. S. Gurin, N. G. Romanov,
A. G. Badalyan, P. G. Baranov**

Ioffe Institute, St. Petersburg 194021, Russian Federation, Roman.Babunts@mail.ioffe.ru

A radio-spectroscopic instrument complex is designed for the study and non-destructive testing of condensed materials, including nanostructured and biological objects, using electron paramagnetic resonance (EPR), electron spin echo (ESE) and optically detected magnetic resonance (ODMR). The complex consists of two complementary systems: a high-frequency EPR/ODMR spectrometer and a magnetic resonance spectrometer, combined with optical confocal and atomic force microscopy.

The high-frequency EPR/ODMR spectrometer operates both in continuous and pulsed modes in W- and D-bands [1]. The main features of the spectrometer are:

The unified design of the microwave bridges 94 and 130 GHz allows you to quickly change the operating frequency.

The compact design of the microwave bridges based on semiconductor components makes it possible to place them directly on the cryostat without using long waveguide lines.

The microwave insert can be made in two versions: with a single-mode resonator and a non-resonant microwave insert [2].

Operation of the closed cycle magneto-optical cryostat with a superconducting magnet (-7 to $+7$ T) and an optical access for photo-EPR and ODMR does not depend on cryogenic infrastructure. The cryostat provides a wide temperature range of 1.5 to 300 K and high temperature stability.

The open design of the spectrometer allows you to quickly change the configuration of the experiment. The spectrometer supports the following operating modes: EPR, ESE, photo-EPR, ODMR, detection of the level anticrossings, ENDOR.

The second part of the radio-spectroscopic complex is the ODMR spectrometer built on the basis of an inverted confocal probe microscope from NT-MDT Company. The combination of high spatial and spectral resolution of the confocal microscope with EPR creates an experimental base for the study of single molecules and defects.

Such an approach allows one to locally diagnose a small region of the material under study and obtain information on the distribution of magnetic fields and temperatures, on the processes of interaction of defects with the environment, on the relaxation characteristics of the defects under study. The possibility of obtaining three-dimensional images the sample structure using atomic force microscopy, measurements of a distribution of luminescent centers using confocal spectroscopy, and obtaining magnetic and temperature maps of the studied materials opens up many diverse prospects for the further use of the developed

probe-optical ODMR spectrometers for the diagnosis of nanostructures and biomaterials .

The radio-spectroscopic instrument complex has already been tested in the study of many objects: rare-earth ions in garnet crystals, vacancy defects in SiC, NV-defects in diamond, etc.

This work was supported by the Russian Science Foundation (Project № 20-12-00216)

1. Babunts R.A., Badalyan A.G., Uspenskaya Yu.A., Gurin A.S., Romanov N.G., Baranov P.G.: RF Patent No. 2711228 (2020)
2. Edinach E.V., Uspenskaya Yu.A., Gurin A.S., Babunts R.A., Asatryan H.R., Romanov N.G., Badalyan A.G., Baranov P.G.: Phys. Rev. B **100**, 104435 (2019)

ORAL TALK

Accounting Material Imperfections in the Design of Halbach Magnets

A. Bogaychuk^{1,2}, V. Kuzmin¹

¹ Institute of Physics, Kazan Federal University, Kazan, 420008, Russian Federation

² Tatarstan Academy of Sciences, Kazan, 420111, Russian Federation

aleksandr.bogaychuk@gmail.com

The performance of permanent magnets is limited not only by their design [1], but also by their high sensitivity to temperature and imperfections of magnetic materials. Whereas the first issue, for example, can be solved by temperature stabilization of environment, the issue of material imperfection will always be an individual problem in each magnet construction. This is because there are always production defects which lead to the variation of the magnetization of individual magnet block by 0.1–5% and additionally deviation of the magnetization angle up to 0.9° compared to ideal magnets [2]. These are the reasons why real magnet systems have always strongly reduced homogeneity when compared to calculations and simulations.

In this work we demonstrate an experimental method for the improvement of the magnetic field homogeneity in Halbach array by taking magnet material imperfection into account.

In Fig. 1b the proposed Halbach array composed of 8 elements is showed. Its dimensions are $40 \times 40 \times 102$ mm and weight is 0.6 kg. The filed homogene-

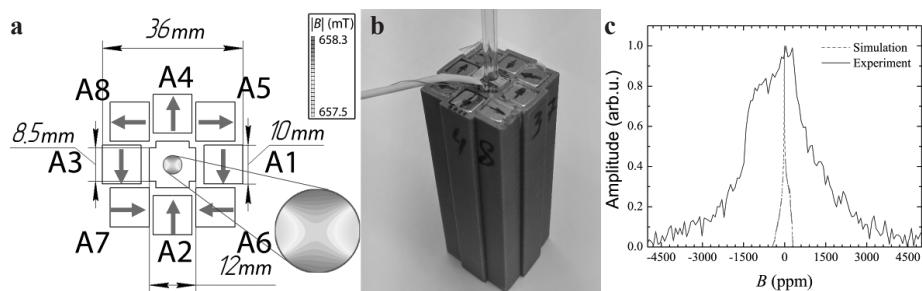


Fig. 1. The Halbach magnet consisted of 8 elements: **a** the drawing and the calculated field map in the sample volume, **b** the photograph of the assembled magnet, **c** the calculated (ideal infinite magnets) and experimentally determined magnetic field distribution in initial configuration.

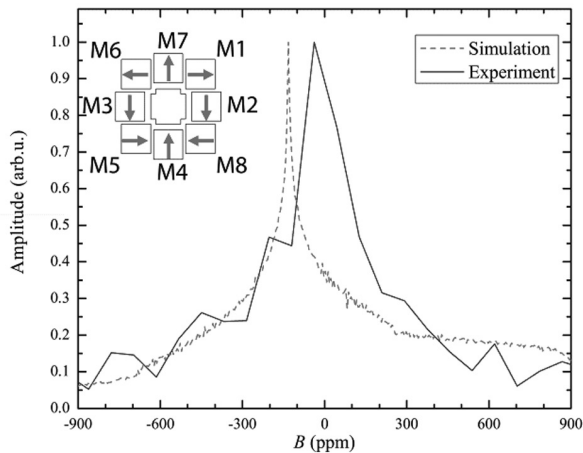


Fig. 2. Computed with neglected angular deviations and measured field distributions in Halbach magnet configuration with the best homogeneity of the magnetic field.

ity was evaluated on a water sample in the working volume with a diameter of 4 mm and a height of 10 mm. The NMR measurements were performed on a home-built pulsed spectrometer [3].

As can be seen from Fig. 1c the experimental field map (solid line) significantly differs from those predicted by the simulation for ideal magnets (dashed line).

The proposed method of field homogeneity improvement relies on determination of the magnetization magnitude for individual magnet blocks based on NMR field measurements in a simplified system which in our case consists of 4 blocks (A1, A2, A3, A4 positions in Fig. 1a). Then a set of configurations with highest homogeneities can be found from simplified field maps simulations of all possible configurations or by applying sophisticated optimum search algorithms if the number of blocks is large. Finally, the residual effect of angular magnetization deviations can be reduced by experimental selection of the best configuration from the set found on simulation step.

By applying the described method we have found the best configuration (Fig. 2) in which the average value of the magnetic field and a half-width were found to be 598.0 mT and 226.9 ppm, respectively. These parameters are sufficient for solid state NMR relaxometry measurements.

1. Müller K.-H., Krabbes G., Fink J., Grub S., Kirchner A., Fuchs G., Schultz L.: *J. Magn. Magn. Mat* **226-230**, 1370–1376 (2001)
2. Blümler P., Casanova F.: *Mobile NMR and MRI. Chapter 5. hardware developments: Halbach magnet arrays*: Royal Society of Chemistry 2016.
3. Kuzmin V., Bogaychuk A., Nekrasov I., Safullin K., Salakhov M., Alakshin E., Klochkov A., Tagirov M.: *Magn. reson. solids* **21**, 1–7 (2019)

SECTION 5

ELECTRON SPIN-BASED METHODS FOR ELECTRONIC AND SPATIAL STRUCTURE DETERMINATION IN PHYSICS, CHEMISTRY AND BIOLOGY

PLENARY LECTURE

Experimental Features of Enhanced Nuclear Magnetic Resonance in Van Vleck Paramagnets

M. Tagirov

Kazan Federal University, Kazan 420008, Russian Federation,
Tatarstan Academy of Sciences, Kazan 420111, Russian Federation

A special class of solid-state magnets – Van Vleck paramagnets – have been studied for quite a long time. The unusual temperature dependence of the magnetic susceptibility of Van Vleck paramagnets, which follows the Curie law at high temperatures and becomes a constant at low temperatures, is due to the fact that the ground state within the lowest magnetic multiplet is either a singlet or a nonmagnetic doublet state. This Van Vleck paramagnetism often occurs in systems of non-Kramer's rare-earth ions (e.g., Pr^{3+} , Eu^{3+} , Tb^{3+} , Ho^{3+} , or Tm^{3+}) in which the crystalline electric field lifts the degeneracy of the J multiplet, giving rise to splitting which are typically of the order of $10\text{--}100\text{ cm}^{-1}$. Because of this splitting observation of electron paramagnetic resonance (EPR) in Van Vleck paramagnets is rare, and has been limited to systems in which the splitting to the first excited levels within the J multiplet is small, or to excited levels within the J multiplet. Usually, however, the conventional EPR microwave frequencies are just too small. Furthermore, to get appreciable changes in the energy splitting of the multiplet sublevels, the Zeeman energy should be of the same order as the crystal-field splitting within the multiplet, and high magnetic fields are necessary. The strong hyperfine interaction makes these substances extremely interesting from the standpoint of studying electronic–nuclear magnetism. The magnetic field induced at the nucleus of the rare-earth Van Vleck ion is by many times higher than the external applied magnetic field, so that the nuclear magnetic resonance NMR frequencies in such systems occupy an intermediate position between the ordinary NMR frequencies and the electron paramagnetic resonance EPR frequencies, and one can therefore speak in terms of a so-called “enhanced” NMR. Intermetallic Van Vleck paramagnets ordinarily have cubic symmetry, while the symmetry of the majority of insulating Van Vleck paramagnets is lower than cubic, so that they are characterized by anisotropy of the effective gyro magnetic ratio of the nuclei of the Van Vleck ions.

Results from enhanced nuclear magnetic resonance (ENMR), which in the absence of direct EPR measurements is one of the principal methods to study the magnetic properties of Van Vleck paramagnets (see reviews by Aminov and

Teplov [1] and Abragam and Bleaney [2]), indicate that the lifetime of rare-earth ions in excited states is rather short and that relatively broad resonances are to be expected. Later, with the help of a superconducting magnet and far-infrared lasers, transitions have been observed between the ground singlet state and each component of the first excited doublet of thulium ethylsulphate. The frequencies used lay in the range 1.04 to 1.18 THz [3].

All magnetically concentrated dielectric Van Vleck paramagnets was intensively investigated by using enhanced nuclear magnetic resonance during more than 65 years mainly in Kazan University as well as in Oxford University. Main problem of spectroscopy and spin kinetics were already solved. At the same time in dilute compounds such experiments was not reliable because of weak signal. Only in last days due to the digital self made experimental set up it became possible to observe and investigate magnetically diluted VV paramagnets. At report it will present a new result in such compound and its will compared with magnetically concentrated VV paramagnets.

This work was financially supported by the Russian Foundation for Basic Research (Grant RFBR 18-42-160012).

1. Aminov L.K., Teplov M.A.: *Usp. Fiz. Nauk* **147**, 49 (1985) [*Sov. Phys. Usp.* **28**, 762 (1985)]; Aminov L.K., Teplov M. A.: *Sov. Sci. Rev. A, Phys. Rev.* **14**, 1 (1990)
2. Abragam A., Bleaney B., *Proc. R. Soc. London A* **387**, 221 (1983)
3. Moll H.P., van Tol J., Wyder P., Tagirov M.S., Tayurskii D.A.: *Phys. Lett.* **77**, 3459–3462 (1996)

INVITED TALK

Enhancing Coordination-Based Copper(II) Spin Labelling for Accurate Distances at Sub-Micromolar Concentrations

**J. L. Wort¹, K. Ackermann¹, A. Giannoulis¹, A. J. Stewart¹,
D. G. Norman², B. E. Bode¹**

¹ Biomedical Sciences Research Complex, and Centre of Magnetic Resonance,
University of St Andrews, St Andrews, KY16 9ST, Scotland, beb2@st-andrews.ac.uk

² School of Life Sciences, University of Dundee, Dundee, DD1 5EH, Scotland

Electron paramagnetic resonance (EPR) distance measurements are making increasingly important contributions to studies of biomolecules underpinning health and disease by providing highly accurate and precise geometric constraints. Combining double-histidine motifs with Cu^{II} spin labels shows promise for further increasing the precision of distance measurements [1], and for investigating subtle conformational changes [2]. It also appeals in proteins containing essential cysteines which can interfere with thiol-specific labelling. However, the non-covalent Cu^{II} coordination approach is vulnerable to low binding-affinity [3]. Here, dissociation constants (K_D) are investigated *via* modulation-depths of relaxation induced dipolar modulation enhancement (RIDME) EPR distance experiments. The superb sensitivity of these experiments reveals low- to sub- μ M Cu^{II} K_D s under EPR distance measurement conditions at cryogenic temperatures. Furthermore, extrapolation of room-temperature ITC-determined K_D s to low temperature using van't Hoff agrees excellently with PDEPR-derived values. We show the feasibility of exploiting the double histidine motif for EPR applications at sub- μ M protein concentrations in orthogonally labelled Cu^{II}-nitroxide systems [4] and investigate factors enhancing the binding affinity.

1. Cunningham T.F., Putterman M.R., Desai A., Horne W.S., Saxena S.: *Angew. Chem. Int. Ed.* **54**, 6330 (2015)
2. Sameach H., Ghosh S., Gevorkyan-Airapetov L., Saxena S., Ruthstein S.: *Angew. Chem. Int. Ed.* **58**, 3058 (2019)
3. Lawless M.J., Ghosh S., Cunningham T.F., Shimshi A., Saxena S.: *Phys. Chem. Chem. Phys.* **19**, 20959 (2017)
4. Wort J.L., Ackermann K., Giannoulis A., Stewart A.J., Norman D.G., Bode B.E.: *Angew. Chem. Int. Ed.* **58**, 11807 (2019)

ORAL TALKS

NMR of ^3He in Contact with Nanoparticles

**E. M. Alakshin¹, G. A. Dolgorukov¹, A. V. Klochkov¹, E. I. Kondratyeva¹,
V. V. Kuzmin¹, K. R. Safiullin^{1,2}, A. A. Stanislavovas¹, M. S. Tagirov^{1,2}**

¹ Kazan Federal University, Kazan 420008, Russian Federation, alakshin@gmail.com

² Institute of Applied Research, 420111, TAS, Russian Federation, murat.tagirov@gmail.com

The study of the spin kinetics of ^3He in contact with nanostructures will be presented.

The spin kinetics data of ^3He in contact with various trifluoride nanosized powders will be presented. Results for LaF_3 nanopowder demonstrated that the nuclear magnetic relaxation of the adsorbed ^3He occurs due to the modulation of dipole-dipole interaction by the quantum motion in the adsorbed two-dimensional film. The analysis of obtained data for PrF_3 nanoparticles testifies in favor of cross-relaxation presence in the nuclear spin-lattice relaxation data, which takes place between ^3He and ^{141}Pr nuclei. The magnetic phase transition in DyF_3 is accompanied by a considerable change in the character of fluctuations of the magnetic moments of dysprosium ions, which affect the spin kinetics of ^3He in contact with the substrate. Significant changes in the relaxations rates of the longitudinal and transverse magnetizations of liquid ^3He have been discovered in the region of magnetic ordering of the solid matrix.

Our group systematically studied the nuclear magnetic relaxation of ^3He in contact with silicate aerogels. The determining role of the adsorbed layer in relaxation processes of gaseous and liquid ^3He was confirmed. It is known that aerogel acts as an impurity and affects phases of superfluid ^3He . Nowadays, it is of interest to study superfluid ^3He in contact with anisotropic aerogels (group of prof. Dmitriev V.V., Moscow). The model of ^3He relaxation in contact with anisotropic aerogels will be proposed.

In recent years nanodiamonds have become a widely investigated material for quantum engineering, biological and electronic applications. The T_1 T_2 relaxation times of ^3He were measured in adsorbed, gas and liquid phases in a detonation nanodiamond sample at the frequency range of 5–18 MHz and at $T = 1.6$ K temperature. Experiments with nanodiamond surface preplated with N_2 or ^4He layers will be presented. The model of ^3He relaxation in contact with detonation nanodiamonds that describes our experimental results will be proposed.

This work was supported by the Russian Science Foundation (project no. 19-72-10061).

Investigations of Substituted Calcium Phosphates for Biomedical Applications Using Double Resonance EPR Techniques

**F. F. Murzakhanov¹, M. R. Gafurov¹, G. V. Mamin¹, S. B. Orlinskii¹,
M. A. Goldberg², S. M. Barinov², V. S. Komlev²**

¹ Kazan Federal University, 18 Kremlevskaya Str., Kazan 420008, Russian Federation, murzakhanov.fadis@yandex.ru

² A. A. Baikov Institute of Metallurgy and Materials Science, Russian Academy of Sciences, 49 Leninsky pr., Moscow, Russian Federation

Orthopedic implants improve the quality of millions patients life every year. Currently calcium phosphate (CP) based bone substitute compounds are most suitable materials in a clinical applications for bone and dental regeneration, repair and replacement. One of their main structural characteristics is an ability to accept a great variety of isomorphous substitutions (Mn^{2+} , Al^{3+} , Mg^{2+} , etc) while retaining the initial space group. These substitutions allow to significantly modify surface reactivity, to promote cell proliferation, contribution to the enhancement of the mechanical properties and to prevent various infections associated with the implantation stage. However, in the domain of bone engineering, doped CPs has not been studied as abundantly as expected. The exact localization of impurity ions, spatial features and interatomic interactions in the CPs based materials are still unclear. A new approaches combining the double electron-electron and electron-nuclear resonance techniques must shed light on the structural insight of the materials under study [1, 2].

The most important and commonly used materials from CPs group are hydroxyapatite (HA), tricalcium phosphate (TCP) and octacalcium phosphate

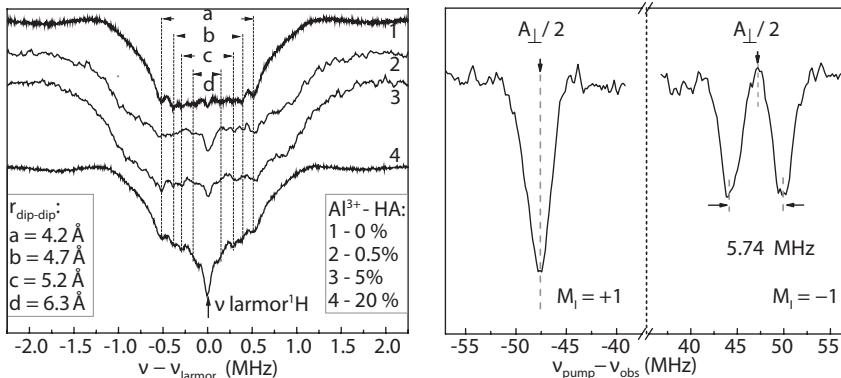


Fig. 1. (left) 1H ENDOR spectra depend on Al^{3+} concentration at W-band (94 GHz), $T = 50$ K. The interatomic distances are calculated in point-dipole approximation; (right) EDNMR spectra for nitrogen radical at $T = 297$ K. The splitting depends on the M_I that confirms the theory of EDNMR transitions.

(OCP) that contain ions with non-zero nuclear magnetic moments (^1H and ^{31}P both $I = 1/2$). In the present study electron nuclear double resonance (ENDOR) method allowed to determine the manganese position in the HA and TCP crystal structures at extremely low concentrations ($x = 0.001$). The thermal transformations of pure HA at different annealing temperatures were clearly detected by ENDOR experiments. Furthermore for Al-doped HA the ENDOR results clearly confirm the possibility of introduction of the high amount of Al^{3+} up to 20 mol.% in the structure due to the creation of vacancy by two protons leave the cell. The same scheme of charge compensation with the trivalent cation introduction was demonstrated and confirmed by ENDOR method for the first time (Fig. 1 left).

It is widely known stable nitrogen radical is routinely spin probe for additional EPR and ENDOR investigations of CP materials [3]. However the ELDOR-detected NMR (EDNMR) method, that based on double electron-electron transitions, significantly expands the capabilities of magnetic resonance approaches to obtain unique structural information [4]. At the present work all experiments were conducted at room temperature ($T = 297$ K) and in X-band range ($\nu = 9.6$ GHz). Under these conditions we have succeeded to measure the value of quadrupole interaction between the nitrogen nuclear and the crystal (electric) field gradient (Fig. 2 right). Owing to the strong anisotropy of EPR signal we successfully carried out selective measurements of quadrupole splitting values depending on angular orientation of nanoparticles. For hydroxyapatite we revealed that the tensors of hyperfine and quadrupole interactions are non-collinear. Since it is known that the quadrupole interaction is sensitive to any changes of crystal field gradients due to impurity ions [4], the EDNMR method opens up new horizons for the investigation of materials doped with various cations.

The work was supported by Russian Foundation for Basic Research grant № 18-29-11086 (magnetic resonance studies), № 18-29-11053 (synthesis of CP) and by the research grant of Kazan Federal University.

1. Dorozhkin S.V.: Progress in biomaterials **5**, 1 (2016)
2. Arcos D., Vallet-Regí M.: Journal of Materials Chemistry B **8**, 9 (2020)
3. Gafurov M., Biktagirov T., Mamin G., Orlinskii S.: Appl. Magn. Reson. **45**, 11 (2014)
4. Goldfarb D.: Emagres **6**, 1 (2007)

On the Manifestation of the Le Chatelier-Braun Principle in Photosystem I Complexes Embedded in Dry Trehalose Matrices

A. Sukhanov¹, M. Mamedov², A. Semenov², K. Salikhov¹

¹Zavoisky Physical-Technical Institute, FRC Kazan Scientific Center of RAS, Kazan 420029, Russian Federation

²A. N. Belozersky Institute of Physical-Chemical Biology, Moscow State University, Moscow, Russian Federation

Disaccharide trehalose prevents protein denaturation caused by freezing, heating, and drying [1]. The existing paradigm of the protective mechanism of the native protein structure by trehalose is based on the assumption that this sugar inhibits protein dynamics [2]. Although this assumption seems to be very interesting, it requires additional details and evidences. Based on our experimental results and analysis of the data available in the literature, we proposed a phenomenological molecular model of the stabilizing and cryoprotective effect of trehalose on the functioning of the reaction center (RC) of photosystem I (PS I) [3]. This model assumes the existence of two pathways for the adsorption of trehalose – endothermic and exothermic, which may differ due to the conformation of this disaccharide or due to the different realization types of formation? of the hydrogen bonds of trehalose with surrounding molecules. In doing so, the effect of trehalose on the functioning of the RC can be explained by the Le Chatelier-Brown principle.

To justify the model, the influence of 4Fe-4S clusters on the spin-lattice relaxation of separated charges in the RC of PS I is of fundamental importance. In this work, using the out-of-phase ESEEM, we measured the distance between the separated charges on the primary donor P_{700}^+ and the phylloquinone acceptor A_1^- in the PS I RC, lacking terminal 4Fe-4S clusters FA and FB, embedded into a dry trehalose matrix. It was shown that this distance does not change when heated from 150 K to room temperature.

This work was supported by the Russian Foundation for Basic Research (project no. 18-43-160017).

1. Palazzo G., Mallardi A., Hochkoeppler A., Cordone L., Venturoli G.: *Biophys. J.* **82**, 558 (2002)
2. Savitsky A., Gupta O., Mamedov M., Golbeck J.H., Tikhonov A., Möbius K., Semenov A.: *Appl. Magn. Reson.* **37**, 85 (2010)
3. Sukhanov A.A., Mamedov M.D., Möbius K., Semenov A.Y., Salikhov K.M.: *Appl. Magn. Reson.* **49**, 1011–1025 (2018)

SECTION 6

MOLECULAR MAGNETS AND LIQUID CRYSTALS

PLENARY LECTURE

EPR Study of Intrinsically Disordered Proteins in Cell

**E. G. Bagryanskaya¹, S. Ovcherenko^{1,2}, O. A. Chinak³,
O. A. Krumkacheva⁴, S. A. Dobrynin¹, V. Tormyshev¹, I. A. Kirilyuk¹**

¹ N. N. Vorozhtsov Novosibirsk Institute of Organic Chemistry SB RAS, Lavrentiev Ave. 9, Novosibirsk 630090, Russian Federation, egbagryanskaya@nioch.nsc.ru

² Novosibirsk State University, Pirogova Str. 2, Novosibirsk 630090, Russian Federation

³ Institute of Chemical Biology and Fundamental Medicine SB RAS, Lavrentieva 8, Novosibirsk 630090, Russian Federation

⁴ International Tomography Center SB RAS, Institutskaya 3A, Novosibirsk 630090, Russian Federation

In this presentation, the peculiarities of applying different spin probes based of sterically substituted nitroxides and triarylmethyl (TAM) radicals to study proteins in cell are discussed. The stability of series of nitroxides and TAMs as well as newly synthesized biradicals aimed to be used as DNP agents was investigated. We used highly stable spin label based on 3-carboxy-2,2,5,5-tetraethylpyrrolidine-1-oxyl (**1**) synthesized by new high yield method for studying the mechanism of Intrinsically Disordered Protein (RL2) penetration into cells using EPR spectroscopy. Intrinsically Disordered Protein (IDP) RL2 is a recombinant analog of human κ -casein fragment, which induces apoptosis of cancer cells with no cytotoxic activity toward normal cells. Spin labeled RL2 was introduced into A549 human lung adenocarcinoma cells. It is shown that spin probe **1** could not penetrate into cells while the attachment of this spin label to human IDP protein, allows us to study spin label stability in A549 human lung adenocarcinoma cells and to follow its transformation inside cells. The stability of spin labels is very high and allows us to investigate the kinetics and changes in the EPR spectra during more than 20 hours. The obtained results showed that the same EPR approach can be used to investigate the kinetics and the mechanism of protein penetrating into cell. It is shown that, reduction-resistant spin labels bound with CPP can be used as DNP agent or EPR tomography. To increase sensitivity the deuteration of the ethyl group in spin label **1** can lead to narrow lines of free nitroxides and increase sensitivity in EPR tomography.

The authors would like to acknowledge financial support by the Ministry of Education and Science of the Russian Federation (state contract No. 14.W03.31.0034).

INVITED TALKS

Tuning the Magnetic Properties of Co(II)-Based Single-Ion Magnets by Magnetic Dilution

**S. L. Veber^{1,2}, J. Nehr Korn³, I. V. Valuev^{1,2}, A. S. Bogomyakov¹,
A. M. Sheveleva^{1,2}, V. I. Ovcharenko¹, M. A. Kiskin⁴, E. A. Suturina^{2,5},
K. Holldack³, A. Schnegg^{3,6}, M. V. Fedin^{1,2}**

¹ International Tomography Center SB RAS, Novosibirsk, Russian Federation,
sergey.veber@tomo.nsc.ru

² Novosibirsk State University, Novosibirsk, Russian Federation

³ Max Planck Institute for Chemical Energy Conversion, Mülheim, Germany

⁴ N.S. Kurnakov Institute of General and Inorganic Chemistry, Moscow, Russian Federation

⁵ University of Bath, Bath, UK

⁶ Helmholtz-Zentrum für Materialien und Energie, Berlin, Germany

Single ion magnets (SIM) are promising unit blocks for ultra-dense data-storage devices and quantum computers. The prerequisite for SIM behavior is large zero-field splitting (ZFS), an intramolecular property. In addition, intermolecular electron spin interactions can strongly influence the macroscopic magnetic properties of SIM bulk materials. When thinking of SIM as a self-sustained device, which can be addressed from outside, the distance between the individual SIMs is the parameter to be controlled when preparing SIM arrays. This urges for an unambiguous determination of inter- and intramolecular electron spin interactions. Spectroscopic methods alone are oftentimes not sufficient to reach this goal. Therefore, magnetic dilution of paramagnetic samples by complexes with diamagnetic ions is a routinely used approach. Yet, as will be shown herein, magnetic dilution, may not only change intermolecular interactions, but also intramolecular properties, determining SIM behavior.

We studied the magnetic properties of the SIM $[\text{Co}(\text{piv})_2(2\text{-NH}_2\text{-Py})_2]$ along with its magnetically diluted analogues with the general formula $[\text{Co}_x\text{Zn}_{(1-x)}(\text{piv})_2(2\text{-NH}_2\text{-Py})_2]$ by XRD, X-band and Frequency-Domain Fourier-Transform THz-EPR (FD-FT THz-EPR) spectroscopy, AC magnetic measurements and quantum chemical calculations (QCC). FD-FT THz-EPR [1] allowed for direct determination of very large ZFS in $[\text{Co}(\text{piv})_2(2\text{-NH}_2\text{-Py})_2]$ and its Zn-diluted analogues down to 10% of Co(II) content. The ZFS was found to be almost constant in the range between 100% to 50% of Co(II) content. However, it drastically decreases from $\sim 75\text{ cm}^{-1}$ to $\sim 50\text{ cm}^{-1}$ while decreasing the Co(II) content below 50%.

The reason for this shift can be rationalized with the help of dilution dependent XRD analyses. XRD showed that dilution with Zn does not only change the average distance between paramagnetic ions, but induces also structural changes at the remaining Co sites. This indicates that $\text{Co}(\text{piv})_2(2\text{-NH}_2\text{-Py})_2$ molecules can be found in one of two geometries which correspond either to Co(II) or Zn(II) lattice. Further evidence could be obtained by QCC, which unveiled that the dilution-induced structural transition in $\text{Co}_x\text{Zn}_{(1-x)}(\text{piv})_2(2\text{-NH}_2\text{-Py})_2$ leads to spin levels inversion of Co(II) ion forming true-SIM spin levels order. This observation was reliably confirmed by X-band EPR and AC magnetometry. The latter also allows one to determine the magnetic relaxation pathways for Co(II) ion spin system in both types of $\text{Co}(\text{piv})_2(2\text{-NH}_2\text{-Py})_2$ geometries.

S.L.V. thanks the Russian Science Foundation (17-13-01412) for support of this work.

1. Nehr Korn J., Holldack K., Bittl R., Schnegg A.: *J. Magn. Reson.* **280**, 10 (2017)

Cation Dynamics in Ionic Liquid Crystals

D. Majhi¹, J. Dai¹, B. B. Kharkov², A. V. Komolkin³, S. V. Dvinskikh^{1,2}

¹ Department of Chemistry, KTH Royal Institute of Technology, Stockholm 10044, Sweden, sergeid@kth.se

² Laboratory of Bio-NMR, St. Petersburg State University, St. Petersburg 199034, Russian Federation

³ Physics Faculty, St. Petersburg State University, St. Petersburg 199034, Russian Federation

Ionic liquid crystals (ILCs) have the typical properties of ionic liquids, as well as nano-scale structures with partial orientational and positional orders. The properties of ILCs are readily modified by selecting cations and anions. The most extensively studied ILCs are based on imidazolium cation. Charge delocalization in the imidazolium core reduced ionic interaction and thus promotes low transition temperatures. The thermal behaviour of ILCs with hydroscopic counter-ions can also be influenced by hydrogen bonding between anion and water. Due to the contribution of the electrostatic interactions, mesophases in ILCs exhibit significantly lower value of the molecular orientational order parameter S as compared to that in non-ionic counterparts.

We report on investigation of the molecular and local bond orientational ordering in a series of ILCs with a fixed imidazolium-based cation and number of anions varying in structure, ionic radius, negative charge localization and hydrogen bonding properties. Molecular and local bond order parameters are estimated via measurement of dipolar spin couplings. A large anisotropy of diamagnetic susceptibility of mesogenic functional groups in ILCs induces macroscopic molecular alignment in the presence of a strong magnetic field of an NMR spectrometer. In this case, NMR spectra are obtained with high resolution and the site-specific anisotropic spin couplings are straightforwardly accessed. We quantify orientational order of C-H bonds of a long-chain imidazolium-based cation in an ionic smectic phase. Molecular order parameter S is also estimated. The observed trends of the bond and molecular order parameter values depending on counter-ion are discussed [1–4].

1. Dai J., Kharkov B.B., Dvinskikh S.V.: *Crystals* **9**, 18 (2019)
2. Dai J., Majhi D., Kharkov B.B., Dvinskikh S.V.: *Crystals* **9**, 495 (2019)
3. Cifelli M., Domenici V., Chizhik V.I., Dvinskikh S.V.: *Appl. Magn. Reson.* **4**, 553 (2018)
4. Dvinskikh S.V.: *Liq. Cryst.*, 2019, <https://doi.org/10.1080/02678292.2019.1647569>.

SECTION 7

OTHER APPLICATIONS OF MAGNETIC RESONANCE

INVITED TALKS

New Insights from the Study of Triplet States

A. Barbon

Department of Chemical Sciences, University of Padova, Via Marzolo 1, 35131 Padova, Italy,
antonio.barbon@unipd.it

Triplet states of organic molecules are involved in a variety of processes and in a wide range of fields, from technology to biology. Despite quite a number of papers have been published in the 60s-70s dealing with such a state, it looks that after so many years the field is still living a green age, and the topic is under revision from many authors. Processes in the past classified as relaxation processes for excited singlets are now considered with care as new ways for the population of these states; the processes can be fine-tuned by a proper design of the molecular system. Also, from a spectroscopic point of view, complications connected with the use of lasers as light sources have been exploited as new tools for obtaining information on the system.

In this contribution, recent studies of charge-transfer Intersystem Crossing (CT-ISC) [1], radical-induced ISC, and enhanced ISC mechanisms [2] will be presented, with a focus on the spin polarization of the triplet state and the opportunities offered by Time-Resolved EPR (TREPR) for the study these processes.

TREPR also offers opportunities to study properties of the excited singlet states with magnetophotoselection experiments [3], which allow to obtain information on the transition dipole moment in the molecular frame directly from isotropic samples.

Examples taken from recent studies on different molecular systems are provided.

1. Hou Y., Zhang X., Chen K., Liu D., Wang Z., Liu Q., Zhao J., Barbon A.: *J. Mater. Chem. C* **7**, 12048–12074 (2019)
2. Zhao Y., Chen K., Akhuseyin E., Li S., Hou Y., Zhang X., Wang, Z. Zhao J., Barbon A., Yaglioglu H., Wu H.: *Che. Europ. J.* **26**, 3591–3599 (2020)
3. Barbon A., Dal Farra M.G., Ciuti S., Albertini M., Bolzonello L., Orian L., Di Valentin M.: *J. Chem. Phys.* **152**, 034201 (2020)

Hydration, Self-Diffusion and Ionic Conductivity of One Charge Cations in Nafion Membranes Studied by NMR

V. I. Volkov^{1,2}, A. V. Chernyak^{1,2}, O. I. Gnezdilov³, V. D. Skirda³

¹ Institute of Problems of Chemical Physics RAS, Chernogolovka, Russian Federation, vitwolf@mail.ru

² Science Center in Chernogolovka RAS, Chernogolovka, Russian Federation

³ Kazan (Volga region) Federal University, Kazan, Russian Federation

The interconnection of transport channel structure, counter ion hydration and mobility in sulfonic cation exchange Nafion membranes as in model system were revealed. The hydration numbers h of H^+ , alkaline and alkaline-earth metal cation were calculated from 1H high resolution NMR [1,2]. The h values are 2 , 6 ± 1 , 6 ± 1 and 0.8 ± 0.2 for H^+ , Li^+ , Na^+ and Cs^+ cation, correspondingly. Self-diffusion coefficients of water molecules and H^+ ions in wide range of temperature and humidity were analyzed [1]. Self-diffusion coefficients of Li^+ , Na^+ , Cs^+ counter ions were measured for the first time by pulsed field gradient NMR technique on $^7Li^+$, $^{23}Na^+$, $^{133}Cs^+$ nuclei. Experimental self-diffusion coefficients and self-diffusion coefficients calculated from translation jump correlation times of counter ions (measured by NMR relaxation techniques) were compared. It was concluded that macroscopic water and ionic transfer is controlled by translational jumping between membrane sulfonate groups [2]. Cation translation mobility is governed by ionic hydration. Cation self-diffusion coefficients are changed in the next row $H^+ \gg Li^+ \leq Na^+ > Cs^+$ in Nafion compare to membrane MSC with more water-absorbing ability [3] and chloride aqueous solutions where $Li^+ < Na^+ < Cs^+$. Low mobility of Cs^+ ion in Nafion is a result of $Cs^+ \rightarrow SO_3^-$ group contact ionic pair forming. Ionic conductivities calculated from self-diffusion coefficients on the basis of Nernst-Einstein equation are in good agreement with experimental values. The similar results were received for other sulfonic cation exchanger polymers [2, 3]. Therefore the detailed NMR investigations gave opportunity to understand the microscopic mechanism of membrane selectivity of sulfo containing membranes to the alkaline metal cations. These results may be a guide for new materials creation.

This work was supported by the Russian Foundation for Basic Research (project no. 18-08-00423 A). NMR measurements were performed using equipment of the Center of Collective Use of the Institute of Problems of Physical Chemistry RAS with the support of State Assignment of the Institute (state registration nos. 0089-2019-0010 and 0089-2019-0002).

1. Chernyak A.V., Vasiliev S.G., Avilova I.A., Volkov V.I.: Appl. Magn. Res. **50**, 667–693 (2019)
2. Volkov V.I., Marinin A.A.: Russ. Chem. Rev. **82** (3), 248–273 (2013)
3. Volkov V.I., Chernyak A.V., Golubenko D.V., Shevlyakova N.V., Tverskoy V.A., Yaroslavtsev A.B.: Membranes and Membr. Technol. **2** (1), 54–62 (2020)

ORAL TALKS

Spin Kinetics of Gaseous ^3He in Nematically Oriented Aerogels at Low Temperatures**V. Kuzmin¹, K. Safiullin¹, A. Stanislavovas¹, M. Tagirov^{1,2}**¹ Institute of Physics, Kazan Federal University, Kazan 420008, Russian Federation, andrey.stanislavovas@gmail.com.²Tatarstan Academy of Sciences, Kazan, 420111, Russian Federation.

Aerogels with open-pore space not only have a wide application in various fields [1] but also present objects of many intensive scientific studies [2–5]. Nowadays, interest in the study of the ^3He -aerogels system increased due to discovery of polar superfluid phases in ordered aerogels [6, 7]. The ballistic mean-free path (mfp) in an aerogel is an important parameter for theoretical models of ^3He superfluidity and can be determined by diffusion experiments, for instance, via magnetic resonance experiments with gradients.

In this work the ^3He gas self-diffusion and relaxation studies were performed in five samples of nematically ordered Al_2O_3 aerogels with different density (82, 125, 180, 597 and 920 mg/cm^3). The samples with higher densities (597 and 920 mg/cm^3) were fabricated from 82 and 125 mg/cm^3 samples, respectively, by the technique described in [8]. The study was carried out using pulsed NMR methods at temperatures of $T = 1.5$ and 4.2 K at frequency of $f_0 = 16$ MHz ($H_0 = 490$ mT) and in constant magnetic field gradient of $G = 2.2$ mT/cm (only for diffusion experiments).

 ^3He gas self-diffusion

The obtained values of ^3He gas diffusion coefficient D in all samples are smaller than expected for the ideal gas in pores of aerogels in low pressure range. It should be noted, that D does not depend on the type of sample surface (raw or covered by N_2 or ^4He) and the observed effect of reduced gas diffusion cannot be explained by the influence of surface diffusion. The simplest Knudsen model, which takes place exactly at low pressure range, cannot describe the suppression of the ^3He diffusion coefficient at low temperatures. Problems with application of Knudsen diffusion model are described by Bhatia and Nicholson [9]. Authors show that Knudsen model overpredicts the value of the diffusivity (or mfp), because it neglects distant van der Waals interactions between the

wall and the diffusing molecules in gas phase. The influence of van der Waals forces on gas diffusion in aerogels was indirectly confirmed by the observed ^3He gas densification.

^3He spin lattice relaxation

The observed values of ^3He spin-lattice relaxation times in gas have an order of magnitude $T_1 \sim 1\text{--}10$ s in all samples with pre-plated surface by ^4He adsorbed layer at 1.5 and 4.2 K. The covering of samples surface by ^4He allows to exclude adsorption of ^3He and the influence of surface relaxation on gas relaxation. Therefore, the ^3He gas relaxation should be governed by other rather weak relaxation mechanisms. It should be noted, that bulk ^3He spin-lattice relaxation time is known to be extremely long and the open-pore structure of aerogels exclude the extensive influence of the mechanism of dipole-dipole relaxation of ^3He gas in restricted geometry considered in [10]. We suppose that the spin-lattice relaxation of gaseous ^3He is governed by atoms motion in inhomogeneous magnetic field created by fibers. We discuss a realization of possible motion regimes [11] in aerogels and a possible sources of inhomogeneity: the paramagnetic centers in the aerogel, the diamagnetic susceptibility of the fibers and a possible existence of “dirty” aerogel fibers surrounded by “clean” fibers. In the latter case the nuclear magnetic relaxation should be governed by the time needed for atoms to diffuse to “dirty” walls (fibers).

More details will be presented in oral report.

This work was financially supported by the Russian Science Foundation (grant RSF 20-42-09023).

1. Akimov Yu.K.: *Instrum. Exp. Tech.* **46**, 287 (2003)
2. Gibbs M. *et al.*: *Physica B: Condensed Matter* **462**, 213 (1995)
3. Candela D., Kalechofsky N.: *J. Low Temp. Phys.* **113**, 3/4, 351 (1998)
4. Alakshin E.M. *et al.*: *JETP Lett.* **104**, 315 (2016)
5. Kuzmin V. *et al.*: *Phys. Chem. Chem. Phys.* **20**, 1476 (2018)
6. Dmitriev V.V. *et al.*: *Phys. Rev. Lett.* **115**, 165304 (2015)
7. Zhelev N. *et al.*: *Nat. Commun.* **7**, 12975 (2016)
8. Volkov V.V. *et al.*: *Instrum. Exp. Tech.* **60**, 737 (2017)
9. Bhatia S.K. and Nicholson D.: *Chem. Eng. Sci.* **66**, 284 (2011)
10. Korb J.P. *et al.*: *J. Chem. Phys.* **98**, 2411 (1993)
11. Pignol G. *et al.*: *Phys. Rev. A* **92**, 053407 (2015)

Magnetoelastic Effect in CoNi Particles Caused by Thermal Resizing of Crystal Substrate

D. A. Bizyaev, A. A. Bukharaev, N. I. Nurgazizov, A. P. Chuklanov, S. A. Migachev

Zavoisky Physical-Technical Institute, FRC Kazan Scientific Center of RAS, Kazan 420029, Russian Federation, niazn@mail.ru

One of the factors defining the magnetic properties of planar particles is mechanical stress. Due to the magnetoelastic effect, stress affect to the magnetic properties, in particular, change the size of the domains of multi-domain particles. Thus, by controlling the uniaxial stress in the particle, it is possible to control its domain structure. In this paper, we studied the change in the size of the magnetic domains of planar CoNi particles having a square shape. For this, computer simulation methods and magnetic force microscopy were used.

For investigation the array of square-shaped CoNi (Co18%, Ni82%) particles ($7.5 \times 7.5 \times 0.03 \text{ mkm}^3$) was formed on the surface of hexagonal LiNbO_3

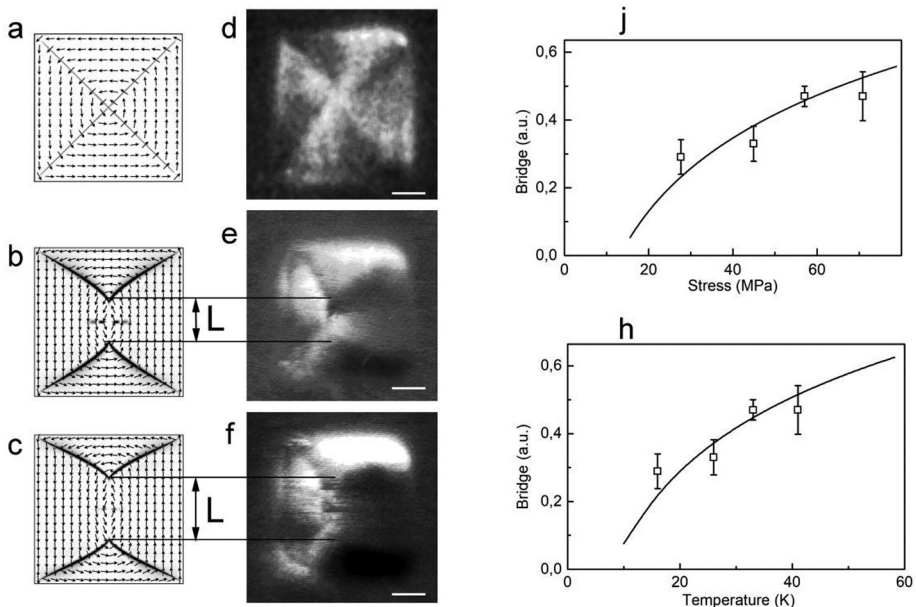


Fig. 1. Magnetization distribution of a CoNi particle ($7.5 \times 7.5 \times 0.03 \text{ mkm}^3$) calculated by OOMMF for K_{eff} values: 0 J/m^3 (a), 1.4 kJ/m^3 (b), 2.2 kJ/m^3 (c). MFM images of the CoNi particle obtained after changing of the substrate temperature on 0 K (d), 26 K (e), 41 K (f). Scale length is 2 mkm . The letter L show a bridge formed as result of influence of mechanical stress. Graphs of the bridge length (L) depending on the mechanical stress (j) and depending on the substrate temperature (h). The solid line is the calculation, the symbols are the experimental data.

crystals with the size of $4 \times 5 \times 6 \text{ mm}^3$. Particles were created by the electron beam evaporation method through metal mesh with square holes, as described in [1]. A magnetic structure of the particle was simulated by the OOMMF [2]. During the simulation, the value of the anisotropy coefficient (K_{eff}) increased sequentially with a step of 100 J/m^3 . Since the modeled particles are polycrystalline, the anisotropy is completely determined by mechanical stresses. Based on K_{eff} value, we can find the value of the mechanical stress (σ) acting on the particle as: $\sigma = 2/3 \cdot K_{\text{eff}}/\lambda_s$, where λ_s is the saturation magnetostriction. As the calculations showed, the unstressed particle ($K_{\text{eff}} = 0$) has a classical four-domain structure (Fig. 1a). As K_{eff} value increases above 300 J/m^3 , domains with direction of magnetization parallel to the anisotropy direction begins to increase and a characteristic bridge (L) is formed between them (Fig. 1b, c). The bridge length is proportional to the area of domains and it can be used for compare of model and experimental images (Fig. 1d–f). The dependence of the bridge length on the value of mechanical stress in the particle was found from calculated images of the magnetization distribution (Fig. 1j).

The scanning probe microscope Solver P47 working in the magnetic force microscope (MFM) mode was used for experimental studies of the particle magnetization. To create uniaxial mechanical stress in the particles, substrate heating was used. It is known that the thermal expansion coefficients of hexagonal LiNbO_3 have different values along different crystallographic axes. Therefore, the dimensions of the crystal in one direction change more than in the other when it heated (or cooled).

This allows to create uniaxial stresses of a predetermined magnitude in particles located on the surface of such a crystal, due to changes in its temperature. Based on the experimental MFM images for each temperature value, the characteristic length of the bridge was found and the mechanical stress created by thermal deformation of the substrate was calculated (Fig. 1h). Due to the technical capabilities of the device, it was possible to change the substrate temperature only within 40 K. It was shown that the dependences of the bridge length on mechanical stress obtained theoretically and experimentally coincide well (Fig. 1j, h). This allows us to conclude, it is possible to precisely change of the magnetic structure of a planar particle by operating the temperature of the crystal substrate.

The sample preparation was partially supported by the Russian Foundation for Basic Research (grant 18-02-00204).

1. Nurgazizov N., Chuklanov A., Biziyayev D. *et al.*: IOP Conference Series: Materials Science and Engineering **699**, 012008 (2019)
2. Donahue M., Porter D.: OOMMF User's Guide, Ver. 1.0. National Institute of Standards and Technology, Gaithersburg, MD, USA (1999). 83 p. <http://math.nist.gov/oommf>

Modern Fundamentals of the Development of Agricultural *Solanum Tuberosum L.* Using Targeted Delivery of Manganese with Novel Bionanocomposites Based on Polysaccharides

**S. S. Khutsishvili¹, A. I. Perfil'eva², O. A. Nozhkina², T. V. Ganenko¹,
N. I. Tikhonov¹, I. A. Graskova², T. I. Vakul'skaya¹**

¹ A. E. Favorsky Irkutsk Institute of Chemistry SB RAS, Irkutsk 664033, Russian Federation, khutsishvili_sp@yahoo.com

² Siberian Institute of Plant Physiology and Biochemistry SB RAS, Irkutsk 664033, Russian Federation

It is known that trace elements, including Mn, occupy an important place in the biochemistry of any plant, and their insufficiency or excess can cause serious diseases and low productivity [1]. The study of biochemical processes and methods for ensuring optimal nutrition of potato crops (*Solanum tuberosum L.*), one of the most important agricultural crops in Russia and around the world, is of great interest to biochemists and plant physiologists. However, despite the scientific experience in this area, still many topical issues remain unresolved. In addition, every year the search for more effective fertilizers that are safe for the environment, especially in the face of climate change, is becoming increasingly important in connection with the problems of healthy diet. Manganese, in particular, is a cofactor of many plant cell enzymes involved in photosynthesis and synthesis of vitamins. Manganese helps to increase the content of sugars and their outflow from the leaves, accelerates plant growth and seed ripening. However, manganese is considered an extremely non-mobile element and in a plant it moves only upward through the xylem to leaves, and, being in the leaves, it is not transferred to other parts of a plant [2].

In this work, we studied and developed a comprehensive modern approach to controlling the qualitative and quantitative effect of manganese during the growing season of potato crops (*Solanum tuberosum L.*), obtaining new information on the mechanism of transformation and migration of biologically significant Mn ions, and developing novel universal trophic low-dose manganese-containing bionanocomposites based on natural polysaccharides (arabinoga-lactan, starch, κ -carrageenan) for targeted delivery of micronutrient fertilizers and plant protection. In the course of the study, several series of potato crops with different manganese contents in the nutrient medium were grown, and the micronutrient fertilizers obtained (bio-nanocomposites) were tested on plants. All plants are characterized by a complex of physiological and biochemical methods. EPR spectroscopy was used as the main method for studying magnetic manganese ions in plant organs (roots, stem, leaves). The structural features of nanocomposites were also characterized by the EPR

method and other modern physicochemical methods, including their biologically active properties for plant protection.

The authors are grateful to the Baikal Analytical Center of Collective Use, SB RAS. The project supported by the Russian Foundation for Basic Research № 20-016-00152.

1. Hopkins W.G., Huner N.P.A.: Introduction to Plant Physiology, 4th edition. New York: J. Wiley & Sons 2008.
2. Graham R.D., Hannam R.J., Uren N.C.: Manganese in Soils and Plants. Developments in Plant and Soil Sciences, vol 33. Dordrecht: Springer 1988.

SECTION 8

PERSPECTIVES OF MAGNETIC RESONANCE
IN SCIENCE AND SPIN TECHNOLOGY.
SPIN-BASED INFORMATION PROCESSING.
THEORY OF MAGNETIC RESONANCE

ORAL TALKS

Magnon Bose Condensed State for Quantum Computing

Yu. Bunkov

Russian Quantum Center, Moscow, Skolkovo 143025, Russian Federation, y.bunkov@rqc.ru.

In this report we will discuss the application of the coherent state of magnons – the Bose-Einstein condensed state for storing and managing quantum information. MBEC is formed in magnetically ordered materials at a sufficiently high concentration of non-equilibrium magnons [1]. The repulsion interaction between magnons is necessary for the stability of mBEC. Otherwise, mBEC loses spatial stability and breaks up into small drops. As a result of this interaction, the magnetic resonance frequency increases with increasing density of non-equilibrium magnons. Due to the repulsion energy, the phenomenon of magnon superfluidity occurs. The resulting energy gap determines the critical Landau velocity for superfluid magnetization flow. The phenomenon of magnon superfluidity has much in common with the phenomenon of superconductivity. In particular, it allows one to construct magnon charge, phase, and flux qubits similar to superconducting qubits. Unlike standard single-particle qubits, quantum information in mBEC states is duplicated in a large number of identical bosonic particles, so it can be considered as a macroscopic qubit. Duplication of quantum information makes them potentially more stable than ordinary qubits, where all quantum information is lost with one error. The advantage of magnetic qubits is that they are insensitive to electrical interference, since they do not contain free electrons. Besides magnon superfluidity exists even at room temperatures. In this case, the question of the temperature range necessary for the stable operation of the magnon qubit remains open. However, it can be significantly higher than the temperature required for the operation of superconducting qubits. The most suitable material for the fabrication of mBEC qubits is the out of plane magnetized Yttrium Iron Garnet film. The properties of magnon qubits and methods of operations on them (quantum gates) were recently considered in [2].

The work was supported by Russian Science Foundation (19-12-00397).

1. Bunkov Yu.M., Safonov V.L.: JMMM **452**, 30 (2018)
2. Bunkov Yu.M.: JETP **158**, 24 (2020)

On Certain Algebraic Properties of the Sub-Block of Zero Field Hyperfine Hamiltonian with Penultimate Total Spin Projection for a Radical with an Arbitrary Set of Spin-1/2 Nuclei and Visualizing its Eigenvalues

D. V. Stass

Voevodsky Institute of Chemical Kinetics and Combustion, Novosibirsk 630090, Russian Federation,
Novosibirsk State University, Novosibirsk 630090, Russian Federation,
stass@ns.kinetics.nsc.ru

Eigenvalue problems for Hamiltonians often lead to algebraic problems too complex to be analytically tractable, and except for the simplest systems of very small or regular structure the problem has to be solved numerically. The reason is that solving a Hamiltonian for a physical system with n free parameters naturally leads to the need to solve an algebraic problem with n free parameters, *e.g.*, derive and solve a secular equation to find the energies of eigenstates as the roots of an n -th order polynomial. The problem then is that, unless the situation is very symmetric, allows a perturbative treatment, or can be physically factored into lower-dimensional subtasks, anything beyond a cubic equation is an analytical dead-end, and one is faced with the usual choice of either resorting to simple model cases with no more than three parameters, or having to go numeric. Here we attempt a somewhat different approach to this complexity for the particular problem of describing the eigenstates of the spin system of an organic radical with electronic spin-1/2 interacting with spin-1/2 nuclei via isotropic hyperfine interaction, as explored in [1]. The paper discusses in details that the “penultimate” sub-block of the hyperfine Hamiltonian in zero field with total electron and nuclei spin projection one step lower than maximum ($M = M_{\max} - 1$) for a radical with an arbitrary set of spin-1/2 nuclei is of key importance for describing recombining spin-correlated radical pairs in zero or weak magnetic field, exemplifying a physically reasonable part representative of pair behavior that still allows a certain analytical insight. In this contribution we shall analyze its general properties for a radical with arbitrary complex isotropic hyperfine structure in zero field, construct a radical pair from such partners and analyze the evolution of this subensemble in zero and weak field, treating Zeeman interaction as perturbation, and describe a simple geometric approach to visualizing the eigenvalues even though they cannot be found analytically.

More specifically, we take a radical with n spin-1/2 nuclei with distinct positive hyperfine coupling constants a_i construct an $(n+1) \times (n+1)$ sub-block with $M = (n - 1)/2$ of its reduced Hamiltonian $\hat{H} \rightarrow 2(\frac{1}{4} \sum_i a_i \hat{I}_i - \hat{H})$ and show that of its $n+1$ roots $\lambda_0 = 0$, $n-1$ of λ_i lie between ordered adjacent pairs of a_i , and the highest one lies beyond the sum of a_i . The $n+1$ eigenvectors form a fully entangled set. Using the guaranteed non-degeneracy of λ_i , we then construct energies and eigenvectors perturbed by $V = \omega_0 S_z$, complement the radical with a second radical partner without nuclei, and show that the probability that a

subensemble of such pairs with all nuclear spins up, starting with singlet electron state, recombines to singlet state is guaranteed linear with ω_0 , while for the mirror block with $M = -(n-1)/2$ and the pair with all nuclear spins down we find identical field dependence of the opposite sign. Thus, for equilibrium nuclear population the linear contributions for mirror-symmetric subensembles compensate each other, and the field dependence is at least parabolic. However, for a polarized nuclear state the compensation may be not complete, and a linear skew proportional to polarization may appear. Then we introduce equivalent nuclei, which brings about degenerate roots of a_q and contracted eigenvectors traceable to pure nuclear functions, introduce nuclei with spin higher than 1/2 as a set of equivalent nuclei, and introduce nuclei in the second partner, and show that the above derivation still holds true. Such an approach explored in [1], although not providing the complete solution, provides useful analytic insights for a representative part of the solution, and may complement the usually needed numerical simulations.

Finally, we show that a simple geometric visualization of the nonzero eigenvalues for a radical with n spin-1/2 nuclei with arbitrary positive couplings a_i is possible: take an n -dimensional hyper-ellipsoid with semiaxes $\sqrt{a_i}$, stretch it by a factor of $\sqrt{n+1}$ along the spatial diagonal $(1,1,\dots,1)$, get the semiaxes of the new hyper-ellipsoid q_i , and obtain the sought n eigenvalues as $E_k = -\frac{1}{2}q_k^2 + \frac{1}{4}\sum_i a_i$. Although this procedure cannot yield analytic expressions for the eigenvalues, it does suggest a way of seeing things that currently can only be solved numerically, which is immensely helpful in unlocking the intuition. This thinking of Hamiltonians in terms of geometric shapes can be a valuable addition to the algebraic toolbox, providing insights that complement the usually inevitable numeric calculations.

1. Stass D.V.: J. Chem. Phys. **151**, 184112 (2019)

Energy Transfer in Spin-Polarized Photo-Excited Triplet States: Two-Site Model

Y. E. Kandrashkin

Zavoisky Physical-Technical Institute, FRC Kazan Scientific Center of RAS, Kazan 420029,
Russian Federation, yuk@kfti.knc.ru

The chemical exchange is known playing a crucial role in evolution of the spin states. The exchange of the transversal magnetization leads to the broadening of the resonance lines, to the changing the line shapes and to the shifting of the resonance conditions observed in magnetic resonance experiments. Generally, these properties are described well by the modified Bloch equations, known as Bloch-McConnell equations. The original Bloch-McConnell equations are applied to the system in the stationary conditions when its spin state remains unchanged in absence of the external MW irradiation. However, this assumption becomes incorrect in the case of the photoexcited spin-polarized molecules when laser flash initiates the reversible intramolecular processes like intramolecular energy transfer processes in covalently tethered chromophores. To investigate the kinetic properties in such a system, the two-site model can be applied.

Based on two-site model, the populations, ρ_{ii} , of the observable triplet state can be described in the interaction representation of the mean spin Hamiltonian H_0 by the following kinetic equations:

$$\partial \rho_{ii} / \partial t = -R(\rho_{ii} - \bar{\rho}_{ii}) - \sum_j K_{ij}(\rho_{ii} - \rho_{jj}).$$

Here, R is the relaxation superoperator, $\bar{\rho}_{ii}$ is the equilibrium density matrix and the rate constant K_{ij} is determined via the energy transfer rate constant k , off-diagonal matrix elements of the alternating part V of the spin-Hamiltonian, and the energy gap between sublevels of $\Delta E_{ij} = H_{ii} - H_{jj}$:

$$K_{ij} = 4k |V_{ij}|^2 / (4k^2 + \Delta E_{ij}^2).$$

These expressions combined with the Bloch-McConnell equations describe well the non-stationary properties of the spin system initiated by the photoexcitation of the molecule. The examination of these equations shows that they can explain several phenomena including the change of the shape of the triplet spectrum, the rise of the net polarization, the anisotropic and multi-exponential decays of the signal, etc. As a result, they can be used for the analytical study and numerical modelling of two-dimensional EPR spectra when the laser flash initiates the reversible energy or charge transfer processes.

The work was supported by the Russian Foundation for Basic Research Project 19-53-53013

Conduction Electron Spin Resonance Study of $\text{Bi}_{1.08}\text{Sn}_{0.02}\text{Sb}_{0.9}\text{Te}_2\text{S}$ Topological Insulator

**V. O. Sakhin, I. I. Gimazov, E. F. Kukovitskii, Yu. I. Talanov,
G. B. Teitel'baum**

Zavoisky Physical-Technical Institute, FRC Kazan Scientific Center of RAS, Kazan 420029,
Russian Federation, sahin@kfti.knc.ru

The magnetism of topological insulators (TI) is due to interplay of magnetic moments from different origin such as doped magnetic moments, intrinsic magnetic moments due to nonmagnetic structural defects, the spins of the surface Dirac charge carriers and of bulk charge carriers. We report here the results of the Conduction Electron Spin Resonance (CESR) studies of $\text{Bi}_{1.08}\text{Sn}_{0.02}\text{Sb}_{0.9}\text{Te}_2\text{S}$ – the 3-dimensional TI with remarkable transport properties/

We studied single crystals of $\text{Bi}_{1.08}\text{Sn}_{0.02}\text{Sb}_{0.9}\text{Te}_2\text{S}$ with no magnetic ions in a structure using the standard X-band ESR spectrometer. Remind, that our previous ESR study [2] of this compound revealed existence of intrinsic magnetic moments that originate from nonmagnetic structural defects. In the course of the present studies by using CESR methods we observed also another kind of magnetic related phenomena in TI. At temperatures below than 16 K in addition to resonance from intrinsic magnetic moments [2] we found a signal consisting of two asymmetric lines at fields of 150–200 Oe. It has a strong dependence on the angle α between the magnetic field and the basal ab plane. The g -factors for both lines were given as follows: $g^2(\alpha) = (g_{\parallel}\cos\alpha)^2 + (g_{\perp}\sin\alpha)^2$, with $g_{\parallel} \approx 26$ and $g_{\perp} \approx 41$ for the first line, whereas for the second one $g_{\parallel} \approx 26$ and $g_{\perp} \approx 46$. Such a large g -factors are due to strong spin-orbital coupling typical for such compounds.

The temperature dependence of integral intensity for both lines contributing to CESR signal follows Curie-like law, which suggests that the signal is due to small metallic particles distributed in bulk of the sample. This assumption allows us to carry out analysis on base of earlier works on tiny metallic particles [3]. We argue that our low field signal corresponds to CESR of nanosize droplets with the electron and hole conductivity which get formed due to the inhomogeneities of forbidden gap randomly distributed in bulk of sample. It worth noting that the low field CESR signals exist on the background of non-resonant microwave absorption curve which reflects the antilocalization regime of magnetoresistance typical for the TI surface.

The work was supported by Foundation for Basic Research (grant 20-02-00910).

1. Kushwaha S.K. *et al.*: Nat. Comm. **7**, 11456 (2016)
2. Sakhin V.O. *et al.*: JETP Letters **109**, 465 (2019)
3. Gor'kov L.P., Eliashberg G.M.: JETP **21**, 940 (1965)

EPR Study of Light-Induced Charges in Ternary Organic Photovoltaic Blend PCDTBT/PC60BM/ICBA

M. N. Uvarov^{1,2}, L. V. Kulik^{1,2}

¹ Voevodsky Institute of Chemical Kinetics and Combustion SB RAS, Institutskaya Str. 3, Novosibirsk 630090, Russian Federation, uvarov@kinetics.nsc.ru

² Novosibirsk State University, Pirogova Str. 2, Novosibirsk 630090, Russian Federation

The ternary composite of an electron donor material – semiconducting polymer PCDTBT and two electron accepting fullerenes PCDTBT/PC60BM/ICBA 1:1:1, as well as the corresponding binary composites PCDTBT/PC60BM 1:2 and PCDTBT/ICBA 1:2, were studied by continuous wave and pulse EPR at a temperature of 80K. Modeling the EPR spectra allowed us to estimate the contributions of PC60BM and ICBA to the light-induced EPR signal of the PCDTBT/PC60BM/ICBA ternary composite as 0.7:0.3. The absence of new lines in the EPR spectrum of the ternary composite, in comparison with the corresponding binary ones, means that the mechanism of the molecular alloy of PC60BM and ICBA, as previously assumed, is not implemented in this system, and the most probable scenario is the existence of two parallel heterojunctions PCDTBT/PC60BM and PCDTBT/ICBA. This conclusion is confirmed by modeling the decay curves of the light-induced EPR upon turning off the light, as well as the out-of-phase electron spin echo from the charge transfer state (the main intermediate of the photoelectric conversion) in these composites. It is noteworthy that in the ternary composite with the same fullerene acceptors, but with a different polymer donor (P3HT), the molecular alloy mechanism of two acceptors is realized [1]. It is likely that the polymer donor has a decisive influence on the morphology and electron-transport properties of such ternary composites. It should be noted that the methods of light-induced EPR and out-of-phase ESE were used for the first time to study ternary donor – acceptor composites [2].

This work was supported by Russian Foundation for Basic Research, grant 19-03-00149.

1. Angmo D. *et al.*: J. Mater. Chem. C **3**, 5541 (2015)
2. Kulik L.V., Uvarov M.N.: Appl. Magn. Reson. (submitted).

Theoretical Basis for Switching a Kramers Single Molecular Magnet by Circularly-Polarized Radiation

A. G. Maryasov¹, M. K. Bowman^{1,2}, M. V. Fedin^{3,4}, S. L. Veber^{3,4}

¹ Novosibirsk Institute of Organic Chemistry of the Siberian Branch of the Russian Academy of Sciences, Novosibirsk 630090, Russian Federation, maryasov@nioch.nsc.ru

² Department of Chemistry & Biochemistry, The University of Alabama, Tuscaloosa, AL 35487, USA, mkbowman@ua.edu

³ International Tomography Center of the Siberian Branch of the Russian Academy of Sciences, 630090 Novosibirsk, Russian Federation, mfedin@tomo.nsc.ru

⁴ Department of Physics, Novosibirsk State University, 630090 Novosibirsk, Russian Federation, sergey.veber@tomo.nsc.ru

The *d*-group Kramers ions, having strong zero field splitting (ZFS) with axial symmetry and a negative *D* value for the ZFS Hamiltonian, are widely considered as candidates for use as single molecular magnets (SMMs). An important need is the means to switch the SMM between its states in a reasonably short and predictable period of time, which is generally not available. We propose an approach, Zeeman-far infrared (ZeFIR) double resonance, in which circularly polarized alternating magnetic fields in the far infrared (FIR) range induce selective magnetic dipole transitions between different Kramers doublets of the SMM and polarized microwave (mw) pulses transfer excitation inside the upper Kramers doublet. A combination of FIR and mw pulses allows unidirectional switching between +*S* and −*S* states of the ion. The proposed approach is considered for a model quartet system with total spin $S = 3/2$, which seems to be the most promising object for selective resonance manipulations of its states by circularly polarized radiation.

SECTION 9

MEDICAL PHYSICS.
MAGNETIC RESONANCE IMAGING

ORAL TALKS

Application of EPR Spectroscopy to Determine the Content of Nitric Oxide in the Brain and Heart of Rats after Some Pathology

**Kh. L. Gainutdinov^{1,2}, V. V. Andrianov^{1,2}, G. G. Yafarova^{1,2},
T. K. Bogodvid², M. N. Paveliev³, N. G. Shayakhmetov⁴,
S. G. Pashkevich⁵, V. A. Kulchitchky⁵**

¹ Zavoisky Physical-Technical Institute, FRC Kazan Scientific Center of RAS, Kazan 420029, Russian Federation, kh_gainutdinov@mail.ru

² Institute of Fundamental Medicine and Biology of Kazan Federal University, Kazan 420008, Russian Federation

³ Danish Research Institute of Translational Neuroscience, Aarhus University, Denmark

⁴ Interregional Clinical Diagnostic Center, Kazan 420101, Russian Federation

⁵ Institute of Physiology of Nat. Acad. of Sci. of Belarus, Minsk 220072, Belarus

Brain ischemia can be caused by a decrease in the oxygen content, which can culminate in ischemic insult defined as acute damage of brain tissue, with a disruption of its functions due to the difficulty or cessation of blood flow to brain areas [1]. It is shown that in the occurrence and development of brain stroke, both the protective role and the destructive role can be attributed to nitric oxide (NO) [2, 3]. Nitric oxide (NO), which is a free radical, is currently considered as a new signal molecule, that regulates the physiological functions of the organism and the metabolism of cells [1, 4]. In animals NO plays an especially important role in the nervous [2, 5, 6] and cardiovascular systems [7, 8]. According to the current understanding the development of cerebral ischemia and the subsequent stroke is associated with impaired cerebral blood flow, as well as violations of its regulation by the NO system [9, 10].

There are many methods of measuring NO production in biological systems. Precise measurement of both the steady concentration of NO and the speed of NO generation in biological systems is a difficult task due to the low activity of NO synthases (NOS) and its short half-life [11]. In the last few years electronic paramagnetic resonance (EPR) proved to be one of the most efficient methods for the detection and quantification of nitric oxide in biological tissues [12, 13, 14]. That is due to the method developed by Vanin et al., in which they used a technique known as spin trapping. Spin trapping is based on the reaction of a radical (in this case NO) with the spin trap. In the subsequent reaction an adduct is formed with a characteristic EPR spectrum. The complex of Fe²⁺ with

diethyldithiocarbamate (DETC) was used to capture NO and to form a stable ternary complex $(\text{DETC})_2\text{-Fe}^{2+}\text{-NO}$ in the animal tissues. Those complexes are characterized by an easily recognizable EPR spectrum with g -factor $g = 2.035 - 2.040$ and a triplet hyperfine structure [14, 15]. The method has a sensitivity of 0.04–0.4 nM, allows direct measurements, and is highly sensitive due to the use of the spin traps. The disadvantages include semi-quantitativity and complicated evolution of the complex of NO with the spin trap [12, 13].

We used EPR spectroscopy to study the dynamics of NO in the brain and heart of rats after modeling a number of pathological processes. The intensity of NO production by EPR spectroscopy was measured using the spin trap technique [12, 15, 16]. The spin trap components were the following: DETC-Na was administered intraperitoneally at a dose of 500 mg/kg in 2.5 ml of water, a mixture of solutions of iron sulphate ($\text{FeSO}_4 \times 7 \text{H}_2\text{O}$, Sigma, USA) at a dose of 37.5 mg/kg and sodium citrate at a dose of 187.5 mg/kg solved in a volume of 1 ml of water per 300 g of the weight of the animal prepared immediately before the injection was injected subcutaneously at the right and left thigh and the rostral part of the interscapular region [5, 15]. As a result, the compound DETC-Fe^{2+} is formed, which forms the stable radical $(\text{DETC})_2\text{-Fe}^{2+}\text{-NO}$ with NO. This $(\text{DETC})_2\text{-Fe}^{2+}\text{-NO}$ complex is characterized by an easily recognizable EPR spectrum with g -factor $g = 2.038$ and a triplet hyperfine structure [2, 15]. The spectra of the complex $(\text{DETC})_2\text{-Fe}^{2+}\text{-NO}$ were measured on Bruker X spectrometers (9.50 GHz) EMX/plus with a temperature module ER 4112HV and ER 200 SRC with a magnetic field modulation of 100 kHz and a modulation amplitude of 2 G, with a microwave power of 30 mW, a time constant of 200 ms and a temperature of 77 K in a finger Dewar of the Bruker company.

By the methods of EPR spectroscopy our team has evaluated effect of ischemic stroke on the intensity of NO production in the tissues of the brain, heart and liver of rats *in vivo* [5]. It was shown that in 5 hours after modeling of ischemia by 5-minute hyperbaric hypoxia double reduction of NO production was observed in the tissues of the hippocampus, heart and liver. Later, a significant reduction of NO content was found in the olfactory bulb and hippocampus of the brain of rats on the 1st and 2nd days after modeling of ischemia simulated by ligation at the level of bifurcation of the common carotid arteries [17, 18]. Earlier, using EPR spectroscopy we found that in the ischemic part of the left hemisphere 5 h after ischemic stroke caused by coagulation in the left middle brain artery, the NO content in the spin trap and R-conformer compositions decreases by 500% and 30%, respectively. This decrease in the NO content remains at 9 and 24 h after the stroke [2]. In the group of animals treated with a blocker of K_{ATP}^+ channels glibenclamide, on the third day after stroke, an increase in NO level of 65% was observed compared to the control, and the introduction of the activator of K_{ATP}^+ channels, diazoxide a day before ischemia has led to a decrease of NO level at all time points on 25–41% [19]. This result demonstrates relationship between K_{ATP}^+ channels and NO in rats with ischemic preconditioning. Studies were also conducted on the dynamics of the NO content in various tissues after various pathologies: heart myocardial infarction [20], pharmacological desympathiza-

tion of the heart [7], limitation of motor activity [16], long-term sensitization [21], spinal cord injury [22].

Supported partially by RFBR (No. 18-515-00003) and partially by BRFFR (B18R-227).

1. Donnan G.A., Fisher M. *et al.*: *Lancet* **371**, 1612–1623 (2008)
2. Gainutdinov Kh.L., Gavrilova S.A. *et al.*: *Appl. Magn. Reson.* **40**, No 3, 267–278 (2011)
3. Terpolilli N.A., Moskowitz M.A. *et al.*: *J. Cereb. Blood Flow Metab.* **32**, 1332–1346 (2012)
4. Vanin A.F.: *Nitric Oxide* **54**, 15–29 (2016)
5. Andrianov V.V., Pashkevich S.G. *et al.*: *Appl. Magn. Reson.* **47**, No 9, 965–976 (2016)
6. Chen Z.Q., Mou R.T. *et al.*: *Med Gas Res.* **7**, No 3, 194–203 (2017)
7. Andrianov V.V., Sitdikov F.G. *et al.*: *Ontogenez* **39**, No 6, 437–442 (2008).
8. Reutov V.P., Okhotin V.E. *et al.*: *Uspekhi Physiol. Nauk* **38**, No 4, 39–58 (2011)
9. Bolanos J.P., Almeida A.: *Biochim. Biophys. Acta.* **1411**, 415–436 (1999)
10. Pacher P., Beckman J.S., Liaudet L.: *Physiol. Rev.* **87**, 315–427 (2007)
11. Csonka C., Pali T. *et al.*: *Brit. J. Pharmacol.* **172**, 1620–1632 (2015)
12. Vanin A.F., Huisman A. *et al.*: *Methods in Enzymology* **359**, 27–42 (2003)
13. Kleschyov A.L., Wenzel P., Munzel T.: *J. Chromatography B* **851** 12–20 (2007)
14. Hawkins C.L., Davies M.J.: *Biochimica et Biophysica Acta* **1840** 708–721 (2014)
15. Mikoyan V.D., Kubrina L.N. *et al.*: *Biochim. Biophys. Acta* **1336**, No 2, 225–234 (1997)
16. Gainutdinov Kh.L., Andrianov V.V. *et al.*: *Biophysics* **58**, No. 2, 203–205 (2013)
17. Andrianov V.V., Yafarova G.G. *et al.*: *Appl. Magn. Reson.* **51**, No 4, 375–387 (2020)

Using of Special MRI-0.4 T for the Selection of Sugar Beets

**Ya. Fattakhov¹, A. Bayazitov¹, A. Fakhrutdinov¹, R. Khabipov¹,
K. Salikhov¹, V. Shagalov¹, A. Kornienko², O. Stognienko²**

¹ Zavoisky Physical-Technical Institute, FRC Kazan Scientific Center of RAS, Kazan 420029, Russian Federation, fattakhov@kfi.knc.ru

² Mazlumov All – Russian Research Institute of Sugar Beet and Sugar, Voronezh, 396030, Russian Federation, kav250240@mail.ru

Until recently, diseases of sugar beet root crops developing during the growing season could be studied only by invasive methods. With the development of magnetic resonance imaging (MRI), which is widely used in medical diagnostics, it became possible to use MRI methods in phytopathology [1]. This allows us to identify consortial relationships in pathosystems and pathogenesis pathways. Compact MRI devices have been created, which can be used in field and vegetative conditions for the diagnosis of diseases in living plants. Modern developments in the field of MRI have made it possible to non-invasively detect the underground symptoms of sugar beet caused by beet cyst nematode and root rot. MRI monitored the synergistic relationship between the two pathogens, providing a new understanding of the interaction of plants and pathogens [2].

Using a prototype developed and manufactured in the laboratory of Methods of Medical Physics of Zavoisky Physical-Technical Institute, FRC Kazan Scientific Center of RAS, a specialized permanent magnet magnetic resonance imaging system with a magnetic field induction of 0.4 T, images of sugar beet root crops in longitudinal and transverse sections were obtained. To obtain images, the T1-weighted images mode was used.

The use of non-invasive MRI methods is a promising direction in plant phytopathology for the diagnosis of latent diseases in the latent stage of development. Using MRI images, you can determine the number of parenchyma rings and predict the productivity of selection samples.

For selection, plant growing, storage and processing, it is necessary to use MRI methods in field and vegetation experiments, selection of the initial selection material of sugar beets for productivity and technological qualities, when stored in sugar bars and processing in sugar factories, for which it is necessary to create mobile compact MRI devices.

1. Borisjuk L., Rolletschek H., Neuberger T.: *The Plant J.* **70**, 1.1, 129 (2012)

2. Hillnhütter C., Sikora R.A., Oerke E.-C., van Dusschoten D.: *J. Exp. Bot.* **63** (2011)

Investigation of Functional Voice Diseases Using MRI and Spectral Voice Analysis Method

M. Fattakhova¹, V. Krasnozhon², R. Khabipov¹, Ya. Fattakhov¹

¹ Zavoisky Physical-Technical Institute, FRC Kazan Scientific Center of RAS, Kazan 420029, Russian Federation, mariam.fattakhova@gmail.com

² Kazan State Medical Academy – Branch Campus of the FSBEIFPE RMACPE MOH Russia, Kazan 420012, Russian Federation, vn_krasnozhon@mail.ru

In recent years MRI has become widespread as a method for diagnosing voice diseases. The main contingent of patients is voice professionals: teachers of universities and schools, vocalists, guides, kindergarten teachers, translators. This group also includes workers in industrial enterprises with high noise, chemical and dust pollution.

MRI can detect both diseases of the organs of voice formation, and concomitant diseases that affect voice formation. The first group includes studies of the physiology of voice formation of professional vocalists [1]. The second group includes: osteochondrosis, hernias of the intervertebral discs of the cervical spine, arthrosis, etc. [2]. A significant group of patients are patients with laryngeal cancer [3]. The technique made it possible to obtain unique information about the size and characteristics of tumor localization, blood flow (with MRI with contrast) for subsequent surgery.

However, in the early stages of functional diseases of the voice, they cannot be diagnosed using standard research methods. Some functional voice diseases are not detected by MRI, but are observed by spectral voice analysis method [4]. We used spectral voice analysis method based on Focusrite Scarlett Solo Studio setup and Fourier analysis. With the combination of two methods – MRI and spectral analysis of voice, good diagnostic results were achieved. The first results obtained by us in the diagnosis of some functional disorders of the voice are presented.

1. Echternach M., Sundberg J., Arndt S., Breyer T., Markl M., Schumacher M., Richter B.: *Logoped Phoniater. Vocol.* **33**, 67 (2008)
2. Alimetov H.A.: *Dissertation – Kazan*, 1995.
3. Maroldi R., Ravanelli M., Farina D.: *Curr. Opin. Otolaryng. Head Neck Surg.* **22**, 131 (2014)
4. Vasilenko Yu.S., Meshcherkin A.P., Pavlikhin O.G., Romanenko S.G.: *Spectral computer voice analysis.* <https://nikio.ru/>

SECTION 10

DIAMOND-BASED QUANTUM SYSTEMS FOR SENSING AND QUANTUM INFORMATION

INVITED TALKS

Color Centers in Diamond for Biological Sensing and Quantum Information

P. Hemmer

Texas A&M University, USA

Diamond Quantum Sensing of Cell Mechanics and Cell Dynamics

Q. Li

Department of Physics, The Chinese University of Hong Kong, Shatin, New Territories, Hong Kong;
Hong Kong Institute of Quantum Information Science & Technology, The Chinese University of Hong
Kong, Shatin, New Territories, Hong Kong, liquan@phy.cuhk.edu.hk

The optical properties of nitrogen vacancy (NV) centers in diamond are sensitive to its spin states, making NV centers effective quantum sensors for applications ranging from condense matter physics to biomedicine. The long spin coherence time of NV center electrons make it particularly attractive in biological applications. The NV centers are particularly sensitive to the magnetic field projected along the NV axis, so that orientation change of a diamond sample (containing NVs) would cause detectable modulation in its optically detected magnetic resonance spectrum, a method known as the vector magnetometry. This method has excellent spatial resolution and measurement sensitivity on the orientation change of NVs in the diamond sample. In this specific application, we show that by recording the three dimensional rotation of nanodiamond (ND) together with the three dimensional translational tracking of the ND trajectories, one can measure the mechanical property of fixed cells, as well as monitor the time dependent activities of live cells. The works are carried out in collaboration with Renbao Liu, Xi Feng, Wenghang Leong, Yue Cui, Kangwei Xia, and Chufeng Liu. We acknowledge funding from CUHK Group Research Scheme (Project No. 31110126); and ANR/RGC (project No. A-CUHK404/18).

Single Nuclear Spin Detection Using Electrical Spin State NV Readout

M. Nesladek

Hasselt University, Belgium

Picoliter NMR Spectroscopy with Diamond NV Centers

V. Acosta

University of New Mexico, USA

Nitrogen-Vacancy (NV) centers in diamond have emerged as a model platform in the field of "quantum sensing", broadly defined as the use of qubit systems to measure environmental parameters. I will discuss ongoing work in my lab to develop new spectroscopic and imaging tools based on diamond quantum sensors. I will focus on recent milestones towards performing Nuclear Magnetic Resonance (NMR) spectroscopy at the picoliter scale (the scale of single cells). These include the use of diamond quantum sensors to perform two-dimensional NMR spectroscopy in a microfluidic chip. I will also outline efforts to improve the spectral resolution and sensitivity of NV NMR spectrometers for the ultimate goal of identifying, quantifying, and monitoring molecular composition under physiological conditions.

Optically Hyperpolarized Nanodiamonds: Applications in Accelerated NMR and Sensing

A. Ajoy

UC Berkeley, Berkeley, USA

NMR spectroscopy, and its imaging counterpart (MRI), is one of the shining successes of the human scientific enterprise. Fundamentally a technique to probe nuclear spins, NMR provides a chemically specific and non-invasive spectroscopic means to peer into local chemical bonding environments and dynamics. However, NMR suffers from *poor resolution* and *low sensitivity*, factors that have locked it up in “central facilities” and prevented its wider use. These restrictions stem from inefficiencies in spin polarization and detection in conventional NMR.

I will describe a new paradigm of NMR that promises to overcome these limitations. Spin polarization and detection are now carried out by light, harnessing “*quantum-sensors*” constructed out of diamond nanoparticles. In particular, I will describe how quantum sensors can be exploited to “*hyperpolarize*” nuclear spins with light, boosting their magnetic resonance signatures by several orders of magnitude. They can also allow sensitive NMR detection over *nano-* and *meso-*scale volumes at high spatial and frequency resolution. Together this opens exciting new avenues ranging from signal enhanced NMR/MRI devices, optical NMR probes of interfaces, transportable nanoscale NMR detectors, and also opens new forays into many-body spin engineering for quantum information science.

Coherent Control of the Single Photon Interaction with Atomic and Nuclear Ensembles of Quantum Emitters in Solids

**Y. Shi¹, A. Akimov¹, P. Hemmer^{1,2,3}, A. A. Kalachev^{3,4}, F. G. Vagizov^{4,3,1},
Y. V. Radeonychev⁵, O. Kocharovskaya¹**

¹ Department of Physics and Astronomy

² Department of Electrical and Computer Engineering, Texas A&M University, TX: 77843, USA,
kochar@physics.tamu.edu

³ Zavoisky Physical-Technical Institute, FRC Kazan Scientific Center of RAS, Kazan 420029,
Russian Federation

⁴ Kazan Federal University, 420008, Russian Federation

⁵ Institute of Applied Physics, Russian Academy of Sciences, 603950, Russian Federation

On-chip quantum optical network's platform based on quantum emitters in solids (such a color centers in diamond or rare-earth ions in crystals) has two important advantages over a leading superconducting qubits platform. Both of them are based on higher photon's frequency. These are the possibility of tight focusing (resulting in miniaturization of quantum circuits) and orders of magnitude higher bandwidth (resulting in higher operation speed).

In spite of the big progress achieved in coherent control of a quantum interface of the single photon with the individual quantum emitter in solids, control of its interface with an ensemble of such emitters remains a challenging task. In particular, all-optical ensemble based quantum memories were not realized yet in solids. One reason for it is a presence of the large inhomogeneous broadening. In this talk we'll discuss the prospects for achieving such interface, in vacancies with inversion symmetry in diamond (such as SiV, GeV, SnV), in particular, for realization of an all-optical quantum memory, based on spatially chirped control field [1].

Both advantages discussed above could be further pushed to their extreme if gamma-photons instead of optical photons and nuclear instead of atomic transitions in solids could be used. The additional advantages in using of nuclear transitions are their insensitivity to external perturbations of the electric and magnetic fields and presence of the strong zero phonon line even at room temperature. At the same time absence of the intense coherent sources in this range makes an implementation of such control difficult.

We'll discuss our recent demonstration of an acoustic control of the nuclear transition frequency via the Doppler effect [2] and our recent proposals for realization of quantum nuclear memories [3].

The work was supported by the National Science Foundation (NSF grant numbers: PHY-2012194 and PHY-150-64-67). AAK, PH, and YVR acknowledge a financial support from the Government of the Russian Federation (Mega-Grant No.14.W03.31.0028). YVR and FGV appreciate a support by support by the Russian Foundation for Basic Research (RFBR, Grants No. 18-32-00774 and

No. 19-02-00852), as well as by the Ministry of Science and Higher Education of the Russian Federation under Contract No. 14.W03.31.0032. YS is supported by the Herman F. Heep and Minnie Belle Heep Texas A&M University Endowed Fund held/administered by the Texas A&M Foundation.

1. Zhang X., Kalachev A.A., Kocharovskaya O.: *Phys. Rev. A* **90**, 052322 (2014)
2. Zhang X., Liao W.-T., Kalachev A.A., Shakhmuratov R.N., Scully M.O., Kocharovskaya O.: *Phys. Rev. Lett.* **123**, 250504 (2019)
3. Radeonychev Y.V., Khairulin I.R., Vagizov F.G., Kocharovskaya O.: *Phys. Rev. Lett.* **124**, 163602 (2020)

Prospects of Tin Vacancy Centers in Diamond for Quantum Sensing and Information

C. Becher

Fachrichtung Physik, Universität des Saarlandes, Campus E2.6, 66123 Saarbrücken, Germany

Quantum bits based on solid-state spins are promising and potentially scalable systems for the implementation of quantum technologies ranging from quantum information processing to quantum-enhanced sensing and metrology. Ideally, they combine individually addressable spins with very long coherence times, optical emission spectra with narrow homogeneous and inhomogeneous broadenings and bright single-photon emission. In this respect, impurity-vacancy color centers in diamond based on group-IV elements (SiV, GeV, SnV, PbV) have emerged as interesting systems promising to combine all desired favorable properties.

Among these centers, the recently discovered negatively charged tin-vacancy center (SnV⁻) in diamond combines high brightness single photon emission [1, 2], large Debye-Waller factors and Fourier-limited linewidths [3, 4]. Furthermore, the ground state fine structure splitting exceeds 800 GHz which potentially suppresses phonon mediated decoherence of the lowest ground state's spin doublet, which is the predominant decoherence mechanism for other negatively charged group-IV – vacancy centers (Silicon-vacancy center (SiV⁻) and germanium-vacancy center (GeV⁻)). We here report on spectroscopy and on all-optical coherent manipulation of the SnV spin states. We observe narrow resonances for a coherent population trapping scheme which should enable all-optical magnetic field sensing.

1. Iwasaki T. *et al.*: Phys. Rev. Lett. **119**, 253601 (2017)
2. Tchernij S.D. *et al.*: ACS Photonics **4**, 25802586 (2017)
3. Trusheim M.E. *et al.*: Phys. Rev. Lett. **124**, 023602 (2020)
4. Görlitz J. *et al.*: New J. Phys. **22**, 013048 (2019)

Quantum Photonics with hBN – from Fundamental Studies to Emerging Applications

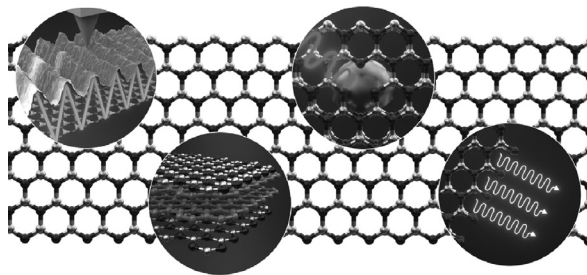
I. Aharonovich

University of Technology Sydney, Ultimo, NSW, 2007, Australia,
ARC Centre of Excellence for Transformative Meta-Optical Systems

Engineering robust solid-state quantum systems is amongst the most pressing challenges to realize scalable quantum photonic circuitry. While several 3D systems (such as diamond or silicon carbide) have been thoroughly studied, solid state emitters in two dimensional (2D) materials are still in their infancy.

In this presentation I will discuss single defects in an emerging 2D material – hexagonal boron nitride (hBN) that as promising qubits for quantum photonic applications. In particular, I will focus on ways to engineer these defects deterministically using either chemical vapour deposition growth or ion implantation, and show results on strain tuning of these ultra bright quantum emitters.

I will then highlight promising avenues to integrate the single defects with photonic cavities, as a first step towards integrated quantum photonics with 2D materials. I will summarize by outlining challenges and promising directions in the field of quantum emitters and nanophotonics with 2D materials.



Photonic Crystal Cavities for GeV SnV Diamond

A. Akimov

Texas A&M University, College Station, 77840, TX, USA, akimov@physics.tamu.edu

Color centers in diamond attract a lot of attention due to unique properties of diamond, such its optical and chemical purity, low concentration of nuclear spins in diamond matrix and also its physical and chemical inertness. Nitrogen vacancy (NV) color centers in diamond is the most studied color center in diamond because its fluorescence rate does depend on spin state this way enabling readout of the spin state. This property opens a lot of opportunities to for its implementation in quantum information processing [1] and sensing [2] applications. Nevertheless, NV color center has number of important disadvantages, such as broad emission spectrum dominated by phonons sideband with only 5% emission in zero-phonon sideband. Another problem is its high sensitivity to surface and structural defects in diamond often introduced by surrounding nanostructures. These disadvantages stimulated search for other color centers, which would have narrow spectrum dominated by zero-phonon line and better behavior in nanostructures.

The silicon-vacancy (SiV) center was suggested as such a center. Due to high symmetry of this center, it does not have dipole moment in the ground state and therefore is not as sensitive to various surface defects and damages as NV center. Moreover, it happens to have narrow zero-phonon line dominating the spectrum. However, unfortunately, excited state decay of this center is dominated by non-radiative relaxation. The next natural candidate is germanium-vacancy (GeV) center since Ge is right under Si in the Mendeleev table. This color center is expected to have less non-radiative decay and therefore could be good replacement for SiV. The key advantage of the group IV color centers in diamond is there relatively low sensitivity to the damages, created by nanofabrication. This opens unique opportunity to use this color centers with nanostructures photonic. It been already successfully demonstrated, that SiV containing nanocavities may significant advance performance of the color centers, making many quantum information processing possible [3, 4]. In our work we are trying to make the next step in the development for such a device by integrating nanodiamonds, containing GeV color center with photonics devices out of more conventional for industry materials.

Another application of GeV color center developed by my group is temperature sensing. Again, the absolute record in combination of spatial resolution and sensitivity in measurement of magnetic fields and temperature belong to NV color centers in diamond. But these measurements require use of microwave radiation of Watts level which somewhat limits its applications in bioscience.

We found that GeV allow different, microwave-free all-optical way of temperature measurements which is already found some application in bio community.

1. Doherty M.W., Manson N.B., Delaney P., Jelezko F., Wrachtrup J., Hollenberg L.C.L.: *Phys. Rep.* **528**, 1 (2013).
2. Ofori-Okai B.K., Pezzagna S., Chang K., Loretz M., Schirhagl R., Tao Y., Moores B.A., Groot-Berning K., Meijer J., Degen C.L.: *Phys. Rev. B – Condens. Matter Mater. Phys.* **86** (2012)
3. Sipahigil A., Evans R.E., Sukachev D.D., Burek M.J., Borregaard J., Bhaskar M.K., Nguyen C.T., Pacheco J.L., Atikian H.A., Meuwly C., Camacho R.M., Jelezko F., Bielejec E., Park H., Lončar M., Lukin M.D.: *Science* **354**, 847 (2016)
4. Sukachev D.D., Sipahigil A., Nguyen C.T., Bhaskar M.K., Evans R.E., Jelezko F., Lukin M.D.: *Phys. Rev. Lett.* **119**, 223602 (2017)

Fiber-Optic Diamond-Based Biothermometry

A. Zheltikov

TAMU/MSU/RQC, Moscow, Russian Federation

Sensitive Magnetometry in Challenging Environments

**Kai-Mei C. Fu¹, G. Z. Iwata^{2,3}, A. Wickenbrock^{2,3},
D. Budker^{2,3,4}**

¹ University of Washington, Physics Department and Electrical and Computer Engineering Department, Seattle, WA, 98105, USA

² Helmholtz-Institut, GSI Helmholtzzentrum für Schwerionenforschung, 55128 Mainz, Germany

³ Johannes Gutenberg-Universität Mainz, 55128 Mainz, Germany

⁴ Department of Physics, University of California, Berkeley, CA 94720-7300, USA

State-of-the-art magnetic field measurements performed in shielded environments with carefully controlled conditions rarely reflect the realities of those applications envisioned in the introductions of peer-reviewed publications. Nevertheless, significant advances in magnetometer sensitivity have been accompanied by serious attempts to bring these magnetometers into the challenging working environments in which they are often required. In this talk, we take a look at the ways in which various magnetometer technologies (mostly, NV-diamond and alkali-vapor magnetometers) have been adapted for use in challenging environments.

ORAL TALKS

Development of Upconversion YVO_4 $\text{Yb}^{3+}\text{Er}^{3+}$ Nanoparticles for Biological Applications

**V. G. Nikiforov¹, D. K. Zharkov¹, A. G. Shmelev¹, A. V. Leontyev¹,
V. S. Lobkov¹, M. H. Alkahtani², P. R. Hemmer^{1,3}**

¹ Zavoisky Physical-Technical Institute, FRC Kazan Scientific Center of RAS, Kazan 420029, Russian Federation

² The National Center for Applied Physics, KACST, PO Box 6086, Riyadh 11442, Saudi Arabia

³ Institute for Quantum Science and Engineering (IQSE) and Department of Physics and Astronomy, Texas A&M University, College Station, TX 77843-4242, USA

We have synthesized YVO_4 : Yb, Er nanoparticles (NPs) with sizes in the range of 10–700 nm. The NPs exhibit bright green luminescence under laser excitations at 257 and 980 nm due to emission from excited levels of Er^{3+} ions. In the downconversion mode, vanadate groups VO_4^{3-} act as sensitizers for UV radiation with an energy transfer to Er^{3+} ions. The upconversion mode occurs under laser irradiation at 980 nm. In this case, Yb^{3+} ions are sensitizers, and Er^{3+} ions excitation results from a two-quantum inter-ion energy transfer. It appears that the efficiency of non-radiative multiphonon transitions is low because of the absence of radiative ${}^4\text{I}_{11/2} \rightarrow {}^4\text{I}_{15/2}$ transitions in Er^{3+} ions at 660 nm. At the same time, under intense irradiation, a wide band in the range of 625–700 nm was observed, which we believe to be the emission of NP crystal lattice defects. An important result of the work is that in the upconversion mode, the luminescence in an aqueous colloidal

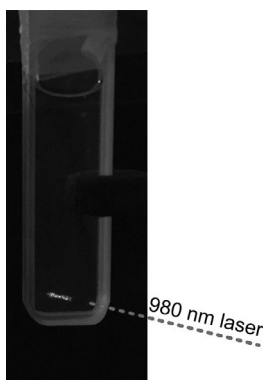


Fig. 1. Photograph of the luminescence in aqueous colloidal solution of YVO_4 : Yb, Er NPs under 980 nm laser irradiation.

solution of NPs was low-sensitive to surface quenchers (Fig. 1). It seems to be that the YVO_4 : Yb, Er NPs are well protected from surface quenchers due to their low defect structure. This interesting fact needs further experimental validation, because it looks very promising to offer advantages over the conventional NPs based on fluoride nanocrystals. As the matter of fact, the synthesized YVO_4 : Yb, Er NPs efficiently producing visible light via upconversion under NIR excitation in the aqueous environment show usefulness for a wide range of biological application.

Biocompatibility Testing of Vanadate Oxide Based Upconversion Nanoparticles with *Helix Lucorum* Grape Snails

**A. G. Shmelev¹, V. G. Nikiforov¹, D. K. Zharkov¹, V. V. Andrianov^{1,2},
L. N. Muranova^{1,2}, A. V. Leontyev¹, Kh. L. Gainutdinov^{1,2}, V. S. Lobkov¹,
P. R. Hemmer^{1,3}**

¹ Zavoisky Physical-Technical Institute, FRC Kazan Scientific Center of RAS, Kazan 420029, Russian Federation, sgartjom@gmail.com

² Institute of Fundamental Medicine and Biology, Kazan (Volga Region) Federal University, Kazan 420008, Russian Federation

³ Institute for Quantum Science and Engineering, Department of Physics and Astronomy, Texas A&M University, TX 77843-4242, College Station, USA

Fluorescence microscopy is a powerful tool for studying real-time biological processes in cells and tissues with high spatial resolution, and sensitivity down to the level of single molecules [1]. In the last decade, luminescent nanoparticles have been actively studied [2]. Progress in the methods of nanoparticle synthesis makes it possible to create nano-phosphores free from blinking and reliably protected from quenchers. This makes it possible to use nanoparticles for non-invasive visualization, characterization and control of biological processes at the cellular and molecular levels.

We synthesized upconversion nanoparticles (UCNP) $\text{YVO}_4: \text{Yb}, \text{Er}$ (size distribution 10 to 700 nm) that absorbs 980 nm light and emits typical Er spectrum (about 520 – 560 nm) [3]. We tested biocompatibility of the UCNPs by model animal *Helix lucorum* grape snail. We used active snails, weight about 25 g, fed 2 weeks in wet atmosphere at room temperature (18–22°C). Colloidal mixture of UCNPs in water (doses are 16 mg/kg and 200 mg/kg of



Fig. 1. Snail nervous system microphotography with optical fiber (left) and upconversion nanoparticles in the tissue illuminated by 980 nm laser through fiber (right).

UCNPs per animal weight) was injected into the snails through sinus node for minimal pain and damage to the snail. One day after injection, before tissue extraction, snails showed no difference in movements and behavior. For tissue extraction snails was anesthetized by ice-water mixture. We extracted samples of liver, skin, nervous system and heart and tried to find UCNPs luminescence by 980 nm diode laser excitation observing samples through microscope with pump radiation absorbance filter, and recording pictures by Canon EOS 650D camera. We found several nanoparticles in nervous system (Fig. 1) and no one in the of liver or skin.

So we made first tests of biocompatibility on model animals (*Helix lucorum* grape snail). The UCNPs are injected into the animals and we found some of them into the animal body (into the nervous system). Unfortunately achieved signals was very weak, so we need to search particles in confocal regime and test another sizes and types of UCNPs.

The financial support of the Foundation for Basic Research (grant 19-02-00569 and 20-02-00545 for spectroscopic study) is gratefully acknowledged. The synthesis of nanoparticles was supported by a grant from the Government of the Russian Federation under order no. 220, contract no. 14.W03.31.0028 with the Zavoisky Physicotechnical Institute.

1. Yan L., Zhao F., Li S., Hu Z., Zhao Y.: *Nanoscale* **3**, 362 (2011)
2. Wolfbeis O.S.: *Chem. Soc. Rev.* **44**, 4743 (2015)
3. Leontyev A.V., Zharkov D.K., Shmelev A.G., Nikiforov V.G., Lobkov V.S.: *Bull. of the RAS: Physics.* **83**, 1484 (2019)

Fluorescent Properties of Diamonds Doped with Germanium and Erbium

**D. K. Zharkov¹, A. G. Shmelev¹, A. V. Leontyev¹, V. G. Nikiforov¹,
R. I. Khaibullin¹, M. H. Alkahtani², P. R. Hemmer^{1,3}**

¹ Zavoiisky Physical-Technical Institute, FRC Kazan Scientific Center of RAS, Kazan 420029, Russian Federation, dzharkov@list.ru

² The National Center for Laser and Optoelectronics, KACST, Riyadh, 11442, Saudi Arabia

³ Institute for Quantum Science and Engineering (IQSE) and Department of Physics and Astronomy, Texas A&M University, College Station, 77843-4242, USA

Ultrathin surface layers (with a thickness of not more than 50 nm) with different color centers were obtained by ion doping of diamond with accelerated ion energies of less than 100 keV. In particular, ions of chemical elements (Ge and Er) were implanted into pure (non-impurity), nitrogen-containing, boron-containing or flint-containing diamond layers, as well as into dry suspensions of nanodiamonds obtained with a diamond anvil. The nanodiamonds synthesized in diamond anvil cells were dispersed in water using an ultrasonic bath and stabilized with polyvinyl acetate. A droplet with a dispersion of nanodiamonds was placed on a coverslip and dried during continuous rotation (spin-coating) for uniform distribution of nanodiamonds on the coverslip. A cover glass with nanodiamonds was placed on a glass slide so that the nanodiamonds remained between the cover glass and the slide. When NV color centers were excited in nanodiamonds using 532 nm laser radiation, fluorescence was recorded in the region of 600–700 nm with a characteristic spectral distribution. The pump radiation was blocked by an interference filter at the input of the radiation registration unit. The spectrum was obtained using a CCD camera, while the pump radiation was focused on a single nanodiamond. The fluorescence spectra of a diamond substrate implanted with germanium were recorded at liquid nitrogen temperature and at room temperature. At a higher temperature, a shift in the fluorescence spectrum to a shorter wavelength region is noticeable. Another interesting feature of this object is the very long-term fluorescence. After turning off the laser radiation, the fluorescence of the excited region of the object continues for several minutes. This phenomenon requires additional research and modernization of equipment for recording long-term luminescence dynamics.

This work was supported by the Mega-grant of the Government of the Russian Federation (Agreement No.14.W03.31.0028)

POSTERS

SECTION CHEMICAL AND BIOLOGICAL SYSTEMS

Kinetics of Paramagnetic Centers Formation in the Calcium Gluconate Subjected to Mechanochemical Treatment

**M. M. Akhmetov¹, G. G. Gumarov¹, V. Yu. Petukhov¹,
G. N. Konygin², D. S. Rybin²**

¹ Zavoisky Physical-Technical Institute, FRC Kazan Scientific Center of RAS, Kazan 420029, Russian Federation, mansik86@mail.ru

² UdmFRC Ural Branch of RAS, Physical-Technical Institute, Izhevsk 426067, Russian Federation, dsrybin@mail.ru

In the calcium gluconate subjected to mechanochemical treatment, the formation of paramagnetic centers (PC) was detected, which were responsible for the appearance of an EPR signal with $g = 2.005$ and a line width of ~ 8.5 G [1]. It was previously established that an increase in the grinding time leads to the accumulation of the number of these centers. However, it is also known that the interaction of radicals arising from mechanical activation with environmental components can significantly affect their appearance and stabilization [2]. In this case, radical acceptance is also possible, preventing further free radical reactions due to changes in the structure of the molecule. The aim of this work was to

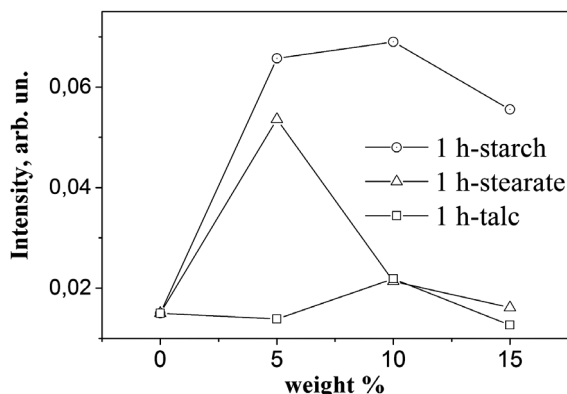


Fig. 1. Dependence of CG EPR line intensity on the amount of additives (weight %).

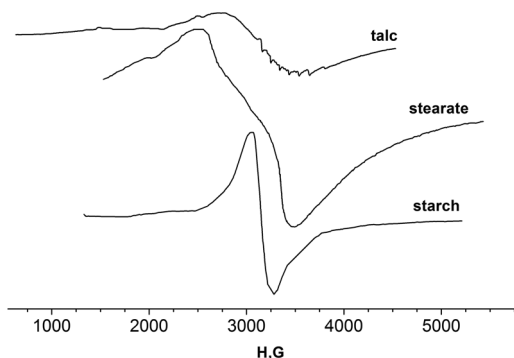


Fig. 2. EPR spectra of excipients (9.5 GHz, $T = 300$ K).

study the effect of additives (excipients) included in the official calcium gluconate (CG) on the formation and accumulation of paramagnetic centers during the mechanical activation of CG. Mechanically activated samples of CG with excipients (talc, starch and calcium stearate) included in the commercial dosage form were obtained by mixing powders of the appropriate weight.

Studies have shown that the concentration of PC that appear in CG as a result of its mechanochemical treatment substantially depends on the type and amount of added additives. As can be seen from Fig. 1, the addition of starch and calcium stearate in an amount up to 5 wt.% significantly increases the intensity of the EPR signal (4 times at $t = 1$ h). A further increase in the amount of starch to 15 wt.% practically does not affect the amplitude of the EPR signal. At the same time, the addition of talc up to 15 wt.% practically does not increase the intensity of the EPR line, regardless of the time of mechanochemical treatment.

To clarify the direct effect of the introduced additives on the changes in the observed spectra, EPR spectra were separately recorded from the powders of the initial excipients and after their mechanical activation. Fig. 2 shows the EPR spectra of the powder of the initial starch and this sample subjected to mechanical activation with different durations. It can be seen from the spectra presented that starch is a paramagnet, and mechanical treatment leads to the appearance of additional paramagnetic centers. However, the parameters of these EPR spectra differ significantly from the parameters of the spectrum of the free radical arising from the mechanical treatment of calcium gluconate. In particular, the g -factor and line width of the original powder and this starch powder after mechanical activation ($t = 10$ min) are $g_K = 2.162$, $\Delta H_K \approx 265$ G and $g_{KMA} = 2.51$, $\Delta H_{KMA} \sim 2000$ G, respectively. Similar results of EPR studies were also revealed for other excipients of officinal calcium gluconate. The EPR spectra of both the initial and mechanically activated samples of calcium stearate and talc are also fundamentally different from the line observed for mechanically activated CG.

Thus, it was found that the intense line observed in the EPR spectrum with $g \approx 2.005$ and a width of ~ 8 G from mechanically activated binary composi-

tions is a line from calcium gluconate and is not a superposition of lines due to excipients present in the compositions. At the same time, the amplitude of the line from mechanically activated CG (and, consequently, the concentration of paramagnetic centers in it) largely depends on both the type of excipient and its concentration. Most likely, the role of excipients is to weaken the process of recombination of radicals and their stabilization immediately upon their occurrence. This is indicated by the fact that among the excipients examined, starch, which significantly enhances the EPR signal with $g \approx 2.005$, is at the same time a high molecular weight compound.

1. Gumarov G.G., Petukhov V.Yu., Konygin G.N., Rybin D.S., Zheglov E.P.: Clinical Medicine Almanac **17**, Part 1, 47 (2008)
2. Baramboim N.K.: Mechanochemistry of macromolecular compounds. - M.: Khimiya, 1970. p. 357.

Quantification of Protein Aggregation using NMR Relaxation of Nuclei of Water and Ions: a Study of the RRM2 Domain of TDP-43 Protein

S. O. Rabdano¹, S. S. Bystrov², C. Cabal³, V. I. Chizhik²

¹ Lab. of Biomolecular NMR, SPbSU, St. Petersburg, Russian Federation, sevastyan.rabdano@spbu.ru

² Faculty of Physics, SPbSU, St. Petersburg, 198504, Russian Federation

³ Faculty of Physics, Havana University, Havana, Cuba

The contemporary set of biophysical and biochemical tools possess a lot of possible ways to study protein aggregation. The magnetic resonance methods such as NMR and EPR are prominent techniques that allow the determination of parameters of structure and dynamics of biomolecular systems under native solution conditions. They usually utilize signals from atoms in the biomolecules, however, for aggregates made from disordered heterogeneous coils of entangled peptide chains measurements become extremely difficult if not impossible. Nevertheless, a lot of information can be obtained from the signals of residual mobile regions of polypeptide chains in large protein agglomerates [1]. Another beneficial approach is to use the NMR signal from solvent nuclei. The global rearrangements in the structure of protein complexes are reflected in significant changes in the resonance parameters for water as the main component [2] and ions of salts in a buffer.

In the present report, the NMR relaxation rates of nuclei in the buffer (¹H, ²H, ²³Na and ³⁵Cl) for control and aggregated samples of the RRM2 domain of TDP-43 protein are considered as probes for changes in protein conformation and aggregation state. It was found that proton relaxation times are sensitive to protein aggregation at low resonance frequencies to a greater extent. The relaxation rates for ions of sodium and chlorine found to be sensitive to the presence of protein in solution. The kinetics of RRM2 aggregation was studied using NMR relaxation of ¹H nuclei of water. The experimental R_1 and R_2 relaxation rates of solvent nuclei for this system were compared to simulated values obtained in the assumption of three-site exchange.

The reported study was funded by RFBR and CITMA according to the research project №18-53-34003.

1. Rabdano S.O. *et al.*: Sci. Rep. **7**, № 1, 11161 (2017)
2. Taraban M.B. *et al.*: Anal. Chem. **91**, 4107–4115 (2019)

Identification of the Radiation-Induced Radicals in Calcium Gluconate

**A. R. Gafarova, G. G. Gumarov, M. M. Bakirov, R. B. Zaripov,
V. Yu. Petukhov**

Zavoisky Physical-Technical Institute, FRC Kazan Scientific Center of RAS, Kazan 420029,
Russian Federation, albina-gafarova@mail.ru

Conformational analysis is one of the rapidly developing branches of modern chemistry. The study of drug conformation plays an important role in predicting not only the physical and chemical properties, but also the biological activity of the drug.

Earlier, we showed the possibility of using the EPR method to determine the conformation of calcium gluconate [1]. When samples were irradiated with gamma rays, paramagnetic centers were found that are stable at room temperature. The obtained spectra in the X- and Q-bands were analyzed using the MatLab EasySpin program. The experimental spectra from all irradiated samples are described by four components: doublet of triplets, triplet, doublet of doublets, doublet. The data obtained by modeling were used to calculate the torsion angles corresponding to the hyperfine interaction constants, which in turn indicates possible conformations of calcium gluconate. Thus, in the study

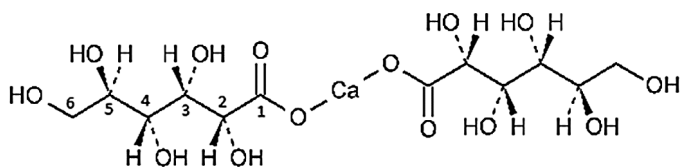


Fig. 1. The chemical formula of calcium gluconate.

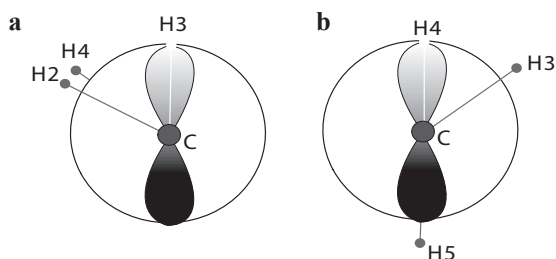


Fig. 2. The Newman projection combined for three carbon atoms for calcium gluconate: **a** for C2-C3-C4 atoms, the radical on C3; **b** for C3-C4-C5 atoms, the radical on C4.

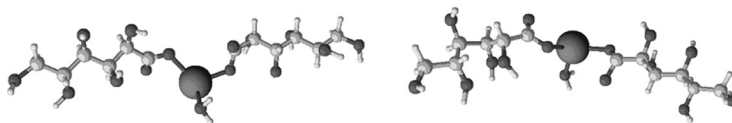


Fig. 3. Calcium gluconate molecule model in planar and cyclic conformation.

of calcium gluconate samples, the exact values of the torsion angles between the C-H bond and the axis of the orbital of the unpaired electron were obtained.

This work shows a method for comparing the position of paramagnetic centers at various carbon atoms with the spectrum components.

According to published data [2], a radical cannot form on the terminal carbon (C6, C1). Then, the radical with the doublet of triplets hyperfine structure binds to the carbon atom located near the terminal (C5), Fig. 1. The doublet corresponds to the only possible position on C2. The remaining signals can be attributed to the radicals at C3 and C4. To determine the position of the remaining signals, we built an idealized model of calcium gluconate, as well as the Newman projection.

Figure 2 shows that the *trans-gauche* conformation must correspond to the radical on C4. However, based on experimental data, the obtained torsion angles correspond to the *gauche-gauche* conformation both in the case of a triplet and in the case of a doublet of doublets. Based on this, we can conclude that the remaining components correspond to position C3.

The presence of two signals on carbon C3 is supposedly due to two possible conformations of calcium gluconate. It is known that gluconic acid and its salts can exist in two forms: planar and cyclic. The cyclic form is formed from a planar one by rotation through the C3-C4 bond of the remainder of the carbon skeleton by 120° .

According to the obtained torsion angles, we constructed a three-dimensional model of calcium gluconate, corresponding to two possible conformations, Fig. 3.

Thus, the results of the study showed the promise of using the EPR method to study the conformation of the molecules of gluconic acid salts, which will determine the reason for increasing the therapeutic efficacy of the drug after mechanical activation.

1. Gafarova A.R. *et al.*: Modern development of magnetic resonance 129 (2018)
2. Kochetkov N.K.: Radiation chemistry of carbohydrates (N.K. Kochetkov, L.I. Kudryashov, M.A. Chlenov). - M., 1978. -288 p.

The Content of Nitric Oxide and Copper in the Olfactory Bulbs of Rat's Brain after Modeling of Brain Stroke and Administration of Mesenchymal Stem Cells

**Kh. L. Gainutdinov^{1,2}, V. V. Andrianov^{1,2}, G. G. Yafarova^{1,2},
S. G. Pashkevich³, M. O. Dosina³, A. S. Zamaro³, Y. P. Tokalchik³,
T. Kh. Bogodvid², L. V. Bazan¹, A. A. Denisov³, V. A. Kulchitchky³**

¹ Zavoijsky Physical-Technical Institute, Kazan 420029, Russian Federation, kh_gainutdinov@mail.ru

² Institute of Fundamental Medicine and Biology of Kazan Federal University, Kazan 420008, Russian Federation

³ Institute of Physiology of Nat. Acad. of Sci. of Belarus, Minsk 220072, Belarus

Nitric oxide (NO) is known as one of the most vital signal molecules, that regulates the physiological functions of the organism and the metabolism of cells [1]. **Its role has been demonstrated for the central and autonomous nervous systems**, for cardiovascular function and blood supply to the brain and the heart [1–5]. In recent years there are many facts indicating that biosynthesis of NO is one of the key factors in the pathophysiological response of the brain to hypoxia-ischemia [2, 5, 6]. One of the reasons of the involvement of NO into the pathological process is the prolonged lack of oxygen, which leads to brain hypoxia. Hypoxia is accompanied by the increase in a tissue ischemia and in present time the development of cerebral ischemia and following stroke is associated with impaired cerebral blood flow, as well as violations of its regulation by the NO system [2, 7]. Previously, by the methods of EPR spectroscopy our team has evaluated effect of ischemic stroke on the intensity of NO production in the tissues of the brain, heart and liver of rats in vivo [8]. It was shown that in 5 hours after modeling of ischemia double reduction of NO production was observed in the tissues of the hippocampus, heart and liver. On the other hand, there is evidence that stem cells, the most important of which are mesenchymal stem cells (MSCs), provide regeneration of animal tissue [9]. In this regard, the aim of this work was to study the intensity of NO production and copper content (as an indicator of superoxide dismutase) in the olfactory bulbs of rat brain by EPR spectroscopy by modeling ischemic stroke of the brain, as well as studying the effect of intranasal administration of MSCs.

Modeling of ischemic stroke was produced on rats according to [10]. The experimental animals were divided into two groups (10 animals in each). The first group represented animals after ischemic damage. Animals of the 2nd group were injected 50 µl of a suspension containing 400 thousand MSCs (intranasal administration) 10 min after the modelling of brain ischemia. After 24 hours it was carried out fence of the olfactory bulbs. A similar extraction of tissue samples were also produced from control animals. In all series, on the day of the experiment, rats were anesthetized by intraperitoneal injection of a mixture of ketamine-chloralose-acepromazine (55.6 mg, 5.5 mg and 1.1 mg/kg, respectively). The components of the spin trap NO (DETC-Na, FeSO₄, sodium

citrate) was injected 30 minutes before the extraction of studied tissue. The measurements of the spectra of the complex $(\text{DETC})_2\text{-Fe}^{2+}\text{-NO}$ were performed on the spectrometer EMX/plus with a temperature module ER 4112HV in the X band (9.50 GHz). The amplitude of the EPR spectra was always normalized to the weight of the sample (details of the EPR signal measurement technique described earlier [5, 11]).

It was found a significant reduction of NO content in the olfactory bulb of the brain of rats 24 hours after modeling of ischemia. The level of NO production was also reduced after ischemia with MSCs administration as compared to intact animals. It was not found the significant difference of the NO content in rats after ischemia with MSCs administration relative to ischemic rats. The copper content in the olfactory bulb of the rat tended to increase after ischemia modeling, which indicates the activation of antioxidant protection in damaged brain tissue 1 day after ischemia. The activation of antioxidant protection in damaged brain tissues was more expressed 1 day after ischemia in case of administration of MSCs.

Supported partially by RFBR (Grant No. 18-515-00003) and partially by BRFFR (Grant B18R-227).

1. Vanin A.F.: Nitric Oxide **54**, 15–29 (2016)
2. Bolanos J.P., Almeida A.: Biochim. Biophys. Acta **1411**, 415–436 (1999)
3. Andrianov V.V., Sitdikov F.G. *et al.*: Ontogenez **39**, No 6, 437–442 (2008).
4. Reutov V.P., Okhotin V.E. *et al.*: Uspekhi Physiol. Nauk **38**, No 4, 39–58 (2011)
5. Gainutdinov Kh.L., Gavrilova S.A. *et al.*: Appl. Magn. Reson. **40**, No 3, 267–278 (2011)
6. Manukhina E.B., Malyshev I.Y. *et al.*: Nitric Oxide **3**, 393–401 (1999)
7. Chen Z.Q., Mou R.T. *et al.*: Med Gas Res. **7** (3), 194–203 (2017)
8. Andrianov V.V., Pashkevich S.G. *et al.*: Appl. Magn. Reson. **47**, No 9, 965–976 (2016)
9. Lukomska B., Stanaszek L. *et al.*: Stem Cells Int. **2019**, 9628536 (2019)
10. Shanko Y., Zamaro A. *et al.*: J. Sci. Tech. Res. **7** (5), MS.ID.001567 (2018)
11. Vanin A.F., Huisman A. *et al.*: Methods in Enzymology. **359**, 27–42 (2003)

Structural and Functional Properties of the Nanosized Al/V₂O₅ Termites Obtained by Mechanochemical Activation

A. I. Kokorin¹, E. A. Konstantinova², A. N. Streletskii¹

¹ Chemistry Department, FRC CP RAS, Moscow 119991, Russian Federation, alex-kokorin@yandex.ru

² Physics Department, Moscow State University, Moscow 119991, Russia Federation, liza35@mail.ru

Thermal transformations of mechanochemically activated (MCA) termites Al/V₂O₅ were analyzed by the method of X-ray diffraction, calorimetry and EPR spectroscopy. The influence of the treatment time of MCA on stages of thermal transformations during oxidation of aluminum in the reaction $10\text{Al} + 3\text{V}_2\text{O}_5 \rightarrow 5\text{Al}_2\text{O}_3 + 6\text{V}$ was revealed and the optimal conditions of MCA were established. Importance of such composites is caused by their activity as perspective termites with high energy production up to explosion [1]. The EPR study of such systems provides valuable information about their structure and features [1, 2].

For the non-activated mixtures and at short-time of MCA, the intensive oxidation of aluminum occurred by the liquid-phase mechanism at $T > 680$ °C, above melting temperatures of the both components. Figures 1 and 2 illustrate some of the results obtained.

Transformations of experimental ESR spectra shown in Fig. 1 and 2 demonstrate serious rearrangements occurring in Al/V₂O₅ mixtures and in comparison with XRD and DSC data permitted explanation of the results. At the optimal conditions of MCA, transformations are started at temperatures only slightly above 150 °C by the solid-phase mechanism. Reduction of V₂O₅ occurs via several lower vanadium oxides: $\text{V}_2\text{O}_5 \rightarrow \text{V}_4\text{O}_9 \rightarrow \text{V}_6\text{O}_{13} \rightarrow \text{VO}_2(\text{I}) \rightarrow \text{VO}_2(\text{II}) \rightarrow \text{V}_3\text{O}_5 \rightarrow \text{V}_2\text{O}_3 \rightarrow \text{VO} \rightarrow \text{V}$, which were revealed by the XRD method. Heating of mixtures is accompanied by the increase of concentrations of paramagnetic

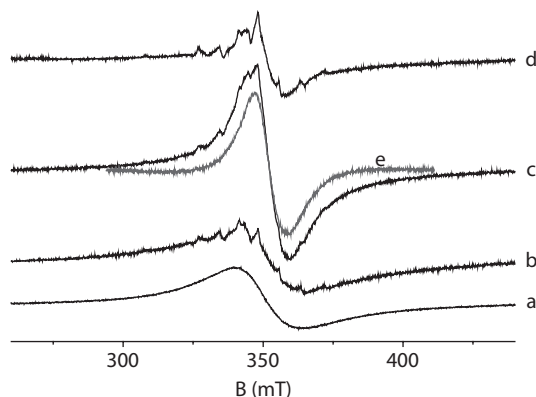


Fig. 1. EPR spectra at 77 K of Al/V₂O₅ composite mechanically treated during 12 min at 25 (a), and heated at 320 (b), 420 (c), 520°C (d). Spectrum (e) is a subtraction of (b) from (c). Spectra are normalized to the equal mass of the sample.

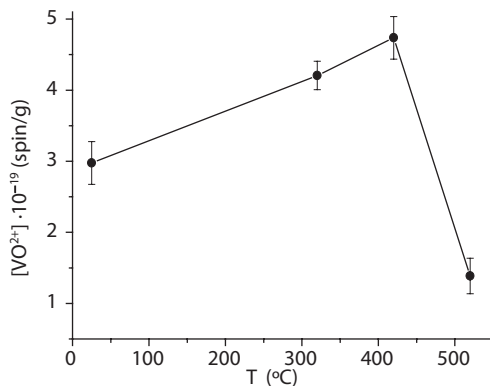


Fig. 2. Dependence of VO²⁺ ions concentration on temperature of Al/V₂O₅ composite after thermal treatment.

centers (PCs) VO²⁺ of two types up to 420 °C, and by their almost complete disappearance at 520 °C. Assumptions concerning relations between PCs and phases V₄O₉ and VO₂(I), and on the effect of PCs on initiation of the solid-phase transitions will be discussed. MCA treatment carried out upon optimal conditions promotes the explosive way of the reaction at firing the activated samples. It was found that the use of nanosized V₂O₅ as the initial component of a mixture does not significantly facilitate the activation processes.

We would note that EPR results are supplementary to all other macroscopic data such as DSC, TG, XRD, and specific surface area, *S*, measurements. Indeed, paramagnetic centers acting as spin probes (various types of VO²⁺ PCs) reflecting partially reduced chemically active centers provided information about microscopic features of the investigated systems. Correlations observed between the number of PCs in the mixture, its activity at one hand and a value of *S*, appearance of a new EPR signal, a singlet at 420 °C, and its intensity and XRD of a new VO₂-I phase, transformations of the EPR spectrum with temperature changes gave really important information on structural peculiarities and the mechanism of this type of thermites.

This work was supported by the State assignment of RF № AAAA-A20-120021390044-2. E.A.K. thanks Russian Foundation for Basic Research (grant 18-53-00020-Bel-a) for financial support.

1. Kokorin A.I., Streletskii A.N., Kolbanev I.V., Borunova A.B., Degtyarev Ye.N., Leonov A.V., Permenov D.G., Konstantinova E.A.: *J. Phys. Chem. C* **123**, 19991 (2019)
2. Kolbanev I.V., Degtyarev E.N., Streletskii A.N., Kokorin A.I.: *Appl. Magn. Reson.* **47**, 575 (2016)

NMR and DLS Study of Intermolecular Interactions of the Blood Plasma Fibrinogen. The pH and Ionic Strength Effects on the Prelude of Fibrin Clotting

A. M. Kusova, A. E. Sitnitsky, Yu. F. Zuev

Kazan Institute of Biochemistry and Biophysics, FRC Kazan Scientific Center of RAS, Lobachevsky Str., 2/31 Kazan, Russian Federation, alexakusova@mail.ru

The protein-protein intermolecular interactions are of considerable importance in thermodynamic properties and phase behavior of protein solutions. In the present work we focused most attention on the protein-protein interactions in fibrinogen (Fg) solutions, which play a fundamental role in the processes of clotting, thrombocytosis and wound healing. In spite of the fact that interactions of Fg with other plasma proteins and receptors are important in hemostasis, thrombosis and other processes, we put emphasis on the Fg-Fg interactions due to high natural concentration of Fg in plasma (2–4 g/L) and their possible prelude to protofibril formation.

Recently, we have proposed a complex approach to study diffusive mobility and interactions of spheroidal protein molecules in a wide concentration range [1]. In the present work self-diffusion and collective (mutual) diffusion of rod-shaped Fg were studied using the pulsed field gradient nuclear magnetic resonance (PFG NMR) and the dynamic light scattering (DLS) techniques. The applied experimental approaches observe different diffusion effects, giving in combination information on the details of inter-protein interactions. The theoretical description of experimental data was based on the friction formalism of nonequilibrium thermodynamics and the potential of mean force analysis. The multi-staged approach obtained the further development to determine the long- and short-range nonspecific interactions of rod-shaped bovine Fg and reveal the effect of protein surrounding (pH and ionic strength) on this interaction. It was found that by varying of external conditions one can manipulate with different contributions of intermolecular forces and potentially operate blood physiological processes.

This work was performed with financial support from the Russian Foundation for Basic Research, Grant № 20-04-00157.

Mechanism of Intrinsically Disordered Protein Penetration into Cells: Monitoring by EPR and Confocal Microscopy

**S. Ovcherenko¹, O. Chinak², O. Krumkacheva³, S. Dobrynin¹,
I. Kirilyuk¹, E. Bagryanskaya¹**

¹ N. N. Vorozhtsov Novosibirsk Institute of Organic Chemistry SB RAS, 630090, Russian Federation

² Institute of Chemical Biology and Fundamental Medicine SB RAS, 630090, Russian Federation

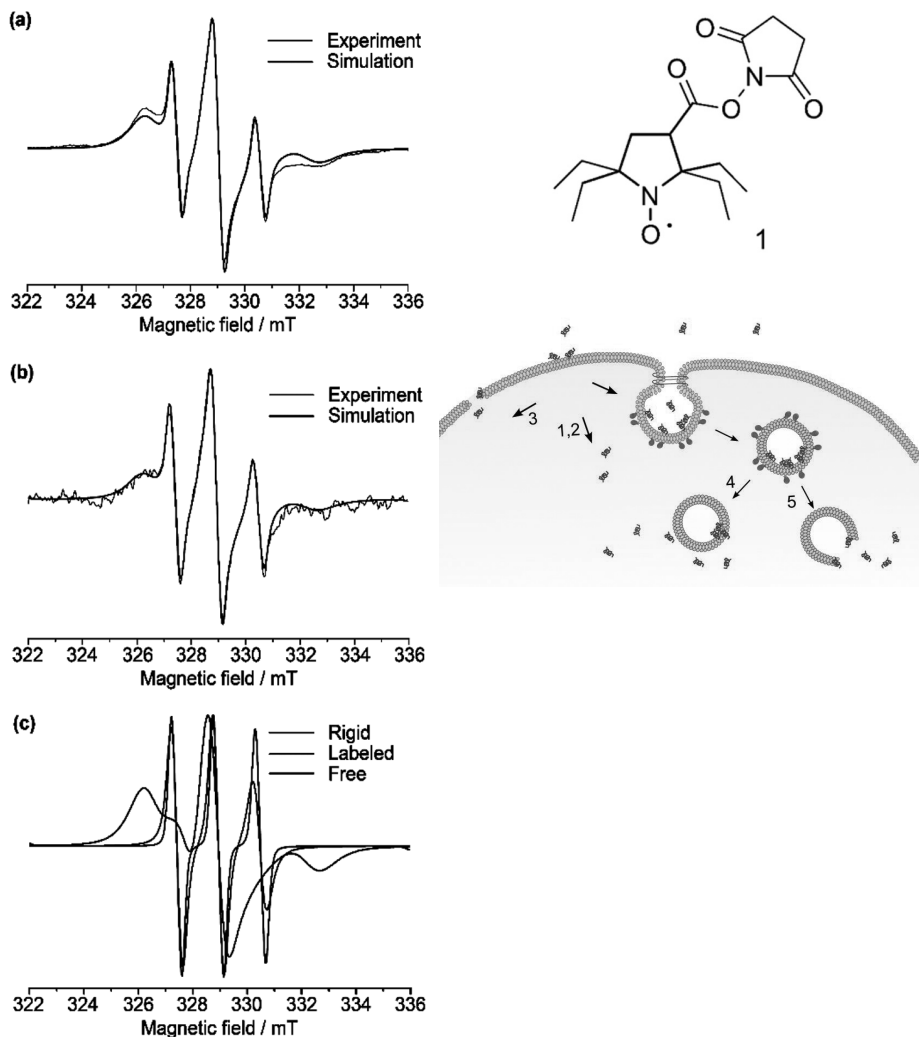
³ International Tomography Center SB RAS, 630090, Russian Federation

Intrinsically disordered protein RL2 – a recombinant analog of human κ -casein fragment – was shown to penetrate cytoplasm of both cancer and normal cells and to induce apoptosis of cancer cells without cytotoxic activity toward normal cells [1]. Since penetration into cells is important step of biological action of any therapeutic molecules, it is relevant knowing the way RL2 penetrates cells. Cell-penetrating peptides are known for their effective penetration cells via direct penetration through the membrane or via endocytosis and for their ability to deliver cargo molecules into cells. Unlike electroporation and microinjection, intracellular delivery of cargo molecules using CPP is suitable for *in vivo* application.

We applied the combination of confocal microscopy and CW-EPR methods to study the protein penetration into cells. RL2 was treated with reduction resistant spin label 3-((2,5-dioxopyrrolidin-1-yloxy)carbonyl)-2,2,5,5-tetraethyl-1-oxyl (**1**) to give spin labelled protein RL2-**1**. The stability of the spin label is very high and allows us to investigate the kinetics and changes in the EPR spectra during more than 20 hours. CW-EPR was used to study the kinetics of single protein states transformations from the data of spin label mobility while confocal microscopy allowed us to trace RL2 location in cells. Taking together these methods provide us with complete picture of RL2 penetration.

The spin labeled peptide RL2-**1** was shown to accumulate in A549 human lung adenocarcinoma cells with the nitroxide half-life of approximately 10 hours inside the cells. EPR spectra revealed superposition of three components with different mobility and rotational correlation times varying by more than one order of magnitude. Confocal microscopy results and simulations of EPR spectra performed allows us to assign these fractions to 1) spin labeled protein with very low mobility which is sticking on the inner membrane surface of endosomes, 2) spin labeled protein with mobility similar to buffer solution and 3) spin labeled amino acids formed in cells due to protein digesting. It allows us to follow the ways of IDP penetration into cell: via endosomes or to cytoplasm directly through the membrane.

CW EPR allows to follow the kinetics of different forms of RL2-**1** and its transformation at minimal concentration 10-60 μM in the cells. It will allow us in future to study the changes in the structure of spin labeled RL2 during penetration into cells by PELDOR.



Possible applications of cell-penetrating peptides/proteins spin labelled with reduction-resistant nitroxides are discussed, including intracellular structural studies and EPRI/OMRI/ODNP tomography.

The work was supported by the Ministry of Science and Higher Education of Russia (project number 14.W03.31.0034).

1. Semenov, D.V. *et al.*: The protein journal **29**(3), 174-180 (2010)
2. Chinak O.A. *et al.*: Molecules **24**(16), 2919 (2019)

DFT Calculations of EPR Parameters for Substituted Calcium Phosphates

**D. Shurtakova¹, G. Mamin¹, M. Gafurov¹, S. Orlinskii¹, F. Murzakhanov¹,
A. Fedotov², V. Komlev²**

¹ Physics Department, Kazan Federal University, Kazan, 420008, Russian Federation,
darja-shurtakva@mail.ru

² A. A. Baikov Institute of Metallurgy and Materials Science, Russian Academy of Sciences,
Moscow, 119991, Russian Federation

Calcium phosphates are widely used in medicine. The main studies of calcium phosphates directed to the study of the properties for their further use as bone tissue's implants. Calcium phosphates can include into its crystal lattice various impurity ions, which can affect the physicochemical and biological properties. Therefore, it is important to study such impurities. EPR spectroscopy is a powerful biophysical tool for this aim [1].

The purpose of this work is to simulate the EPR spectrum of manganese ion in synthetic hydroxyapatite from first principles and to compare this spectrum with the experimental one.

Hydroxyapatite (HAP) $\text{Ca}_{10}(\text{PO}_4)_6(\text{OH})_2$ samples were synthesized on the Faculty of Science of New Materials at Moscow State University. EPR spectra were simulated in the Matlab program using the EasySpin module. For the simulation, the g -factor parameters and the hyperfine interaction constant A were used. These parameters calculated by the Quantum espresso program. The crystal field was also taken into account in the simulation. To calculate the parameters of the crystal field, a program was written by Python. This program is based on the Coulomb interaction using the electron density which was calculated by Quantum

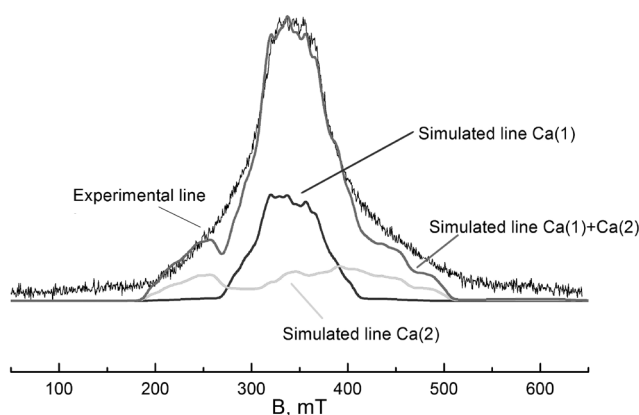


Fig. 1. Simulated and experimental EPR spectra of synthetic hydroxyapatite.

espresso. Mn^{2+} ions can replace Ca^{2+} ions in hydroxyapatite in two positions Ca (1) and Ca (2). Therefore, all calculations were made for both positions.

The best agreement between the experimental and simulated spectrum is achieved by taking into account the contributions from manganese ions in two possible positions. This suggests that manganese ions can be in both positions.

This research has been supported by RFBR grant 18-29-011086 and by the subsidy allocated to Kazan Federal University for state assignment No. 0671-2020-0051.

1. Epple M.: *Acta biomaterialia* **77**, 1–14 (2018)

^1H NMR Study of Blood Plasma of Rats with the Experimental Model of SCI

S. V. Yurtaeva¹, M. Yu. Volkov¹, G. G. Yafarova^{1,2}

¹ Zavoisky Physical-Technical Institute, FRC Kazan Scientific Center of RAS, Kazan 420029, Russian Federation, S.Yurtaeva@kfti.knc.ru

² Institute of Fundamental Medicine and Biology, Kazan Federal University, Kazan, Russian Federation

The study of traumatic damage of the spinal cord is still of great importance due to the ongoing search for the effective methods of treating of spinal cord injury (SCI).

The developing of new approaches to SCI treatment require deeper study of the molecular processes and mechanisms arising under SCI. Along with traditional biochemical and clinical methods, unconventional experimental methods of obtaining new molecular information may be used. One of the sources of new metabolic experimental data concerning SCI may be NMR spectroscopy of blood plasma. Blood plasma includes many hydrogen-containing metabolites, so ^1H NMR is widely used for quantification of metabolites.

In this research, the blood plasma samples of rats with 3 and 7 day experimental SCI model and control rats were studied by ^1H NMR spectroscopy. NMR experiments were performed on “Avance 400” NMR spectrometer (Bruker, Germany). The following metabolites and compounds were detected in the ^1H NMR spectra: EDTA, Mg^{2+} -EDTA²⁻ complexes, lactate, alanine, glutamine, glucose, lipides. The most evident effect of variation of line intensities after SCI was observed for the lines with ~ 2.6 – 2.7 ppm, ~ 2.46 ppm, ~ 2.16 ppm. The comparison of the blood plasma of rats with SCI and the blood plasma of control rats showed that the amount of ionic magnesium and glutamine increases after SCI. Mechanisms underlying the detected metabolic changes are discussed.

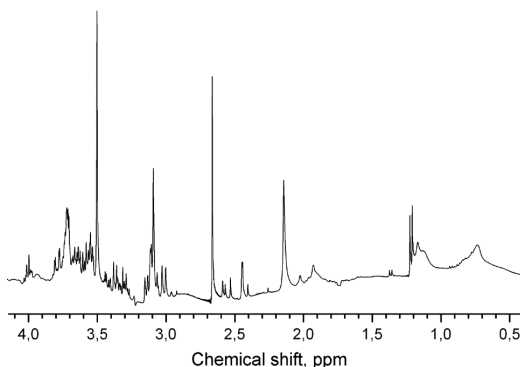


Fig. 1. The typical ^1H NMR spectrum of rat blood plasma after SCI.

Photoinduced States of Some Compact Electron Donor/Acceptor Dyads

A. A. Sukhanov¹, V. K. Voronkova¹, J. Zhao²

¹ Zavoiisky Physical-Technical Institute, FRC Kazan Scientific Center of RAS, Kazan 420029, Russian Federation, vio@kfti.knc.ru

² State Key Laboratory of Fine Chemicals, School of Chemical Engineering, Dalian University of Technology, 116024, P. R. China, zhaojzh@dlut.edu.cn

Photoinduced charge separation processes, recombination reactions, and intersystem crossing (ISC) determine the basic properties of optically active materials, such as photocatalysts, elements of optoelectronics and organic photovoltaics. The study of these processes creates a fundamental basis for the development of promising new materials. The possibilities of using these or those systems are determined by the properties of triplet states, such as the effectiveness of the ISC and the lifetime of the triplet state.

Using the time-resolved (TR) EPR method, new donor-acceptor dyads were studied, more precisely, several series of dyads with different types of partners and their mutual orientation. The chromophores are directly related to each other in the studied dyads, and a rather strong connection between partners is expected, which distinguishes them from previously studied ones. The experimental TR EPR spectra are described by model spectra, the parameters of photoinduced states and the nature of the polarization of the electron spins of these states are determined. The dependence of these properties on the type of donors and acceptors in dyads and their mutual orientation is analyzed.

Studies have shown that photoinduced charge separation and recombination processes in such compact dyads make a significant contribution to the formation of metastable triplet states, which can significantly exceed the contribution of ISC of the monomer [1–4]. For the first time, the possibility of the coexistence of photoexcited donor-acceptor dyads in the excited triplet state localized on one of the chromophores and in the triplet state formed by the delocalization of unpaired electrons by both partners is shown [1,4].

This work was supported by the Russian Foundation for Basic Research (project no. 19-53-53013)

1. Dong Y., Sukhanov A.A. *et al.*: *J.Phys. Chem. C* **123**, 22793–22811 (2019)
2. Imran M., Sukhanov A.A. *et al.*: *J.Phys. Chem. C* **123**, 7010–7024 (2019)
3. Zhao J., Sukhanov A.A. *et al.*: *J. Phys. Chem. C* **123**, 18270–18282 (2019)
4. Tang G., Sukhanov A.A., Zhao J. *et al.*: *J. Phys. Chem. C* **123**, 30171–30186 (2019)

Nitric Oxide in Restriction of Motor Activity, Including Spin Cord Injury

**G. G. Yafarova^{1,2}, V. V. Andrianov^{1,2}, V. S. Iyudin¹, T. V. Baltina²,
A. A. Ereemeev², I. A. Lavrov², R. I. Zaripova², T. L. Zefirov²,
Kh. L. Gainutdinov^{1,2}**

¹ Zavoiisky Physical-Technical Institute, FRC Kazan Scientific Center of RAS, Kazan 420029, Russian Federation

² Institute of Fundamental Medicine and Biology of Kazan Federal University, Kazan 420008, Russian Federation, gusadila@mail.ru

Nitric oxide's system (NO) is one of the most studied systems of the organism [1, 2]. Its participation in the mechanisms of development of various pathological states of the body is attracted great interest [3, 4]. The NO system is also essential in adaptation to environmental changes and external conditions [5]. In addition to vasodilation, NO participate in reactions of oxidative stress, glutamate-calcium cascade, and inflammation [2]. There are disputes about the role of NO in the injury of the central nervous system, including insufficient research of the dynamics of NO production at different stages of spinal cord injury (SCI). SCI is a serious and destructive neurological disorder, which can lead to loss of sensory and motor function and, depending from the degree of damage, to paralysis and death [6]. The high frequency of SCI is combined with the complexity of SCI pathogenesis, and the current lack of adequate treatment and rehabilitation for patients with SCI takes the problem beyond purely medical aspects. One of the problems occurs during SCI is the restriction of motor activity, which is a significant social problem caused by lifestyle, professional activity, prolonged bed rest, etc [7–9]. In this case, oxygen consumption by tissues and the activity of oxidative processes are significantly reduced [10]. Presumably, the role of NO in this pathology depends on the concentration range, the type of source cell and the medium in which NO was obtained.

We used a model of SCI at the level of the first lumbar vertebra (L1) according to the modified method of A. Allen [7, 8] and used a model of restriction of motor activity [9]. We studied the tissue samples of the spinal cord (SC), liver and heart in intact animals and in different periods of traumatic disease of the SC and restriction of motor activity by EPR spectroscopy using the method of spin traps [11, 12]. As spin trap were applied the complex of Fe^{2+} with diethyldithiocarbamate (DETC)₂- Fe^{2+} -NO. The records were carried out on EPR spectrometer X-band firm "Bruker" ER 200E SRC. In intact rats the production of NO in the SC was on average 1.3 nm/g·hour and in the heart of 5.2 nm/g·hour. It was found that the production of NO in these tissues after a long time restriction of motor activity increases by 2-3 times. At the same time, the dynamics of NO production in SCI is wave-like, when the level of NO production in SC tissues sometimes increased or decreased. Thus, it is shown that during consideration of the consequences of SCI it is necessary to take into account the component of restriction of motor activity. Thus, the dynamics of the intensity of formation

of NO after SCI indicates its possible role as an inducer of apoptosis in the tissue of the damaged SC, and generalized activation of NO-ergic stress-limiting system in the early stages of SCI.

At the same time, the dynamics of NO formation after SCI is waved when the level of NO production sometimes increases or decreases. A decrease in the intensity of NO production was observed up until 3 days after SCI; further, generalized activation of the NO-ergic stress-limiting system was observed: NO production increased in all studied tissues. In the late period after SCI, an increase in the intensity of NO formation was persisted only in the tissue of the damaged spinal cord, which indicates its possible role as an apoptosis inducer in the area of damage. Thus, during considering of the consequences of SCI, it is necessary to take into account the component of restriction of motor activity.

Supported partially by RFBR (Grant 18-515-00003) and partially by BRFFR (Grant B18R-227) and also by government assignment for FRC Kazan Scientific Center of RAS.

1. Vanin A.F.: *Biohimia* **63**, 924–938 (1998)
2. Terpolilli N.A., Moskowitz M.A. *et al.*: *J. Cereb. Blood Flow Metab.* **32**, 1332–1346 (2012)
3. Pacher P., Beckman J.S. *et al.*: *Physiol. Rev.* **87**, 315–427 (2007)
4. Andrianov V.V., Sitdikov F.G. *et al.*: *Ontogenez* **39**, No 6, 437–442 (2008)
5. Manukhina E.B., Malyshev I.Y. *et al.*: *Nitric Oxide* **3**, 393–401 (1999)
6. Dumont R.J., Okonkwo D.O. *et al.*: *Clin. Neuropharmacol.* **24**, No 5, 254–264 (2001)
7. Yafarova G.G., Andrianov V.V. *et al.*: *BioNanoScience* **6**, No 4, 332–334 (2016)
8. Yafarova G.G., Andrianov V.V. *et al.*: *Bull. Experim. Biol. Med.* **162**, No 3, 316–319 (2017)
9. Gainutdinov Kh.L., Faisullina R.I. *et al.*: *Bull. Experim. Biol. Med.* **154**, 635–637 (2013)
10. Kwak, E.K.: *Korean Med. Sci.* **20**, 663–669 (2005)
11. Mikoyan V.D., Kubrina L.N. *et al.*: *Biochim. Biophys. Acta* **1336**, No 2, 225–234 (1997)
12. Gainutdinov Kh.L., Gavrilova S.A. *et al.*: *Appl. Magn. Reson.* **40**, No 3, 267–278 (2011)

Study of the Radiation-Induced at Room Temperature Stable Radicals in Octacalcium Phosphate Synthesized by Wet Method with XRD and EPR

**B. Yavkin¹, D. Shurtakova¹, F. Murzakhanov¹, M. Gafurov¹,
G. Mamin¹, S. Orlinskii¹, V. Smirnov², V. Sirotinkin², A. Fedotov²,
V. S. Komlev², A. Shinkarev³**

¹ Kazan Federal University, 18 Kremlevskaya Str., Kazan, Russian Federation

² A.A. Baikov Institute of Metallurgy and Materials Science, Russian Academy of Sciences,
49 Leninsky pr., Moscow, Russian Federation

³ Kazan National Research Technological University, 68 Karl Marx Str., Kazan, Russian Federation

Octacalcium phosphate (OCP, chemical formula $\text{Ca}_8\text{H}_2(\text{PO}_4)_6 \times 5\text{H}_2\text{O}$) is increasingly attracting attention in last decade as a transient intermediate to the biogenic apatite for bone regeneration and study the processes of pathological calcification. We have synthesized stable OCP powders obtained by double transformation of α -tricalcium phosphate. X- and gamma ray radiation induced defects are studied by means of pulsed electron paramagnetic resonance (EPR) at 9 and 94 GHz microwave frequencies. Multicomponent EPR spectra were deconvoluted into three types of the paramagnetic centers, their spectroscopic parameters (g-factors and hyperfine constants) are defined. Based on the extracted parameters these paramagnetic centers were ascribed to H^0 , CO_2^- and NO_3^{2-} radicals. The spectroscopic parameters of NO_3^{2-} stable radical in the obtained samples are markedly different from these in hydroxyapatite [1]. In addition coherent dynamics of different electron-nuclear systems containing nuclei ^1H , ^{31}P and ^{23}Na nuclei with various strength of hyperfine interaction have been observed. The obtained results could be used for the tracing of the mineralization processes from its initiation to the completion of the final product and for the identification of the OCP phase.

This research has been supported by RFBR grant 18-29-011086 and by the subsidy allocated to Kazan Federal University for the state assignment No. 0671-2020-0051.

1. Shurtakova D. *et al.*: Magn. Reson. Solids **21**, 19105 (2019)

SECTION

STRONGLY CORRELATED ELECTRON SYSTEMS

NMR Study of the Ion Mobility in Frustrated $\text{Li}_{1-x}\text{CuSbO}_4$ Compound

D. Gafurov^{1,2}, M.-I. Sturza³, E. Vavilova²

¹ Institute of Physics, Kazan Federal University, Kazan, 420008, Russian Federation,
londonstyle1998@gmail.com

² Zavoisky Physical-Technical Institute, FRC Kazan Scientific Center of RAS, Kazan 420029,
Russian Federation

³ Leibniz Institute for Solid State and Materials Research IFW Dresden, Dresden 01069,
Germany

The Li diffusion in $\text{Li}_{(1-x)}\text{CuSbO}_4$ with lithium deficiency $x = 2\%$, 5% , 7% and 10% was studied by investigation of motional narrowing of the central ${}^7\text{Li}$ NMR line in the temperature range from 290 K to 470 K. The activation energy of hopping of lithium ions was determined from the temperature dependence of the NMR linewidth. It was found that at relatively small deficiency of lithium the activation energy changes slightly, while at x of the order of 0.1 a clear decrease of E_a is observed. The dependence of the obtained activation energy on the lithium content indicates the opening of motion channels in the crystals at x close to 0.1 due to the formation of free vacancies at the lithium position, which favors the thermally activated hopping of ions [1].

The work was supported by RFBR through grant No. 18-02-00664.

1. Gafurov D. et.al.: Magnetic Resonance in Solids. Electronic Journal. **21**, 19602 (2019)

ESR Investigation of Magnetic Properties and Vanadium Oxidation State in α -Li₃V₂(PO₄)₃/C Composite

**T. P. Gavrilova¹, S. M. Khantimerov¹, R. R. Fatykhov¹, I. V. Yatsyk¹,
P. Balaya², N. M. Suleimanov¹**

¹ Zavoisky Physical-Technical Institute, FRC Kazan Scientific Center of RAS, Kazan 420029, Russian Federation

² National University of Singapore, 119077, Singapore

One of the most important problems for the development of new generation of lithium-ion accumulators (LIA) is the search for new promising materials with increased energy density and lifetime. The use of polyanionic compounds consisting of octahedral complexes of transition metals (Mn, Co, V) as a cathode material with a well-developed three-dimensional crystal structure, the interstitial positions of which are filled with lithium ions, is a very interesting approach to increase the efficiency of LIA. Here we present the investigations of Li₃V₂(PO₄)₃ compound with LISICON (Li Super Ionic Conductor) structure as a potential cathode material for LIA. Intensive investigations of the such type of compounds are of great interest due to a large range of possible changes in the valence state of the transition element. Indeed, the transition of electron to the structure of metal-oxygen bonds and vice versa in the process of Li intercalation/deintercalation plays a fundamental role in transport properties of electrode materials. Electron spin resonance method can give the necessary information about the transition element, its valence state and the local electronic structure of complex formed by the interaction of d and p orbitals of metal and ligand, respectively.

The investigated here α -Li₃V₂(PO₄)₃/C was synthesized by the solvothermal method and has the monoclinic structure with $P2_1/n$ space group and lattice parameters: $a = 8.605 \text{ \AA}$, $b = 5.591 \text{ \AA}$, $c = 12.038 \text{ \AA}$, $\beta = 90.6^\circ$ [1]. ESR measurements were performed both for as-prepared α -Li₃V₂(PO₄)₃/C composite and for α -Li₃V₂(PO₄)₃/C sample after Li deintercalation and intercalation processes. In the as-prepared α -Li₃V₂(PO₄)₃/C V³⁺ ions have d-electronic configuration 3d² and ground state ³F with spin $S = 1$. For such ions with an even number of electrons in the respective electronic shells singlet ground-state levels may result such that no ESR is observable. Indeed, we did not observe the ESR signal in as-prepared α -Li₃V₂(PO₄)₃ samples which would be expected for vanadium ions in [3+] valence state. At the same time using low temperatures we were able to resolve a weak resonance signal in the ESR spectra of as-prepared compound. Approximation of these spectra yielded the best fit of experimental data for the powder spectrum corresponding to paramagnetic centers with effective spin $S = 1/2$ and anisotropic g -factor. Obtained anisotropic g -factor $g_{\perp} = 1.972$, $g_{\parallel} = 1.933$ (at $T = 100 \text{ K}$) is close to the g -factor of V⁴⁺ ions in tetragonally distorted VO₆ octahedra [2]. We suggest that ESR spectra of the as-prepared compound corresponds to V⁴⁺ ions. The presence of V⁴⁺ ions in the initial samples of α -Li₃V₂(PO₄)₃/C can be associated with small lithium non-stoichiometry.

Typical ESR spectra of delithiated (obtained by the full charge of an electrochemical cell) $\alpha\text{-Li}_3\text{V}_2(\text{PO}_4)_3/\text{C}$ can be approximated, as in the previous case, by the powder spectrum, corresponding to the paramagnetic centers with effective spin $S = 1/2$ and anisotropic g -factor. We suggest that vanadium ions in the delithiated sample can change their valency state from [3+] to [4+/5+] during charging. It should be noted that V^{5+} ion has no electrons in 3d electron shell and therefore this ion is ESR silent. Since vanadium has a nuclear spin $I = 7/2$, we observed the exchange-narrowed resonance line, which is typical for magnetically concentrated compounds [3]. The estimation of V^{4+} ions' relative concentration in the as-prepared phase of $\alpha\text{-Li}_3\text{V}_2(\text{PO}_4)_3/\text{C}$ in respect to the delithiated phase gives the value of 1.5–2.5%.

It should be noted that ESR signal discussed above was not observed in the ESR spectra of relithiated (obtained after one full charge/discharge cycle) $\alpha\text{-Li}_3\text{V}_2(\text{PO}_4)_3/\text{C}$ which has the same composition as as-prepared $\alpha\text{-Li}_3\text{V}_2(\text{PO}_4)_3/\text{C}$. This fact indicates that vanadium ions giving rise to the ESR signal in the as-prepared samples change their valence state during the cycling of $\alpha\text{-Li}_3\text{V}_2(\text{PO}_4)_3/\text{C}$ cell. The reduction of all vanadium ions to the valence state [3+] after the first charge/discharge cycle corresponds to reversible intercalation of all lithium ions to the $\alpha\text{-Li}_3\text{V}_2(\text{PO}_4)_3$. Thereby, the host structure of $\alpha\text{-Li}_3\text{V}_2(\text{PO}_4)_3$ samples allows to use its maximum capacity during the first charge/discharge cycle.

The reported research was funded by Russian Science Foundation (grant No 19-79-10216).

1. Patoux S., Wurm C., Morcrette M. *et al.*: Journal of Power Sources **119–121**, 278 (2003)
2. Gallay, van der Klink J.J., Moser J.: Phys. Rev. B **34**, 3060 (1986)
3. Abragam A., Bleaney B.: "Electron paramagnetic resonance of transition ions", Oxford University Press, 1970.

Zn-Doped Frustrated $S = 1/2$ Spin Chains $\text{LiCu}_{(1-x)}\text{Zn}_{(x)}\text{SbO}_4$ Studied by NMR

A. Kamalov^{1,2}, M.-I. Sturza³, H.-J. Grafe³, E. Vavilova²

¹ Institute of Physics, Kazan Federal University, Kazan, 420008. Russian Federation,
alen.kamalov@gmail.com

² Zavoisky Physical-Technical Institute, FRC Kazan Scientific Center of RAS, Kazan 420029,
Russian Federation

³ Leibniz Institute for Solid State and Materials Research IFW Dresden, Dresden 01069,
Germany

The problem of the influence of nonmagnetic impurities on the properties of highly frustrated magnets has been very actively studied in recent years. This is explained not only by the problems of fundamental solid state physics, but also by the possible practical applications of such compounds, since real samples always contain a certain number of defects. The theory predicts various ground states depending on the ratio of factors such as frustration parameter, concentration of defects, and their type.

In this work a system with well-isolated frustrated chains of Cu^{2+} Heisenberg spins $\text{LiCu}_{(1-x)}\text{Zn}_{(x)}\text{SbO}_4$ with $x = 0.1\%$ was investigated by ^7Li NMR in different external magnetic fields (1.8–16 T) and temperature range 1.2–300 K. The local static and dynamic susceptibility probed by line shift and nuclear spin-lattice relaxation were compared with a bulk susceptibility and with the corresponding characteristics of undoped sample in different field-induced phases [1].

The work was supported by RFBR through grant no. 18-02-00664.

1. Grafe H.-J. et al.: Scientific Reports **7**, 6720 (2017)

Modification of the Properties of Barium Strontium Titanate Films on Silicon Substrate

D. P. Pavlov¹, R. I. Batalov¹, A. V. Leontyev¹, D. K. Zharkov¹,
S. A. Migachev¹, I. V. Lunev², T. S. Shaposhnikova¹, R. F. Mamin^{1,2}

¹ Zavoiisky Physical-Technical Institute, FRC Kazan Scientific Center of RAS, Kazan 420029, Russian Federation, mamin@kfti.knc.ru

² Institute of Physics, Kazan Federal University, Kazan 420000, Russian Federation

To improve the properties of solar cells, primarily to increase the absorptivity of solar cells in a wider region of the light spectrum [1], various films are applied to their surface. Also recently, the photovoltaic effect is often used [2], which is the direct conversion of light into electricity and is considered one of the most reliable and abundant sources of renewable and clean energy. A high-mobility electron gas was observed in 2004 [3] at the interface of LaAlO₃/SrTiO₃ heterostructure. In this regard, barium strontium titanate (BST), being a ferroelectric with Curie temperature close to room temperature and having a band gap $E_g = 3.7$ eV (with a photoresponse appearing at energy above 2.5 eV [3]), can be considered as a potential material for use in solar power engineering, as well as for the detection of UV light [4] when grown on Si substrate. In this work we solve these problems by creating such a special state of the interface when applying a thin ferroelectric film on silicon. The properties of the heterostructures obtained by dielectric and various optical methods are measured and characterized. It was found that changes of the capacity of the heterostructure are related to increase of conductivity through the Si layer with increasing frequency based on the results of the study of the frequency dependences of the BST/Si heterostructure. The reflection spectrum from the BST film was studied. Based on these results, the absorption spectrum was modeled, which has a peak in the region of 3 eV. There is also an inflection in the region of 2.6–2.8 eV, which can correspond to energy from the top of the valence band to the lower levels of the BST film defect system. The surface was tested by atomic force microscopy before and after modification. The laser annealing method did not yield any significant results. The most promising method was the modification of barium-strontium titanate films on a silicon substrate by the ion implantation method with the introduction of chromium atoms with energy of 40 KeV. The measurement of the photoconductivity has shown that current at the interface increases substantially when illuminated by the ultraviolet light. This increase is particularly high for samples modified by ion implantation. The possibility of carrier concentration increasing by this way is discussed when exciting the p/n junction for use as an operating element in solar batteries. The properties of barium-strontium titanate films on a silicon substrate and the possibility of their modification are investigated. The photoconductivity of the heterostructure interface and the possibility of modifying the properties of barium-strontium titanate films by the laser annealing method and the ion implantation method

are studied. The effect of modification on photoconductive properties of the films was revealed.

The reported study was supported of the Russian Foundation for Basic Research and the Government of the Republic of Tatarstan (grant 18-42-160005). The work of R.F.M. is partially performed according to the Russian Government Program of Competitive Growth of Kazan Federal University.

1. Solankii Ch.S., Singh H.K.: *Anti-refraction and Light Trapping in c-Si Solar Cells*. Singapore: Springer. 2, 186 p., 2017.
2. Yang S.Y., Seidel J., Byrnes S.J., Shafer P., Yang C.-H., Rossell M.D., Yu P., Chu Y.-H., Scott J.F., Ager III J.W., Martin L.W., Ramesh R.: *Nature Nanotechnology* **5**, 143 (2010)
3. Ohtomo A., and Hwang H.: *Nature* **427**, 6973 (2004)
4. Putra I.R., Syafutra H., Alatas H.: *Procedia Environ. Sci.* **33**, 607 (2016)
5. Sharma S., Tomar M., Puri N.K., Gupta V.: *Sensors and Actuators A: Phys.* **230**, 175 (2015)

The Delay Time of Phase Transition to the Polar Phase in Relaxors

T. S. Shaposhnikova¹, S. A. Migachev¹, R. F. Mamin^{1,2}

¹ Zavoisky Physical-Technical Institute, FRC Kazan Scientific Center of RAS, Kazan 420029,
Russian Federation, vixsup@mail.ru

² Institute of Physics, Kazan Federal University, Kazan 420000, Russian Federation

Relaxor ferroelectrics have been subject to intensive research. The distinguishing features of relaxors are a strongly diffuse maximum in the temperature behavior of permittivity, the shift of this maximum toward higher temperatures with rising measuring field frequency, and a strong frequency dependence of permittivity at very low frequencies. Numerous experimental data show that the properties of the low-temperature phase depend on the history of samples, so nonergodic behavior is observed in the low-temperature phase [1]. In an applied electric field, the transition to a uniform state of polarization is observed in the low-temperature phase after zero-field cooling. Such a phase transition is observed in [1] after a sufficiently long delay time had passed from the beginning of field application. The dependences of delay time t_0 of the phase transition on temperature T and external electric field E were established. The observed regularities have been discussed using an approach [2] developing on the basis of the model of diffuse phase transition in the system with defects [3]. It is shown that in the frame of that approach the delay phase transition in polar phase in relaxors could be explain if the dynamic of electron system would be take in consideration [2]. For examine that model we investigate the effect of illumination on the delay time t_0 of the phase transition in $\text{PbMg}_{1/3}\text{Nb}_{2/3}\text{O}_3$.

The time dependence behavior of the dielectric permittivity of lead lanthanum zirconate titanate transparence ceramic sample from the moment of the field application at certain temperatures after the zero-field cooled regime is compared to that exhibited by a single-crystal lead magnoniobate in [110] orientation. The delay time t_0 of the phase transition have been measured for different temperatures and applied electric field. The photoconductivity has been investigated and the correlation of observed results with developed model is discussed. The delay time of the phase transition from the glasslike to the field-induced ferroelectric state was determined for the sharp change in the dielectric permittivity at several temperatures in a lead magnoniobate single crystal. But the same transition in lead lanthanum zirconate titanate has more smooth behavior. In the case of ultraviolet illumination the delay time becomes a few times shorter for both cases.

The reported study was supported by Foundation for Basic Research (grant 18-02-00675). The work of R.F.M. is performed according to the Russian Government Program of Competitive Growth of Kazan Federal University.

1. Colla E.V., Koroleva E.Yu., Okuneva N.M., Vakhrushev S.B.: Phys. Rev. Lett. **74**, 1681 (1995)
2. Mamin R.F., Blinc R.: Physics of the Solid State **45**, 942 (2003)
3. Mamin R.F.: Physics of the Solid State **43**, 1314 (2001)

Cluster Spin Glass State as a Result of Lithium Deficiency in the Honeycomb System $\text{Li}_3\text{Ni}_2\text{SbO}_6$

E. Vavilova¹, T. Salikhov¹, E. Zvereva², V. Nalbandyan³

¹ Zavoisky Physical-Technical Institute, FRC Kazan Scientific Center of RAS, Kazan 420029, Russian Federation, jenia.vavilova@gmail.com

² Faculty of Physics, Moscow State University, Moscow 119991, Russian Federation

³ Chemistry Faculty, Southern Federal University, Rostov-on-Don 344090, Russia

The impact of defects on the balance of interactions in the frustrated layered honeycomb magnets is a topic that has been actively discussed in recent years. Here we present the results of studies of compound $\text{Li}_{0.8}[\text{Ni}_{0.6}\text{Sb}_{0.4}]\text{O}_2$ where structural defects are created by the deficient of Li ions, which occupy the positions between the magnetic Ni-Sb-O honeycomb planes. Such defects lead to various changes in the system: first, due to the requirements of the charge balance, one can expect changes in the oxidation state of Ni and Sb ions in planes. Secondly, structural studies favor a small change in the Sb ions content in this compound and the related structural defects of planes and local breaks of the periodicity of the magnetic lattice. Thirdly, one can, in principle, expect the appearance of mobile charge carriers in metal-oxide planes. And finally, fourthly, vacancies at lithium positions lead to hopping mobility of these ions at high temperatures [1]. The data obtained in the studies of AC and DC susceptibility and ^7Li NMR indicate that the ground state of the system is transformed from zigzag AF order to cluster spin glass, which, in principle, is expected when defects are introduced into a frustrated magnetic system. Based on the research results, the features of the critical regime and the parameters of the ground state in the system under study are determined.

The work was supported by RFBR through grant No. 18-02-00664.

1. Salikhov T. et al.: Magnetic Resonance in Solids. Electronic Journal **18**, 16207 (2016)

Superparamagnetic Properties in $\text{La}_{0.83}\text{Sr}_{0.17}\text{Mn}_{0.9}\text{Zn}_{0.1-x}\text{Fe}_x\text{O}_3$ ($x = 0, 0.025, 0.075, 0.1$)

R. M. Eremina¹, I. V. Yatsyk¹, Z. Y. Seidov², A. Badelin³

¹ Zavoisky Physical-Technical Institute, FRC Kazan Scientific Center of RAS, Kazan 420029, Russian Federation

² Institute of Physics, Azerbaijan National Academy of Sciences, Baku, Azerbaijan

³ Astrakhan State University, Astrakhan, Russia Russian Federation

Hole doped manganites having the general formula $\text{A}_{1-x}\text{B}_x\text{MnO}_3$, where A is one or several trivalent cations from the group of lanthanides and B is a divalent alkaline-earth metal such as Ca, Ba, or Sr, have a quite rich phase diagram resulting from the interplay between the spin, orbital, charge, and lattice degrees of freedom. In addition to the problems related to the orbital, charge, and magnetic ordering, these materials attract considerable current interest owing to such phenomena as the colossal magnetoresistance and phase separation [1, 2].

In this work, we studied $\text{La}_{0.83}\text{Sr}_{0.17}\text{Mn}_{0.9}\text{Zn}_{0.1-x}\text{Fe}_x\text{O}_3$ ($x = 0, 0.025, 0.075, 0.1$) by the magnetic resonance method. Temperature dependencies of the ESR linewidth for $\text{La}_{0.83}\text{Sr}_{0.17}\text{Mn}_{0.9}\text{Zn}_{0.1-x}\text{Fe}_x\text{O}_3$ are presented in Fig.1. A shift in the temperature of magnetic ordering with increasing iron concentration was detected.

The work was supported by RFBR (grant 18-52-06011).

1. Deisenhofer J., Braak D., Krug von Nidda H.-A., Hemberger J., Eremina R.M., Ivanshin V.A., Balbashov A.M., Jug G., Loidl A., Kimura T., Tokura Y.: Phys. Rev. Lett. **95**, 257202 (2005)
2. Kadomtseva A.M., Popov Yu.F., Vorobiev G.P., Kamilov K.I., Mukhin A.A., Ivanov V.Yu., Balbashov A. M.: Phys. Solid State **48**, 2134 (2006)

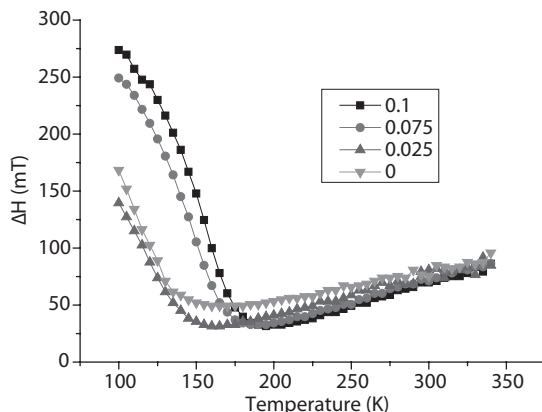


Fig. 1. Temperature dependence of the ESR linewidth for $\text{La}_{0.83}\text{Sr}_{0.17}\text{Mn}_{0.9}\text{Zn}_{0.1-x}\text{Fe}_x\text{O}_3$ ($x = 0, 0.025, 0.075, 0.1$).

Photostimulated Properties of Ferroics and Photoconductivity at the Interface of the $\text{Ba}_{0.8}\text{Sr}_{0.2}\text{TiO}_3/\text{LaMnO}_3$

**D. P. Pavlov, T. S. Shaposhnikova, A. V. Leontyev,
D. K. Zharkov, T. M. Salikhov, R. F. Mamin**

Zavoisky Physical-Technical Institute, FRC Kazan Scientific Center of RAS, Kazan 420029,
Russian Federation, mamin@kfti.knc.ru

We present the results of a theoretical investigation of the dynamical states in ferroics arising under the illumination in the vicinity of phase transitions. The regions of phase coexistence as well also the emergence of unstable states arise in the ferroelectrics in the vicinity of the photostimulated phase transition [1–3]. We have investigated the appearance of a dynamical regime in ferromagnetic and antiferromagnetic semiconductors [4] in the vicinity of the phase transition in depending on the illumination conditions. The dynamics of the system is considered by analysis of the behavior of the order parameter and the charge carrier concentration on the defects. It is shown that the existence of the nonequilibrium and spatial nonuniform states and, as well, the dynamical and auto-oscillation regimes of the system is possible in the vicinity of a phase transition under the illumination. The corresponding time and spatial change of the order parameter and the concentration of charge carriers on the defects are obtained. The intensity of illumination - temperature region of the hysteresis state is estimated. A phase diagram of the various states of the system in the parameter space “the intensity of illumination - the temperature” is obtained. The new possibilities of dynamical regimes for the case of layered structures are discussed.

The thin film of epitaxial $\text{Ba}_{0.8}\text{Sr}_{0.2}\text{TiO}_3$ (BSTO) was sputtered on the top of single crystalline LaMnO_3 samples using the magnetron sputtering technique. Antiferromagnetic LaMnO_3 might be transferred to ferromagnetic state by increasing the concentration of free carriers by injection. This means that increasing the free charge carriers might lead to the local ferromagnetic state and magneto-resistivity in a system with 2DEG. Therefore, there is an opportunity to switch both conductivity by an electric field (trigger effect), and the magnetic order (magnetoelectric effect) in the heterostructures similar to BTO/LMO. Conductivity measurements of the heterostructure were performed by a four-point probe method. Our measurements demonstrated that the resistivity of samples with deposited film of BSTO decreases strongly, and below the temperature of 160 K passes to a metallic-like behavior. Dependencies of the electrical resistance on temperature were studied for $\text{Ba}_{0.8}\text{Sr}_{0.2}\text{TiO}_3/\text{LaMnO}_3$ heterostructure. Green (514 nm) pulsed light induces transient resistance component. In 80–200 K range this transient component is positive and ~15%

of the steady-state resistance, the time constant associated with the transient component is ~ 12 s.

The study of photostimulated phenomena financial was supported from the government assignment for FRC Kazan Scientific Center of RAS. The reported study of photoconductivity was funded by Russian Scientific Foundation according to the research project No. 18-12-00260.

1. Mamin R.F., Teitel'baum G.B.: JETP Lett. **44**, 420 (1986)
2. Mamin R.F.: JETP Lett. **60**, 52 (1994)
3. Mamin R.F.: JETP Lett. **84**, 808 (1997)
4. Nagaev E.L.: Sov. Phys. Usp. **18**, 863 (1975)

Electron Spin Resonance Study of $\text{Sm}_{1-x}\text{Yb}_x\text{B}_6$ Solid Solutions

S. V. Demishev¹, M. I. Gilmanov¹, A. N. Samarin¹, A. V. Semeno^{1,2},
N. E. Sluchanko^{1,2}, N. Yu. Shitsevalova³, V. B. Filipov³, V. V. Glushkov¹

¹ Prokhorov General Physics Institute of RAS, Vavilov str., 38, Moscow 119991,
Russian Federation, gilmanov@lt.gpi.ru

² Moscow Institute of Physics and Technology, Dolgoprudny 141700 Moscow region,
Russian Federation

³ Institute for Problems of Materials Science of NASU, Kiev 03680, Ukraine

In a recent investigation of topological Kondo insulator candidate SmB_6 by means of electron spin resonance (ESR) [1] arose a question of the nature of the magnetic centers in this mysterious compound. Various possibilities were discussed including the formation of spin-polaron states on the surface of SmB_6 [2]. One of the ways to shade more light on this problem is to study ESR in doped SmB_6 system, which is the subject of present work.

A series of solid solutions $\text{Sm}_{1-x}\text{Yb}_x\text{B}_6$ with $x = 0.005, 0.05, 0.1$ has been studied. It is very surprising that the general temperature behavior (abrupt decrease of intensity below $T^* \sim 7$ K) as well as g -factor and 4-line structure of ESR spectrum seems to be similar to the case of pure SmB_6 (fig. 1). The main difference introduced by Yb doping appears in intensity and line width of the components of the ESR spectrum, which most likely means that Yb^{3+} ions are ESR-silent and the observed signal has the same nature as for undoped compound. In the same time the components of the signal are much better resolved, allowing for more clear separation and analysis, while having an additional control parameter of doping concentration.

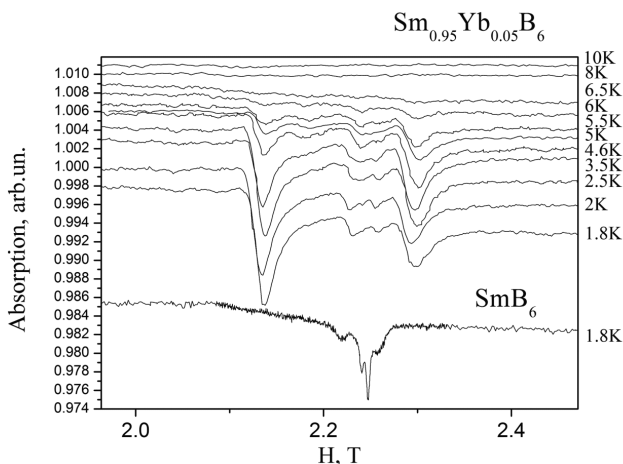


Fig. 1. Temperature dependence of $\text{Sm}_{1-x}\text{Yb}_x\text{B}_6$ ESR spectra on $f = 60$ GHz for $x = 0.05$ (upper curves) and a single ESR spectrum of pure SmB_6 for a reference.

The data obtained in a frequency range 28–60 GHz shows, that the *distance* between the components of the ESR spectra remains constant, while the left-most component have *g*-factor $g = 2$, i.e. with a change of a frequency the signal moves as a whole. Such an unusual behavior seems to be quite unlikely in case of a single ion nature of ESR signal, and strongly favors the hypothesis of the spin-polaron states formation [2].

This work was supported by programmes of Russian Academy of Sciences “Electron spin resonance, spin-dependent electronic effects and spin technologies”, “Electron correlations in strongly interacting systems”.

1. Demishev S.V., Gilmanov M.I., Samarin A.N., Semeno A.V., Sluchanko N.E., Samarin N.A., Bogach A.V., Shitsevalova N.Yu., Filipov V.B., Karasev M.S., Glushkov V.V.: *Sci. Rep.* **8**, 7125 (2018)
2. Demishev S.V., Gilmanov M.I., Samarin A.N., Semeno A.V., Sluchanko N.E., Samarin N.A., Bogach A.V., Shitsevalova N.Yu., Filipov V.B., Karasev M.S., Glushkov V.V.: *Appl. Magn. Reson.* **51**, 71 (2020)

SECTION
ELECTRON SPIN-BASED METHODS
FOR ELECTRONIC AND SPATIAL STRUCTURE
DETERMINATION IN PHYSICS, CHEMISTRY
AND BIOLOGY

**Comparative Analysis of Electro-surface Properties
of Mesoporous Alumina Grafted with Silanes
Using EPR of pH-Sensitive Nitroxide Radicals**

D. Tambasova, P. Lyubyakina, E. Kovaleva

Institute of Chemical Engineering, Ural Federal University, 19 Mira St., Yekaterinburg, 620002,
Russian Federation, d.p.tambasova@urfu.ru

Composite materials are attracting more and more scientists' attention, allowing to combine the advantages of previously developed carriers, such as simple silicate matrices, polymer gels and nanoparticles [1]. Mesoporous materials, including mesoporous alumina, have been actively studied in diverse areas including adsorption processes and heterogeneous catalysis including enzymatic [2]. In this study we used EPR spectroscopy of pH-sensitive nitroxides as spin probes to evaluate the surface charge and interfacial acid-base equilibria in the modified surface of mesoporous white powdered γ -Al₂O₃ of a granular structure, with a specific surface of 173.28 m²/g, an average pore diameter of 2.40 μ m, particle diameter of the predominant fraction of 0.41 μ m [3]. The γ -Al₂O₃ were grafted with 3-aminopropyltriethoxysilane (APTES), 3-(2,3-epoxypropoxy)-propyltrimethoxysilane (EPPMS), 3-methoxymethylsilane (TMOMS) and 3-mercaptopropyltrimethoxysilane (MPP-TMOS). pH-sensitive nitroxide probe, 2-(4-(chloromethyl)phenyl)-5,5-dimethyl-2-ethyl-2,5-dihydro-1H-imidazole-1-oxyl, has been synthesized at the Institute of Organic Chemistry, Siberian Branch of the Russian Academy of Sciences, Novosibirsk. It was found that the conditions of samples pretreatment exerted a significant effect on the apparent pK_a of nitroxides measured from EPR titration curves (Fig.1). In the series of intrinsic γ -Al₂O₃ and γ -Al₂O₃ grafted with APTES, EPPMS, TMOMS and MPP-TMOS pK_a shifts of EPR titration curves of the NR used in the aluminum oxides about those for the radical bulk solution (ΔpK_{a1-a5}) were found

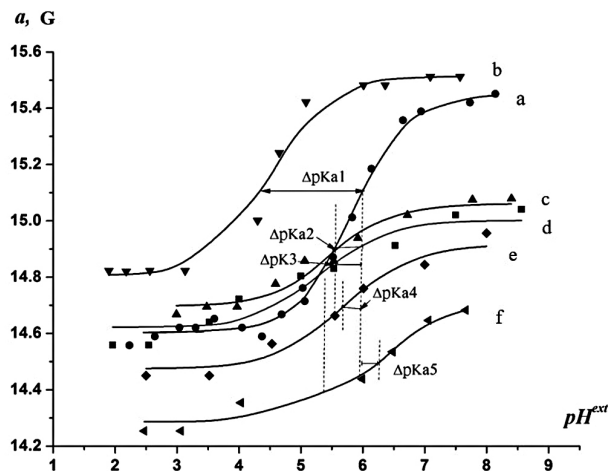


Fig. 1. EPR titration curves for NR titration in an aqueous solution with $\mu = 0.1$ (a), in the pores of $\gamma\text{-Al}_2\text{O}_3$ (b), $\gamma\text{-Al}_2\text{O}_3$, grafted with APTES (c), EPPMS (d), TMOMS (e) and MPP-TMOS (f), solution ($\text{pH}_{\text{ext}} = 4\text{--}4.2$).

to be equal to -1.5 , -0.4 , -0.3 and -0.25 , $+0.22$, respectively. It means that in this series surface electrical charge first becomes less positive and then for the sample modified with MPP-TMOS surface recharges from positive to negative. For the series of the above-mentioned modified $\gamma\text{-Al}_2\text{O}_3$ there was observed a decrease in hyperfine interaction constant (a , G) that caused by a decrease in surface polarity [4,5].

The results of the research showed that $\gamma\text{-Al}_2\text{O}_3$ surface grafted with different silanes leads both to a decrease in the polarity of the oxide surface and to an increase in its negative charge. They allowed to establish the relationship between the surface charge and the catalytic activity of heterogeneous catalytic systems (in some model reactions of decomposition of natural polysaccharides and to optimize conditions for the HCS) formation of GCS with the highest catalytic activity.

The research was supported by the Foundation for Basic Research (grant 18-29-12129mk).

1. Paul D.R., Robeson L.M.: Polymer, Polymer nanotechnology: Nanocomposites **49**, 3187–3204 (2008).
2. Muhammad Azam Khan. Hydrolysis of Hemicellulose by Commercial Enzyme Mixtures. Lulea University of Technology, Lulea, 2010.
3. Akrapopulu K.C., Vordonis L., & Lycourghiotis A.: Effect of temperature on the point of zero charge and surface dissociation-constants of aqueous suspensions of gamma- Al_2O_3 . Journal of the Chemical Society-Faraday Transactions I, **82**, 3697–3708 (1986)
4. Fernandez M.S., Fromherz P.: Lipoid pH indicators as probes of electrical potential and polarity in micells. J. Phys.Chem. **81(18)** 1755 (1977)
5. Khramtsov V.V., Marsh D., Weiner L.M. *et al.*: The application of pH-sensitive spin labels to studies of surface potential and polarity of phospholipid membranes and proteins. Biochim. Biophys. Acta. **1104** 317 (1992)

EPR Study of Yb³⁺ Impurity Ions in Mg₂SiO₄ Single Crystals

**V. Tarasov¹, A. Sukhanov¹, R. Zaripov¹, K. Subbotin², E. Zharikov²,
V. Dudnikova³**

¹ Zavoisky Physical-Technical Institute, FRC Kazan Scientific Center of RAS, Kazan, 420029, Russia, tarasov@kfti.knc.ru

² Laser Materials and Technology Research Center, Prokhorov General Physics Institute of RAS, Moscow, 119991, Russian Federation

³ Moscow State University, Moscow, 119991, Russian Federation

Continuous wave EPR spectroscopy is used to obtain crystal structure and magnetic properties of paramagnetic centers formed by Yb³⁺ impurity ions in forsterite (Mg₂SiO₄) single crystals. The measurements were performed at helium temperatures by the ELEXSYS E580 EPR spectrometer in the X-band. It is found that Yb³⁺ ions in Mg₂SiO₄ substitute Mg²⁺ ions in M1 site with the C_i point symmetry group of the crystal field and enter the crystal lattice in the form of single ions and dimer associates. The concentration of the dimer associates is several orders of magnitude higher than the concentration of associates formed randomly at the statistical distribution of impurity ions over the crystal. It is assumed that mechanism leading to the association of the impurity ions into the dimers is related with the necessity to conserve the total cation charge during the heterogeneous substitution. In this case three Mg²⁺ cations are replaced by the dimer associate of the two trivalent impurity ions with magnesium vacancy nearby them. Orientation dependencies of the EPR spectra were measured for the rotations of external magnetic field around *a*, *b* and *c* crystal axes. It enables us to determine directions of the principal magnetic axes and the parameters of the effective spin Hamiltonian that describe the magnetic characteristics of the ytterbium impurity centers in forsterite.

The work was supported by Russian Foundation for Basic Research (project 18-07-01144 a).

Development of Fullerene-Based Spin Label for Nanometer Distance Measurements

**I. Timofeev^{1,3}, E. Tretyakov^{2,3}, G. Fazleeva⁴, P. Troshin⁵,
E. Bagryanskaya^{2,3}, M. Fedin^{1,3}, O. Krumkacheva^{1,3}**

¹ International Tomography Center SB RAS, Novosibirsk, 630090, Russian Federation,
ivan.timofeev@tomo.nsc.ru

² Vorozhtsov Institute of Organic Chemistry SB RAS, Novosibirsk 630090, Russian Federation

³ Novosibirsk State University, Novosibirsk 630090, Russian Federation

⁴ Arbuzov Institute of Organic and Physical Chemistry RAS, Kazan 420088, Russian Federation

⁵ Skolkovo Institute of Science and Technology, Moscow 143026, Russian Federation

Pulsed dipolar EPR spectroscopy has been proved a valuable tool for extracting structural and dynamic data from spin-labeled biomolecules. Since widely used nitroxide spin labels give insufficient sensitivity, new kinds of labels appear intended to improve data quality. Recently, our group proposed triplet fullerene as a perspective spin label for DEER distance measurements [1]. Triplet fullerene hyperpolarization reduces DEER accumulation time by a factor of 10–1000 compared to nitroxide radicals, which is greatly important for acquiring long distances. One of our problems today is the development of fullerene-based spin label featuring the outstanding properties of pristine fullerene and applicable to measure distances in water-soluble biomolecules.

In this work we attempted different strategies to achieve high EPR signal and long phase memory times for water-soluble fullerene derivatives. We characterize the derivatives using EPR at 20 K and UV-vis spectroscopy and compare to pristine fullerene. Derivatization of fullerenes does not lead to full dissolution in water to monomers, so derivatives exhibit poor triplet EPR signal in water. To improve their water solubility and obtain magnetic properties we employed non-covalent formation with gamma-cyclodextrins. The fullerene:cyclodextrin complexes are dissolved then to monomers and feature triplet EPR spectra as of pristine fullerene dissolved in toluene. Similar to nitroxides, transverse relaxation at low temperatures is determined by nuclear spin diffusion, so deuteration increases phase memory times. The work is continued with tethering of the studied fullerene derivatives to biopolymers.

The work was supported by Russian Foundation for Basic Research (grant 19-29-10035).

Synthesis and ESR Study of Copper Doped CdSe and “Core-Shell” CdSe/CdS Quantum Dots

**D. O. Sagdeev¹, R. R. Shamilov¹, V. K. Voronkova², A. A. Sukhanov²,
Yu. G. Galyametdinov^{1,2}**

¹Kazan national research technological university, Kazan, Russia, demsagdi@yandex.ru

²Zavoisky Physical-Technical Institute, FRC Kazan Scientific Center of RAS, Kazan 420029, Russian Federation, ansukhanov@mail.ru

Combination of magnetic and luminescent properties make Cu doped quantum dots a perspective material for creation of bifunctional agent for multimodal medical imaging [1].

We developed the synthesis method of the magnetic Cu:CdSe colloidal quantum dots with hydrophilic stabilizer (mercaptoacetic acid). Nanoparticles show two types of strong ESR spectra (Fig. 1) of Cu²⁺ located at the CdSe surface (broaden line) and single ions in the bulk of crystal lattice (hyperfine splitting). These QDs have luminescence spectra at orange-red wavelengths. However, “core” quantum dots usually have low luminescence intensity. The one of the ways for solving that problem is covering QDs with semiconductor with wide band gap like CdS [2]. But there is no data how shell growth influent on surface-located Cu²⁺ ions.

In our experiment, CdS shells also were grown by colloidal method but using the mixture of hydrophobic stabilizers – oleic acid and dodecanethiol. We observed that core-shell QDs also show ESR spectra, but only characteristic for Cu²⁺ ions located on the CdS surface (Fig. 1). This may indicate the process of

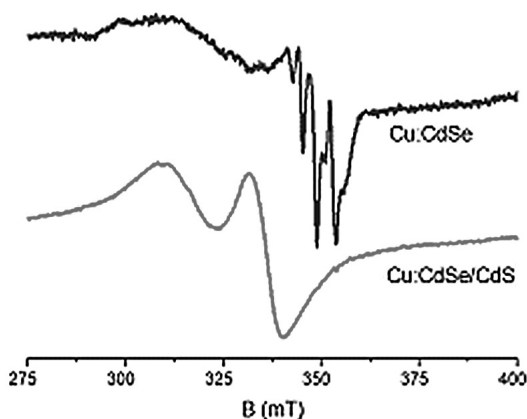


Fig. 1. ESR spectra of the Cd_{0.95}Cu_{0.05}Se quantum dots powder before and after the CdS shell growth

displacement of impurity ions from the CdSe crystal lattice during shell formation and ligand replacement and re-adsorption at the CdS surface.

Any changes in the location of luminescence peak were not observed. This may indicate the absence of the influence of presence of copper ions in the semiconductor crystal lattice on the luminescence of Cu:CdSe quantum dots.

The work was supported by the Russian Foundation for Basic Research, project 20-03-00620 A.

1. Zhang F., He X.W., Li W.Y., Zhang Y.K.: *J. Mater. Chem.* **22**, 22250 (2012)
2. Galyametdinov Y.G. *et al.*: *Rus. Chem. Bul.* **67**, 1, 172 (2018)

Determination of the Energy Level Position of Radicals in the Band Gap of TiO₂ Based Microspheres Using EPR Spectroscopy

E. V. Kytina¹, E. R. Parkhomenko¹, E. A. Konstantinova^{1,2}

¹ Department of Physics, M. V. Lomonosov Moscow State University, Russian Federation

² National Research Center Kurchatov Institute, Moscow, Russian Federation, liza35@mail.ru

Nowadays, titania based species widely used for air purification, gas sensors, water photosplitting, photovoltaic application [1, 2]. The most active research is currently underway in the development of energy-efficient photocatalysts operating under illumination in the visible region of the spectrum [3]. The behavior of such photocatalysts is very sensitive to the structure of energy levels arising in their band gap as the result of bulk doping and surface modification [1–3]. Really, intraband optical transitions, a recombination of photogenerated charge carriers and redox reactions in the nanostructured semiconductors occur with the participation of these energy levels. Therefore the aim of this work was to demonstrate the possibility of determining the position of photoactive energy levels in the band gap of titania based nanostructured microspheres from the electron paramagnetic resonance (EPR) spectroscopic measurements under the “in situ” illumination of the samples.

All the samples under investigation were synthesized by the modified aerosol pyrolysis method (see details in [4]). EPR spectra were recorded with an ELEXSYS-E500 (Bruker, Germany) spectrometer (X-band, the sensitivity up to 10^{10} spin/G). The samples were illuminated directly in the spectrometer cavity in the range of 270–1000 nm. As the light source, a high pressure mercury lamp with the diffraction monochromator was used. The illumination intensity was of ca. $40 \text{ mW} \cdot \text{cm}^{-2}$.

Light irradiation induces fundamental and impurity absorption

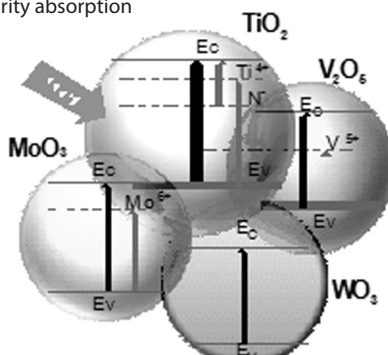


Fig. 1. Diagram of the band structure of microspheres, consisting of TiO₂, MoO₃, V₂O₅, WO₃ nanocrystals.

We have studied nitrogen doped microspheres ($\text{TiO}_2/\text{MoO}_3$, TiO_2/WO_3 , $\text{TiO}_2/\text{V}_2\text{O}_5$, $\text{TiO}_2/\text{MoO}_3/\text{V}_2\text{O}_5$, $\text{TiO}_2/\text{WO}_3/\text{V}_2\text{O}_5$, $\text{TiO}_2/\text{MoO}_3/\text{WO}_3$, $\text{TiO}_2/\text{MoO}_3/\text{V}_2\text{O}_5/\text{WO}_3$) using our new method based on EPR spectroscopy for constructing the band diagram of nanostructured semiconductors. Different paramagnetic centers (Ti^{3+} , Mo^{5+} , V^{4+} , N^{\cdot}) were found in the microspheres depending on their composition. The EPR signal intensity of the revealed radicals was changing under illumination. We have measured the dependence of the EPR signal intensity of different paramagnetic centers on the photon energy ($h\nu$). Let us discuss as example the results obtained for the $\text{TiO}_2/\text{MoO}_3/\text{V}_2\text{O}_5/\text{WO}_3$ samples.

It was found that at values of the photon energy $h\nu = 2.7$ eV, an increase in the intensity of the EPR signal from Ti^{3+} centers occurs, and at $h\nu = 1.55$ eV, the EPR signal from N^{\cdot} radicals increases (TiO_2 nanocrystals, $E_g = 3.2$ eV). We suppose, taking into account the data of [2], that the defects are recharged under illumination due to impurity absorption: $\text{N}^- + h\nu \rightarrow \text{N}^{\cdot} + e$ (in the conduction band); $\text{Ti}^{4+} + h\nu \rightarrow \text{Ti}^{3+} + h$ (in the valence band). It was found that at values of the photon energy $h\nu = 2.8$ eV, an increase in the intensity of the EPR signal from Mo^{5+} centers occurs (MoO_3 nanocrystals, $E_g = 3.1$ eV), and at $h\nu = 2.1$ eV, the EPR signal from V^{4+} radicals increases (V_2O_5 nanocrystals, $E_g = 2.5$ eV). No paramagnetic centers were detected in WO_3 . Using the obtained values, we can estimate the position of the energy levels of these defects in the band gap [2]. This result is shown in Fig. 1.

The obtained results can be useful for understanding the mechanism of photocatalytic behavior of titania based microspheres.

The reported study was funded by RFBR according to the research project № 18-29-23051.

1. Chen X., Mao S.: Chem. Rev. **107**, 2891 (2007)
2. Hoffmann M.R., Martin S.T., Choi W., Bahnemann D.W.: Chem. Rev. **95**, 69 (1995)
3. Konstantinova E.A., Kokorin A.I., Minnekhanov A.A., Sviridova T.V., Sviridov D.V.: Catal. Lett. **149**, 1147 (2019)
4. Tarasov A., Hu Z., Meledina M., Trusov G., Goodilin E., Dobrovolsky Y.: J. Phys. Chem. C: **121**, 4443 (2017)

Specific Features and Application Examples of a High-Frequency Electron Spin Resonance Spectrometer with Frequency Modulation

**Yu. A. Uspenskaya¹, R. A. Babunts¹, E. V. Edinach¹, A. S. Gurin¹,
H. R. Asatryan¹, D. O. Tolmachev², N. G. Romanov¹, A. G. Badalyan¹,
P. G. Baranov¹**

¹ Ioffe Institute, Russian Academy of Sciences, St. Petersburg, Russian Federation,
yulia.uspenskiya@mail.ioffe.ru

² Experimentelle Physik III, Technische Universitat Dortmund, Dortmund, Germany

The EPR spectrometer that operates in a continuous mode in W- (wavelength – 3 mm) and D- (2 mm) bands with frequency modulation has been developed. As a rule, EPR spectrometers operate in a continuous wave mode with low-frequency modulation of the magnetic field and lock-in detection at the modulation frequency. The method of low-frequency modulation of the operating frequency has been tested and patented [1].

Figure 1 shows the EPR spectra of the yttrium-aluminum garnet (YAG) crystal doped with rare-earth ions (Tb^{3+} and Ce^{3+}) at a frequency of 94 GHz using the nonresonant microwave insert [2]. The spectra were recorded at low-frequency (680 Hz) modulation of the operating frequency with modulation amplitude $f_{mod} = 2.5$ MHz.

For comparison, the spectrum obtained according to the standard technique of recording EPR spectra with low-frequency modulation of the magnetic field with the amplitude of 0.1 mT is shown in Fig. 1. The correlation between the

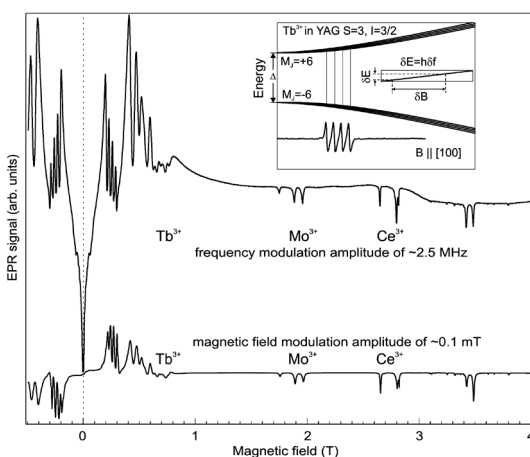


Fig. 1. EPR spectra of YAG:Tb,Ce recorded at a frequency 94 GHz at the temperature of 1.5 K with modulation of the magnetic field and frequency modulation.

frequency modulation amplitude and the magnetic field modulation amplitude can be defined by the following formula:

$$\Delta\nu = (g_e\mu_B/h)\Delta B,$$

i.e., 1 mT = 28 MHz for $g_e = 2.00$. It is obvious that the intensity of the EPR spectra of Tb^{3+} ions recorded by the frequency modulation technique increases. The spectra are normalized by signals of Ce^{3+} . A further decrease in the frequency modulation amplitude is possible based on the signal-to-noise ratio. In a high-frequency range the frequency modulation can be used in both systems: with low Q factor and with cavities application.

At a standard cavity Q factor, about 500–1000, the half-width of the resonance curve in the W range is 95–190 MHz; i.e., even at the maximum frequency modulation amplitude of 15 MHz, frequency changes will be close to the dip point. For the frequency of 130 GHz, the conditions are more favorable.

The method of low-frequency modulation of the operating frequency makes it possible to exclude modulation coils and increase sensitivity in studies of spin systems with weak divergence of the Zeeman levels in the magnetic field.

This work was supported by the Russian Foundation for Basic Research under Grant No. 19-52-12058, Deutsche Forschungsgemeinschaft (DFG) within the framework of the ICRC project TRR 160.

1. Babunts R.A., Badalyan A.G., Uspenskaya Yu.A., Gurin A.S., Romanov N.G., Baranov P. G.: RF Patent No. 2711228 (2020)
2. Edinach E.V., Uspenskaya Yu.A., Gurin A.S., Babunts R.A., Asatryan H.R., Romanov N.G., Badalyan P.G., Baranov A.G.: Phys. Rev. B **100**, 104435 (2019)

SECTION MEDICAL PHYSICS

Connective Tissue Dysplasia: Computer Analysis of Serum Fe³⁺-Transferrin ERR Spectra

**G. Gumarov¹, M. Ibragimova¹, A. Chushnikov¹, D. Khaibullina²,
V. Petukhov¹, I. Yatsyk¹**

¹ Zavoisky Physical-Technical Institute, FRC Kazan Scientific Center of RAS, Kazan 420029,
Russian Federation, ibragimova@kfti.knc.ru

² Kazan state medical Academy, Kazan 420012, Russian Federation, dina.khaibullina@mail.ru

The use of various physical methods, in particular the EPR-spectroscopy, for the diagnosis of pathological changes in the organism using blood analysis is an urgent task of modern medicine. One of the serum proteins is human transferrin (Tf) consisting of two homologous lobes which each strongly bind an iron ion in the high-spin ferric form ($S = 5/2$). The absorption line with effective g -factor $g' = 4.3$ assigned to the Tf-Fe³⁺ ions (at 9.7 GHz – X-band) has complicated shape (a double peak and shoulder) flanked by exceptionally broad asymmetric tails. The aim of this work was to establish the peculiarities of such a pathology as connective tissue dysplasia based on created computer analysis of the high-spin serum Fe³⁺-Tf lineshape by using EPR spectra recorded at 80 K on X-band spectrometer Bruker EMX-300"

To simulate EPR spectra from Fe³⁺ the Easyspin software package was used, a pepper utility for performing EPR calculations of powdered solid-state samples. In accordance with M. Azarkh *et al.* [1] for description the EPR spectra was used the spin Hamiltonian including the fine structure terms up to 4th order:

$$\mathbf{H} = \mu_B \mathbf{B}_0 \mathbf{gS} + \text{SDS} + \sum_q B_4^q \mathbf{O}_4^q(\mathbf{S})$$

The second term describes the second-order zero-field splitting (ZFS) of the six magnetic sublevels into three Kramers doublets. The tensor \mathbf{D} is symmetric and taken traceless, which means that the three principal values of \mathbf{D} can be expressed in just two parameters $D = 3/2D_z$ and $E = 1/2(D_x - D_y)$. The ratio E/D is referred to as the rhombicity of the D -tensor.

Computer analysis was carried out in three stages. Preliminary modeling was performed using the anisotropic broadening of the splitting in zero field. In this

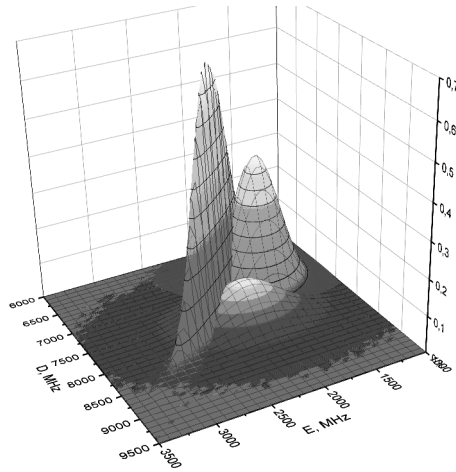


Fig. 1. The result of computer analysis.

case the area of the studied values and the distribution center were approximately determined. Three systems were introduced, each with its own orthorhombicity parameter. The results of this stage were used as the starting values of the desired parameters for the next stages. In the second stage, three two-dimensional Gaussian distributions were established, each of which has the form:

$$f(D, E) = A \exp \left[- \frac{((D - D_0) \cos \alpha + (E - E_0) \sin \alpha)^2}{2\sigma_D^2} - \frac{(-(D - D_0) \sin \alpha + (E - E_0) \cos \alpha)^2}{2\sigma_E^2} \right]$$

where D_0, E_0 – the distribution coordinates, σ_D and σ_E – the distribution width parameters, α – the rotation angle, A – the amplitude. Considering the sum of distributions as weights of spectra with corresponding parameters, the simulation spectrum was calculated. Variation of these parameters was used to achieve a minimum standard deviation of the model spectrum from the experimental one. Calculations of model spectra library were performed on a rectangular grid, the step for parameters D and E was 50 MHz. At the third stage, the “error grid” method described in work [1] was applied. In this case, the output is a distribution that is not associated with any initial assumption about the form of the distribution. In Fig. 1 and 2 the results of computer analysis and fitting of experiment spectrum are shown.

Thus, taking into account the splitting in the zero field and the fine structure terms up to 4th order in spin Hamiltonian showed that the proportion of components with different parameters of orthorhombicity E/D allowed us to describe obtained spectra satisfactorily. It was established that the proportion of

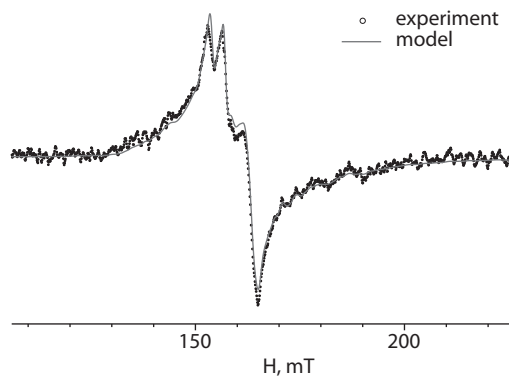


Fig. 2. The result of experiment spectrum fitting.

components with different parameters of ratio E/D for patients with back pain associated with connective tissue dysplasia (CTD) differs from each other, but they all differ significantly from the control ones. The obtained results indicate that the use of the EPR method with subsequent computer analysis of the spectra from serum $\text{Fe}^3\text{-Tf}$ can allow to identify and evaluate occult anomalies of iron turnover in patients with CTD. This is consistent with current concepts that trace elements play an important role in the development and implementation of clinical manifestations of this pathology. At the same time, the main part is given to Mg^{2+} but are almost no data on the influence of other trace elements, in particular iron, in the pathogenesis of CTD within the human body.

1. Mykhailo Azarkh, Peter Gast, Anne B. Mason, Edgar J. J. Groenen and Guinevere Mathies.: Phys. Chem. Chem. Phys. **21**, 16937 (2019)

Inter-Protein Molecular Interactions in Solutions of Human Serum Albumin, Studied by NMR-Diffusometry and Dynamic Light Scattering

A. K. Iskhakova^{1,2}, A. M. Kusova¹, A. E. Sitnitsky¹, Yu. F. Zuev¹

¹ Kazan Institute of Biochemistry and Biophysics, FRC Kazan Scientific Center, Russian Academy of Sciences, Kazan 420111, Russian Federation, presidium@knc.ru, knc@knc.ru

² Physics Department, Kazan Federal University, Kazan 420111, Russian Federation, phys.dep@kpfu.ru.

Estimation of protein-protein interactions is important for understanding biological processes in vivo and in vitro, as well as for developing and optimizing of biotechnological processes. The role of intermolecular interactions increases sharply in undiluted protein solutions, where they affect the protein structure and conformation, protein functioning, thermodynamics and kinetics of biochemical reactions.

Nuclear magnetic resonance (NMR) and dynamic light scattering (DLS) methods were used to determine collective and self-diffusion coefficients for rigid globular protein HSA (Human Serum Albumin). In this work, we used the theoretical Vink's approach to study inter-protein interactions analyzing the concentration dependences of collective and self-diffusion coefficients by means of friction and virial coefficients [1]. To evaluate the second virial coefficient as the measure of paired protein-protein interactions, the DLVO and Mac-Millan theories were used. The positive second virial coefficient usually corresponds to repulsive intermolecular interactions. On the ground of obtained virial coefficients, we evaluated the specificity of intermolecular interactions in solutions of globular proteins HSA and described them according to the data of collective and self-diffusion.

This work was performed with financial support from the Russian Foundation for Basic Research, Grant № 20-04-00157.

1. Vink H.: Mutual diffusion and self-diffusion in the frictional formalism of non-equilibrium thermodynamics, *J. Chem. Soc., Faraday Trans. 1*, 81, 1725–1730 (1985)

SECTION
THEORY OF MAGNETIC RESONANCE

**Collective Modes in Solutions of Nitroxyl Radicals
Detected by CW EPR**

M. M. Bakirov¹, K. M. Salikhov^{1,2}, I. T. Khairutdinov¹, B. Bales³

¹Zavoisky Physical-Technical Institute, FRC Kazan Scientific Center of RAS, Kazan 420029, Russian Federation, pinas1@yandex.ru

²Kazan Federal University, 18 Kremlyovskaya St., Kazan 420008, Russian Federation

³Western Institute of Nanoelectronics, University of California, Los Angeles 18111, USA

In contrast to the linear response region, CW EPR in the saturation region is an example of a signal from a system in strong magnetic fields. In the presence of spin exchange, new collective states forms in the spin system under the saturation condition. It is theoretically demonstrated (Fig. 1) that in the system, consisting of two homogeneous lines in the presence of spectral diffusion V , the resonance frequencies of the collective modes changes from the amplitude of the microwave field (ω_1) [1].

Tempol nitroxyl radical were studied by CW EPR. The existence of these collective states from the analysis of the EPR spectra of nitroxyl radicals in

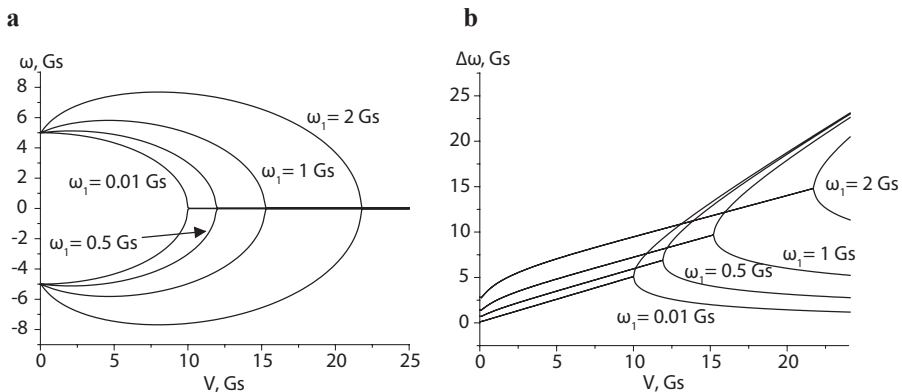


Fig. 1. Resonant frequencies of components (a) and the observed line widths of the EPR spectrum components (b) dependences on spectral diffusion V ($\gamma^{-1}T_1^{-1} = 0.05$ G, $\gamma^{-1}T_2^{-1} = 0.1$ G).

solution was experimentally established. These systems were also studied by pulsed EPR spectroscopy for the reliability of the results. The experimental data were simulated using spin density matrix formalism with spin-Hamiltonian model taking into account the hyperfine interaction of unpaired electrons with magnetic nitrogen nuclei and environment protons, dipole-dipole interaction, and isotropic exchange interaction between radicals.

1. Salikhov K.M.: Current state of the spin exchange theory in dilute solutions of paramagnetic particles. New paradigm of spin exchange and its manifestations in EPR spectroscopy. *Phys. Usp.* 951–975, **62**, (2019)

Spin-Echo Diffusion Attenuation and Spin Relaxation of a Particle Moving in a Random Magnetic Field

R. Shagvaleev¹, N. Fatkullin²

¹ Institute of Physics, Kazan Federal University, Kazan, 420008, Russian Federation,
shagvaly@yandex.ru

² Institute of Physics, Kazan Federal University, Kazan, 420008, Russian Federation,
nail.fatkullin@kpfu.ru

The magnetic susceptibility variation in spatially inhomogeneous media induces random magnetic fields, which may have strong impact on the effective self-diffusion and nuclear spin-relaxation rates as probed using nuclear magnetic resonance. In this work, we consider three different spatial correlation functions describing the random magnetic field, i.e., of the Yukawa, of the Gaussian and of the exponential types. We show that the effect of the random magnetic field on the quantities measured can differ substantially for different relative magnitudes of the characteristic parameters, such as the correlation length or time intervals in the NMR pulse sequences.

SECTION

LOW-DIMENSIONAL SYSTEMS AND NANO-SYSTEMS

Abnormal Magnetism of Nano- and Microscaled Tetrafluorites LiTbF_4 and LiDyF_4

**G. Yu. Andreev¹, A. G. Kiyamov¹, S. L. Korableva¹, A. A. Rodionov¹,
I. V. Romanova¹, A. S. Semakin¹, M. S. Tagirov^{1,2}**

¹ Kazan Federal University, Kremlevskaya 18, Kazan 420008, Russian Federation, ujif28@mail.ru

² Institute of Applied Research, Tatarstan Academy of Sciences, Levobulachnaya 36a,
Kazan 420111, Russian Federation

Rare earth tetrafluorides LiReF_4 , $\text{Re} = \text{La—Lu}$, are a promising material for laser technology [1, 2], medicine and biotechnology[3]. LiTbF_4 is an Ising dipolar uniaxial ferromagnet; $T_C = 2.8741(16)$ K [5]. LiDyF_4 is a layered antiferromagnet; $T_N = 0.610(15)$ K [5].

Nanosized powders of LiTbF_4 were synthesized using hydrothermal method[6]. Microsized LiTbF_4 and LiDyF_4 powders were baked at 650. XRD patterns, TEM HR and optical microscope were used for characterization. Temperature and field dependencies of magnetization were measured at the vibrational magnetometer. LiTbF_4 nanopowder at $B = 10$ mT showed reduction of Curie temperature compared with monocrystal. Field dependence of LiDyF_4 micropowder's magnetization at temperatures below 7 K takes the form of antiferroelectric hysteresis. Temperature dependence of loops' area is measured. Also, this sample's magnetisation does not set instantly when the external field is set, but follows exponential law $\exp(-t/\tau)$. Values of τ are different for magnetization and demagnetization of LiDyF_4 micropowder.

The financial support of the Russian Foundation for Basic Research and the Government of the Republic of Tatarstan (project 18-42-160012 p_a) is gratefully acknowledged.

1. Zhai X., Lei P., Zhang P. *et al.*: *Biomaterials* **65**, 115–123 (2015)
2. Castellano-Hernández E., Kalusniak S., Metz P.W., Kränkel C.: *Laser & Photonics Reviews* **14**, no. 2, 1900229 (2020)
3. Zelmon D.E., Erdman E.C., Stevens K.T. *et al.*: *Applied Optics* **55**, 834–837 (2016)
4. Als-Nielsen J., Holmes L.M., Krebs Larsen F., Guggenheim H.J.: *Phys. Rev. B* **12**, 191–197 (1975)
5. Mennenga G., de Jongh L.J., Huiskamp W.J.: *Journal of Magnetism and Magnetic Materials* **44**, 48–58 (1984)
6. Zhang Q., Yan B.: *Inorganic Chemistry* **49**, no. 15, 6834–6839 (2010)

Spin-Polarized Current in Non-Collinear Magnetic Tunnel Junction

Ch. A. Fam¹, N. Kh. Useinov¹, A. P. Chuklanov², A. A. Bukharaev²

¹ Institute of Physics, Kazan Federal University, Kazan 420008, Russian Federation,
nuseinov@mail.ru

² Zavoisky Physical-Technical Institute, FRC Kazan Scientific Center of RAS, Kazan 420029,
Russian Federation

In the last decade scientists have turned their great interest in magnetic tunnel junctions (MTJs). This growing interest is associated with the probability of using MTJ in straintronics devices [1].

When an insulator layer with the thickness of several nanometers is placed between two ferromagnetic (FM) layers, as shown in Fig. 1, the electron may tunneling through the insulator layer due to its wave nature. Among other things the probability of tunneling depends on magnetization orientation of FM layers. As a result, the spin-polarized current occurs, that can be measured experimentally. For calculation of current-voltage characteristics and angular dependence of the spin-polarized current the modified theory of MTJ is used.

The equation for calculation of the spin-polarized current is following [2]:

$$I(V, \theta) = \sum_{\alpha, \alpha'} \frac{e^2 (k_{F, \alpha}^{\text{TS}})^2 A V}{4\pi^2 \hbar} \int_0^{\gamma_{\text{cr}}} \sin(\gamma_{\text{TS}, \alpha}) \cos(\gamma_{\text{TS}, \alpha}) T_{\alpha, \alpha'} [\cos(\gamma_{\text{TS}, \alpha}), V, \theta] d\gamma_{\text{TS}, \alpha},$$

where $\alpha = \uparrow \downarrow$ is the spin index, $k_{F, \alpha}^{\text{TS}}$ is the wave vector, which is connected with the voltage applied (TS (Top Side) indicates from which side positive voltage is applied), A is the contact area, V is the bias voltage applied to the contact, $T_{\alpha, \alpha'}$ is the transmission coefficient, γ_{cr} is the critical angle, which is derived from the conservation law for the parallel to the boundary components of Fermi wave vectors, $\gamma_{\text{TS}, \alpha}$ is the angle between axis z and direction of an electron in the top layer (see Fig. 1), θ is the angle between the magnetization directions in ferromagnetic layers.

The current-voltage characteristics of MTJ are calculated for non-symmetric case, when the properties of FM layers are different, Fig. 2. The analysis of angular dependence of spin-polarized current was made. It was revealed that the values of current flowing at $\theta = 0^\circ$ (i.e. when the magnetization of FM layers are parallel) and at $\theta = 180^\circ$ (antiparallel case) are significantly differ.

For example this theory can find application in the cases when FM layers have configurational anisotropy. The magnetization orientations of such the layers are differing from point to point and the angle between magnetization of layers can vary from 0 to 180° [2].

Thus, the theory of MTJ was developed for calculating spin-polarized current through magnetic structures with configurational anisotropy. The calculations of

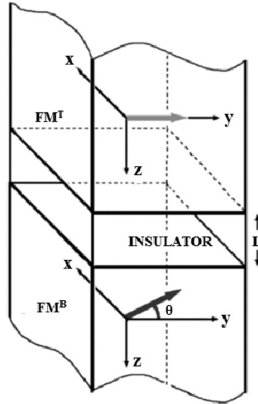


Fig. 1. Scheme of the MTJ, FMT/I/FMB, is placed on the piezoelectric substrate, see [2]. Arrows show the magnetization direction of ferromagnetic layers. FMT is magnetically hard, while FMB is magnetically soft; θ is an angle between the magnetization directions in ferromagnetic layers.

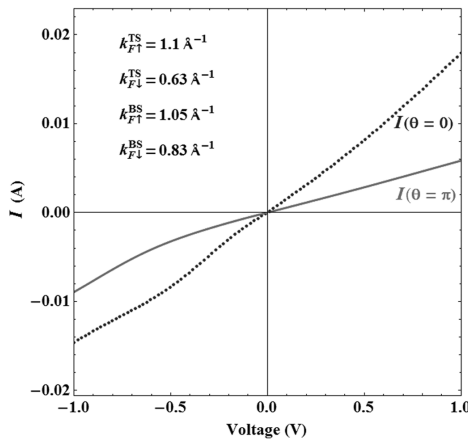


Fig. 2. The tunnel current on the applied voltage V at two values of the angle: $I(\theta = 0)$ is the parallel (dot line) and $I(\theta = \pi)$ is the antiparallel (solid line) orientation with non-identical FM of layers. The legend shows the MTJ parameters: $k_{F\alpha}^{TS(BS)}$ are the values of the wave vectors for the FM layers, $U = 3.8$ eV is the height of the barrier, $L = 20.0$ Å is the barrier thickness and $m_{\text{eff}} = 0.6m_e$ is the effective mass of electron in the barrier.

current-voltage characteristics with different distribution of top and bottom FM layers were performed.

The work was supported by the Russian Foundation for Basic Research (project 18-02-00204) and Program of Competitive Growth of Kazan Federal University.

1. Bukharaev A.A., Zvezdin A.K., Pyatakov A.P., Fetisov Yu.K.: Phys. Usp. **61**, 1175 (2018)
2. Bukharaev A.A., Bizyaev D.A., Nurgazizov N.I., Chuklanov A.P., Useinov N.Kh.: J. Magn. Magn. Mater. **500**, 166315 (2019)

Epitaxial Growth and Ferromagnetic Resonance Study of Magnetic Anisotropies in Thin Pd_{1-x}Fe_x Films on the Single-Crystal MgO(110) Substrate

**B. F. Gabbasov¹, A. I. Gumarov¹, A. A. Rodionov¹, I. V. Yanilkin¹,
R. R. Khabibullin¹, R. V. Yusupov¹, L. R. Tagirov^{1,2}**

¹ Institute of Physics, Kazan Federal University, Kazan, Russian Federation

² Zavoisky Physical-Technical Institute, FRC Kazan Scientific Center of RAS, Kazan 420029, Russian Federation, bulgabbasov@gmail.com

Palladium-rich Pd_{1-x}Fe_x ($x < 0.10$) alloys that possess face-centered cubic structure attract the attention of the researchers due to a promise of its use as magnetically-soft weak low-temperature ferromagnets in heterostructures of superconducting spintronics. Recently, the procedure [1] has been developed for a synthesis of the high-quality epitaxial Pd_{1-x}Fe_x thin films on a popular (001)-oriented single crystal MgO substrate with the “cube-on-cube” type epitaxy. It has been found with ferromagnetic resonance (FMR) and dc-magnetometry that these films are easy-plane ferromagnets with the four-fold in-plane anisotropy which magnitude increases with an increase of the iron content in the alloy [1]. However, for cryogenic memory applications the uniaxial in-plane anisotropy is requested. It is known that in the bulk crystalline Pd_{1-x}Fe_x alloys the true easy axes correspond to the <111>-type crystallographic directions. If this holds for epitaxial Pd_{1-x}Fe_x thin films as well, the uniaxial anisotropy can be achieved if the film is grown on a properly oriented substrate.

We report here on the successful application of the proposed earlier synthesis procedure to the growth of 20-nm thick epitaxial Pd_{0.92}Fe_{0.08} film on (110)-oriented MgO substrate. Film structure has been characterized *in situ* with LEED and *ex situ* with XRD techniques. Its magnetic properties were studied with vibrating sample magnetometry (VSM) and FMR. In particular, it was shown that indeed in-plane easy axes are parallel to the <111>-type crystallographic directions of MgO substrate. We find also that the orientation dependence of the FMR resonance field can be successfully described assuming the magneto-crystalline anisotropy with the orthorhombic symmetry. The symmetry lowering from cubic occurs due to the film and the substrate notable lattice mismatch and subsequent structure distortion.

This work was supported by the RSF project No. 18-12-00459. Synthesis and analysis of the films were carried out at the PCR Federal Center of Shared Facilities of KFU.

Ultrafast Magnetization Dynamics in Thin Films of L1₀-Ordered FePt and FePd Compounds

A. V. Petrov¹, M. V. Pasynkov¹, R. V. Yusupov¹, S. I. Nikitin¹,
A. I. Gumarov¹, I. V. Yanilkin¹, A. G. Kiiamov¹, L. R. Tagirov^{1,2}

¹ Institute of Physics, Kazan Federal University, Kazan 420111, Russian Federation, mike_p95@mail.ru

² Zavoisky Physical-Technical Institute, FRC Kazan Scientific Center of RAS, Kazan 420029, Russian Federation

Intermetallic compounds and heterostructures based on elements of the platinum group are the basis of modern media for super-dense magnetic recording of information. The choice is determined by the unique magnetic properties of such compounds and long-term stability, as well as the insensitivity of their magnetic properties to the corrosive effects of oxygen and air humidity. [1]

Thin films of FePd and FePt compounds 10 nm thick were grown by molecular beam epitaxy (MBE) on MgO (001) substrates at room temperature in an ultrahigh-vacuum chamber on a 3 nm thick chromium (Cr) seed layer deposited at a substrate temperature of 600 °C. To transfer the equimolar systems FePd and FePt to the ordered tetragonal phase L1₀, the film was annealed for 30 minutes at a temperature of 650 °C.

The crystal structure and epitaxiality of the grown FePd and FePt films were studied by low-energy electron diffraction (LEED) methods directly in the ultrahigh-vacuum chamber and X-ray diffraction (XRD) analysis. The contrasting patterns of the LEED maxima indicate the single-crystal nature of the films and their coherent growth on substrates, that is, cube by cube type epitaxy. The observation of the (001) maximum along with (002) in the X-ray diffractogram indicates the tetragonal symmetry of the crystal lattice of the films, which, in turn, indicates their successful synthesis in the desired ordered L1₀ phase.

Using femtosecond optical and magneto-optical spectroscopy, it was shown that thin films of the L1₀ phases of FePd and FePt compounds are characterized by different times of photoinduced demagnetization. Such a difference is a prerequisite for the creation of artificial multilayer ferrimagnetic structures of the F1/N/F2 type, where F1 and F2 are ferromagnetic layers, the nature of the interaction between which is determined by the thickness of the separator made of normal metal N. The difference in the demagnetization rates is a necessary condition for ultrafast photoinduced handling magnetization.

In the future, the synthesis of three-layer structures based on L1₀-FePd and L1₀-FePt is supposed. The latter are isostructural and have very close lattice constants, both with respect to each other and to the Fe_{0.08}Pd_{0.92} system. This makes it possible to create perfect heteroepitaxial structures based on them.

This work was supported by the RSF project No. 18-12-00459. Synthesis and analysis of the films were carried out at the PCR Federal Center of Shared Facilities of KFU.

Femtosecond Optical and Magneto-Optical Studies of Magnetic and Electronic Inhomogeneities in Pd_{1-x}Fe_x Thin Films

**A. V. Petrov¹, R. V. Yusupov¹, I. V. Yanilkin¹, A. I. Gumarov¹,
A. G. Kiiamov¹, S. I. Nikitin¹, L. R. Tagirov^{1,2}**

¹ Institute of Physics, Kazan Federal University, Kazan, Russian Federation, flypetrov@yandex.ru

² Zavoisky Physical-Technical Institute, FRC Kazan Scientific Center of RAS, Kazan 420029, Russian Federation

Palladium-iron Pd_{1-x}Fe_x alloys with cubic fcc crystal structure at low Fe-content ($x < 0.10$) are soft low-temperature ferromagnets promising for fast and energy-efficient superconductor (S) / ferromagnet (F) heterostructure-based superconducting spintronic devices [1], both logical elements and memory cells. Iron content x in the alloy determines its Curie temperature, magnetization as well as the magnetic anisotropy [2]. F-layer in S/F/S heterostructures serves as a phase shifter of the superconducting wavefunction between two S-layers, with the phase shift value related to the magnetization and layer thickness [3]. For this reason, one of the key features of the F-layer is its magnetic homogeneity, as inhomogeneous magnetization over the contact area destroys the coherence and smears out Josephson effect associated with it.

One should note that palladium-rich Pd_{1-x}Fe_x alloys are in fact solid solutions and therefore are intrinsically inhomogeneous systems. Magnetic inhomogeneity in these materials had been studied in the bulk crystalline samples by neutron diffraction [4]. This method however is not suitable for ultrathin weakly ferromagnetic films, and complementary approaches are required.

Here we present the results of a systematic study of a series of 20-nm epitaxial high-quality Pd_{1-x}Fe_x thin films ($x = 0; 0.012; 0.034; 0.062$ and 0.080) on MgO (001) substrate with ultrafast optical and magneto-optical spectroscopy methods. Details on the film synthesis can be found elsewhere [2]. Chemical composition, crystalline structure and magnetic properties of all the samples have been thoroughly investigated before [5].

For studies of both the reflectivity transients and the time-resolved magneto-optical Kerr effect the sensitive pump-probe setup was used. Experimental results for pure Pd and Pd_{0.94}Fe_{0.06} films are shown in Fig. 1a. In the reflectivity transients of the Pd film the relaxation after an instantaneous (with our temporal resolution) rise can well be described by a sum of the fast (~ 0.24 ps) and the slow (~ 400 ps) components. No any qualitative or quantitative modification of the transient took place on cooling the Pd film. Results for the Pd_{0.94}Fe_{0.06} film are similar in the temperature range above Curie temperature ($T_C \sim 190$ K), only the lifetime of the slow component is somewhat shorter, ~ 240 ps. On further cooling below T_C the transient experiences a drastic, both quantitative and qualitative, evolution. Namely, while the fast relaxation component is left essentially untouched, the amplitude of the slow component decreases by more than 80%, and its lifetime shortens down to ~ 40 ps below 100 K (Fig. 1b).

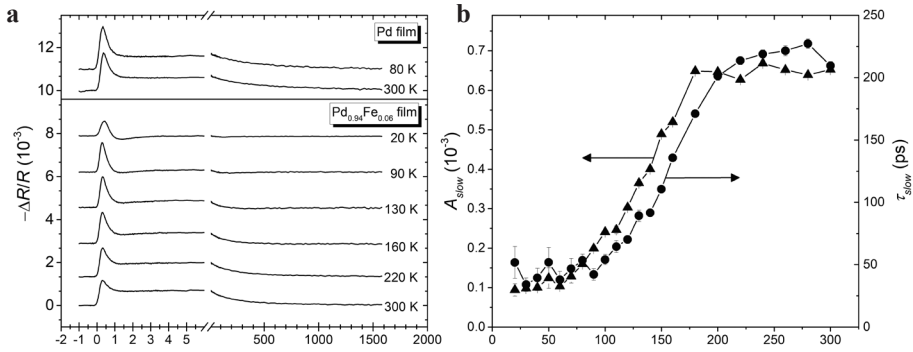


Fig. 1. **a** Temperature evolutions of the reflectivity transients for epitaxial Pd and $\text{Pd}_{0.94}\text{Fe}_{0.06}$ films. **b** Temperature dependencies of the amplitudes and the lifetimes for selected exponential components that describe the responses of $\text{Pd}_{0.94}\text{Fe}_{0.06}$ film presented in (a).

Moreover, additional relaxation components of an opposite sign develop on cooling: an intermediate with the lifetime of ~ 0.8 ps and a very long one ~ 1 ns.

We will argue basing on the data on a whole series of our samples that the complex multi-component character of the reflectivity transients originates from the magnetic inhomogeneity of the films. Nature of the developing and vanishing components will be discussed.

This work was supported by the RSF project No. 18-12-00459. Synthesis and analysis of the films as well as the ultrafast studies were carried out at the PCR Federal Center of Shared Facilities of KFU.

1. Ryazanov V.V., Bol'ginov V.V., Sobanin D.S. *et al.*: Phys. Procedia **36**, 35 (2012)
2. Esmaeili A., Yanilkin I.V., Gumarov A.I. *et al.*: Thin Solid Films **669**, 338 (2019)
3. Vernik I.V., Bol'ginov V.V., Bakurskiy S.V. *et al.*: IEEE Trans. Appl. Supercond. **23**, 1701208 (2013).
4. Low G.G., Holden T.M.: Proc. Phys. Soc. **89**, 119 (1966)
5. Esmaeili A., Yanilkin I.V., Gumarov A.I. *et al.*: <https://arxiv.org/pdf/1912.04852>

Hidden Magnetic Order in Triangular-Lattice Magnet $\text{Li}_2\text{MnTeO}_6$

**G. V. Raganyan¹, T. M. Vasilchikova¹, V. B. Nalbandyan², D. A. Gafurov³,
E. L. Vavilova³, A. E. Susloparova⁴, A. I. Kurbakov⁴, M.-H. Whangbo⁵,
E. A. Zvereva¹**

¹ Faculty of Physics, Lomonosov Moscow State University, Moscow, 119991, Russian Federation

² Chemistry Faculty, Southern Federal University, Rostov-on-Don, 344090, Russian Federation

³ Zavoisky Physical-Technical Institute, FRC Kazan Scientific Center of RAS, Kazan 420029,
Russian Federation

⁴ NRC “Kurchatov Institute” – PNPI, Gatchina 188300, Russian Federation

⁵ Department of Chemistry, North Carolina State University, Raleigh, NC 27695-8204, USA

The static and dynamic magnetic properties of a new quasi-two-dimensional magnet with a triangular lattice $\text{Li}_2\text{MnTeO}_6$ are investigated. The data on the specific heat and low-temperature neutron diffraction reveal the onset of long-range magnetic order, despite the absence of any pronounced features on the temperature dependence of magnetic susceptibility in weak magnetic fields upon cooling to 2 K and essentially reduced magnetic moment as determined from neutron studies (*hidden magnetic order* effect). The temperature dependence of the magnetic susceptibility obeys the Curie-Weiss law at high temperatures but involves a wide range of short-range magnetic correlations and a relatively large negative Weiss temperature, which indicates the predominance of antiferromagnetic exchange interactions and a noticeable spin frustration. With an increase in the magnetic field, the behavior of the temperature dependence of the magnetic susceptibility changes noticeably, and a characteristic maximum is observed at the Neel temperature. The magnetic structure of $\text{Li}_2\text{MnTeO}_6$, determined by neutron powder diffraction measurements at 1.6 K, is described by the 120° non-collinear spin structure with the propagation vector $\mathbf{k} = (1/3, 1/3, 0)$. Consistent with this finding, the spin exchange interactions evaluated for $\text{Li}_2\text{MnTeO}_6$ by density functional calculations are dominated by the nearest-neighbor antiferromagnetic exchange within each triangular spin lattice.

This work was financially supported by the RFBR grant 18-02-00326.

Magnetic Properties of $\text{La}_{1-x}\text{Sr}_x\text{Mn}_{0.9}\text{Fe}_{0.1-y}\text{Mg}_y\text{O}_3$

R. M. Eremina¹, A. V. Shestakov¹, I. V. Yatsyk¹, D. V. Mamedov¹,
A. G. Badelin², V. K. Karpasyuk²

¹ Zavoisky Physical-Technical Institute, FRC Kazan Scientific Center of RAS, Kazan 420029, Russian Federation, aleksey665@gmail.com

² Astrakhan State University, Astrakhan, 414056, Russian Federation, alexey_badelin@mail.ru

The properties of manganites that are phases of variable composition substantially depend on the concentration of different-valence ions, their electronic configuration and localization, concentration of oxygen, and defects of nonstoichiometry. The structure of the electron shells of the ions replacing manganese ions plays an important role together with their ionic radii. Fe^{3+} ions do not participate in the double exchange interaction that is the basis of the existence of the ferromagnetism of manganites and effects of interrelation of their electrical and magnetic properties. In addition, iron ions intercalating into the $\text{Mn}^{3+}\text{-O}^{2-}\text{-Mn}^{4+}$ chains break some exchange bonds between the Mn^{3+} and Mn^{4+} ions, which leads to a decrease in the ferromagnetic parameters and conductivity. The aim of this work is the investigation of the influence of the replacement of magnesium by iron in lanthanum– strontium manganite $\text{La}_{0.7}\text{Sr}_{0.3}\text{Mn}_{0.9}\text{Fe}_{0.1-y}\text{Mg}_y\text{O}_3$. The electron paramagnetic resonance (EPR) spectra (see Fig. 1) were measured (at $f = 9.4$

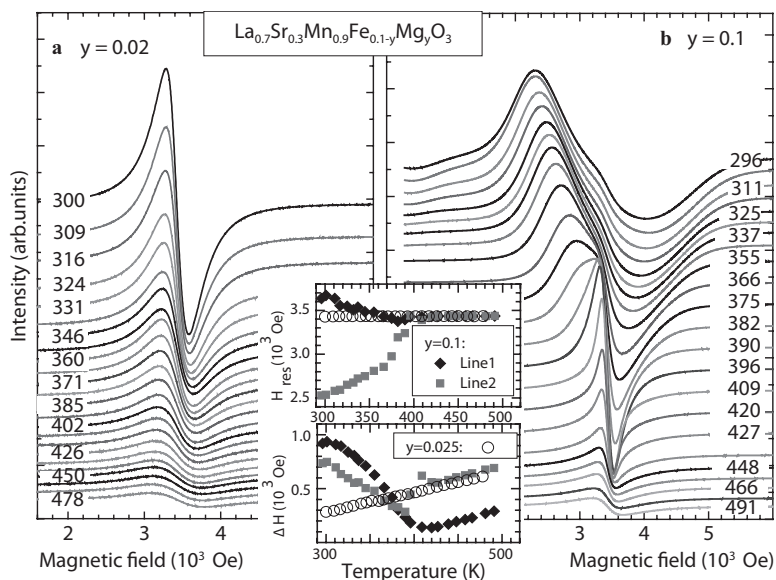


Fig. 1. Temperature evolution of EPR spectra in $\text{La}_{0.7}\text{Sr}_{0.3}\text{Mn}_{0.9}\text{Fe}_{0.1-y}\text{Mg}_y\text{O}_3$ (a) $y = 0.025$; (b) $y = 0.1$.

GHz) on a Varian E-12 spectrometer in a range of temperatures of 300 to 600 K and on a Bruker EMX plus spectrometer in a range of 100–300 K. Temperature dependencies of the resonance fields and linewidths are presented in the insert Fig. 1. According Fig. 1, doping by iron ions decreases the temperature of the magnetic phase transition.

This work was supported by the Russian Foundation for Basic Research (grant no. 18-52-06011).

EPR Study of Highly Branched Mesomorphic Iron(III) Complexes

V. Vorobyeva¹, U. Chervonova², M. Gruzdev², A. Kolker²

¹ Zavoisky Physical-Technical Institute, FRC Kazan Scientific Center of RAS, Kazan 420029, Russian Federation, vvalerika@gmail.com

² G. A. Krestov Institute of Solution Chemistry of the Russian Academy of Sciences, Ivanovo, 153045, Russian Federation, gms@isc-ras.ru

The magnetic properties of five novel highly branched mesomorphic iron(III) complexes with 3,4,5-tris-(tetradecyloxy)-fragments on periphery with PF_6^- , Cl^- , ClO_4^- , BF_4^- and NO_3^- counter ions have been studied for the first time by EPR spectroscopy in the wide (4.2–340 K) temperature range. One low-spin ($g_{\perp} = 2.21$, $g_{\parallel} = 1.935$) and two high-spin ($g_{\perp} = 4.2$, $g_{\parallel} = 2$ and broad line with effective $g = 2$) centers are observed in EPR spectra for all five complexes.

The number of LS centers is small and decreases with temperature. The temperature dependences of integrated intensity of I-type iron centers observed the maximum at low temperatures (Fig. 1 left). The probable cause of that can be that these centers are coupled by antiferromagnetic exchange interactions and are linked into dimers [1]. The exchange constant J_1 between high-spin centers were estimated with the help of Bleaney-Bowers equation [2], with follow exchange constants $J_1 = 14.39$ K (Cl^-), $J_1 = 7.2$ K (PF_6^-), $J_1 = 14.39$ K (ClO_4^-), $J_1 = 21.3$ K (NO_3^-), $J_1 = 14.39$ K (BF_4^-). Negative coupling constant J confirms the presence of the antiferromagnetic interactions between iron centers.

Behavior of II-type of iron(III) centers is typical for the ferromagnetic resonance line. The temperature dependences of this type of centers has a broad peak at $T_{\text{max}} = 50$ K for compound with Cl^- counter ion and $T_{\text{max}} = 240$ K for all other compounds (Fig. 1 right). A broad maximum in the magnetic susceptibility can be interpreted as an exchange line from chains with Heisenberg antiferromagnetic

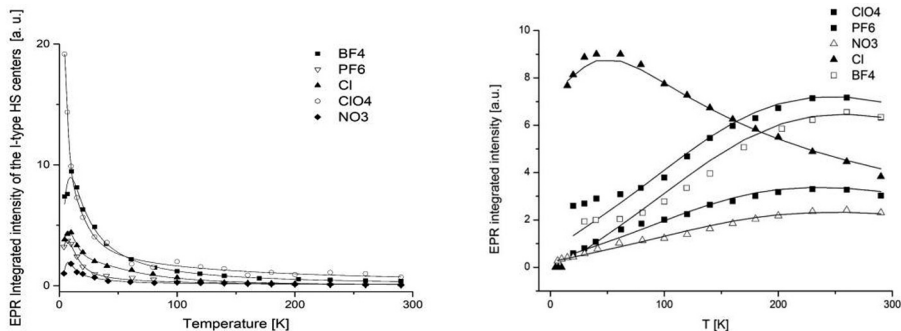


Fig. 1. The temperature dependences of the EPR lines integrated intensity of the I-type (left) and II-type (right) HS iron(III) centers for all five compounds. The solid lines represent the best fit to the experimental data with coupling constants mentioned in the text.

behavior [3], and it reflects the influence of the magnetic coupling along the chain of iron ions. Exchange constants $J_2 = 41 \text{ cm}^{-1}$ (Cl^-), $J_2 = 197 \text{ cm}^{-1}$ (PF_6^-), $J_2 = 205 \text{ cm}^{-1}$ (ClO_4^-), $J_2 = 208 \text{ cm}^{-1}$ (NO_3^-), $J_2 = 214 \text{ cm}^{-1}$ (BF_4^-) in Fisher model of magnetic susceptibility in an infinite spin chain with account for the real spin $5/2$ were used. Coupling constant J is defined to be positive for an antiferromagnetic bond. It should be noted that the position of a broad maximum in the curve I vs. T essentially depends on the type of anion and the broad maximum shifts to lower temperatures [1].

For study liquid-crystalline properties the magnetic behavior was studied in heating-cooling cycle in the temperature range from 260 to 340 K. The small hysteresis loop observed above 290 K is due to the supercooling of the mesophase. Probably, phase transition from crystal phase to smectic is likely observed.

Thus, we can assume that the studied such magnetic systems are inhomogeneous and consists of two magnetic sub-lattices. The HS Fe(III) centers with weakly distorted octahedral environment most probably form chain in layers. The HS Fe(III) centers with strongly distorted octahedral environment form dimers, that are likely arranged between the layers. Examples of such inhomogeneous magnetic systems based on Fe(III) ionic bilayers in crystalline state and smectic type in mesophase are known in the literature [4].

The work was supported by Russian Foundation for Basic Research (grant 18-29-04016_mk).

1. Domracheva N., Vorobeva V., Pyataev A., Tamura R., Suzuki K., Gruzdev M., Chervonova U., Kolker A.: *Inorg. Chim. Acta* **439**, 186 (2016)
2. Guskos N., Zolnierkiewicz G., Typek J., Szymczak R., Blonska-Tabero A.: *Mater. Sci. Poland* **30**, 1 (2012)
3. Caputo R.E., Willett R.D.: *Phys. Rev. B* **13**, 3956 (1976)
4. Seredyuk M., Gaspar A.B., Ksenofontov V., Galyametdinov Yu., Kusz J., Gutlich Ph.: *Adv. Funct. Mater.* **18**, 2089 (2008)

Epitaxial Growth, Structural and Magnetic Properties of $\text{Pd}_{0.95}\text{Fe}_{0.05}/\text{Pd}_{0.92}\text{Fe}_{0.08}$ Bilayers

A. I. Gumarov^{1,2}, I. V. Yanilkin^{1,2}, R. V. Yusupov¹, R. I. Khaibullin²,
M. N. Aliyev³, L. R. Tagirov^{1,2}

¹ Institute of Physics, Kazan Federal University, Kazan 420008, Russian Federation

² Zavoisky Physical-Technical Institute, FRC Kazan Scientific Center of RAS, Kazan 420029,
Russian Federation, amir@gumarov.ru

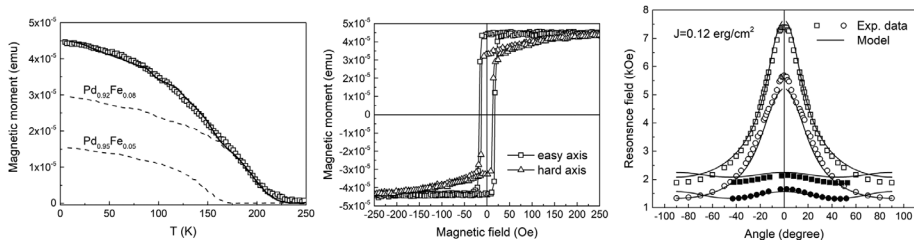
³ Baku State University, Baku 1148, Azerbaijan

The interest to the dilute $\text{Pd}_{1-x}\text{Fe}_x$ ($x = 0.01\text{--}0.10$) alloy originates from its potential applications in superconducting spintronics [1]. We have developed a procedure of the epitaxial growth of thin-film palladium-iron heterostructures [2], which may shed light on unusual magnetic properties of thin $\text{Pd}_{1-x}\text{Fe}_x$ films produced by implantation of iron ions into an epitaxial palladium film.

The $\text{Pd}_{0.95}\text{Fe}_{0.05}/\text{Pd}_{0.92}\text{Fe}_{0.08}$ heterostructure with the thickness of both layers of 20 nm was synthesized by molecular-beam epitaxy technique (MBE system by SPECS) under ultra-high, $3 \cdot 10^{-10}$ mbar, vacuum conditions on (001)-oriented epi-polished single-crystal MgO substrate. The epitaxial growth mode of the films was verified by the LEED and XRD techniques. Magnetic properties were studied using VSM magnetometry (QD PPMS-9) and ferromagnetic resonance (FMR, X-band Bruker ESP300 spectrometer).

The dependence of the magnetic moment on temperature $M(T)$ is shown in the Figure, left panel, open symbols. It reveals a kink at ~ 160 K and can be decomposed into the magnetic responses of the constituent layers (shown by dash lines) using the $M(T)$ data for individual $\text{Pd}_{0.95}\text{Fe}_{0.05}$ and $\text{Pd}_{0.92}\text{Fe}_{0.08}$ films from Refs. [2, 3]. The magnetic hysteresis loops (middle panel) measured at $T = 20$ K demonstrates a consolidated reversal of the magnetic moments of the layers with a unified coercive field. This is most probably a consequence of the strong inter-layer coupling due to the direct contact between the layers.

FMR technique was applied to study the magnetic anisotropies in the $\text{Pd}_{0.95}\text{Fe}_{0.05}/\text{Pd}_{0.92}\text{Fe}_{0.08}$ bilayer. The FMR spectra were recorded at $T = 20$ K in the in-plane and out-of-plane geometries of the experiment [4]. Two resonance lines were observed, simultaneously reflecting the presence of two oscillators in the system. The angular dependences of the resonance fields (H_{res}) for these



lines are presented in the right panel of the Figure. The stronger ferromagnetic $\text{Pd}_{0.92}\text{Fe}_{0.08}$ layer is expected to have a higher resonance field at $\theta_H = 0^\circ$ (along the film normal) and a lower resonance field at $\theta_H = 90^\circ$ (in-plane alignment) compared with a weaker ferromagnetic $\text{Pd}_{0.95}\text{Fe}_{0.05}$ layer. Then, the out-of-plane angular dependences of the two independent resonances must intersect at an angle of about $\theta_H = 20^\circ$ between the film normal and the film plane. The experimentally observed angular dependence of H_{res} does not show this crossing (see square and circle symbols in the Figure, right panel). This may occur due to repulsion of resonances at the intersection point because of the interaction between the ferromagnetic layers. Then, instead of two independent resonances, the collective oscillations of the two occur in terms of in-phase (“acoustic”) and anti-phase (“optical”) modes. The FMR resonance lines observed around the expected crossing angle are, in fact, these collective modes [5]. Modelling of the angular dependences of the FMR fields for resonance (black solid lines) provides the magnetic anisotropy parameters of the adjacent $\text{Pd}_{1-x}\text{Fe}_x$ layers and the strength of the coupling between them.

This work was supported by the RFBR project No. 20-02-00981. Synthesis and analysis of the films were carried out at the PCR Federal Center of Shared Facilities of KFU.

1. Ryazanov V.V., Bol'ginov V.V., Sobanin D.S. *et al.*: Phys. Procedia **36**, 35 (2012)
2. Esmaili A., Yanilkin I.V., Gumarov A.I. *et al.*: Thin Solid Films **669**, 338 (2019)
3. Esmaili A., Yanilkin I.V., Gumarov A.I. *et al.*: <https://arxiv.org/pdf/1912.04852>
4. Farle M.: Rep. Progr. Phys. **61**, 755 (1998)
5. “Ultrathin Magnetic Structures II”, ed. by B. Heinrich and J.A.C. Bland. Springer-Verlag Berlin-Heidelberg 1994, 361 p.

2D Triangular Lattice Magnet GdFeTeO_6 with Large Magnetocaloric Characteristics

T. Vasilchikova¹, V. Nalbandyan², M. Evstigneeva², E. Zvereva¹

¹ Faculty of Physics, Moscow State University, Moscow 119991, Russian Federation

² Chemistry Faculty, Southern Federal University, Rostov-on-Don 344090, Russian Federation

We report on static and dynamic magnetic properties of GdFeTeO_6 with superstructure of the rosielite type. Both the magnetic susceptibility and the specific heat of GdFeTeO_6 unambiguously confirm the onset of long range ordering at $T_N = 2.4$ K, which is suppressed quickly in applied external magnetic fields. This suppression is accompanying by appearance of Gd-related Shottky-type anomaly on the $C_p(T)$. Based on the thermodynamic studies, the magnetic B - T phase diagram was constructed.

Spin dynamic properties investigated by electron spin resonance (ESR) corroborate static magnetic ones and indicate rather 2D character of magnetic interactions. ESR spectra in the paramagnetic phase demonstrate a single broad line, which can be assigned to averaged response from gadolinium and iron subsystems and characterized by the isotropic effective g -factor $g = 2.00 \pm 0.1$, typical for S-type ions Gd^{3+} ($S = 7/2$) and Fe^{3+} ($S = 5/2$) in octahedral oxygen coordination. Broadening of the ESR line as temperature decreases is typical for AFM compounds and the critical exponent corresponds to rather 2D character of AFM magnetic correlations.

In accordance with our magnetocaloric data, for a magnetic field change of 9 T, the maximum values of $-\Delta S_M(T) = 35.3$ J/kg K, $\Delta T_{\text{ad}} = 27$ K, relative cooling power (RCP) and refrigerant capacity (RC), are 580 J/kg and 465 J/kg, respectively. So, all MCE parameters are remarkably large in GdFeTeO_6 , that makes this system interesting for potential application as low-temperature magnetic refrigerator (MR), for example for design of hydrogen liquefier MR.

This work has been supported by Russian Foundation for Basic Research through grant 18-03-00714.

EPR in Conductive Polymer Composites with Carbon Nanotubes

A. M. Zyuzin, N. V. Yantsen, A. A. Karpeev, V. V. Naumkin

Mordovia State University. Saransk, 430005, Russian Federation, nkyancen@yandex.ru

The studies results of EPR spectra parameters temperature dependences of a peroxide-crosslinked electroconducting composite based on ethylene vinyl acetate (EVA), are presented. Single-wall carbon nanotubes (CNT) and carbon black (BC) were used as conductive fillers. Two series of samples were studied, the first containing 10% BC and 0.1–0.2% CNT, the second – 35% BC. EPR spectra were recorded on a PS100X radio spectrometer at a frequency of 9.4 GHz microwave field in the temperature range from 20 °C to 150 °C. In the studied temperature range, the g -factor value in all samples remained equal to 2.0.

It was found (Fig. 1) that the paramagnetic centers concentration, which is proportional to the integral intensity $J(T)$, in an electrically conducting composite samples with CNT increases significantly with increasing temperature compared to a composite containing only carbon black.

The temperature dependences of $J(T)$ of pure CNT and BC, in contrast to composites, show a slight decrease, which is explained by changes in the populations of the upper and lower zeiman levels due to the action of the temperature factor.

The reported research was funded by Russian Foundation for Basic Research and the government of Mordovia Republic of the Russian Federation, grant № 18-48-130015 r_a.

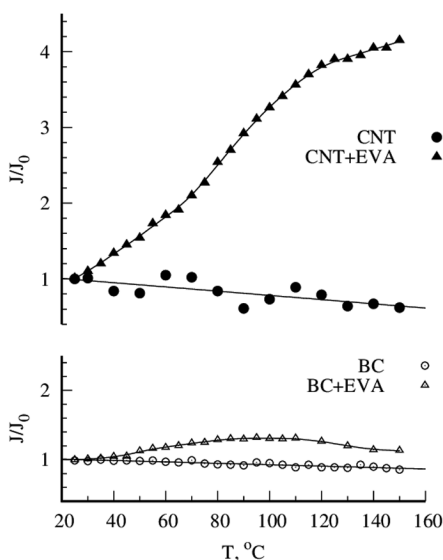


Fig. 1. The integral intensity temperature dependences.

High Temperature Ferromagnetism in Thin Films of $\text{Mn}_x\text{Si}_{1-x}$ ($x \approx 0.5$) Nonstoichiometric Alloys: Ferromagnetic Resonance Studies

**A. B. Drovosekov¹, A. S. Barkalova^{1,2}, L. S. Parshina³,
O. A. Novodvorsky³, O. D. Khramova³, D. S. Gusev³, E. A. Cherebilo³,
K. Yu. Chernoglazov⁴, A. S. Vedeneev⁵, V. V. Rylkov^{4,5}**

¹ P. L. Kapitza Institute for Physical Problems RAS, Moscow 119334, Russian Federation,
drovosekov@kapitza.ras.ru

² National Research University “Higher School of Economics”, Moscow 101000, Russian Federation

³ Institute on Laser and Information Technologies – Branch of the Federal Scientific Research Center
“Crystallography and Photonics” of Russian Academy of Sciences, Moscow region, Shatura 140700,
Russian Federation

⁴ National Research Center “Kurchatov Institute”, Moscow 123182, Russian Federation

⁵ Kotel’nikov Institute of Radio Engineering and Electronics RAS, Fryazino Branch, Moscow region,
Fryazino 141190, Russian Federation

The development of $\text{Mn}_x\text{Si}_{1-x}$ ($x \approx 0.5$) alloy films with composition close to the manganese monosilicide MnSi attracts a lot of attention, since these films demonstrate unusual magnetic and transport properties and can be easily incorporated into existing microelectronic technology. The stoichiometric $\varepsilon\text{-MnSi}$ with B20 structure has the Curie temperature $T_C \approx 29$ K and demonstrates a complex magnetic phase diagram including the region of unusual magnetic states, skyrmions. At the same time, the T_C value of nonstoichiometric $\text{Mn}_x\text{Si}_{1-x}$ ($x \approx 0.51 - 0.53$) alloy films obtained by the pulsed laser deposition (PLD) was found to increase by more than an order of magnitude as compared with $\varepsilon\text{-MnSi}$ [1]. It was shown that a polycrystalline structure, sizes and shapes of nanocrystallites as well as the tension between the film and substrate arising in the growth process play an important role in the formation of the high-temperature ferromagnetism (HT FM) in such alloys [2, 3]. However, up to now the effect of substrate crystal structure on the properties of the HT FM phase was not investigated.

In this work, we perform comparative studies of the nonstoichiometric $\text{Mn}_x\text{Si}_{1-x}$ ($x \approx 0.5$) alloy films prepared by PLD on the *c*- and *r*- Al_2O_3 substrates. A set of such films were deposited on the substrates from the polycrystalline MnSi target at different laser energy density $E = 4.5 - 7.5$ J/cm² on the target. X-ray diffraction (XRD) studies show a high degree of amorphousness in the synthesized films with a strong diffusion signal in the spectra which is a sign of nanocrystalline structure of the samples. The maximal value of the diffusion signal demonstrates a dependence on both the laser energy density on the target and the type of the substrate used in the growth process.

The magnetic properties of the grown films were investigated by ferromagnetic resonance (FMR) at a frequency $f = 17.3$ GHz in the temperature range $T = 4 - 330$ K in the magnetic field up to $H = 10$ kOe applied in the sample plane. It is shown that the use of the high laser energy density $E \approx 7.4$ J/cm² on the target initiates the formation of a homogeneous HT FM phase in the

films with the Curie temperature $T_{\text{Ch}} \approx 330$ K. The deposition of the films with lower E leads to a decrease in T_{Ch} and the formation of an additional “low-temperature” FM phase with $T_{\text{Cl}} \approx 50$ K. It is found that the Curie temperature coincides for the films grown on different substrates at the same laser energy density on the target. On the contrary, the effective demagnetization field $4\pi M_{\text{eff}}$, determined by FMR, depends on the used substrate and correlates with the maximal value of the diffusion signal in the XRD spectra. The observed effect indicates a significant influence of structural defects in the synthesized films on the formation of the high-temperature FM phase, since the concentration of such defects and the induced magnetic anisotropy are strongly defined by the degree of a film-substrate crystal structure mismatch.

This work was supported by the Ministry of Science and Higher Education within the State assignment FSRC “Crystallography and Photonics” RAS and IRE RAS in part of “thin films synthesis”, the Russian Foundation for Basic Research (projects No. 18-07-00772, 18-07-00729, 19-29-03032, 19-07-00471, 19-07-00738) in part of “thin films analysis”.

1. Rylkov V.V. *et al.*: *Europhys. Lett.* **103**, 57014 (2013)
2. Nikolaev S.N. *et al.*: *AIP Advances* **6**, 015020 (2016)
3. Drovosekov A.B. *et al.*: *Europhys. Lett.* **115**, 37008 (2016)

SECTION OTHER APPLICATIONS OF MAGNETIC RESONANCE

The Effect of Halloysite Nanotubes Surface Modification on its Acid-Base Properties

D. O. Antonov¹, D. P. Tambasova¹, D. D. Davydov¹, E. G. Kovaleva¹

¹ Ural Federal University, Yekaterinburg 620100, Mira str., 19, Russian Federation
d.o.antonov@urfu.ru

The modification of halloysite nanotubes with various functional groups, such as carboxyl, aminocarboxyl, thiol, mercapto and phosphonic groups, has been of great interest in recent years [1]. Due to such modifications, halloysite found new applications in the process of sorption of dyes, biologically active substances, enzymes and metal ions [2]. Modification of the surface by new functional groups leads to subsequent changes in the surface charge and electric potential, local pH inside the pores (pH^{loc}), and ionization constants of functional groups. These characteristics can directly affect many processes on a surface, including heterogeneous catalysis and adsorption. The electro-paramagnetic resonance (EPR) of the pH-sensitive stable nitroxyl radicals as labels and probes allows to track these changes [3].

The purpose of this research is to study the changes in the local pH inside the pores (pH^{loc}) and the ionization constants of the functional groups of halloysite nanotubes upon modification of their surface with glycidoxypolytrimethoxysilane. The nitroxyl radical 4-dimethylamine-2-ethyl-5,5-dimethyl-2-pyridin-4-yl-2,5-dihydro-1H-imidazol-1-oxyl with two pKa ($\text{pK}_{\text{a}1} = 2.92$, $\text{pK}_{\text{a}2} = 5.06$), which was synthesized at the Institute of Organic Chemistry SB RAS (Novosibirsk, Russia). Modified samples of halloysite nanotubes were synthesized in an organic synthesis laboratory at the Ural Federal University. Two selected samples with degrees of functionalization of 46% (HNTM-1) and 51% (HNTM-2) were used for studies. Figure 1 shows the dependence of the average hyperfine splitting constant of the nitroxyl radical (a , %) on the solution pH. From the figure it is seen that the pH^{loc} of the solution near the surface of the samples in neutral and slightly acidic media slightly differ from the pH of the external solution, whereby there have been observed an increase in hydrogen protons near the surface as compared to their concentration in the external solution at $\text{pH} < 4$.

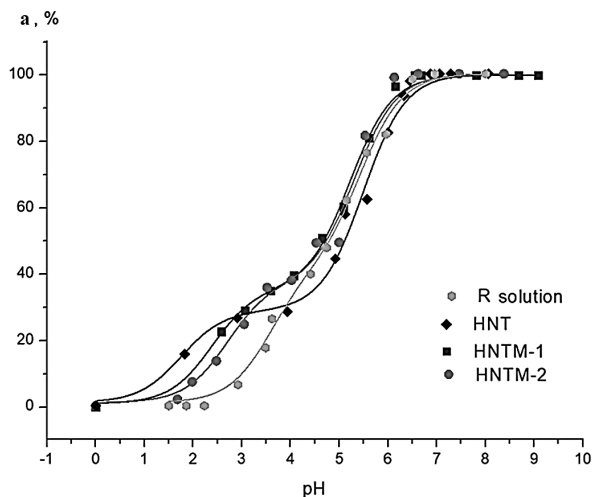


Fig. 1. EPR titration curves of the pH-sensitive nitroxyl radical near the surface of halloysite samples, $a, \% = (a - a_{\text{NRH}^{++}}) / (a_{\text{NR}} - a_{\text{NRH}^{++}}) \times 100\%$

The horizontal plateaus on the titration curves of the samples indicate the process of titration of siloxane functional groups [4]. A decrease in length of these plateaus on the titration curves for the modified samples can be explained by the fact that these groups react with the modifying agent and therefore their quantity decreases. We can suppose that epoxy groups of the modifying agent are located on the halloysite nanotubes outer surface.

The research was supported by the Foundation for Basic Research (grant 18-29-12129mk).

1. Massaro M., Cavallaro G., Colletti C.G., Lazzara G., Milioto S., Noto R., Riela S.: *J. Mater. Chem. B* **6**, 3415 (2018)
2. Lvov Y., Wang W., Zhang L., Fakhrullin R.: *Adv. Mater.* **28**, 1227 (2016)
3. Kovaleva E.G., Molochnikov L.S., Antonov D.O., Tambasova D.P., Stepanova, Hartmann M., Tsmokalyuk A.N., Marek A., Smirnov A.I.: *J. Phys. Chem. C* **122**, 20527 (2018)
4. Bretti C., Cataldo S., Gianguzza A., Lando G., Lazzara G., Pettignano A., Sammartano S.: *J. Phys. Chem. C* **120**, 7849 (2016)

TR EPR Study of Spin-Orbit Charge Transfer Intersystem Crossing in Bodipy-Anthracene Compact Dyads

A. A. Sukhanov¹, Z. Mahmood², J. Zhao², V. K. Voronkova¹

¹ Zavoisky Physical-Technical Institute, FRC Kazan Scientific Center of RAS, Kazan 420029, Russian Federation

² State Key Laboratory of Fine Chemicals, School of Chemical Engineering, Dalian University of Technology, 116024, P. R. China, zhaojzh@dlut.edu.cn

In electron donor/acceptor dyads, the formation of a metastable triplet state of the chromophore can occur due to intersystem crossing (ISC) through states with charge transfer, so-called spin-orbit charge transfer-induced intersystem crossing (SOCT-ISC) mechanism. This mechanism is of particular interest for preparation of heavy atom-free triplet photosensitizers (PSs). It is necessary to study the conditions of formation and manifestation of the SOCT-ISC mechanism for preparation of new effective heavy atom-free triplet PSs. The time-resolved electron paramagnetic resonance (TREPR) spectroscopy allows to study the photoinduced triplet states. We studied a series of Bodipy-anthracene (BDP-An) compact electron donor/acceptor dyads using TREPR to establish manifestation feature of SOCT-ISC mechanism and the possibility of discriminate SOCT-ISC and normal ISC mechanisms.

Early, we studied a series of BDP-An dyads without heavy atom with different mutual orientations between the Bodipy and the anthracene moieties. We observed three triplet excited states for some BDP-AN donor/acceptor dyads, that are triplet states confined on the AN and the BDP moieties as well as triplet state of charge transfer state [1]. Based on the electron spin polarization (ESP) pattern of the three triplet states, we proposed that triplet states are not the dominant ISC channel; the SOCT-ISC mechanism as the main ISC channel.

In this work we study new AN-BDP dyads with different number of iodination (heavy atom) attached to the core of Bodipy (BDP) acceptor. Same ESP pattern and increase of zero field splitting parameters of triplet state of BDP moiety with increase of iodination are observed for dyads. The three triplet excited states are observed for AN-BDP with one iodine and the charge transfer state not observed for AN-BDP with two iodine atoms.

This work was supported by the Russian Foundation for Basic Research (project no. 19-53-53013).

1. Wang Z., Sukhanov A.A., Toffoletti A. *et al.*: J. Phys. Chem. C **123** (1), 265–274 (2019)

Capabilities of Nuclear-Magnetic Resonance Tools for Detailed Scanning of Fluid Properties in Core Samples and in Wells Under Drilling.

**V. Murzakaev¹, N. Belousova¹, A. Bragin¹, D. Kisler¹, V. Skirda²,
A. Alexandrov²**

¹ TNG-Group, Bugulma, Russian Federation, Murzakaev.VM@tng.ru

² Institute of Physics, Kazan Federal University, Kazan, Russian Federation, kazanvs@mail.ru

Nuclear Magnetic Resonance has various applications in different fields of science and technology: medicine, physics, chemistry, biology. Major success has been achieved by developers of equipment for studying the subsoil for oil and gas using instruments based on Nuclear Magnetic Resonance, and a sufficient number of articles and monographs have been written about the results of such works. Amidst depletion of conventional hydrocarbon reserves, thin-layer deposits, including saturated fluids of various viscosities and mobilities, are making an increasing contribution to field research. More detailed information about the properties of the studied survey object, along with multi-dimensional representations of the results, allows interpreters to more deeply understand fluid properties in a reservoir and to acquire more reliable information about production potential in difficult geological conditions.

TNG-Group has equipment developed in conjunction with Kazan Federal University, which has a resolution that is not inferior to international counterparts, and when studying a core sample, an NMR-based installation has no analogues in its class at all. Resolution of downhole and surface equipment is of comparable size and shows identical resulting interpretation parameters. This allows to replace one recording method (technology) with another one when necessary or if it is impossible to perform research applying one of the presented technologies. Thus, a core research facility has the ability to scan the NMR properties of a full-sized core sample directly at the wellsite with a 2 cm detailing along the length of the core sample.

A counter-magnet downhole tool has a resolution of about 5 cm for detailed studies and measurements in a stationary mode (i.e. in a standstill state) and about 15–20 cm in a continuous recording mode. The data acquired using both instruments are important for the optimal selection of points for sampling reservoir fluid, which are then used to access reservoir properties in the laboratory. Acquisition of information about the section with high accuracy will not allow to miss impermeable layers, which is important in the end when choosing the shooting range points and when estimating the hydrocarbon reserves.

Information on the types of fluid saturating the pore space and their volumes is very important for geophysicists, field development specialists, geologists, and petrophysicists. Such information can be acquired using the technique for analysis of two-dimensional distributions of relaxation times acquired using NMR equipment. The results of applying this technique for a downhole tool and a surface unit are presented in the Fig. 1.

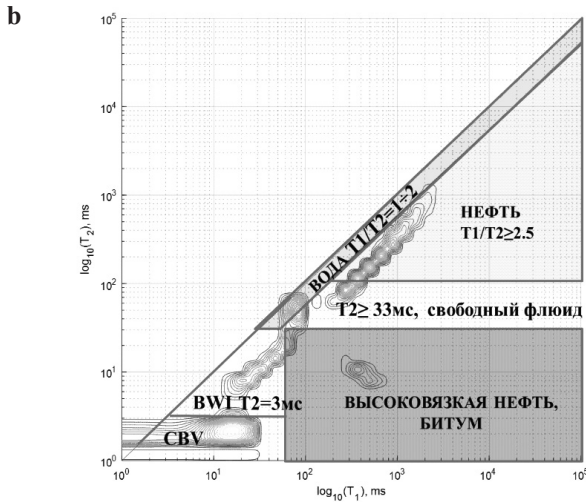
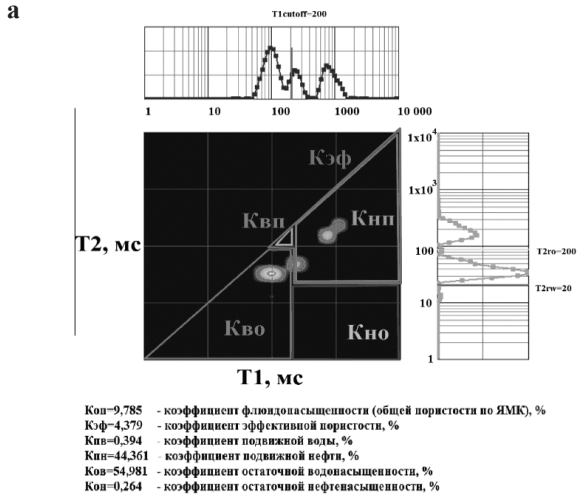


Fig. 1. Measurement and analysis of 2D distribution of relaxation times in borehole (a) in core samples (б).

The above examples indicate that the fluid typification technique for the distribution of relaxation times T1-T2 was successfully tested on a large number of samples saturated with various types of oils and selected in different regions, and can be used in the future. For a more correct interpretation of multi-variate NMR measurements, it is necessary to create a library of “2D maps” from places where core studies or borehole studies using NMR have been performed. Preliminary information (laboratory NMR studies of samples and fluids, mineralogical and lithological features of the studied rocks, NMR of neighboring wells in 1D and 2D modes, etc.) and calibration measurements on drilling fluid samples and oil samples from the studied sediments will provide additional information for correct interpretation of measurement results in typization mode.

Spin Properties of the Fe(III) Complexes with Tetradentate Schiff Bases and Photosensitive 4-Alkoxystryrylpyridine Axial Ligands

**E. N. Frolova, L. V. Bazan, O. A. Turanova, M. Yu. Volkov,
L. G. Gafiyatullin, I. V. Ovchinnikov, A. N. Turanov**

Zavoisky Physical-Technical Institute, FRC Kazan Scientific Center of RAS, Kazan 420029,
Russian Federation, fro-e@yandex.ru

Spin state of a Fe(III) ion may depend on a small change in the number of links in the long alkyl chain of the ligand, which influence the ion through intermolecular interaction. Previous studies [1] showed that the complexes with the general chemical formula $[\text{Fe}(\text{SB})\text{Sp}_2]\text{BPh}_4 \times n\text{MeOH}$ (Sp is 2-stryrylpyridine and SB is a Schiff base: salen, vanen, bzacen and acen $\{\text{H}_2\text{salen} = \text{N},\text{N}'\text{-ethylenebis}(\text{salicylideneimine}), n = 1; \text{H}_2\text{vanen} = \text{N},\text{N}'\text{-ethylenebis}(3\text{-methoxysalicylideneimine}), n = 4; \text{H}_2\text{acen} = \text{N},\text{N}'\text{-ethylenebis}(\text{acetylacetyloneimine}), n = 1; \text{H}_2\text{bzacen} = \text{N},\text{N}'\text{-ethylenebis}(\text{benzoylacetylone}), n = 1\}$) demonstrate high spin ($S = 5/2$), low spin ($S = 1/2$) and thermo-induced SCO ($1/2 \leftrightarrow 5/2$) for central Fe(III) with the variation of the SB in the equatorial plane of the complexes. It was expected that irradiation, which causes a *trans-cis* transition of the axial ligand, will lead to significant changes in the SCO parameters of the central Fe(III) ion of complexes solved in dichloromethane. However, it turned out that irradiation can lead not only to isomerization, but also to irreversible cyclization of 4-stryrylpyridine molecules with their separation from the central ion and, accordingly, destruction of the studied complexes. It seemed reasonable to us to use longer molecules of stryrylpyridines that are not subject to cyclization upon irradiation as a photoisomerizable ligand (they can also cyclize, but the process is much slower). This work presents the results of studies of the first obtained complex compounds containing 4-alkoxystryrylpyridines as axial ligands. The presence of a long alkyl chain in the transposition of 4-stryrylpyridine leads to the manifestation of liquid crystal properties not only in the ligand itself, but also in some complexes obtained on its basis.

The resulting compounds were characterized by UV, EPR, and NMR magnetometry.

1. Turanova O.A., Volkov M.Y., Frolova E.N., Bazan L., Garifzianova G.G., Gafiyatullin L.G., Turanov A.N.: Journal of Chem. Phys. **152**(1), 014306. doi:10.1063/1.5124369 (2020)

EPR Measurements of Guest Diffusion in Magneto-Concentrated Porous Metal Organic Frameworks (MOFs)

D. Polyukhov¹, A. Poryvaev¹, M. Fedin¹

¹International Tomography Center SB RAS, Novosibirsk 630090, Russian Federation, daniil@tomo.nsc.ru

Metal Organic Frameworks (MOFs) are porous materials having prospective applications in many fields of science. Molecular separation of similar components is one of the most promising applications of MOFs. Developing materials with required properties needs complex approaches to investigate diffusion inside the porous system. MOF ZIF-8 represents large cavities (~ 12 Å) and small windows (~ 7 Å) that separate cavities. Therefore, this material has molecular sieving properties and high uptake.

Recently, we developed novel approach to measure guest diffusion rates in ZIF-8 using incorporated paramagnetic spin probes [1]. This method is based on an effect of oxygen displacement by guest molecules, which leads to a dramatic narrowing of the EPR lines of spin probe. ZIF-8 is a diamagnetic MOF. However, ZIF-8 versions with modified paramagnetic metal ion can be magnetically-concentrated. In particular, ZIF-67 (Co^{2+} -substituted ZIF-8) is paramagnetic. The dipolar interactions between Co^{2+} and spin probe (nitroxide TEMPO radical) lead to severe broadening of the EPR spectrum, thus complicating the study of diffusion kinetics. The detection using second harmonic regime compensates for the information losses due to the broadening. Therefore, TEMPO@ZIF-67 was also well suitable for EPR studies of guest diffusion into MOF. Figure 1 shows the obtained EPR data for diffusion of xylenes and ethylbenzene in ZIF-67.

In summary, we developed useful approach to measure guest diffusion rates in both diamagnetic and paramagnetic MOFs with cavities-windows structure via EPR spectroscopy using spin probes.

The reported study was funded by RFBR, project number 19-33-90035.

1. Polyukhov D.M., Poryvaev A.S., Gromilov S.A., Fedin M.V.: Nano Letters **19**, 6506 (2019)

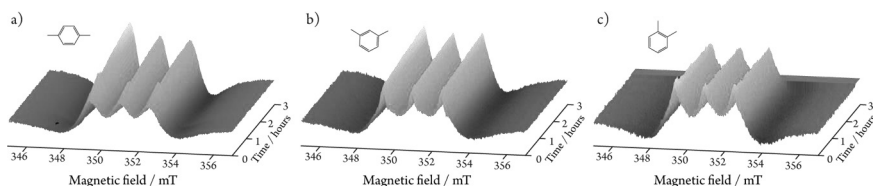


Fig. 1. *In situ* time-resolved EPR measurements of guest diffusion. a, b, c show examples of time-resolved EPR spectra upon *in situ* *p*-xylene (top) and ethylbenzene (bottom) diffusion into ZIF-67.

SECTION

MAGNETIC RESONANCE IMAGING

Development of a Conform Sensor “Hand” for Receiving an NMR Signal in a Small-Size Traumatological MRI System with a Field of 0.4 T

A. A. Bayazitov, Ya. V. Fattakhov, A. R. Fakhrutdinov, V. A. Shagalov

Zavoisky Physical-Technical Institute, FRC Kazan Scientific Center of RAS, Kazan 420029,
Russian Federation, bayazitov.alfis@kfti.knc.ru

The work is devoted to the receiving-transmitting system for a small-sized specialized traumatological magnetic resonance scanner with 0.4 T magnetic field induction. The scanner with permanent magnet has compact dimensions due to the small gap of the magnet and can be installed in mobile specialized transport.

When developing a sensor for these types of MRI scanner, features are provided for the small size of the gap between the poles of the magnet. The size of the gap (and so the sensor) does not exceed 206 mm, the working area of the sensor is a space of 200×120×60 mm. Region of interest (ROI) of the MRI scanner is a space of 200×180×180 mm. The contour shape is chosen so that the fill factor is maximum. The sensor includes a receiving coil, a transmit coil, an external shield [1]. In the work, mathematical modeling of the receiving part of the sensor for a rectangular structure was carried out. The axis of the receiving coil is directed along the X axis. The coil is made using of thickness 0.2 mm copper tape.

When developing and customizing the sensor with various coils, their location relative to each other was taken into account. The paper also analyzes the uniformity of the field and the quality factor of the receiving coil and the possibility of improving them. A homogeneous field promotes uniform reception of the NMR signal. In the calculations, we consider that the distribution of the transmission and reception fields of the same coil is equivalent. Deviations of the field from the maximum value should be within 10%.

When simulating the coil, parameters such as the number of turns and the distance between the turns were set. Based on the simulation results, a layout was developed and its characteristics were measured.

1. Polonskij N.B.: Konstruirovaniye elektromagnitnykh ekranov dlya radioelektronnoy apparatury. M.: Sovetskoye radio (1979)

The First Results of Using a Specialized MRI System with Magnetic Field of 0.4 T

**Ya. Fattakhov¹, A. Anikin¹, A. Bayazitov¹, A. Fakhрутдинov¹,
R. Khabipov¹, V. Odivanov¹, K. Salikhov¹, V. Shagalov¹, N. Reshetnikov²,
D. Abdulganieva³, M. Mikhailov⁴, S. Ryzhkin⁴, V. Anisimov⁵**

¹ Zavoisky Physical-Technical Institute, FRC Kazan Scientific Center of RAS, Kazan 420029, Russian Federation, fattakhov@kfti.knc.ru

² Health Center, FRC Kazan Scientific Center of RAS, Kazan Russian Federation, reshnicolaj@yandex.ru

³ Kazan State Medical University, Kazan, 420012, Russian Federation, diana.abdulganieva@kazangmu.ru

⁴ KSMA – Branch Campus of the FSBEIFPE RMACPE MOH Russia, Kazan 420012, Russian Federation, rsa777@inbox.ru

⁵ Republican Clinical Hospital, Kazan 420064, Russian Federation, vianisima@mail.ru

The work presents the first results of the diagnosis of joint diseases using a new developed of a specialized magnetic resonance imager with magnetic field induction of 0.4 T.

Earlier, the team developed and manufactured low-field medical magnetic resonance imaging scanners with a resistive magnet. On these tomographs in medical institutions, over 30.000 patients were examined. At present, a joint effort of “Gradient MRT” LLC and KPhTI FIC of FRC KazSC RAS is developing a specialized magnetic resonance imager for the diagnosis of diseases and injuries of joints. The magnetic system is made on a permanent magnet with a magnetic field induction of 0.4 T and a gap of about 200 mm. The main technical characteristics of the magnet: the region of uniformity 180×180×200 mm, the heterogeneity of the magnetic field in the region of uniformity of about 20 ppm. All studies were conducted on volunteers.

To check the diagnostic capabilities of the device, together with a team of doctors from, test measurements of the knee joint and hand joints were carried out.

Trial images of patient limbs were obtained in T1 and T2-weighted images. The cortical plates of the articular surfaces are satisfactorily visualized in the images. Such pathologies are diagnosed as: unevenness of the joint space, unevenness and marginal osteophytes of the articular surfaces of the metacarpophalangeal joint. When examining the knee joint, the posterior cruciate ligament is well defined without significant changes.

It is known that proton-weighted images with suppression of fat are most optimal for joint diagnostics; work is currently underway to develop such research protocols.

SECTION RELATED PHENOMENA

Photon Echo Oscillations in $\text{LuLiF}_4:\text{Er}^{3+}$ (0.025%) Depending on the Magnetic Field Perpendicular to the C Axis of the Sample

V. Lisin, A. Shegeda, V. Samartsev

Zavoisky Physical-Technical Institute, FRC Kazan Scientific Center of RAS, Kazan 420029,
Russian Federation, valerylisin@gmail.com

The report shows preliminary experimental results on the observation of the dependence of the photon echo (PE) intensity vs dc magnetic field. The following experimental geometry is considered when the directions of laser pulses k are perpendicular to the sample's C axis and the direction of the magnetic field H . The direction of the laser's electric field E is parallel to the C axis (π -polarization). It was found that the intensity of the photon echo oscillates depending on H (Fig. 1), in the case when the magnetic field H is directed exactly at an angle

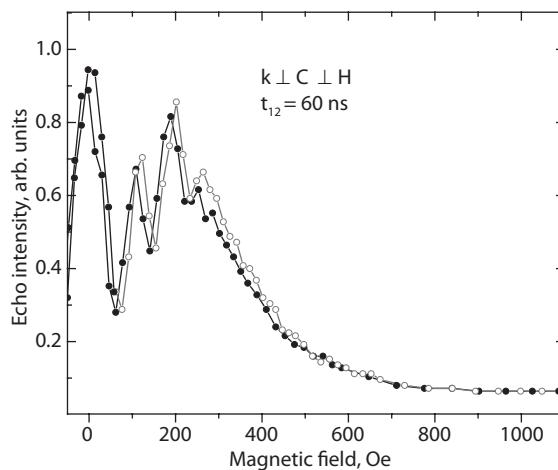


Fig. 1. Photon echo intensity vs dc magnetic field. Delay time between laser pulses t_{12} is equal 60 ns.

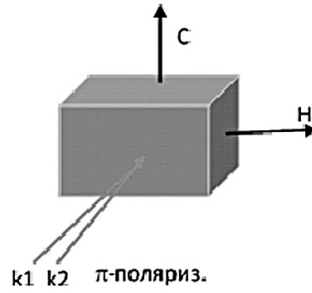


Fig. 2. The geometry of the experiment in which PE oscillations are observed.

of 90° to the C axis (Fig. 2). The oscillations are caused by a dc, not a pulsed magnetic field, in contrast to [1, 2].

The oscillations disappear when the angle between the C axis and the magnetic field differs from 90° by at least 1.5° . A theoretical description of these results is assumed.

The work was supported by Foundation for Basic Research (grant 20-02-00545a).

1. Lisin V., Shegeda A., Gerasimov K.: JETP Lett. **95**, 61 (2012)
2. Lisin V., Shegeda A.: JETP Lett. **96**, 328 (2012)

Propagation Single-Photon Wave-Packet with Orbital Angular Momentum in a Turbulent Atmosphere

**D. O. Akatiev, D. A. Turaikhanov, A. V. Shkalikov, I. Z. Latypov,
A. A. Kalachev**

Zavoisky Physical-Technical Institute, FRC Kazan Scientific Center of RAS, Kazan 420029,
Russian Federation

Studies of fields with nonzero orbital angular momentum (OAM) have been going on for several decades since the work [1]. OAM appears in optical beams with spiral wave fronts [2, 3], and its effect can be seen using optical tweezers [4]. Recently, OAM of light has become interesting for research due to its potential in quantum information processing and communication in higher orders of dimensions. Since single-mode fiber, which is ubiquitous in fiber-optic infrastructure, only supports zero-OAM modes, free space is naturally a possible medium for OAM-based quantum communication. Unfortunately, the OAM value is spoiled by decoherence in a turbulent atmosphere – random phase modulations caused by spatial fluctuations in the refractive index that scatter the initial OAM states into other OAM states. A large number of studies have already been carried out on the effect of turbulence on classical optical beams with certain OAM modes [5, 6]. Therefore, the purpose of this work was to study the behavior of single photons with OAM of in a turbulent atmosphere under the conditions of calculating the modulation of turbulence based on the Kolmogorov model.

Atmospheric turbulence is small-scale irregular air movements characterized by winds that vary in speed and direction. Turbulence is important because it mixes and agitates the atmosphere and causes water vapor, smoke and other substances and energy to be distributed both vertically and horizontally. Turbulent flow is very complex and still not fully understood. Andrey Kolmogorov has developed a simple physical model of turbulence that can be used to analytically evaluate its effects. Kolmogorov's model assumes that energy is introduced into turbulent medium at large spatial scales and a form eddies. They then break up into smaller vortices in the form of a self-similar cascade, until the vortices become small enough for energy to dissipate due to the viscous properties of the medium. In the inertial range between the inner and outer scales, Kolmogorov predicted a power-law distribution of turbulent power with a spatial frequency of $-5/3$ [7], which formed the basis of the modern theory of turbulence [8].

Displacement of the air mass with a different temperature changes the density and, as a consequence, the stream flow. Arises destructive optical turbulence, for description which is commonly used with this parameter, how the structural characteristics of the refractive index C_n^2

In the case of atmospheric turbulence, it is solar heating and wind shear that provide initial energy on a large scale, and it is dissipated in the form of heat due to viscous air friction on the internal scales [9]. On the basis of this

model, phase screens were calculated, which subsequently simulated a turbulent atmosphere in the experimental setup.

An experimental setup for studying the effect of turbulence on states with orbital angular momentum was assembled on the basis of a setup for studying spontaneous parametric down conversion (SPDC) of light. Laser radiation at a wavelength of 532 nm passing through a spatial light modulator was endowed with a non-zero OAM ($L = 1 \dots 5$) and “pumped” a nonlinear PPLN crystal with nonlinearity modulation. In the process of SPDC of light, a pair of photons is generated in it at wavelengths of 1550 nm and 810 nm (signal and idler photons), to which the pumping OAM can be transferred according to the calculations made in [15]. Then the signal and idler photons are divided by a dichroic mirror into two channels. Photons at a wavelength of 1550 nm hit a spatial light modulator, where a mask defining turbulence is set, and introduces a different phase value at each point of the beam profile. Further, the radiation again falls on the spatial light modulator, where there is a mask corresponding to the value of the orbital angular momentum of the beam. Thus, a graph of the dependence of the counting rate of coincidences on the degree of turbulence is studied for different values of the OAM. This work was supported by the Russian Foundation for Basic Research, project No. 18-29-20091.

1. Allen M.W. *et al.*: Phys. Rev. A **45**, 8185 (1992)
2. Abramochkin E., Volostnikov V.: Optics Communications **102**, 336 (1993)
3. Abramochkin E., Volostnikov V.: Optics Communications **125**, 302 (1996)
4. Korobtsov A.V., Kotova S.P., Losevsky N.N., Mayorova A.M., Klenov R.O.: Izvestiya of the Samara Scientific Center of the Russian Academy of Sciences **11**, 76 (2009)
5. Gibson G., Courtial J., Padgett M., Vasnetsov M., Pas’ko V., Barnett S., Franke-Arnold S.: Opt. Express **12**, 5448 (2004)
6. Paterson C.: Phys. Rev. Lett. **94**, 153901 (2005)
7. Kolmogorov A.N.: Dokl. USSR Academy of Sciences **30**, 299 (1941)
8. Frisch W.: Turbulence. Kolmogorov’s legacy. Moscow (1998)
9. Roddier F.: In Progress in Optics **19**, 281 (1981)

Electric Polarization in Small Particles of Multiferroics

T. S. Shaposhnikova, R. F. Mamin

Zavoisky Physical-Technical Institute, FRC Kazan Scientific Center of RAS, Kazan 420029,
Russian Federation, vixsup@mail.ru

Phase transitions in spherical particles of a cubic ferromagnetic was considered in the frame-work of the Ginzburg-Landau phenomenological theory. Concentrating on depolarizing field effects, we study the competition between states with homogeneous magnetization and vortex structures. For large sphere radii ($R > R_c$), a phase transition to a vortex state is possible, while for $R < R_c$ it can be in a homogeneous state. We obtain the inhomogeneous distribution of the ferromagnetic order parameter in the form of 2D and 3D vortices, for which the absolute value of the local magnetization depends on the distance from the center of the vortex. This approach have meaning for mesoscopic-sized particles. Such softening of the amplitude variations of magnetization was considered, for example, in the papers of Levanyuk [1] in the analysis of the ferroelectric near the phase transition and the Robler *et al.* [2] in the analysis of the ferromagnet near the phase transition.

It is known that there is a connection between magnetic frustration and ferroelectricity in multiferroics [3]. In multiferroics, the simultaneous existence of magnetic and electric dipoles does not always cause a strong connection between them, since the microscopic mechanisms of ferroelectricity and magnetism are different. A probable microscopic mechanism inducing ferroelectricity in magnetic spirals was discussed, for example, in reference [4]. It involves the antisymmetric Dzyaloshinsky-Moriya (DM) interaction [5, 6]. The DM interaction causes a non-collinear spin ordering. If the magnetic ordering is inhomogeneous, it can lead to polarization [3, 7]. In our work, using the expression for free energy for spherical nanoparticles we obtained an expression for the inhomogeneous distribution of magnetization in the form of 2D and 3D magnetic vortices. The non-uniform electric polarization was calculated. In our case, electric polarization has the form of 2D or 3D hedgehogs. The results are used to discuss the formation of “polar clusters”.

1. Levanyuk A.P., Blinc R.: Phys. Rev. Lett. **111**, 097601 (2013)
2. Robler U.K., Bogdanov A.N., Pfeleiderer C: Nature **442**, 797 (2006)
3. Cheong S.-W., Mostovoy M.: Nature Materials **6**, 13 (2007)
4. Sergienko I.A., Dagotto E.: Phys. Rev. B **73**, 094434 (2006)
5. Dzyaloshinskii I.E.: Sov. Phys. JETP **10**, 628 (1960); **19**, 960 (1964)
6. Morya T.: Phys. Rev. **120**, 91 (1960)
7. Mostovoy M.: Phys. Rev. Lett. **96**, 067601 (2006)

Effect of UV Laser Modification on Intramolecular Energy Transfer Processes in a Vitrified Film Based on a Europium(III) β -Diketonate Complex

**D. V. Lapaev¹, V. G. Nikiforov¹, V. S. Lobkov¹, A. A. Knyazev²,
Yu. G. Galyametdinov^{1,2}**

¹ Zavoisky Physical-Technical Institute, FRC Kazan Scientific Center of RAS, Kazan 420029, Russian Federation

² Kazan National Research Technological University

We revealed the effect of the prolonged UV irradiation with a 337 nm pulsed nitrogen laser on luminescent behavior of a 3 μm vitrified film (sandwiched between two quartz plates) fabricated from an amorphous powder of an anisometric europium(III) β -diketonate complex through a melt-processing technique. It is established, that the film exhibits a bright luminescence of Eu^{3+} ions with the most intense peak at 612 nm caused by efficient ligand-to-metal energy transfer. Despite the fact that usually prolonged UV irradiation leads to irreversible *photofragmentation* of ligands, we had observed no photodecomposition of the complexes after the irradiation of the film with the 337 nm laser for 5 h. The spectroscopic study revealed (i) a 12-fold decrease in the mean luminescence intensity of Eu^{3+} ions in the film due to laser-induced changes in inner coordination spheres of the Eu^{3+} ions and (ii) the main channel of non-radiative energy losses from the Eu^{3+} ions through the multiphonon relaxation. These features open up new possibilities for designing advanced photonics materials with excellent photostability and luminescent properties controlled during operation.

The work was supported by the Russian Foundation for Basic Research (Grants No. 19-02-00569, and No. 19-03-00635)

SECTION
PERSPECTIVES OF MAGNETIC RESONANCE
IN SCIENCE AND SPIN TECHNOLOGY

**Effect of Random Flips of Spins and Conformational
Transitions in PELDOR Signal of Spin Labels with Overlapping
EPR Spectra**

I. T. Khairutdinov, K. M. Salikhov

Zavoisky Physical-Technical Institute, FRC Kazan Scientific Center of RAS, Kazan 420029,
Russian Federation, semak-olic@mail.ru

Due to the molecular motion including the conformational transitions of molecular systems, the dipole-dipole interaction can be randomly modulated as well. This will also affect the manifestation of the dipole-dipole interaction of the spin labels in the PELDOR signal. The conformational transitions produce the random change of the vector \mathbf{r} which connects the spin labels in the pair.

Due to the anisotropy of the g -tensor of spin labels, the conformational transitions can change the resonance frequencies. As a result, the same MW pulse can excite different EPR frequency regions of the spin labels in the course of the molecular conformational transitions. This effect is disturbing the PELDOR

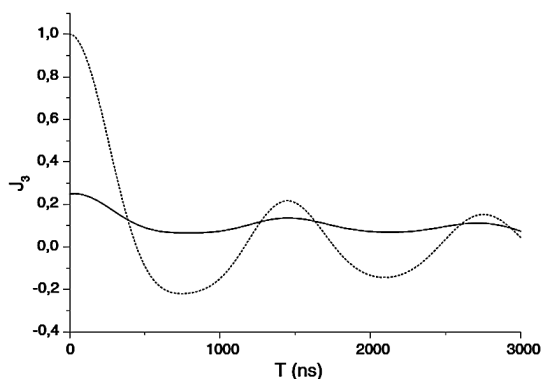


Fig. 1. Effect of spin flips on the contribution of the dipole-dipole interaction to the PELDOR signal for the pairs when the EPR spectra of partners do not overlap (the distance between partners in pairs $r = 4$ nm). Dashed line – the static limit, $W = 0$. Solid line – $W = 3.9 \cdot 10^5$ s $^{-1}$.

signal formation. To illustrate how the molecular conformational transitions affect the PELDOR signal, let us consider a simple model situation, when the change of the spin-label resonance frequencies as a result of the conformational transitions can be ignored. This model situation refers to the spin labels which have practically isotropic g -tensors and which have relatively small anisotropic terms in their hyperfine interaction [1].

Figure 1 illustrates how random spin flips with the rate W can affect the three-pulse PELDOR signal.

1. Salikhov K.M., Khairuzhdinov I.T., Zaripov R.B.: Appl. Magn. Reson. **45**, 573–620 (2014)

NMR Study ^{169}Tm in Diluted Van Vleck Paramagnet $\text{LiTm}_{0.02}\text{Y}_{0.98}\text{F}_4$

**A. S. Parfishina¹, A. V. Egorov², S. L. Korableva¹, I. V. Romanova¹,
K. R. Safiullin¹, M. S. Tagirov^{1,2}**

¹ Institute of Physics, Kazan Federal University, Kremlyovskaya 18, Kazan 420008,
Russian Federation, arina.parfishina@gmail.com

² Institute of Applied Research, Tatarstan Academy of Sciences, Levobulachnaya 36a,
Kazan 420111, Russian Federation

Van Vleck paramagnets (VVP) are compounds which have a singlet ground state and the nearest (10–100 cm^{-1}) excited doublet state of the ground multiplet in a paramagnet rare-earth ion [1]. Detailed study of the NMR spectra and relaxation characteristics in the concentrated Van Vleck paramagnets were reviewed earlier in work [1]. We reported the first NMR study of ^{169}Tm nucleus in a diluted single crystal VVP $\text{LiTm}_{0.02}\text{Y}_{0.98}\text{F}_4$ and comparing our results with LiTmF_4 .

The single crystal $\text{LiTm}_{0.02}\text{Y}_{0.98}\text{F}_4$ has a tetragonal structure of scheelite (CaWO_4) with the space group C_{4h}^6 [2]. LiYF_4 crystals activated by Ho^{3+} , Er^{3+} , Tm^{3+} , Dy^{3+} ions are used in lasers as a converter of the frequencies from radiation to the infrared and visible spectral regions [3]. NMR studying of the VVP single crystal was carried out using pulse home-built spectrometer. The range of magnetic field was 0–0.8 T, working frequencies were 14.15 MHz and 8.43 MHz, temperature region was 2–4.2 K.

As for the single crystal LiTmF_4 [1], we observed a strong anisotropy of the effective gyromagnetic ratio in the single crystal $\text{LiTm}_{0.02}\text{Y}_{0.98}\text{F}_4$. The angular dependence of the effective gyromagnetic ratio for the diluted single crystal $\text{LiTm}_{0.02}\text{Y}_{0.98}\text{F}_4$ completely coincided with the same angular dependence for the concentrated VVP LiTmF_4 [1]. An angular dependence of the spin-lattice relaxation rate (T_1^{-1}) were measured and anisotropy close to the direction [001] were obtained. In this work angular dependence of the spin-spin relaxation rate (T_2^{-1}) relatively to a crystallographic axis were measured and calculated. The inhomogeneous linewidth was obtained and compared with the results for the concentrated VVP LiTmF_4 [1]. Temperature dependencies of the spin-lattice and spin-spin relaxation rates were measured. An interval between the singlet of the ground state to the first excited doublet state was determined equals to $25.9 \pm 0.2 \text{ cm}^{-1}$. The value that was obtained earlier for the concentrated LiTmF_4 was 31 cm^{-1} [1]. According to this result, we assumed a different roots of correlation time in cases of diluted and concentrated Van Vleck paramagnets LiTmF_4 .

The reported study was funded by Russian Foundation for Basic Research, project №18-42-160012 r_a.

1. Aminov L.K., Teplov M.A.: Sov. Phys. Usp. **28**, 762–783 (1985)
2. Garcia E., Ryan R.R.: Acta Cryst. C **49**, 2053–2054 (1993)
3. Walsh B.M.: Laser Physics **19**, 855–866 (2009)
4. Salaun S., Fornoni M.T., Bulou A., Rousseau M., Simon P., Gesland J.Y.: Phys.:Condens. Matter J. **9** 6941–6957 (1997)

Jahn-Teller Centers of Cr²⁺ in a CdSe Crystal

**G. S. Shakurov¹, V. V. Gudkov², I. V. Zhevstovskikh^{2,3}, M. N. Sarychev²,
Yu. V. Korostelin⁴**

¹ Zavoisky Physical-Technical Institute, FRC Kazan Scientific Center of RAS, Kazan 420029,
Russian Federation, shakurov@kfti.knc.ru

² Ural Federal University, 620002, Yekaterinburg, Russian Federation, vlgud@ya.ru

³ Mikheev Institute of Metal Physics, Ural Branch of RAS, Yekaterinburg 620108,
Russian Federation, zhevstovskikh@imp.uran.ru

⁴ Lebedev Physical Institute, 119991, Moscow, Russian Federation, yukor@x4u.lebedev.ru

The CdSe:Cr²⁺ crystal is used as an active medium for mid-IR lasers [1]. It belongs to the II-VI semiconductors. These compounds with an admixture of divalent chromium were studied in detail earlier, including by the EPR method. It was found that when doping crystals with chromium, the symmetry of the environment decreases due to the static Jahn-Teller effect. In all the crystals studied, tetragonal distortions were observed. For crystals with a sphalerite structure consisting of regular tetrahedra, the EPR spectra of Cr²⁺ are described by the spin Hamiltonian of tetragonal symmetry. For compounds with a wurtzite lattice, where tetrahedra are slightly distorted along the sixth order axis, the rhombicity parameter has to be additionally introduced into the Hamiltonian. Different symmetries of the crystalline matrix lead to different numbers of magnetically nonequivalent centers of the Cr²⁺ ion: three for sphalerite and six for wurtzite. Although almost all crystals of this series were studied and spectral parameters were obtained for them, the CdSe:Cr²⁺ compound remained unexplored.

The Cr²⁺ impurity ions were studied in a CdSe crystal by tunable EPR spectroscopy in the frequency range 70–320 GHz. The discovered Jahn-Teller tetragonal distortions of the nearest environment of the chromium ion confirm the results of recent ultrasound studies. A set of spectroscopic parameters is obtained that allows one to obtain agreement between the calculated and experimental angular and field-frequency dependences of the EPR spectra.

1. Antipov O.L., Eranov I.D., Frolov M.P., Korostelin Yu.V., Kozlovsky V.I., Skasyrsky Y.K.: Optics Letters **44**, 1285 (2019)

Features of the ESR on the Mn^{2+} Impurities in the 3D Dirac Semimetal Cd_3As_2

Yu. Goryunov¹, A. Nateprov²

¹ FRC “Kazan scientific center RAS”, Kazan, 420029, Russia, goryunov@kfti.knc.ru

² Institute of Applied Physics, Chisinau, MD-2028, Moldova, nateprov@phys.asm.md

The behaviour of Mn impurities in ESR and transport properties of 3D topological Dirac semimetal Cd_3As_2 has been experimentally studied. It is found that alloying with manganese does not change the sign of magnetoresistance in contrast to Eu alloyed samples [1]. Ions of transition d metals (Fe and Mn) with configuration $3d^5$ are in the S state, and the total orbital momentum of their electrons is zero. Therefore, the magnetic state of these ions is traditionally assumed to be purely spin state with the g -factor equal to that of a free electron (2.0023). Strong ESR signals from Mn^{2+} ions have been detected in the temperature range of 10–300 K. The single ESR line had a typical almost symmetric exchange-narrow Lorentzian shape without superfine structure. However, a complete description with an accuracy of no worse than 0.5% was achieved by superimposing close Lorentzian lines with a width of about 130 and 180 Oe (at room temperature). With decreasing temperature, there was a multiple broadening of the lines and their very weak displacement (see Fig. 1). The temperature dependences are well described by the root term, which would indicate the fluctuation origin of the broadening. But a better description can be achieved by superimposing two exponentials, indicating the presence of gaps in the excitation spectrum. The magnetic state of the Mn^{2+} ion is weak affected by the orbital degrees of freedom but in the case of Dirac quasiparticles one might expect that this influence would be amplified in the case of exchange interaction between localized magnetic moments and free carriers, the spins of which rigidly bound with their orbital motion. The report is devoted to a discussion of these results.

1. Goryunov Yu.V., Nateprov A.N.: Phys. Solid State **60**, 68 (2018)

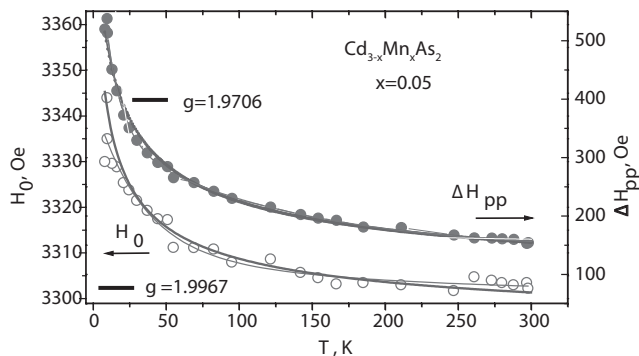


Fig. 1. Temperature dependence of the resonance field and linewidth pic-to-pic.

Electron Spin Relaxation of Photoexcited Porphyrin in Water-Glycerol Glass

**N. Sannikova^{1,2}, I. Timofeev¹, E. Bagryanskaya³, M. Bowman^{3,4},
M. Fedin¹, O. Krumkacheva¹**

¹ International Tomography Center SB RAS, Novosibirsk 630090, Russian Federation, sannikova.epr@gmail.com

² Novosibirsk State University, Novosibirsk 630090, Russian Federation

³ N. N. Vorozhtsov Institute of Organic Chemistry SB RAS, Novosibirsk 630090, Russian Federation

⁴ Department of Chemistry & Biochemistry, University of Alabama, Tuscaloosa, AL 35487-0336, USA

Recently, the photoexcited triplet state of porphyrin was proposed as a promising spin-label for pulsed dipolar electron paramagnetic resonance (EPR). Herein, we report the factors that determine the electron spin echo dephasing of the photoexcited porphyrin in a water-glycerol matrix. The electron spin relaxation of a water-soluble porphyrin was measured by Q-band EPR, and the temperature dependence and the effect of solvent deuteration on the relaxation times were studied. The phase memory relaxation rate ($1/T_m$) is noticeably affected by solvent nuclei and is substantially faster in protonated solvents than in deuterated solvents. The T_m is as large as 13–17 μs in deuterated solvent, potentially expanding the range of distances available for measurement by dipole spectroscopy with photoexcited porphyrin. The $1/T_m$ depends linearly on the degree of solvent deuteration and can be used to probe the environment of a porphyrin in or near a biopolymer, including the solvent accessibility of porphyrins used in photodynamic therapy. We characterized the noncovalent binding of porphyrin to human serum albumin (HSA) from $1/T_m$ and electron spin echo envelope modulation (ESEEM) and found that porphyrin is quite exposed to solvent on the surface of HSA. The $1/T_m$ and ESEEM are equally effective and provide complementary methods to determine the solvent accessibility of a porphyrin bound to protein or to determine the location of the porphyrin.

The experimental investigation of electron spin relaxation of porphyrin and its complex with HSA was supported by Russian Science Foundation (number 18-73-00292). The theoretical description of spin relaxation was supported by the Ministry of Science and Higher Education of the Russian Federation (grant 14.W03.31.0034).

ESR of Dy^{3+} Ions at Cubic Sites in Cs_2NaYF_6 and CsCaF_3 Single Crystals

M. L. Falin¹, V. A. Latypov¹, S. L. Korableva², N. M. Khaidukov³

¹ Zavoisky Physical-Technical Institute, FRC Kazan Scientific Center of RAS, Kazan 420029,
Russian Federation, falin@kfti.knc.ru

² Kazan (Volga Region) Federal University, 42008 Kazan, Russian Federation

³ Institute of General and Inorganic Chemistry, 119991 Moscow, Russian Federation

Fluoroelpasolities $\text{A}_2\text{B}^+\text{C}^{3+}\text{F}_6^-$ ($\text{A} = \text{Cs}$, $\text{B} = \text{Na}$, $\text{C} = \text{Y}$, Sc) having the cubic structure in the wide temperature interval are perfect model systems in which the isomorphous substitution of cations by trivalent rare-earth ions provides an opportunity to study optical and magnetic properties of dopants in a wide concentration range. Double fluoride crystals with perovskite structure $\text{A}^+\text{B}^{2+}\text{F}_3^-$ ($\text{A} = \text{Cs}$, $\text{B} = \text{Ca}$) are very interesting because, on the one hand, they find extensive application in practice, and, on the other hand, they are convenient model systems for studying magneto-optical properties of impurity dopant ions. In principle, it is possible to substitute two various cations in inequivalent positions in these matrices. This enables one to carry out investigations of impurity dopant ions in sixfold or uncommon twelfold coordination. The recent research indicate that the conditions are possible in the process of growth of the CsCaF_3 crystals, at which fluorite nano- or micro-crystallites CaF_2 are formed [1].

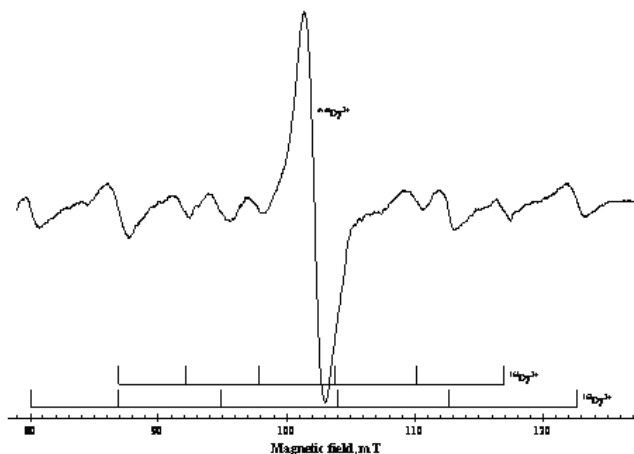


Fig. 1. EPR spectrum of Dy^{3+} in Cs_2NaYF_6 . $\nu = 9330$ MHz, $T = 4.2$ K.

Crystals of cubic elpasolites A_2BCF_6 doped with rare-earth ions were grown under hydrothermal conditions. Under these conditions, spontaneously nucleated crystals of up to 0.5 cm^3 were grown in the upper crystallization zone of the autoclave for 200 h. The crystals $CsCaF_3$ were grown using the Bridgman-Stockbarger method. The concentration of the impurity ion was 1 w%.

EPR experiments was carried out using an X-band spectrometer ERS – 231 (Germany) at $T = 4 \text{ K}$.

The parameters of the corresponding spin Hamiltonians, the ground states and their wave functions were determined. Structural models of the observed complexes were proposed. The experimental results were analyzed in comparison with those for the same paramagnetic ion in other hosts [1, 2].

This work was supported by the program of the Presidium of the Russian Academy of Sciences no. 5 “Electron spin resonance, spin-dependent electron effects and spin technologies”.

1. Falin M.L., Latypov V.A., Gerasimov K.I.: Appl. Magn. Reson. **45**, 707 (2014)
2. Abraham M.M., Finch C.B., Kolopus J.L., Lewis J.T.: Phys. Rev. B **3**, 2855 (1971)
3. Falin M.L., Latypov V.A., Bill H., Lovy D.: Appl. Magn. Reson. **14**, 427 (1998)

SECTION

DIAMOND-BASED QUANTUM SYSTEMS FOR SENSING AND QUANTUM INFORMATION

Specific Features of High-Frequency EPR/ESE/ODMR Spectroscopy of NV Defects in Diamond

**R. A. Babunts, D. D. Kramushchenko, A. S. Gurin, A. P. Bundakova,
M. V. Muzafarova, A. G. Badalyan, N. G. Romanov, P. G. Baranov**

Ioffe Institute, St. Petersburg 194021, Russian Federation, Roman.Babunts@mail.ioffe.ru

High-frequency electron paramagnetic resonance (EPR), electron spin echo (ESE), and optically detected magnetic resonance (ODMR) were applied to study the unique properties of nitrogen-vacancy (NV) defects in diamond in strong magnetic fields. It has been shown that the effective optically-induced alignment of spin level populations, with filling of the $M_S = 0$ level and empty-

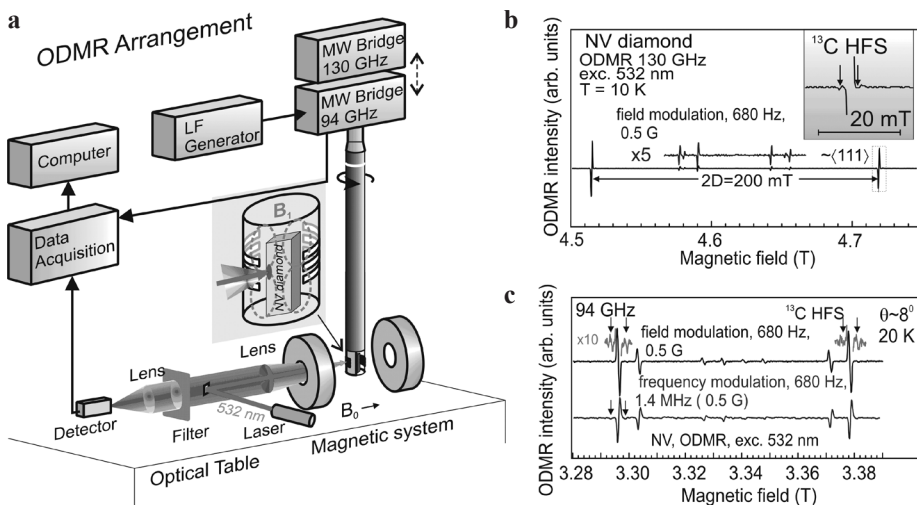


Fig. 1. **a** Schematic diagram of the spectrometer operating in the high-frequency 2 mm (130 GHz) and 3 mm (94 GHz) ranges in strong magnetic fields (up to 7 T). The inset shows on an enlarged scale the scheme of optical excitation and registration of photoluminescence. The sample is placed in a cylindrical waveguide with slots for optical access. This design can be used when tuning the wavelength in the 2 to 3 mm range. **b, c** ODMR spectra of NV centers, measured at 130 GHz and 94 GHz, respectively.

ing of the $M_S = \pm 1$ levels, in magnetic fields of 3 to 5 T, is of the same order as that studied previously [1–3] in zero and low magnetic fields. This allowed observing ODMR at 130 GHz and 94 GHz via variations of the photoluminescence intensity, reaching 10% at resonance.

The samples were preliminarily studied by ODMR in zero magnetic fields, which made it possible to accurately determine the main parameters of the fine structure and hyperfine interactions with nitrogen nuclei, as well as dipole-dipole interactions between the NV center and deep nitrogen donors N^0 , i.e. nitrogen atoms replacing carbon.

In high-frequency ODMR spectra, hyperfine (HF) interactions with the nearest carbon atoms (^{13}C isotope) were observed, which opens up possibilities for an optical study of the dynamic processes of nuclear polarization of carbon nuclei. Narrow ODMR lines that were observed in high magnetic fields are supposed to be used to measure these fields with submicron spatial resolution. One of the concerns with magnetometers is remote calibration. By measuring the HF structure splitting one can calibrate the magnetic field scale. Additional information can be obtained by measuring the distance between the fine-structure lines.

A new technique was developed for detecting ODMR of NV centers with modulation of the microwave frequency, which can simplify the measurement of high magnetic fields. A significant increase in the ODMR signal intensity was demonstrated when the magnetic field was oriented along the symmetry axis of the NV center.

N.G.R and A.S.G. acknowledge partial support from the Russian Foundation for Basic Research under Grant No. 19-52-12058, Deutsche Forschungsgemeinschaft (DFG) within the framework of the ICRC project TRR 160. R.A.B, A.P.B, M.V.M and P.G.B acknowledge the partial support of the Russian Science Foundation (Project No. 20-12-00216).

1. Gruber A., Dräbenstedt A., Tietz C., Fleury L., Wrachtrup J., von Borczyskowski C.: *Science* **276**, 2012 (1997)
2. Jelezko F., Popa I., Gruber A., Tietz C., Wrachtrup J., Nizovtsev A., Kilin S.: *Appl. Phys. Lett.* **81**, 2160 (2002)
3. Baranov P.G., von Bardeleben H.J., Jelezko F., Wrachtrup J.: *Magnetic Resonance of Semiconductors and Their Nanostructures: Basic and Advanced Applications: Springer Series in Materials Science*, Vol. 253, 2017.

Investigation of Vacancy Diffusion and NV Center Formation in the Annealed Electron Beam Irradiated Diamond

**A. M. Gorbachev, S. A. Bogdanov, M. A. Lobaev, A. L. Vikharev,
D. B. Radishev, V. A. Isaev, M. N. Drozdov, V. A. Gusev, D. A. Tatarsky**

Federal Research Center Institute of Applied Physics of the Russian Academy of Sciences,
Nizhny Novgorod, Russian Federation

In this work, the results of optical investigation of the electron beam irradiated diamond sample are presented. The sample contains 3 nm-thick nitrogen-doped delta layer grown by the CVD method. Delta layer is located at the depth of about 50 nm below the substrate surface, and nitrogen concentration is about $1.4 \cdot 10^{19} \text{ cm}^{-3}$ as determined by SIMS. After the irradiation, the sample was annealed at 1200 °C during 4 hours. Electron beam irradiated areas were investigated by photoluminescence spectroscopy before and after annealing. Spatial distribution of emission intensity corresponding to the defects, formed due to irradiation (vacancies, NV centers) was studied for the irradiation dose $2 \cdot 10^{22} \text{ e/cm}^2$. During the annealing, vacancies become mobile and can diffuse forming NV centers even outside the irradiated area.

The study was performed by a grant from the Russian Science Foundation (Project no 16-19-00163).

The Study of SiV Centers Formation in Diamond During the Process of CVD Growth by Optical Emission Spectroscopy

**S. A. Bogdanov, A. M. Gorbachev, A. L. Vikharev,
D. B. Radishev, M. A. Lobaev**

Federal research center Institute of Applied Physics of the Russian Academy of Sciences,
Nizhny Novgorod, Russian Federation, bogser@appl.sci-nnov.ru

SiV centers in diamond are of interest for quantum communication, in particular, for creating single photon sources. To obtain a controlled concentration of such centers in CVD diamond during its growth, it is necessary to have data on the silicon content in the gas phase in the CVD reactor. In this work, the method of optical emission spectroscopy was used to monitor the silicon content. The radiation of the discharge through the fiber was fed to the input of the spectrometer, and a CCD camera connected to its output was used to record the spectra. Silicon atoms in the optical region have fairly bright emission lines at wavelengths of 288.16, 298.76, and 390.55 nm. Radiation at long wavelengths is superimposed on the emission lines of molecular hydrogen. As an intense source of silicon, small pieces of silicon were used, which were placed in the reactor and had contact with the microwave plasma. This method allows a fairly simple and controlled change of the silicon source by varying the number and total area of the pieces.

All of the above mentioned lines corresponding to silicon atoms were observed. However, the emission line of 298.76 nm has a very low intensity, and the line of 390.55 nm is superimposed on the emission line of the CH radical. By varying the amount of silicon, several epitaxial layers of silicon doped with silicon with a thickness of 17 to 32 μm were grown. To control the silicon content in the discharge, a line of 288.16 nm was used. The obtained layers were studied by photoluminescence and Raman spectroscopy. The width of the diamond peak was 1.7–1.8 cm^{-1} for all samples, which corresponds to a diamond with high crystalline perfection, the photoluminescence line of SiV centers is clearly visible.

The study was supported by the Ministry of Science and Higher Education of the Russian Federation under Contract 14.W03.31.0028.

Electroluminescence of Silicon Vacancy Centers in Diamond p-i-n Diode

**M. A. Lobaev¹, D. B. Radishev¹, S. A. Bogdanov¹, A. L. Vikharev¹,
A. M. Gorbachev¹, V. A. Isaev¹, S. A. Kraev², A. I. Okhapkin²,
E. A. Arhipova², M. N. Drozdov²**

¹The Institute of Applied Physics of the Russian Academy of Sciences (IAP RAS), 46 Ulyanov Street, Nizhny Novgorod, Russian Federation, lobaev@appl.sci-nnov.ru

²The Institute of Physics of Microstructure of the Russian Academy of Sciences (IPM RAS), 7 Academicheskaya Street, Afonino, Nizhny Novgorod region, Russian Federation

In this work the results of studying the electroluminescence in diamond p-i-n diode with intrinsic region containing silicon with concentration about 10^{17} cm^{-3} are presented. To obtain high current densities in the p-i-n diode created on the HPHT substrate with the (001) orientation, the regions doped with boron and phosphorus had the concentrations of $5 \cdot 10^{20} \text{ cm}^{-3}$ and 10^{20} cm^{-3} , respectively. The current – voltage characteristics of diodes with different sizes of the undoped region were studied. The electroluminescence and photoluminescence spectra of the emission of SiV centers were studied, and the simultaneous effect of the electric current flow through the diode and laser irradiation on the emission characteristics of SiV centers was studied.

The study was supported by the Ministry of Science and Higher Education of the Russian Federation under Contract 14.W03.31.0028.

Bose Condensation and Spin Superfluidity of Magnons in YIG Film

**P. M. Vetoshko¹, G. A. Knyazev¹, A. N. Kuzmichev¹, A. A. Kholin²,
V. I. Belotelov¹, Yu. M. Bunkov¹**

¹ Russian Quantum Center, Skolkovo, Moscow 143025, Russian Federation
² Crimean Federal University. V. I. Vernadsky, Simferopol 295007, Russian Federation

The formation of a Bose condensate of magnons in a perpendicularly magnetized film of yttrium iron garnet (YIG) under RF pumping in a strip line is experimentally investigated. The characteristics of nonlinear magnetic resonance and the spatial distribution of magnon Bose condensate in the magnetic field gradient are investigated [1]. In these experiments, the Bosonic system of magnons behaves similarly to the Bose condensate of magnons in the antiferromagnetic superfluid ³He-B, which was studied in detail earlier [2]. Magnonic BEC forms a coherently precessing state with the properties of magnonic superfluidity [3]. Its stability is determined by the repulsive potential between excited magnons, which compensates for the inhomogeneity of the magnetic field. We have found the superfluid transport of magnons from the region of strip line 1 (Fig. 1) to the region of strip line 2 and RF signal radiation [1] in a strong gradient of magnetic field.

This work was financially supported by the Russian Ministry of Education and Science, Megagrant project 075-15-2019-1934.

1. Vetoshko P.M. *et al.*: JETP Letters **112**, 290 (2020)
2. Bunkov Yu.M.: J. Mag. Mag. Mat. **310**, 1476 (2007)
3. Bunkov Yu.M.: J. Appl. Mag. Res. (2020)

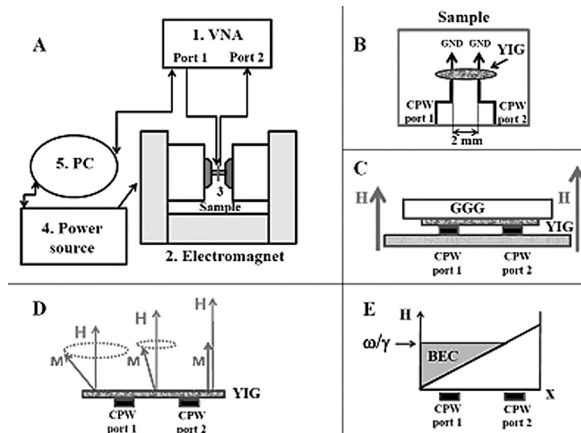


Fig. 1.

AUTHOR INDEX

Abdulganieva, D.	184
Ackermann, K.	55
Acosta, V.	92
Aharonovich, I.	97
Ajoy, A.	93
Akatiev, D. O.	187
Akhmetov, M. M.	108
Akimov, A.	94, 98, 100
Alakshin, E. M.	56
Alexandrov, A.	179
Aliyev, M. N.	170
Alkahtani, M. H.	102, 106
Andreev, G. Yu.	158
Andrianov, V. V.	83, 104, 114, 125
Anikin, A.	184
Anisimov, A. N.	48
Anisimov, V.	184
Antonov, D. O.	12, 176
Arhipova, E. A.	203
Arteaga, A.	33
Asanbaeva, N.	14
Asatryan, H. R.	149
Babunts, R. A.	48, 149, 199
Badalyan, A. G.	48, 149, 199
Badelin, A. G.	32, 136, 166
Bagryanskaya, E. G.	9, 14, 61, 119, 144, 196
Bakirov, M. M.	112, 155
Balaya, P.	129
Bales, B.	155
Balevičius, V.	6
Baltina, T. V.	125
Baranov, P. G.	48, 149, 199
Barba, A. N.	29
Barbon, A.	66
Barinov, S.M.	57
Barkalova, A. S.	30, 174
Batalov, R. I.	132

Bayazitov, A. A.	86, 183, 184
Bazan, L. V.	114, 181
Becher, C.	96
Belotelov, V. I.	204
Belousova, N.	179
Bizyaev, D. A.	70
Bode, B. E.	55
Bogaychuk, A.	50
Bogdanov, S. A.	201, 202, 203
Bogodvid, T. Kh.	83, 114
Bogomyakov, A. S.	62
Bowman, M. K.	81, 196
Bragin, A.	179
Budker, D.	101
Bukharaev, A. A.	70, 159
Bundakova, A. P.	199
Bunkov, Yu. M.	75, 204
Buntkowsky, G.	2
Bystrov, S. S.	6, 111
Cabal, C.	111
Cherebilo, E. A.	174
Chernoglazov, K. Yu.	174
Chernyak, A. V.	67
Chervonova, U.	168
Chinak, O. A.	61, 119
Chizhik, V. I.	6, 111
Chovan, J.	23
Chubarov, A. S.	9
Chuklanov, A. P.	70, 159
Chushnikov, A.	151
Dai, J.	64
Davydov, D. D.	176
Demishev, S. V.	18, 139
Denisov, A. A.	114
Dinse, K.-P.	1
Dobrynin, S.	14, 61, 119
Dolgorukov, G. A.	56
Dong, Y.	10
Dosina, M. O.	114
Drovosekov, A. B.	30, 174
Drozdov, M. N.	201, 203
Dudnikova, V.	143
Dvinskikh, S. V.	64
Edinach, E. V.	149
Egorov, A. V.	6, 193
Eremeev, A. A.	125

Eremina, R. M.	32, 136, 166
Evstigneeva, M.	172
Fakhrutdinov, A.	86, 183, 184
Falin, M. L.	197
Fam, Ch. A.	159
Fatkullin, N.	157
Fattakhov, Ya.	86, 87, 183, 184
Fatykhov, R. R.	129
Fazleeva, G.	144
Fedin, M. V.	9, 62, 81, 144, 182, 196
Fedotov, A.	11, 121, 127
Filipov, V. B.	139
Frolova, E. N.	181
Fu, Kai-Mei C.	101
Fuentes, S.	33
Gabbasov, B. F.	161
Gafarova, A. R.	112
Gafiyatullin, L. G.	181
Gafurov, D.	128, 165
Gafurov, M.	11, 57, 121, 127
Gainutdinov, Kh. L.	83, 104, 114, 125
Galyametdinov, Yu. G.	145, 190
Ganenko, T. V.	72
Gavrilova, T. P.	129
Geru, I. I.	29
Giannoulis, A.	55
Gilmanov, M. I.	139
Gimazov, I. I.	79
Glazkov, V. N.	23
Glushkov, V. V.	139
Gnezdilov, O. I.	67
Goldberg, M. A.	11, 57
Gorbachev, A. M.	201, 202, 203
Gorincioi, E. C.	29
Goryunov, Yu.	195
Gotovko, S.	42
Grafe, H-J.	131
Graskova, I. A.	72
Grishin, P.	11
Gruzdev, M.	168
Gudkov, V. V.	194
Gumarov, A. I.	35, 38, 39, 161, 162, 163, 170
Gumarov, G. G.	108, 112, 151
Gurin, A. S.	48, 149, 199
Gusev, D. S.	174
Gusev, V. A.	201

Hara, S.	47
Hemmer, P. R.	89, 94, 102, 104, 106
Holldack, K.	62
Ibragimova, M.	151
Ignatyev, I.	11
Isaev, V. A.	201, 203
Iskhakova, A. K.	154
Iwata, G. Z.	101
Iyudin, V. S.	125
Kalachev, A. A.	94, 187
Kálai, T.	16
Kamalov, A.	131
Kandrashkin, Y. E.	78
Karpasyuk, V. K.	32, 166
Karpeev, A. A.	173
Kataev, V.	4, 25
Khabibullin, R. R.	161
Khabipov, R.	86, 87, 184
Khaibullin, R. I.	39, 106, 170
Khaibullina, D.	151
Khaidukov, N. M.	197
Khairutdinov, I. T.	16, 155, 191
Khantimerov, S. M.	129
Kharkov, B. B.	64
Kholin, A. A.	204
Khramova, O. D.	174
Khutsishvili, S. S.	72
Kiiamov, A. G.	35, 162, 163
Kirilyuk, I.	14, 9, 61, 119
Kish, K.	16
Kiskin, M. A.	62
Kisler, D.	179
Kiyamov, A. G.	158
Klochkov, A. V.	56
Knyazev, G. A.	204
Knyazev, A. A.	190
Kocharovskaya, O.	94
Kokorin, A. I.	7, 16, 116
Kolker, A.	168
Komlev, V. S.	11, 57, 121, 127
Komolkin, A. V.	64
Kondratyeva, E. I.	56
Konstantinova, E. A.	7, 116, 147
Konygin, G. N.	108
Korableva, S. L.	158, 193, 197
Kornienko, A.	86

Korostelin, Yu. V.	194
Kovaleva, E.	12, 141, 176
Kraev, S. A.	203
Kramushchenko, D. D.	199
Krasnikova, Yu. V.	23
Krasnozhon, V.	87
Kreine, N. M.	30
Krumkacheva, O. A.	9, 61, 119, 144, 196
Kukovitskii, E. F.	79
Kulchitchky, V. A.	83, 114
Kulik, L. V.	80
Kurbakov, A. I.	165
Kusova, A. M.	118, 154
Kuzmichev, A. N.	204
Kuzmin, V.	50, 56, 68
Kytina, E. V.	7, 147
Lapaev, D. V.	190
Latypov, V. A.	197
Latypov, I. Z.	187
Lavrov, I. A.	125
Lebedeva, N. Sh.	9
Leontyev, A. V.	102, 104, 106, 132, 137
Li, Q.	90
Lisin, V.	185
Lobaev, M. A.	201, 202, 203
Lobkov, V. S.	102, 104, 190
Lunev, I. V.	132
Lyubyakina, P.	141
Mahmood, Z.	178
Majhi, D.	64
Mamedov, D. V.	166
Mamedov, M.	59
Mamin, G.	11, 57, 121, 127
Mamin, R. F.	132, 134, 137, 189
Marek, A.	12
Maryasov, A. G.	81
Matveev, V. V.	6
Midoni, I. E.	29
Migachev, S. A.	70, 132, 134
Mikhailov, M.	184
Mohammed, W. M.	35
Morozov, D.	14
Muranova, L. N.	104
Murzakaev, V.	179
Murzakhanov, F. F.	57, 121, 127
Muzafarova, M. V.	199

Nakamura, T.	27
Nalbandyan, V. B.	135, 165, 172
Nateprov, A.	195
Naumkin, V. V.	173
Nefedov, D.	33
Nehrkorn, J.	62
Nesladek, M.	91
Nikiforov, V. G.	102, 104, 106, 190
Nikitin, S. I.	162, 163
Nikolaev, S. N.	30
Norman, D. G.	55
Novodvorsky, O. A.	174
Nozhkina, O. A.	72
Nurgazizov, N. I.	70
Nuzhdin, V. I.	39
O divanov, V.	184
Ohmichi, E.	47
Ohta, H.	47
Okhapkin, A. I.	203
Okubo, S.	47
Orendáčová, A.	23
Orlinskii, S.	11, 57, 121, 127
Ovcharenko, V. I.	62
Ovcharenko, S.	61, 119
Ovchinnikov, I. V.	181
P aduan-Filho, A.	21
Parfishina, A. S.	193
Parkhomenko, E. R.	147
Parshina, L. S.	174
Pashkevich, S. G.	83, 114
Pasynkov, M. V.	162
Paveliev, M. N.	83
Pavlov, D. P.	132, 137
Perfil'eva, A. I.	72
Petrakova, N.	11
Petranovskii, A. V.	33
Petrov, A. V.	162, 163
Petukhov, V. Yu.	108, 112, 151
Polyukhov, D.	182
Poryvaev, A.	182
Povarov, K. Yu.	21
Prando, G.	25
R abdano, S. O.	111
Radeonychev, Y. V.	94
Radishev, D. B.	201, 202, 203
Raganyan, G. V.	165

Reshetnikov, N.	184
Rodionov, A. A.	35, 38, 158, 161
Rodygina, I. K.	23
Romanova, I. V.	158, 193
Romanov, N. G.	48, 149, 199
Rybin, D. S.	108
Rylkov, V. V.	30, 174
Ryzhkin, S.	184
Safiullin, K. R.	56, 68, 193
Sagdeev, D. O.	145
Saito, Y.	47
Sakhin, V. O.	79
Sakurai, T.	47
Salikhov, K. M.	3, 16, 59, 86, 155, 184, 191
Salikhov, T.	135, 137
Samarin, A. N.	139
Samartsev, V.	185
Sannikova, N. E.	9, 196
Sarychev, M. N.	194
Schnegg, A.	62
Seidov, Z. Y.	32, 136
Semakin, A. S.	158
Semeikin, A. S.	9
Semenov, A. V.	139
Semenov, A.	59
Shagalov, V.	86, 183, 184
Shaginyan, V. R.	20
Shagvaleev, R.	157
Shakurov, G. S.	194
Shamilov, R. R.	145
Shaposhnikova, T. S.	132, 134, 137, 189
Shayakhmetov, N. G.	83
Shegeda, A.	185
Shelyapina, M. G.	33
Shestakov, A. V.	166
Sheveleva, A. M.	62
Shi, Y.	94
Shinkarev, A.	127
Shitsevalova, N. Yu.	139
Shkalikov, A. V.	187
Shmelev, A. G.	102, 104, 106
Shurtakova, D.	121, 127
Sirotkin, V.	127
Sitnikov, A. V.	30
Sitnitsky, A. E.	118, 154
Skirda, V. D.	67, 179

Sluchanko, N. E.	139
Smirnov, A. I.	12, 21
Smirnov, V.	127
Soldatov, T. A.	21
Stanislavovas, A. A.	56, 68
Stass, D. V.	76
Stewart, A. J.	55
Stognienko, O.	86
Streletskii, A. N.	116
Sturza, M.-I.	128, 131
Subbotin, K.	143
Sukhanov, A. A.	59, 124, 143, 145, 178
Suleimanov, N. M.	129
Susloparova, A. E.	165
Suturina, E. A.	62
Svistov, L.	42
Tagirov, L. R.	35, 38, 39, 161, 162, 163, 170
Tagirov, M. S.	53, 56, 68, 158, 193
Takahashi, H.	47
Talanov, Yu. I.	79
Tambasova, D. P.	12, 141, 176
Tarasenko, R.	23
Tarasov, V.	143
Tatarsk, D. A.	201
Teitel'baum, G. B.	79
Tikhonov, N. I.	72
Timofeev, I. O.	9, 144, 196
Tokalchik, Y. P.	114
Tolmachev, D. O.	149
Tormyshev, V.	14, 61
Tretyakov, E.	144
Troshin, P.	144
Trusov, G. V.	7
Tsentelovich, Y. P.	9
Turaikhanov, D. A.	187
Turanov, A. N.	181
Turanova, O. A.	181
Tyurtyaeva, A.	33
Useinov, N. Kh.	159
Uspenskaya, Yu. A.	149
Uvarov, M. N.	80
Vagizov, F. G.	94
Vakhitov, I. R.	39
Vakul'skaya, T. I.	72
Valeev, V. F.	39
Valuev, I. V.	62

-
- Vasilchikova, T. M. 165, 172
Vavilova, E. L. 25, 128, 131, 135, 165
Veber, S. L. 62, 81
Vedeneev, A. S. 174
Vetoshko, P. M. 204
Vikharev, A. L. 201, 202, 203
Volkov, M. Yu. 123, 181
Volkov, V. I. 67
Vorobyeva, V. 168
Voronkova, V. K. 124, 145, 178
Whangbo, M.-H. 165
Wickenbrock, A. 101
Wort, J. L. 55
Yafarova, G. G. 83, 114, 123, 125
Yanilkin, I. V. 35, 38, 39, 161, 162, 163, 170
Yantsen, N. V. 173
Yan, Y. 10
Yatsyk, I. V. 32, 129, 136, 151, 166
Yavkin, B. 127
Yocupicio-Gaxiola, R. 33
Yurtaeva, S. V. 123
Yusupov, R. V. 35, 38, 39, 161, 162, 163, 170
Zamaro, A. S. 114
Zaripov, R. B. 16, 112, 143
Zaripova, R. I. 125
Zefirov, T. L. 125
Zhang, X. 10
Zhao, J. 10, 124, 178
Zharikov, E. 143
Zharkov, D. K. 102, 104, 106, 132, 137
Zheludev, A. 21
Zhevstovskikh, I. V. 194
Zhivov, G. A. 38
Ziatdinov, A. M. 44
Zuev, Yu. F. 118, 154
Zvereva, E. A. 135, 165, 172
Zyuzin, A. M. 173

© Федеральное государственное бюджетное учреждение науки
Казанский физико-технический институт имени Е. К. Завойского
ФИЦ КазНЦ РАН, 2020

Ответственный редактор: В. К. Воронкова; редакторы С. М. Ахмин, Л. В. Мосина; технический редактор
О. Б. Яндуганова. Издательство ФИЦ КазНЦ РАН,
420029, Казань, Сибирский тракт, 10/7, лицензия № 0325 от 07.12.2000.

Отпечатано с оригиналов заказчика

АО «Информационно-издательский центр» · Казань, ул. Чехова 28, телефон +7 (843) 236 94 26

